# TEMPERATURE DEPENDENCE OF THE CARDIAC SODIUM CALCIUM EXCHANGER

by

Christian R. Marshall
BSc (Kinesiology) Simon Fraser University 1999

THESIS SUBMITTED IN PARTIAL FULFILLMENT OF
THE REQUIREMENTS FOR THE DEGREE OF

DOCTOR OF PHILOSOPHY

In the
Department
of
Molecular Biology & Biochemistry



SIMON FRASER UNIVERSITY

Summer 2005

# APPROVAL

**Name:** **Christian R. Marshall**

**Degree:** **Doctor of Philosophy**

**Title of Thesis:** **Temperature Dependence of the Cardiac Sodium Calcium Exchanger**

**Examining Committee:**

**Chair:** **Dr. Dipankar Sen**
Professor, Department of Molecular Biology & Biochemistry

---

**Dr. Glen F. Tibbits**
Senior Supervisor, Professor
School of Kinesiology

---

**Dr. Eric A. Accili**
Committee Member, Assistant Professor
School of Kinesiology

---

**Dr. Rosemary B. Cornell**
Committee Member, Professor
Department of Molecular Biology & Biochemistry

---

**Dr. Michel R. Leroux**
Committee Member, Assistant Professor
Department of Molecular Biology & Biochemistry

---

**Dr. Edgar C. Young**
**Internal Examiner,** Assistant Professor
Department of Molecular Biology & Biochemistry

---

**Dr. Kenneth D. Philipson**
**External Examiner,** Professor and Chair
Department of Physiology
David Geffen School of Medicine at UCLA

**Date Approved:** _____

# SIMON FRASER UNIVERSITY

# PARTIAL COPYRIGHT LICENCE

# ABSTRACT

Calcium ($Ca^{2+}$) is a ubiquitous and highly versatile intracellular messenger as exemplified by the numerous mechanisms nature has evolved to facilitate $Ca^{2+}$ transport. One of these mechanisms is $Na^{+}/Ca^{2+}$ exchange. The $Na^{+}/Ca^{2+}$ exchanger (NCX) is an integral membrane protein that catalyzes the counter-transport of $Na^{+}$ for $Ca^{2+}$ ions. NCX is expressed in a wide variety of tissues throughout a diverse group of organisms. NCX expression is especially high in the heart where NCX mainly functions to extrude $Ca^{2+}$ from the cytosol to allow relaxation. Cardiac function in ectotherms, such as the trout, is distinguished by its ability to maintain adequate contractility in temperatures that are cardioplegic to mammals. Using cloned trout NCX-TR1.0 and mammalian NCX1.1 expressed in *Xenopus* oocytes, we measured NCX mediated currents and showed that the NCX-TR1.0 isoform is relatively insensitive to temperature compared with NCX1.1. Furthermore, our results indicate that this phenomenon is intrinsic to the NCX protein itself and is not due to differences in regulatory properties between isoforms. Using chimeras, we determined that the region of the NCX protein responsible for this differential temperature dependence is located within the N-terminal transmembrane domain of the protein. However, further chimeric studies within this region have produced equivocal results. To aid in generation of hypotheses as to which amino acids are likely to confer NCX temperature dependence, we employed bioinformatics and comparative analyses. Cloning of tilapia NCX-TL1.0 provided a useful comparative model to NCX-TR1.0, since tilapia share a close phylogenetic relationship with trout while adapted to live in warm waters. Despite high overall sequence identity with NCX-TR1.0, we found NCX-TL1.0 to have mammalian like temperature dependence. Coupled with measurements using squid and fruit fly NCX isoforms and subsequent sequence analyses, these comparative studies provided insight into the relationship between NCX genotype and temperature phenotype. Finally, data mining of genomic data yielded 13 new NCX sequences, including a fourth NCX gene member that is present only in fish and amphibian genomes. Phylogenetic and evolutionary analyses indicate three serial gene duplication events occurred early in the evolution of vertebrates, giving rise to the four members of the NCX gene family.

For my parents and grandparents

# ACKNOWLEDGEMENTS

I owe many thanks to those who I have encountered over my extended academic training at Simon Fraser University. First and foremost I would like to thank my senior supervisor Dr. Glen Tibbits for his guidance during my tenure in the Cardiac Membrane Research Laboratory. His enthusiasm for research and meticulous approach is contagious and I have grown immensely as a scientist under his tutorage. I would also like to thank my supervisory committee, Dr. Rosemary Cornell, Dr. Michel Leroux, and Dr. Eric Accili for constantly challenging me through insightful and productive discussions. I also thank Dr. Ken Philipson from UCLA for giving my work credence and validity as my defense external examiner.

The breath of my work would not be possible without the help and collaboration of many fine investigators that I have had the privilege to work with over the past 6 years. I would especially like to thank Dr. Larry Hryshko of the University of Manitoba and his lab for the testing all constructs made in this study. I would also like to thank Francis Ouellette, Stefanie Butland, and Joanne Fox of the UBC Bioinformatics Centre for providing excellent consultation with the bioinformatics experiments. In addition, I would like to thank Dr. Fiona Brinkman in the Department of Molecular Biology for help with molecular evolution and phylogenetics.

Thank you to the members, both past and present, of the Cardiac Membrane Research Laboratory but especially to Xiao-Hua Xue who taught me everything I know about molecular biology and gave me the tools to succeed in this project. Thanks also to all the friends I have made at SFU during my degree for providing support and breaks in the tediousness of the laboratory.

Finally, I would like to thank my family for their support and understanding during my long academic career.

# TABLE OF CONTENTS

# LIST OF FIGURES

## CHAPTER 1



## CHAPTER 2



## CHAPTER 3



## CHAPTER 4

**CHAPTER 5**



**CHAPTER 6**

# LIST OF TABLES

# LIST OF ABBREVIATIONS

| | |
|---|---|
| ANOVA | Analysis of Variance between groups |
| CAX | $H^+/Ca^{2+}$ exchangers |
| CaCA | Cation:$Ca^{2+}$ antiporter |
| CCX | Cation/$Ca^{2+}$ exchangers |
| CICR | $Ca^{2+}$ induced $Ca^{2+}$ release |
| DHPR | Dihydropyridine Receptor or L-type $Ca^{2+}$ channel |
| $E_{act}$ | Energy of Activation |
| EGTA | Ethyleneglycol-bis(β-aminoethylether)-N,N,N',N'-tetracetic acid |
| $E_m$ | Membrane potential |
| $E_{Na}$ | Equilibrium potential of $Na^+$ |
| $E_{Ca}$ | Equilibrium potential of $Ca^{2+}$ |
| $E_{Na/Ca}$ | Equilibrium potential of $Na^+/Ca^{2+}$ Exchange |
| $F_{ss}$ | Fraction of steady-state to peak current |
| HEPES | 4-(2-hydroxyethyl)-1-piperazineethanesulfonic acid |
| $I_{Na/Ca}$ | $Na^+/Ca^{2+}$ Exchange current |
| ME | 2-Mercaptoethanol |
| MES | Methanesulfonate acid |
| NCX | $Na^+/Ca^{2+}$ Exchanger |
| NCKX | $K^+$-dependent $Na^+/Ca^{2+}$ exchanger |
| NMG | N-methylglucamine |
| PCR | Polymerase chain reaction |

| | |
|---|---|
| $Q_{10}$ | Temperature Coefficient |
| RACE | 5'- and 3'- rapid amplification of cDNA ends |
| RyR | Ryanodine Receptor |
| SDS-PAGE | sodium dodecyl sulfate-polyacrylamide gel electrophoresis |
| SEM | Standard Error of Means |
| SERCA2a | Sarcoplasmic Reticulum $Ca^{2+}$-ATPase |
| SL | Sarcolemma |
| SLC8A | Solute Carrier Family 8A or NCX Gene Family |
| SR | Sarcoplasmic Reticulum |
| TCDB | Transport Classification Database |
| TEA-OH | Tetraethylammonium hydroxide |
| TMS | Transmembrane segment |
| XIP | E***X***changer ***I***nhibitory ***P***eptide |
| YRBG | Bacterial and Archaea related exchanger proteins |

# LIST OF ORIGINAL PUBLICATIONS

This dissertation is based largely on the following research articles, reproduced by permission of the journals below.

## CHAPTER 2

Elias CL, Xue XH, **Marshall CR**, Omelchenko A, Hryshko LV, Tibbits GF. Temperature dependence of cloned mammalian and salmonid cardiac $Na^+/Ca^{2+}$ exchanger isoforms. *Am J Physiol Cell Physiol.* 2001 Sep;281(3):C993-C1000. PMID: 11502576

In this study, I was responsible for NCX molecular biology and synthesis of NCX cRNA *in vitro*. In addition, I had a limited role in writing and editing the manuscript.

## CHAPTER 3

**Marshall C**, Elias C, Xue XH, Le HD, Omelchenko A, Hryshko LV, Tibbits GF. Determinants of cardiac $Na^+/Ca^{2+}$ exchanger temperature dependence: N-terminal transmembrane segments. *Am J Physiol Cell Physiol.* 2002 Aug;283(2):C512-20. PMID: 12107061

My contribution to this study involved construction of NCX chimeras, synthesis of NCX cRNA *in vitro* and interpretation and analysis of the results. I was responsible for putting together and writing the manuscript.

## CHAPTER 5

**Marshall CR**, Fox JA, Butland SL, Ouellette BF, Brinkman FS, Tibbits GF. Phylogeny of $Na^+/Ca^{2+}$ exchanger (NCX) genes from genomic data identifies new gene duplications and a new family member in fish species. *Physiol Genomics*. 2005 Apr 14;21(2):161-73. Epub 2005 Mar 1. PMID: 15741504

This study was fully conceived and written by me under the advisement of the co-authors.

## CHAPTER 6

**Marshall CR**, Pan TC, Le HD, Omelchenko A, Hwang PP, Hryshko LV, Tibbits GF. cDNA cloning and expression of cardiac $Na^+/Ca^{2+}$ exchanger (NCX) from mozambique tilapia (*Oreochromis Mossambicus*) reveals teleost membrane transporter with mammalian temperature dependence. *J Biol Chem*. 2005 Jun 3; [Epub ahead of print] PMID: 15937330

I was responsible for the overall design of this study in addition to contributing to the cloning and expression of the tilapia NCX. The paper was put together and written by me.

# CHAPTER 1
# GENERAL INTRODUCTION AND LITERATURE REVIEW

## 1.1 Introduction

Transport across biological membranes is a fundamental process in all cells, and its complexity is exemplified by the diversification of ~400 families of membrane transport proteins that have evolved to manage this task (1,2). Calcium ($Ca^{2+}$) is a ubiquitous and highly versatile intracellular messenger used in cell types spanning plant (3), animal (4), protist (5) and bacterial (6) kingdoms. $Ca^{2+}$ ions are in constant flux across the membrane underscored by a concentration differential of approximately four orders of magnitude between the extracellular (mM) and cytosolic spaces (nM). Finely tuned changes in cytosolic $Ca^{2+}$ concentrations allow activation/deactivation of proteins which, in turn, modulate a variety of cellular functions (7). Although necessary for graded responses, $Ca^{2+}$ concentration modulation must be tightly controlled since overload can have potentially deleterious effects by inducing lethal cellular perturbations. As such, the interplay between $Ca^{2+}$ influx and efflux is intricately balanced and regulated by myriad $Ca^{2+}$ transport mechanisms. One of these systems is $Na^+/Ca^{2+}$ exchange.

The $Na^+/Ca^{2+}$ exchanger (NCX) is a polytopic membrane transporter that catalyzes the countertransport of $Na^+$ for $Ca^{2+}$ ions. $Na^+/Ca^{2+}$ exchange is electrogenic, and thus the net direction in which the NCX transports $Ca^{2+}$ is dependent on the membrane potential ($E_m$) in addition to intracellular and extracellular concentrations of $Na^+$ and $Ca^{2+}$. The stoichiometry of this exchange is generally accepted to be $3Na^+:1Ca^{2+}$ (8,9); however a stoichiometry of 4:1 may also possible (10-12). Ion exchange direction is also reversible but NCX primarily functions as a part of the $Ca^{2+}$ efflux system, utilizing the energy of the inward $Na^+$ electrochemical gradient maintained by the $Na^+$-

$K^+$-ATPase. In this manner NCX competes with other $Ca^{2+}$ transport systems to restore resting cytosolic levels, thereby maintaining $Ca^{2+}$ homeostasis.

Attesting to its importance as a $Ca^{2+}$ transport mechanism, NCX is found in the plasma membranes of a phylogenetically diverse group of organisms. In vertebrate species, NCX is present in most tissues where its relative abundance is correlative with the importance of $Na^+/Ca^{2+}$ exchange in that cell type. Expression is high in excitable tissues (heart, brain) and those involved in osmoregulartion (kidney), but low in other tissues (e.g. liver) (13,14). Although the role of NCX in neurons (15,16) and smooth muscle (17,18) has gained recent high profile attention, it is NCX function in the heart that has garnered the most interest. In cardiac tissue, NCX expression is especially high and $Na^+/Ca^{2+}$ exchange clearly plays an important role in cardiomyocyte $Ca^{2+}$ homeostasis on a beat-to-beat basis (see below).

Two seminal events in the early 1990's greatly accelerated our understanding of NCX function. First, the NCX was cloned from canine heart by Nicoll *et al* (19), which provided the impetus for a more detailed biochemical and functional characterization of NCX from a molecular perspective. Cloning of NCX paralogs from other tissues (20,21) and orthologs from other species (22-24) soon followed with the ensuing comparative analyses giving novel insights into NCX function. Secondly, the giant excised patch technique developed by Hilgemann (25) provided a sensitive assay to examine NCX electrophysiology. These seminal developments gave researchers the necessary tools for detailed analyses of NCX from both the molecular and cellular levels.

The following literature review is by no means comprehensive but rather will focus on selected topics pertinent to NCX temperature dependence. The focus will include the physiological relevance of NCX in the heart; the molecular biology, structure and function of the NCX; and adaptation of proteins to temperature.

## 1.2 Physiological Role of NCX in the Heart

It has been known for some time that a rise in cytosolic $Ca^{2+}$ concentration is responsible for triggering the intracellular events leading to muscle contraction. In some instances as exemplified by the rhythmic contraction of cardiac muscle, the elevated free

$Ca^{2+}$ in the cytosol is required for only brief periods of time (e.g. ~50-100 ms). The strength of cardiac muscle contraction is dependent upon this cytosolic $Ca^{2+}$ concentration on a beat-to-beat basis. $Ca^{2+}$ must be rapidly removed from the cytosol for relaxation to occur and therefore its concentration must be tightly regulated in both spatial and temporal domains. The particular role of NCX in $Ca^{2+}$ transport within the heart has been studied extensively and is well documented (see reviews (8,9,26-28). In addition, NCX has been implicated in several cardiac pathophysiologies including arrhythmogenesis (29-31) and cellular damage associated with ischemia/reperfusion injury (32,33).

Reuter and Seiz (34) first identified $Na^{+}/Ca^{2+}$ exchange in 1968 using guinea pig atria. In the thirty-five years since, the role of NCX in excitation-contraction (E-C) coupling in adult mammalian cardiomyocytes has become more clearly defined. In E- C coupling the $Ca^{2+}$ signal responsible for contraction in the heart originates from two primary sources. With depolarization of the sarcolemma (SL), $Ca^{2+}$ enters the cell through voltage-dependent L-type $Ca^{2+}$ channels (DHPR). This $Ca^{2+}$ then triggers $Ca^{2+}$ release from the sarcoplasmic reticulum (SR) through activation of the ryanodine receptors (RyR) in a process known as $Ca^{2+}$-induced $Ca^{2+}$ release (CICR). $Ca^{2+}$ from either source raises the free intracellular $Ca^{2+}$ concentration several fold and induces contraction by binding to site II of troponin C. For relaxation to occur, an amount of $Ca^{2+}$ equal to that entering the cytosol must be extruded within a single heartbeat. This requires $Ca^{2+}$ removal via at least four competing transport mechanisms: sarcolemmal $Ca^{2+}$-ATPase (PMCA), mitochondrial $Ca^{2+}$ uniport, SR $Ca^{2+}$-ATPase (SERCA2a) and $Na^{+}/Ca^{2+}$ exchange. The relative contribution of each of these systems in the removal of $Ca^{2+}$ from the cytosol varies considerably with species (35-37), developmental stage (38) and pathophysiology (39,40). The sarcolemmal $Ca^{2+}$-ATPase and mitochondrial $Ca^{2+}$ uniporter have small roles in relaxation and have collectively been referred to as the slow removal system. Estimates from adult rabbit myocytes indicate that 70% of the $Ca^{2+}$ is removed by SERCA2a, 28% by NCX, and the remaining 2% by the slow removal system (36). These ratios are typical of most mammals, with the NCX responsible for removing ~25-35% of cytosolic $Ca^{2+}$ during relaxation in cats (41), ferrets (41), dogs (40), and humans (39). The lone exception is in murine species where the SERCA2a has high

activity and accounts for ~92% of the intracellular $Ca^{2+}$ removal leaving only ~7% transported by the NCX (~7-9%) (36,42). Conversely, a more substantial role for NCX extrusion of $Ca^{2+}$ has been proposed in lower vertebrates such as fish where transarcolemmal $Ca^{2+}$ flux is more important for direct activation of contraction compared with mammalian species (43,44). In rainbow trout, the NCX is responsible for extruding the majority (~55%) of the $Ca^{2+}$ from the cytosol during myocyte relaxation (45). During cardiac development, neonate NCX expression is several fold higher than in the adult heart (46,47) which is reflected in increased mRNA levels during this stage of development (48,49). Interestingly, these conditions are echoed in the failing heart, with increased mRNA levels, protein levels, and exchanger activity (50,51). In this condition the NCX may be responsible for extruding up to 50% of the $Ca^{2+}$ from the cytosol during relaxation (39,40). The NCX is dominant mode of transsarcolemmal $Ca^{2+}$ removal in adult mammals, extruding anywhere from 7-35% of the $Ca^{2+}$ responsible for inducing contraction. In addition, the NCX may play a more substantial role in cardiac relaxation of lower vertebrates, neonates, and in the failing heart.

The NCX operates well as a $Ca^{2+}$ efflux mechanism and its function in relaxation is well documented. However, more controversial roles for NCX as a contributor to $Ca^{2+}$ influx under certain conditions have been suggested (52). Assuming a transport stoichiometry of 3 $Na^+$ for 1 $Ca^{2+}$, the current produced by NCX ($I_{Na/Ca}$) exhibits a reversal potential analogous to that of ion channels ($E_{Na/Ca}= 3E_{Na} -2E_{Ca}$ where $E_{Ca}$ and $E_{Na}$ are the equilibrium potentials of $Ca^{2+}$ and $Na^+$, respectively (26)). The relationship between the $E_{Na/Ca}$ and $E_m$ determines the net direction of $Ca^{2+}$ transport. For example, if $E_m<E_{Na/Ca}$, then $Ca^{2+}$ extrusion (inward $I_{Na/Ca}$) is favoured as is the case at resting membrane potentials or in the latter stages of myocyte contraction. Under these normal physiological conditions, the NCX responds to increases in cytosolic $Ca^{2+}$ and functions to lower $Ca^{2+}$ to resting levels. However, under certain situations in which $E_m$ exceeds $E_{Na/Ca}$, net transport will reverse and favour $Ca^{2+}$ influx (outward $I_{Na/Ca}$) through NCX. Mechanisms of reverse exchange include depolarization-induced $Ca^{2+}$ influx (53-55) and $Na^+$ current-induced $Ca^{2+}$ influx (56). Clearly, $Ca^{2+}$ influx from NCX can trigger muscle contraction in an experimental setting but the physiological significance remains controversial (57,58) despite extensive investigation. However, in situations discussed

previously where trans-sarcolemmal $Ca^{2+}$ flux is more important for contraction (i.e. neonate, lower vertebrate, failing myocardium), reverse mode NCX may play a more prominent role in eliciting contraction. However, in the healthy adult human heart, it seems likely that the NCX serves primarily as a $Ca^{2+}$ efflux mechanism in relaxation, and that the DHPR is the main source of $Ca^{2+}$ influx for triggering contraction.

## 1.3 The CaCA Superfamily and Molecular Evolution

The NCX is a member of the cation:$Ca^{2+}$ antiporter (CaCA) family, which corresponds to family 2.A.19 of the Transport Classification Database (TCDB) (2). The CaCA family falls within the general class of electrochemical potential-driver transporters and under the subclass of membrane porters. Recently, Cai and Lytton (59) performed an extensive sequence comparison and phylogenetic analysis of 147 sequences in the CaCA family. They defined five major branches based on the names of characterized proteins within the branch: $Na^+/Ca^{2+}$ exchangers (NCX), $K^+$-dependent $Na^+/Ca^{2+}$ exchangers (NCKX), $H^+/Ca^{2+}$ exchangers (CAX), bacterial and archaeal proteins (YRBG), and a group provisionally named cation/$Ca^{2+}$ exchangers (CCX) (59). Approximately a third of the 147 sequences belong to prokaryotes, of which only the *E. coli* inner membrane protein YRBG has been cloned and expressed (60,61). The CAX family branches with the YRBG family but contains sequences from fungi and plants in addition to those with archaea and bacterial origins. Both bacterial (62) and fungi (63) $H^+/Ca^{2+}$ exchangers have been cloned, however, functional characterization is limited to CAXs from the model plant *A. thalina* (64,65). The NCX and NCKX are almost exclusively composed of sequences with animal origins and have been well characterized functionally (9). So far the 24 metazoan originating sequences from the final CaCA group lack sufficient molecular characterization, and have been temporarily named CCX until further information on substrate specificities is available (59).

Encompassing a diverse group of members from all three domains of life – Archaea, Bacteria, and Eukarya – the CaCA family is defined by both functional and sequence similarities that provide insight into the molecular evolution of the family. Functionally, the CaCA family utilizes the inwardly directed electrochemical gradient of cations ($Na^+$, $H^+$, or $K^+$) to transport $Ca^{2+}$ against its electrochemical gradient in a tightly

coupled process. Overall sequence similarity within the CaCA family is low, however, the family does possess conserved α-repeats in the TMS (23). In addition, members of the CaCA family display similar hydrophobicity plots (8) and have between 9 and 11 putative TMS (59). The intramolecular homology of YRBG from *E. coli* extends beyond the α-repeats to include two homologous hydrophobic clusters of 5 TMS with opposite orientations in the membrane (61). The presence of intramolecular homology and relative conservation of TMS throughout the CaCA family suggests its members arose from an ancient intragenic gene duplication event in which a primordial 5-6 TMS protein encoding gene duplicated internally to give one encoding a protein with twice the number of TMS (1). To date, no primodial 'half' exchanger has been found and it appears that – at least for NCX – both the N- and C- terminal hydrophobic domains are required for proper membrane trafficking and function (66) (but also see Gabellini *et al* (67), Li and Lytton (68) and Van Eylen *et al* (69) for an alternative view).

The residue size and relative number of each CaCA homolog within a species also gives clues to the evolution of the CaCA family. The bacterial and archaea members of the CaCA family are only ~half the size of their eukaryotic homologs which is consistent with other transport membrane proteins (70). The size disparity is due to the presence of a central hydrophilic domain (~200-550 residues) in eukaryote CaCA members, linking the N- and C-terminal hydrophobic domains. This cytoplasmic loop is poorly conserved between CaCA groups (59) and is not required for ion transport (66,71). Instead, it is thought that the hydrophilic loop evolved within CaCA subfamilies to gain specific regulatory functions and alternative splice variant capability (8). In addition, eukaryotes have more exchanger isoforms within a species compared with prokaryotes (59), consistent with the idea that eukaryotic gene families expanded through gene duplication and divergence. These facts suggest that the gene duplication event giving rise to the CaCA family occurred before the split of the three domains of life, or that horizontal gene transfer occurred between these domains (72). The NCX group is one of these families that have evolved independently to become a prominent $Ca^{2+}$ exchanger in animals.

## 1.4 NCX Molecular Biology

### 1.4.1 Overall Topology

Historically, molecular studies involving the NCX have lagged due to the relatively low abundance and lability of the exchanger. The molecular investigation of the NCX was greatly facilitated with the cloning and expression of the NCX from the canine heart (NCX1.1) in 1990 (19). A clear topological structure of NCX is beginning to emerge as previous models are tested and reworked with new methods. The most current NCX topology is based on the findings of Iwamoto *et al* (73) and Nicoll *et al* (19) and is shown in Figure 1.

The NCX protein varies in size anywhere from 880 to 970 residues, depending on the isoform, with a deduced molecular weight of ~108 kDa. Initial purification of native NCX from cardiac sarcolemma and subsequent SDS-PAGE identified proteins of 70, 120, and 160 kDa, with the smallest thought to be a proteolytic fragment (74). NCX undergoes several post translational modifications which account for the disparity between the deduced and actual molecular weight of the protein. The first TMS or ~32 residues comprise a signal peptide that is cleaved during initial processing in the endoplasmic reticulum (75,76). The N-terminus of the mature protein is extracellular and glycosylated at an asparagine residue, giving the NCX an apparent molecular weight of 120 kDa (76). An extracellular disulfide bond has been shown to exist between cysteines in the N-terminus and the extracellular loop between TMS 6-7 (77). Under non-reducing gel conditions, the NCX runs as a single band with an apparent molecular weight of 160 kDa (74). Cleavage of the signal peptide (78,79), glycosylation (76), and disulfide bond formation (80) do not appear to be functionally important according to current NCX assay methods.

Initial hydropathy analysis of NCX, indicated a mature protein with 12 TMS (19). More recent studies using epitope-specific antibodies and sulfhydryl modification of substituted cysteines indicates nine putative TMS organized in N and C-terminal hydrophobic domains of 5 and 4 TMS, respectively (73,80,81). Within the hydrophobic domains are the α-1 and α-2 repeats, which and are important for ion translocation (82) and define NCX as a member of the CaCA family (8). These repeats are on opposite

sides of the membrane with α-1 spanning TMS 2 and 3 and α-2 spanning TMS 8 and 9. The intracellular loop spanning the hydrophobic domains comprises more than half the protein and contains sites important for $Ca^{2+}$ regulation, $Na^{+}$-dependent inactivation and alternative splicing (see below for more detailed discussion of these regions and their contribution to NCX function). So far, little information on NCX tertiary structure is available, although Qui *et al* (83) found the helix packing of TMSs 2, 3, 7 and 8 is such that the α-repeats may be aligned in tertiary space.

Some groups have shown exchange activity in truncated NCX proteins lacking the C-terminal portion of the protein (67-69). These investigators proposed that dimerization of the N-terminal TMS region can form a functional exchanger. However, according to the current topological model, this type of arrangement would place both α-regions facing the extracellular side. Ottolia *et al* (66) refuted this possibility by showing that the C-terminal TMS domain is required for proper expression and exchange function and Kasir *et al* (84) demonstrated that constructs with truncations up to the last TMS of NCX do not express.

### 1.4.2 NCX Gene Family

The NCX family (also SLC8A) contains three separate gene products, NCX1 (19), NCX2 (21), and NCX3 (20). It appears that two sequential gene replication events gave rise to the three NCX genes however, the evolutionary timeframe of these replications is unknown. The early evolutionary emergence of NCX predicts that all metazoans should express some exchanger isoform. So far, most cloned NCX genes are from mammalian origins; however, NCX1 orthologs have been cloned and characterized from lower vertebrates such as trout (22) and frog (85), and NCX homologs have been cloned from the invertebrate *Drosophila* (23,86), squid (24) and *C. elegans* (87). In addition, no NCX2 or NCX3 orthologs have been found in non-mammalian species leading to the hypothesis that non-mammalian exchangers diverged before mammalian exchangers split into NCX1, NCX2 and NCX3 (59). Phylogenetic analysis of the NCX family has been hindered by the lack of non-mammalian NCX sequences.

### 1.4.3 Gene Expression and Regulation

The three NCX family members display differential expression patterns in mammalian tissues. Of the three, NCX1 expression has been the most highly characterized, where it has been found in virtually all tissues including heart, brain, kidney, spleen, liver, pancreas, skeletal muscle, smooth muscle and intestine (13). NCX1 mRNA quantities in these tissues have a high degree of variability, exhibiting a 100-fold difference in the highest level expression (heart), to the lowest (liver) (14). Differential expression of the NCX1 gene is directed by three alternative 5'untranslated exons, which are under the control of tissue specific promoters (88-90). The cardiac specific promoter, designated H1, is controlled by a minimum promoter region and two GATA sites (90,91) and is sufficient to direct NCX1 expression in the neonate, adult, and failing heart (92). The K1 promoter has a typical TATA box and regulates expression in the kidney, whereas the GC rich Br1 promoter regulates expression in the brain and low-level expression in other tissues (88,90). Less is known of the regulation of NCX2 and NCX3, which are found exclusively in brain and skeletal muscle (13,20,89).

### 1.4.4 Gene Structure

The human chromosomal location of all three NCX genes has been determined, with NCX1 (93), NCX2 (94), and NCX3 (95) having gene loci of 2p23-p22, 19q13.3, 14q24.1, respectively. The NCX1 gene is organized into 12 exons, with the first exon being a 5'-untranslated region and the last containing a long 3'-untranslated region (87). For all three isoforms, the start codon is in exon 2 which is unusually long (~1.8 kb) and encodes two thirds of the protein (87). Exons 3-8 comprise a relatively small piece of the full coding transcript (~330 bp) and are alternatively spliced in a tissue specific manner. NCX2 and NCX3 have a total of 9 exons, missing the homologs to NCX1 exons 6-8 (only 102 bp) in the alternative splice region. In mammalian isoforms, the exon boundaries of all three NCX genes are identical, except that the long coding exon 2 found in NCX1 and NCX3 is split into three exons in NCX2 (21,87,95). The protein products of all three NCX genes display ~70% identity, which rises to greater than 80% in the TMS (20). To date, no major functional differences have been found to exist between NCX gene products using techniques currently available for NCX assays (96,97).

### 1.4.5 Alternative Splicing

In addition to having three separate gene products under alternative promoter control, tissue specific expression of NCX is further diversified through alternative splicing (13,89,98). NCX splice variants arise from different combinations of exons 3-8, which encode a region in the C-terminal portion of the large intracellular loop as shown in Figure 2. This relatively small region is also known as the alternative splice region and the spliced exons are commonly known as A-F, instead of 3-8. Exons A and B are mutually exclusive but all splice variants must express either one of these exons to maintain an open reading frame (99). To express splice variants in a tissue specific manner, exons A and B are used in combination with cassette exons C-F (98). Of the 32 possible combinations exons A-F can confer, at least 15 NCX1 splice variants have been detected to date for the NCX1 gene (Table 1). In general, excitable tissues (e.g. heart, brain, skeletal muscle) express exon A, whereas splicing variants with exon B predominate in other tissues (e.g. kidney) (13). In addition, all NCX1 splice variants contain the 6-mer, exon D; however, no functional role for this exon has been proposed. In mammals, the NCX1 isoform predominating in cardiac muscle uses the exon combination of ACDEF, and is designated NCX1.1. This cardiac specific variant is conserved in an NCX1 ortholog cloned from frog heart (85) and similar to one cloned from trout heart (NCX-TR1.0) (22). Trout NCX-TR1.0 appears to lack exon E, expressing instead the exon combination of ACDF. Similar to exon D, the physiological role of exon E, which is only five amino acids in length, is not known.

Alternative splicing is less extensive in NCX2 and NCX3, which contain a 34 residue deletion in this region equivalent to NCX1 exons D, E, and F (Table 1). NCX2 expresses only exons A and C as no alternative splicing of NCX2 has been detected to date (13). Conversely, four splice variants of NCX3 have been identified in brain and skeletal muscle (13,95). NCX3.4, found in skeletal muscle, reportedly lacks exons from the alternative splice region, causing a frameshift and premature stop codon downstream in exon 6 (95). This truncated NCX3 isoform is missing about a third of the coding sequence, including part of the intracellular loop and all of the C-terminal TMS domain. Whether the NCX3.4 gene produces a functional exchanger is not known.

The physiological significance of NCX alternative splicing remains unclear as deletion mutants have shown it is not essential for ion transport (71). Potential roles of the region including modulation of NCX current through PKA sensitivity (100,101), $Ca^{2+}$-dependent activation (100,102), and $Na^{+}$ inactivation (102,103) have been suggested. Interestingly, there are more functional differences apparent amongst alternatively spliced isoforms of the same NCX gene than there are between NCX genes. This is the case even in invertebrate NCX isoforms, in which two different splice variants of the *Drosophila* CALX display different ionic regulation (104). It has therefore been proposed that the structural complexity of the NCX gene allows it to respond independently to unique ionic environments and exchange demands in a tissue or cell specific manner (89). More sensitive and physiological relevant NCX assays should provide insight into the functional diversity and differences of NCX alternative splicing, since such small changes in sequence likely evolved to serve some physiological purpose.

## 1.5 NCX Structure and Function

### 1.5.1 Transport Mechanism and Kinetics

The NCX exchange cycle can be described as separate movements of $Na^{+}$ and $Ca^{2+}$ ions through the exchanger in a consecutive or 'ping pong mechanism' (105-108) similar to that described for the $Na^{+}$-$K^{+}$ ATPase (109). A schematic of this mechanism is shown in Figure 3. According to the consecutive model, $Na^{+}/Ca^{2+}$ movement must involve common routes in which the ion binding sites are alternatively exposed to each side of the membrane (110). For example, $Ca^{2+}$ ions bind the exchanger from the intracellular side and are transported by a conformational change across the membrane. After dissociation of the $Ca^{2+}$ ions, $Na^{+}$ ions are free to bind and are translocated to the intracellular side of the membrane, completing a cycle. As previously mentioned, this ion exchange is reversible as the NCX can operate in either $Ca^{2+}$ efflux or $Ca^{2+}$ influx modes (more commonly known as forward and reverse modes, respectively). The NCX can also operate in $Na^{+}/Na^{+}$ and $Ca^{2+}/Ca^{2+}$ exchange modes in the absence of $Ca^{2+}$ and $Na^{+}$, respectively (111-113). However, these latter forms of transport do not produce a

net movement of ions and NCX shows no detectable conductance when $Na^+$ is present without $Ca^{2+}$, and visa versa (25,106).

Modelling the $Na^+/Ca^{2+}$ exchange cycle has proven difficult, as it is not yet clear how the net charge transfer occurs at various stages of the cycle since the pathway involves many steps. Voltage analysis suggests a model in which $Na^+$-bound species are positively charged while the $Ca^{2+}$-bound species is 'electroneutral' indicating that the 'unloaded' cation-binding domain carries two negative charges (114,115). Using electrophysiological techniques, charge movements have been used to measure 'half reaction cycles'. These studies have shown that the binding of $Na^+$ or $Ca^{2+}$ is a weakly voltage sensitive process and the rate-limiting step is the transfer of the charge carrying intermediate (tentatively attributed to the $Na^+$ half cycle) (106,108). This is again consistent with two negative charges crossing the membrane during an exchange cycle. It is estimated that the fully activated NCX is capable of a maximal turnover rate of 5000 $s^{-1}$ (106,115); however, this rate is probably more like ~300-500 $s^{-1}$ under physiological conditions (52). Interestingly, He *et al* (24) showed that the charge movement in squid NCX-SQ1 gave the opposite result of mammalian NCX1. Using half reaction cycles, it was shown that $Na^+$ transport is less electrogenic, while $Ca^{2+}$ transport is more electrogenic for NCX-SQ1. Evidently, more than two negative charges must move into the membrane electrical field when $Ca^{2+}$ is occluded by the NCX-SQ1 from the cytoplasmic side. It has been suggested that $Ca^{2+}$ transport is rate-limiting in the NCX-SQ1, and not $Na^+$ transport as in NCX1 (24).

Currently there exists some controversy over the actual stoichiometry of $Na^+/Ca^{2+}$ exchange, which may not be as rigidly fixed as once thought. A ratio of $3Na^+:1Ca^{2+}$ has been suggested by $Ca^{2+}$ flux studies (116) and comparison of nifedipine-sensitive $Ca^{2+}$ current with NCX inward current (117). These results are supported in a variety of studies using multiple isoforms and measurement techniques (118-122); whereas others (10,11) indicate an exchange ratio closer to $4Na^+:1Ca^{2+}$ using current voltage potentials. A recent study by Kang and Hilgemann (12) suggests that the discrepancy in stoichiometry lies in the NCX having multiple transport modes. Using an ion-selective electrode to quantify ion flux, they showed a ratio of ~3.2 $Na^+:1Ca^{2+}$ for maximal transport in either direction. Kang and Hilgemann (12) propose a new $Na^+/Ca^{2+}$

exchange transport model in which NCX can transport one $Ca^{2+}$ for one $Na^{+}$ at a low rate in addition to the normal transport of one $Ca^{2+}$ for three $Na^{+}$.

#### 1.5.1.1 Ion Translocation and the α-repeats

The molecular determinants of the $Na^{+}/Ca^{2+}$ transport mechanism has been greatly facilitated though mutational analysis of the α-repeat regions shown in Figure 4. The α-1 and α-2 repeats display intramolecular homology (23) and consist of 37 and 33 residues, respectively. The α-repeats have been remodelled in recent years to be located on opposite sites of the membrane (73,80) and facing each other in a helix packing model (83). In addition, loops that connect TMS 2 and 3 at the extracellular surface and TMS 7 and 8 at the cytosolic surface are thought to be asymmetric re-entrant loops that are aligned in 3D topology (73,80). Together with the immediate surrounding TMS, the α-repeats are central to the $Na^{+}/Ca^{2+}$ translocation and are thus extremely sensitive to mutation, especially the acidic (glutamate and aspartate), polar (threonine, serine, asparagine), and flexible (glycine, proline, alanine) groups of amino acids (8,81,123).

There are several conserved acidic residues in the α-repeats and surrounding TMS. E148 in TMS2 and D849 in TMS7 (using human NCX1.1 from start codon GI 10863913 as reference) are completely conserved throughout the CaCA family (59) and are absolutely required for NCX ion translocation function (123). TMS 2 has an additional conserved glutamate at position 155, which would place the charged residue on the same side of the helix as E148. Mutational studies have shown that mutation of E155 reduces NCX activity by 50% (123). TMS 3 lacks the presence of charged amino acids, but the proximal end of the re-entrant loop between TMS 7 and 8 has two conserved aspartate residues at positions 860 and 864. The aspartate located at position 860 is very sensitive to mutation, but D864 is not (8). These conserved acidic residues throughout the region are likely involved in neutralizing the positive charges of $Na^{+}$ and $Ca^{2+}$, thereby allowing transport of the cations through the membrane (59).

In addition to negatively charged residues, the α-repeats and surrounding TMS have a number of conserved polar amino acids. In TMS2, 3, and 7, the polar residues are spaced at regular intervals of 3-4 residues, making these helices amphipathic. Sensitivity

of the NCX to mutation of these polar residues varies. In the α-1 region, S144, S145, S174 and N178 are very sensitive to mutation whereas mutation of T138 and S152 do not alter NCX activity (123,124). Similarly, mutation of T845, S846, S853 and S873 in the α-2 region abolish NCX function, whereas T871 and N874 are not sensitive to mutation (123). The pairs of neighbouring polar residues in TMS 2 (S144, S145) and TMS 7 (T845, S846) that are essential to NCX function, may be in proximity according to the helix packing model of Qui *et al* (83). These residues, in conjunction with other polar residues, may help coordinate cation binding or provide the hydrophilic environment necessary for ion translocation (59).

The α-repeat regions and surrounding TMS are also rich in conserved glycine and proline residues. The α-1 region has 3 proline and 2 glycine residues that are conserved across all species and isoforms. These residues do not appear to be absolutely required for ion translocation, but not all have been tested. In contrast, the α-2 region has 1 conserved proline and 5 conserved glycine residues, with the glycines at positions 845, 881, and 883 being sensitive to mutation. The latter two glycine residues flank a G(I/L)G sequence that is similar to the GYG motif in the P-loop of $K^+$ channels (125). However, other than being a tight turn within the re-entrant loop, this motif in NCX has not been shown to have any functional significance. The presence of proline residues in the middle of TMS 2 and 7 may induce 'kinks' in the helix that allow the appropriate structural geometry for NCX function. An alternative theory postulates that prolines within TMS of membrane proteins promote folding by disfavouring the formation of a misfolded structure (126). The glycine residues may provide the structural flexibility needed for the conformational changes that occur upon ion binding and translocation (59).

It should be noted that most of the mutations mentioned above are in the TMS of the α-repeats. Recent mutational analysis has confirmed that mutations in the TMS of α-1 are important for ion translocation but the proposed re-entrant loops do not appear sensitive to mutation (124).

### 1.5.2 Regulation of NCX

NCX function is dynamically modulated by many factors including stimulation by alkalosis (127), ATP (25,113), PIP2 (128,129), proteinase treatment (130), phospholipases (131), reducing agents (DTT) (132); and inhibition by acidosis (127), XIP (133), inorganic cations (134) and isothiourea derivatives (135,136). In addition to being substrates, $Na^+$ and $Ca^{2+}$ have their own autoregulatory effects on NCX currents collectively referred to as I1 inactivation and I2 modulation, respectively. This regulation arises from the intracellular loop since deletion of the loop abolishes allosteric regulation of NCX activity by intracellular $Na^+$ and $Ca^{2+}$ (71). Not all of the aforementioned factors are within the scope of this thesis and hence the following discussion will be limited to NCX modulation by the lipid bilayer, followed by the effects of $Ca^{2+}$ and $Na^+$ on exchanger function.

#### 1.5.2.1 Lipid Bilayer Composition

$Na^+/Ca^{2+}$ exchange is very sensitive to alteration of the lipid bilayer as shown by the reconstitution of purified NCX into liposomes of varying lipid composition. Increase of negative charge through reconstitution of acidic phospholipids (e.g. phosphatidylserine) (137), addition of exogenous negatively charged amphiphiles (e.g. SDS) (138), or phospholipase cleavage (131) can greatly stimulate NCX. In addition, incorporation of cholesterol greatly facilitates $Na^+/Ca^{2+}$ exchange with an optimal reconstituted lipid environment being 30% phosphatidylcholine, 50% phosphatidylserine, and 20% cholesterol (137,139). Conversely, NCX reconstitution into membranes rich in phosphatidylinositol and phosphatidylglycerol showed diminished exchange (137). Some anionic head groups were found to have a greater stimulatory effect than others (e.g. lauryl sulfate > dodecyl sulfonate > lauric acid) whereas cationic lauryl derivatives (dodecylamine, dodecyltrimethylamine, laurylcholine) were found to be potent inhibitors of $Na^+/Ca^{2+}$ exchange (138). It was also shown that modulation of NCX by amphiphiles was dependent on alkyl chain length as the longer the chain (i.e. more hydrophobic), the greater the stimulatory or inhibitiory effect on $Na^+/Ca^{2+}$ exchange. Presumably more hydrophobic amphiphiles embed in the membrane lipid bilayer where they can mimic phosopholipids and modulate exchange (138). Regardless, the stimulatory effects of a

negatively charged membrane are not due to an altered membrane surface potential since Bers *et al* (140) showed that NCX function is unaffected by changes in surface charge or surface $Ca^{2+}$ concentrations. Thus it is likely that negatively charged amphiphiles enhance NCX function through an interaction with the protein itself.

#### 1.5.2.2 $Ca^{2+}$ Regulation

Early studies showed stimulation of NCX current by intracellular $Ca^{2+}$ (141-143) suggesting regulatory $Ca^{2+}$ was required for exchange activity. This regulatory calcium is not translocated, but rather activates the exchanger upon binding a region in the intracellular loop. α-chymotrypsin treatment eliminates $Ca^{2+}$-dependent activation of NCX outward currents in giant excised patches (71). Measurements of $Ca^{2+}$ affinities in excised patches yielded $K_d$ values of 0.1-0.3 μM, giving little physiological relevance to the sites since they would always be saturated *in situ* (8). Other studies indicate higher affinities in intact myocytes (~20-50 nM) (143) and when expressing only the $Ca^{2+}$-binding domain (~140 nM) (144) meaning the exchanger would be activated upon elevated cytosolic $Ca^{2+}$ concentrations during muscle contraction.

The NCX $Ca^{2+}$ binding region does not resemble other known $Ca^{2+}$ binding sites. Ottolia *et al* (144) expressed the $Ca^{2+}$-binding domain linked with yellow and cyan fluorescent proteins at the N- and C-termini, respectively. Using FRET efficiency measurements, the $Ca^{2+}$-binding domain was shown to 'open' upon $Ca^{2+}$ binding (144). Expressed in myocytes, changes in FRET were observed upon contraction suggesting that NCX is regulated by fluctuations of $Ca^{2+}$ concentration in EC-coupling.

A high affinity $Ca^{2+}$ binding region of 130 residues in length was identified by Levitsky *et al* (145) in the centre of the intracellular (or f) loop. This region has two neighbouring acidic sites of 9 and 12 residues. Each site begins with three consecutive aspartates and is separated by ~35 residues. Mutations in this region – especially the first trio of aspartates in each site – do not effect ion translocation, but do alter $Ca^{2+}$ binding and regulatory properties (146). The region shows high identity across NCX isoforms, and $Ca^{2+}$-dependent activation has been demonstrated in NCX paralogs (96) and orthologs (24). An interesting exception occurs in *Drosophila* CALX where regulatory

$Ca^{2+}$ has the opposite effect and decreases NCX activity (147). This result is indicative of $Ca^{2+}$ binding having an allosteric effect on another area of the exchanger, since the binding sites themselves have high amino acid identity (148). Supporting this idea, a six residue deletion mutant ~180 residues downstream of the $Ca^{2+}$ binding region abolishes regulation by $Ca^{2+}$ (149,150).

#### 1.5.2.3 $Na^+$ Regulation

NCX outward current partially decays to a steady state level in a time dependent manner analogous to that of ion channels (25). This process is exponential and is referred to as $Na^+$-dependent, or I1, inactivation. The physiological significance of $Na^+$-dependent inactivation is unclear since it is only prominent at concentrations of intracellular $Na^+$ (i.e. >30 mM) that are unlikely to be attained during normal conditions (52). The exchanger does not appear to have a regulatory $Na^+$ binding site separate from the translocation sites as is the case with $Ca^{2+}$ binding (8). Rather, inactivation is modelled as a two step process in which $Na^+$ ions bind the transport site at the intracellular surface and can either be transported or induce a state of inactivation (151). $Na^+$-dependent inactivation in excised patches is absent in the presence of high concentrations of regulatory $Ca^{2+}$ (10 μM) (8) and after chymotrypsin treatment (25,152).

The region responsible for $Na^+$-dependent inactivation is attributed to the XIP site, located in the intracellular loop immediately distal to TMS5. This site is 20 residues in length, including 8 basic residues interspersed with hydrophobic residues, and resembles a calmodulin binding domain (133). XIP is short for e*X*changer *I*nhibitory *P*eptide, so named because a peptide with the same sequence is a relatively potent inhibitor of the NCX (133). The inhibitory action of the peptide is non-competitive with $Na^+$ and $Ca^{2+}$ binding and acts at the cytoplasmic surface. Based on these observations the endogenous XIP region of NCX was postulated to have an autoinhibitory effect on ion translocation. Subsequent mutational analysis of the XIP region confirmed that the region does not effect ion translocation per se, but rather has modulating effects on $Na^+$-dependent inactivation (153,154). Some substitutions decreased or even eliminated $Na^+$-dependent inactivation (K229Q, mature canine NCX1.1), while others increased the rate of inactivation (F223E and Y226T). Using synthetic peptides, He *et al* (154) showed the

aromatic (F223 and Y224) and basic residues (R230 and R232) are important for full XIP inhibition of NCX. $Na^+$-dependent inactivation has been demonstrated in different NCX genes (96) and in NCX from different species including squid (24) and fly (147). However, the XIP site shows relatively low evolutionary conservation compared to other regions of the NCX, which could potentially be due to $Na^+$-dependent inactivation not involving the binding of $Na^+$ directly to the XIP site. The XIP site likely interacts with other regions of the intracellular loop to alter the inactivation process. For example, a five residue deletion mutant ~180 residues downstream of the $Ca^{2+}$ binding region abolishes allosteric regulation by $Na^+$ (149,150) implicating this region in the ionic regulation of NCX.

## 1.6 NCX temperature dependence

The temperature dependence of proteins can be quantitatively measured using several parameters. Two of these measures, temperature coefficient ($Q_{10}$) and Energy of Activation ($E_{act}$), are used in these studies to quantify NCX temperature dependence. $Q_{10}$ values reflect the fold change in protein activity for a 10 °C (10 K) change in temperature, or in this case the rate of ion exchange for NCX. The Eact is proportional to $Q_{10}$ and in a typical chemical reaction is defined as the minimal energy required for a reaction to occur or rate-governing activation barrier to a chemical reaction. In the context of our experiments, the physical basis of $E_{act}$ is an estimation of the minimum energy needed for an ion translocation event in NCX to occur. The $E_{act}$ was determined in this study from the slope of an Arrhenius plot, in which the logarithm of either peak or steady-state current was plotted against the inverse of temperature in Kelvin.

Active transporters, such as NCX1.1, involved in ion translocation in the mammalian heart are highly temperature dependent. Despite this, data on the temperature dependence of the NCX1 are somewhat limited. It has been demonstrated that the $Q_{10}$ (fold change in activity for a 10 °C change in temperature) for NCX1.1 is in the range of 2.2 to 4.0 in mammals (151,155). Cardiac function in teleost species such as rainbow trout (*Oncorhynchus mykiss*) is distinguished by its ability to maintain adequate contractility under hypothermic conditions that are cardioplegic to mammals. To account for this phenomenon, it is very likely that some of the proteins involved in E-C coupling

have evolved differently in teleost species (156). $Na^+/Ca^{2+}$ exchange in trout sarcolemmal vesicles show that more than 75% of NCX activity is maintained after reducing the temperature from 21 to 7 °C, whereas NCX activity in canine vesicles is diminished to <10% (44). This result is also observed when both the canine and trout NCX proteins are reconstituted into asolectin vesicles, indicating that potential differences in membrane compositions between species do not explain the observed findings in NCX temperature dependence. Tibbits *et al* (44) measured the energy of activation values to be 62 kJ/mol for canine NCX and only 7 kJ/mol for trout NCX. A similar study using mammalian and amphibian native vesicles measured energy of activation values for NCX activity to be 58 kJ/mol and 25 kJ/mol, respectively (157). The same study also found that reconstitution into artificial lipid vesicles had little effect on the temperature dependence of $Na^+/Ca^{2+}$ exchange velocity. Using immunoblots of trout sarcolemma probed with antibodies raised against canine NCX cDNA, Tibbits *et al* (44) showed a similar pattern of banding compared with immunoblots of mammalian SL. They also found similarities in electrogenicity and stimulation by chymotrypsin treatment between canine and trout NCX. Together, these studies suggest that the differential temperature dependencies between isoforms reflect the intrinsic properties of the exchanger, rather than properties of the lipid environment. Differences in the primary structure between isoforms is likely responsible for their respective temperature sensitivities.

## 1.7 General Adaptation of Proteins to Temperature

The study of protein adaptation to temperature has garnered a lot of attention over the years since it encompasses a broad spectrum of disciplines from protein structure and function to protein evolution. Orthologous proteins of organisms living over a range of environmental temperatures do not employ special mechanisms to maintain function. Rather, subtle redistributions of the same intramolecular interactions confer the appropriate stability or flexibility that allow proteins to function in warm or cold environments. The fact that homologs can maintain function at extreme temperatures is a testament to the extraordinary plasticity available in the 20 amino acids that make up all proteins. There have been myriad recent papers attempting to uncover a molecular

consensus of protein temperature adaptation (see references (158-161) for reviews). Recent advances in computational biology combined with the ever increasing availability of genomic data have complemented traditional laboratory methods and led to significant advances in the field (162-164). A quick search of the subject on PUBMED yields over 800 articles published within the last 5 years.

The majority, but not all, of temperature adaptation studies have focused on proteins derived from prokaryotes that have adapted to live in extreme environments. These 'extremophiles' have proven useful comparative models because of their small genome size and large range of optimal growth temperature. Studies have ranged from the functional comparison of extremophile orthologs (165-169) to structural comparisons of extremophile orthologs (170-172) to comparative genomics and proteomics (162-164,173-175). To date, there is no consensus as to which molecular mechanisms are responsible for allowing proteins to function at extreme temperatures; however, general trends present in the above studies that afford stability in thermophilic proteins include: 1) a decrease in uncharged non-polar residues (especially glutamine and threonine, but also serine); 2) an increase in charged residues (glutamate, aspartate, lysine, arginine, histidine) and therefore ion pairs or salt bridges; 3) an increase in residue hydrophobicity and hydrogen bonding and 4) deletions of surface loops and an overall smaller protein size. All of these modifications are thought to increase the stability of thermophilic proteins, thereby allowing them to function at higher temperatures. The reverse is true for cold-adapted proteins where maintaining conformational flexibility is important for protein function at low temperatures. So far, no cold or warm adaptive protein has been found that displays all of these features. Rather proteins use combinations of these mechanisms to confer the necessary balance between stability and flexibility needed for protein function to occur at an organism's body temperature (161).

Traditional laboratory and new computational methods both have their caveats. Traditional methods rely on the functional comparison of a few proteins, and therefore lack the data necessary to make a consensus statement regarding which amino acids are important in temperature adaptation. The reverse is true for computational methods, which tend to treat whole proteomes in an indiscriminate manner while lacking hypothesis driven data and tangible evidence. It has been suggested that psychrophilic,

mesophilic, and thermophilic prokaryotes can be distinguished by their relative compositions of hydrophobic residues, charged residues, and non-charged polar amino acids (162,176,177) However, these observed trends across genomes may not apply to single proteins. In addition, both methods have failed to obtain specific data on the temperature adaptations of membrane proteins. Almost all studies using functional data to investigate protein temperature adaptation have dealt with soluble proteins, or in the case of comparative proteomics, have failed to treat soluble and membrane proteins differently in their analysis. Because of this, the study of temperature adaptation in membrane proteins has lagged behind. This is due, in part, to the fact that despite membrane proteins may account for up to 30% of an organism's proteome, only 3% of known 3D structures are of membrane proteins (178). This disparity reflects problems of overexpression and crystallization of membrane proteins as well as not knowing how to computationally treat them differently. These caveats advocate the study of membrane protein temperature dependence on a case-by-case basis, preferably using orthologs that are highly conserved.

## 1.8 Thesis Overview

The specific goal of this project is to elucidate the molecular determinants of NCX temperature dependence. However, in a broader context, a unifying theme present throughout is how NCX temperature sensitivity offers insight into the function of the exchanger in general. The approach we have used is multidisciplinary in nature, combining traditional molecular biology techniques such as mutagenesis and chimera studies, with electrophysiology and bioinformatic analyses, including comparative genomics, phylogenetics, and sequence analysis. Temperature is used as a probe to link phenotypic responses with genotypic differences amongst NCX homologs, chimeras and mutants. Interpretation of these results highlights NCX residues potentially important for conferring the necessary flexibility or stability to operate over a range of temperatures. These results are not only applicable to the mechanism of ion translocation in NCX, but can be generally applied to the temperature dependence of all membrane proteins.

The middle chapters of this thesis consist of studies presented roughly in the order in which they were completed. Each chapter represents a separate and self contained set

of experiments complete with methods, results, and discussion. Chapters 2, 3, 5 and 6 are original published research articles, whereas the data in chapter 4 are unpublished at this time. Chapter 2 is a study that highlights the differences in cloned trout and mammalian NCX isoforms with respect to temperature dependence. The trout NCX-TR1.0 was shown to be significantly less sensitive to changes in temperature compared to canine NCX1.1, despite a high overall identity of ~75% at the amino acid level. It was also found that this differential temperature dependence existing between isoforms was an intrinsic property of each protein, and further was not due to potential differences in transport regulation. Chapter 3 attempts to elucidate the molecular determinants underlying the differential temperature dependence of NCX isoforms using a chimeric approach. Using trout-dog NCX chimeras, it was shown that the region responsible for NCX temperature dependence is solely attributable to the N-terminal TMS domain. This region contains the first five TMS up to the end of the XIP site, composing approximately the first quarter of the mature protein. Chapter 4 consists of unpublished data and is an expansion of the previous chapter. Continuing with the chimeric approach, four new chimeras show that each region within in the N-terminal TMS domain is important for NCX temperature dependence. To supplement the chimeric data, the temperature dependence phenotypes of NCX isoforms from other ectotherms – fruit fly CALX and squid NCX-SQ1 – were recorded and compared to trout NCX-TR1.0 and dog NCX1.1. A multiple sequence alignment of these species showed high conservation within the TMS, but many non-conserved residue positions throughout the N-terminal region. Taken together, these results indicate that a series of mutations throughout the N-terminal TMS domain are responsible for NCX temperature dependence. From these results it was evident that a more comprehensive sequence analysis was needed, meaning an expansion of available NCX sequences and subsequent clarification of NCX phylogeny. With this in mind, Chapter 5 addresses the molecular evolution and phylogeny of NCX. Data mining of whole genomes provided 13 new NCX sequences that were added to the already available sequences in GenBank. As expected, multiple sequence alignments showed high conservation in regions known for NCX function and regulation. Data mining of genomes uncovered multiple NCX isoforms from lower vertebrate species, indicating that at least two NCX gene duplications occurred before the divergence of

vertebrates. In addition a putative fourth member of the NCX gene family was found only in fish species suggesting a separate gene duplication event after the divergence of fishes from the rest of the vertebrates. Chapter 6 describes the cloning and characterization of NCX from the *Oreochromis mossambicus*, or Mozambique tilapia. Our motivation was to obtain the temperature phenotype of a species that was more closely related to trout NCX-TR1.0, since our current comparative model – dog NCX1.1 – is ~450 million years removed from teleost species. The tilapia has recently gained prominence in both aquaculture and in the laboratory since it is a fast growing and environmentally robust fish. Most importantly for this study, the tilapia is capable of living at temperatures even greater than mammalian core temperatures of ~37 °C. Thus, tilapia cardiac proteins such as the NCX have adapted to live at temperatures that are lethal to trout providing an excellent comparative model to study NCX temperature dependence. Cloning of an NCX isoform from the tilapia heart yielded an NCX1 isoform named NCX-TL1.0 with ~80% identity to trout NCX-TR1.0 and similar functional and regulatory properties. However, in response to decreasing temperature, tilapia NCX-TL1.0 behaved very different than trout NCX-TR1.0 displaying mammalian-like temperature dependence. A comparison of sequences in the N-terminal domain highlighted ten residues common to tilapia NCX-TL1.0 and dog NCX1.1 that may be involved in NCX temperature sensitivity. Finally, Chapter 7 incorporates the main findings of each chapter to draw a general conclusion of NCX temperature dependence and the significance and applicability of the results, and suggests future studies.

## 1.9 Tables

**Table 1:** Summary of Alternatively Spliced Isoforms of NCX1, NCX2, and NCX3

| Splice Variant | Exons |
|---|---|
| NCX1.1 | ACDEF |
| NCX1.2 | BCD |
| NCX1.3 | BD |
| NCX1.4 | AD |
| NCX1.5 | ADF |
| NCX1.6 | ACD |
| NCX1.7 | BDF |
| NCX1.8 | ACDE |
| NCX1.9 | BDE |
| NCX1.10 | BDEF |
| NCX1.11 | BCDEF |
| NCX1.12 | ADEF |
| NCX1.13 | BCDE |
| NCX1.14 | ACDF |
| NCX1.15 | BCDF |
| NCX2.1 | AC |
| NCX3.1 | AC |
| NCX3.2 | B |
| NCX3.3 | BC |
| NCX3.4 | none |

## 1.10 Figures

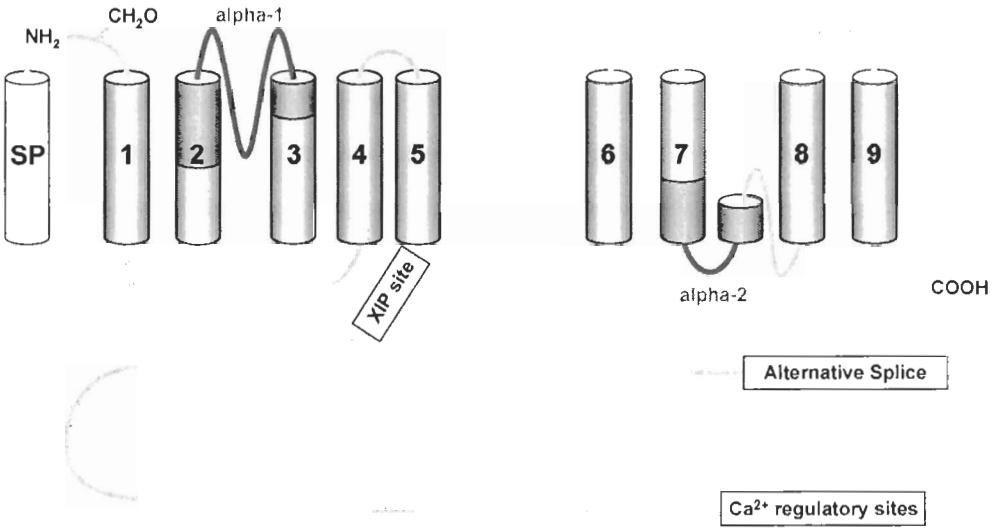


**Figure 1**

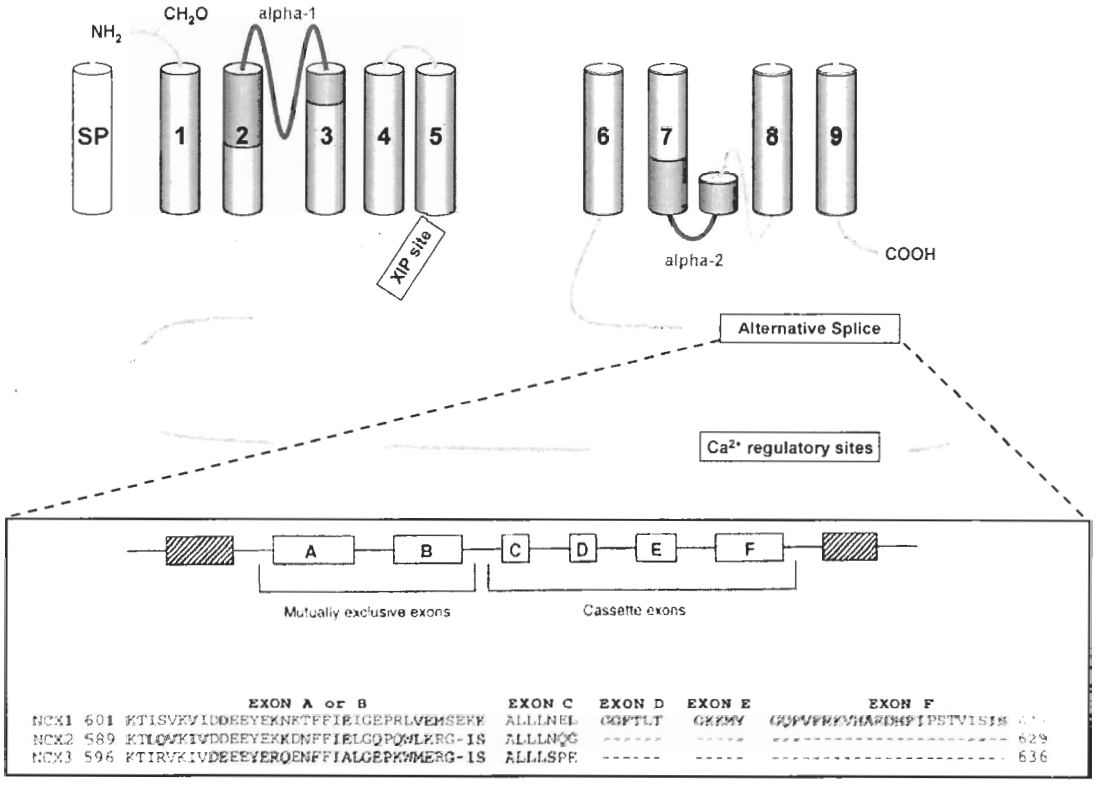
NH2
CH2O
alpha-1
SP
1
2
3
4
5
6
7
8
9
XIP site
alpha-2
COOH
Alternative Splice
Ca2+ regulatory sites
A
B
C
D
E
F
Mutually exclusive exons
Cassette exons
EXON A or B
EXON C
EXON D
EXON E
EXON F
NCX1 601 KTISVKVIDDEEYEKNKTFFIEIGEPRLVEMSEKE ALLLNEL QGPTLT GKKMV
NCX2 589 KILQVKIVDDEEYEKKDNFFIELGQPQWLKRG-IS ALLLNQG
NCX3 596 KTIRVKIVDEEEYERQENFFIALGEPKWMERG-IS ALLLSPE

**Figure 2**

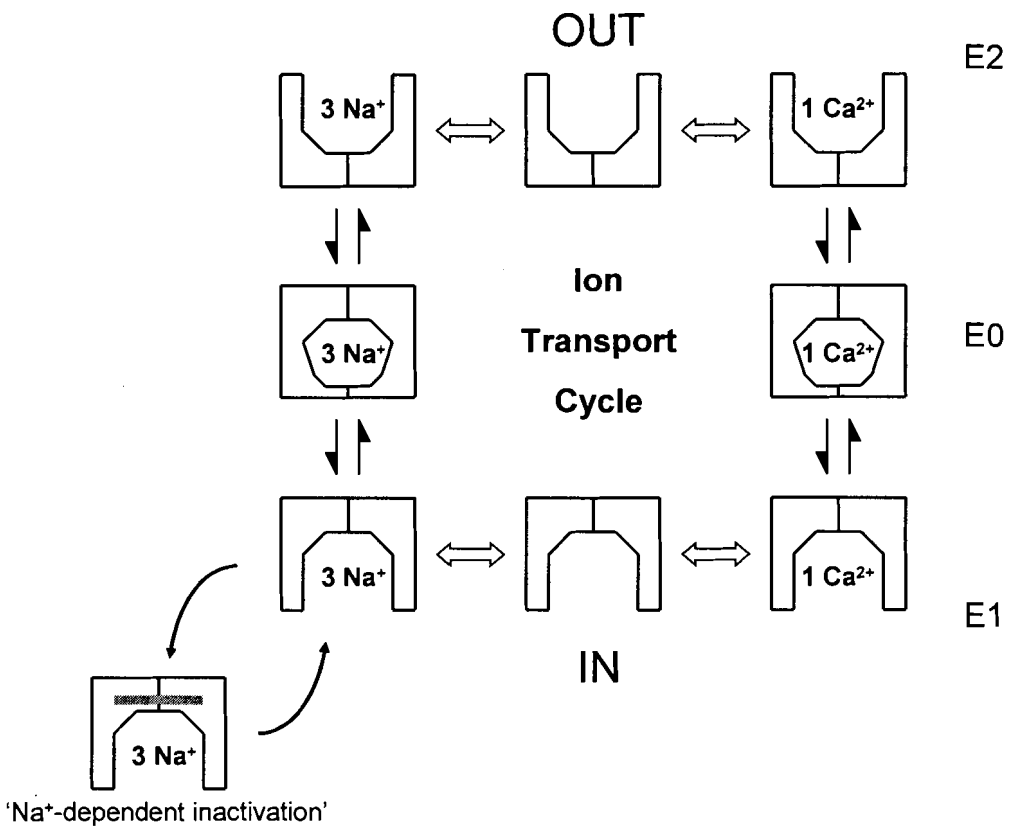
OUT
E2
3 Na+
1 Ca2+
Ion
Transport
Cycle
3 Na+
1 Ca2+
E0
3 Na+
1 Ca2+
E1
IN
3 Na+
'Na+-dependent inactivation'

**Figure 3**

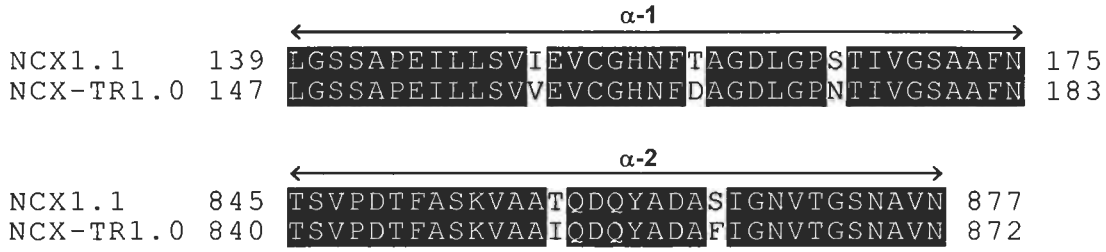
α-1
NCX1.1 139 LGSSAPEILLSVIEVCGHNFTAGDLGPSTIVGSAAFN 175
NCX-TR1.0 147 LGSSAPEILLSVVEVCGHNFDAGDLGPNTIVGSAAFN 183
α-2
NCX1.1 845 TSVPDTFASKVAATQDQYADASIGNVTGSNAVN 877
NCX-TR1.0 840 TSVPDTFASKVAAIQDQYADAFIGNVTGSNAVN 872

**Figure 4**

## 1.11 Figure Legends

**Figure 1: Current Topology of the $Na^+/Ca^{2+}$ Exchanger**
Based on the models of Nicoll *et al* (80) and Iwamoto *et al* (73) the NCX is currently modelled to have nine transmembrane spanning segments (TMS) with five in the N-terminal domain separated from four in the C-terminal domain by a large intracellular loop. TMS are depicted as numbered *grey cylinders* with a *hollow cylinder* representing the signal peptide (SP) that is cleaved during initial processing. *Dark grey* shading within the cylinders shows the alpha-1 and alpha-2 repeats located in the N- and C-terminal TMS domains, respectively. The alpha repeats have intra-molecular homology and are important for ion translocation. The large intra-cellular loop separating the N- and C-terminal TMS domains contains regions important for regulatory function such as the e*X*changer *I*nhibitory *P*eptide (XIP) site and $Ca^{2+}$ binding regions. In addition, the distal portion of the intracellular loop has an alternative splice region (see Figure 2 for more details).

**Figure 2: The Alternative Splice Region of the $Na^+/Ca^{2+}$ Exchanger**
The top panel shows the topological model of NCX as described in Figure 1. The intracellular loop contains an alternative splice region, which is shown in more detail below the topological model. Adapted from Quednau *et al* (13), the lower panel shows the genomic organization of the NCX1 gene along with the amino acid sequence of the exons A-F from the NCX1, NCX2, and NCX3 gene family. Exons A and B are mutually exclusive and are expressed in combination with exons C-F to create alternatively spliced NCX isoforms (see Table 1). NCX2 and NCX3 lack cassette exons D, E and F. Exon A is shown for NCX1 and NCX2, while exon B is shown for NCX3.

**Figure 3: $Na^+/Ca^{2+}$ Exchange Cycle**
Hypothetical $Na^+/Ca^{2+}$ exchange cycle based on the minimal consecutive model of Hilgemann (115). In the E1 state, the cation binding sites of NCX are exposed to the intracellular surface and can bind either $3Na^+$ or $1Ca^{2+}$. Upon binding, the exchanger enters a transition state (E0) where the cations are occluded and allowed to pass through the hydrophobic lipid bilayer. In E2 state, the binding pocket of NCX is exposed to the extracellular surface and the cation released. At this point, a half reaction cycle has occurred and the binding site is free to bind either $3Na^+$ or $1Ca^{2+}$ and transport the cation through the membrane to the cytosolic space. When $3Na^+$ are bound to the E1 state, the exchanger can enter an inactive state as depicted by the reaction in the lower left corner.

**Figure 4: Sequence alignment of the α-1 and α-2 regions**
Sequence alignments are shown for the α-1 (*top*) and α-2 (*bottom*) regions of the canine NCX1.1 and trout NCX-TR1.0. Shading denotes complete identity and numbers are from the start codon. α-1 is located in the N-terminal TMS domain and α-2 is located in the C-terminal TMS domain.

## 1.12 References


1. Saier, M. H., Jr. (2003) *Mol Microbiol* **48**, 1145-1156
2. Busch, W., and Saier, M. H., Jr. (2003) *Methods Mol Biol* **227**, 21-36
3. White, P. J., and Broadley, M. R. (2003) *Ann Bot (Lond)* **92**, 487-511
4. Berridge, M. J., Lipp, P., and Bootman, M. D. (2000) *Nat Rev Mol Cell Biol* **1**, 11-21
5. Moreno, S. N., and Docampo, R. (2003) *Curr Opin Microbiol* **6**, 359-364
6. Norris, V., Grant, S., Freestone, P., Canvin, J., Sheikh, F. N., Toth, I., Trinei, M., Modha, K., and Norman, R. I. (1996) *J Bacteriol* **178**, 3677-3682
7. Macrez, N., and Mironneau, J. (2004) *Curr Mol Med* 4, 263-275
8. Philipson, K. D., and Nicoll, D. A. (2000) *Annu Rev Physiol* **62**, 111-133
9. Blaustein, M. P., and Lederer, W. J. (1999) *Physiol Rev* **79**, 763-854
10. Dong, H., Dunn, J., and Lytton, J. (2002) *Biophys J* **82**, 1943-1952
11. Fujioka, Y., Komeda, M., and Matsuoka, S. (2000) *J Physiol* **523 Pt 2**, 339-351
12. Kang, T. M., and Hilgemann, D. W. (2004) *Nature* **427**, 544-548
13. Quednau, B. D., Nicoll, D. A., and Philipson, K. D. (1997) *Am J Physiol* **272**, C1250-1261
14. Kofuji, P., Hadley, R. W., Kieval, R. S., Lederer, W. J., and Schulze, D. H. (1992) *Am J Physiol* **263**, C1241-1249
15. Choi, D. W. (2005) *Nature* **433**, 696-698
16. Bano, D., Young, K. W., Guerin, C. J., Lefeuvre, R., Rothwell, N. J., Naldini, L., Rizzuto, R., Carafoli, E., and Nicotera, P. (2005) *Cell* **120**, 275-285
17. Danilczyk, U., and Penninger, J. (2004) *Nat Med* **10**, 1163-1164
18. Iwamoto, T., Kita, S., Zhang, J., Blaustein, M. P., Arai, Y., Yoshida, S., Wakimoto, K., Komuro, I., and Katsuragi, T. (2004) *Nat Med* **10**, 1193-1199
19. Nicoll, D. A., Longoni, S., and Philipson, K. D. (1990) *Science* **250**, 562-565
20. Nicoll, D. A., Quednau, B. D., Qui, Z., Xia, Y. R., Lusis, A. J., and Philipson, K. D. (1996) *J Biol Chem* **271**, 24914-24921
21. Li, Z., Matsuoka, S., Hryshko, L. V., Nicoll, D. A., Bersohn, M. M., Burke, E. P., Lifton, R. P., and Philipson, K. D. (1994) *J Biol Chem* **269**, 17434-17439
22. Xue, X. H., Hryshko, L. V., Nicoll, D. A., Philipson, K. D., and Tibbits, G. F. (1999) *Am J Physiol* **277**, C693-700
23. Schwarz, E. M., and Benzer, S. (1997) *Proc Natl Acad Sci U S A* **94**, 10249-10254

24. He, Z., Tong, Q., Quednau, B. D., Philipson, K. D., and Hilgemann, D. W. (1998) *J Gen Physiol* **111**, 857-873

25. Hilgemann, D. W. (1990) *Nature* **344**, 242-245

26. Bers, D. M. (2002) *Nature* **415**, 198-205

27. Hilgemann, D. W. (2004) *Am J Physiol Cell Physiol* **287**, C1167-1172

28. Hryshko, L. V., and Philipson, K. D. (1997) *Basic Res Cardiol* **92**, 45-51

29. Pogwizd, S. M., Schlotthauer, K., Li, L., Yuan, W., and Bers, D. M. (2001) *Circ Res* **88**, 1159-1167

30. Pogwizd, S. M., and Bers, D. M. (2004) *Trends Cardiovasc Med* **14**, 61-66

31. Sipido, K. R., Volders, P. G., Schoenmakers, M., De Groot, S. H., Verdonck, F., and Vos, M. A. (2002) *Ann N Y Acad Sci* **976**, 438-445

32. Kusuoka, H., Camilion de Hurtado, M. C., and Marban, E. (1993) *J Am Coll Cardiol* **21**, 240-248

33. Imahashi, K., Kusuoka, H., Hashimoto, K., Yoshioka, J., Yamaguchi, H., and Nishimura, T. (1999) *Circ Res* **84**, 1401-1406

34. Reuter, H., and Seitz, N. (1968) *J Physiol (Lond)* **195**, 451-470

35. Sham, J. S., Hatem, S. N., and Morad, M. (1995) *J Physiol (Lond)* **488**, 623-631

36. Bassani, J. W., Bassani, R. A., and Bers, D. M. (1994) *J Physiol* **476**, 279-293

37. Bassani, R. A., Bassani, J. W., and Bers, D. M. (1994) *J Physiol* **476**, 295-308

38. Bassani, R. A., and Bassani, J. W. (2002) *Am J Physiol Heart Circ Physiol* **282**, H2406-2413

39. Pieske, B., Maier, L. S., Bers, D. M., and Hasenfuss, G. (1999) *Circ Res* **85**, 38-46

40. O'Rourke, B., Kass, D. A., Tomaselli, G. F., Kaab, S., Tunin, R., and Marban, E. (1999) *Circ Res* **84**, 562-570

41. Puglisi, J. L., Bassani, R. A., Bassani, J. W., Amin, J. N., and Bers, D. M. (1996) *Am J Physiol* **270**, H1772-1778

42. Li, L., Chu, G., Kranias, E. G., and Bers, D. M. (1998) *Am J Physiol* **274**, H1335-1347

43. Tibbits, G. F., Kashihara, H., Thomas, M. J., Keen, J. E., and Farrell, A. P. (1990) *American Journal of Physiology* **259**, R453-460

44. Tibbits, G. F., Philipson, K. D., and Kashihara, H. (1992) *Am J Physiol* **262**, C411-417

45. Hove-Madsen, L., Llach, A., and Tort, L. (2000) *Am J Physiol Regul Integr Comp Physiol* **279**, R1856-1864

46. Artman, M., Ichikawa, H., Avkiran, M., and Coetzee, W. A. (1995) *Am J Physiol* **268**, H1714-1722

47. Haddock, P. S., Coetzee, W. A., and Artman, M. (1997) *Am J Physiol* **273**, H837-846

48. Qu, Y., Ghatpande, A., el-Sherif, N., and Boutjdir, M. (2000) *Cardiovasc Res* **45**, 866-873

49. Boerth, S. R., Zimmer, D. B., and Artman, M. (1994) *Circ Res* **74**, 354-359.

50. Reinecke, H., Studer, R., Vetter, R., Holtz, J., and Drexler, H. (1996) *Cardiovasc Res* **31**, 48-54

51. Studer, R., Reinecke, H., Bilger, J., Eschenhagen, T., Bohm, M., Hasenfuss, G., Just, H., Holtz, J., and Drexler, H. (1994) *Circ Res* **75**, 443-453

52. Bers, D. M. (2001) *Excitation-Contraction Coupling and Cardiac Contractile Force*, Second Edition Ed., Kluwer Academic Publishers

53. Levi, A. J., Spitzer, K. W., Kohmoto, O., and Bridge, J. H. (1994) *Am J Physiol* **266**, H1422-1433

54. Litwin, S. E., Li, J., and Bridge, J. H. (1998) *Biophys J* **75**, 359-371

55. Wasserstrom, J. A., and Vites, A. M. (1996) *J Physiol* **493 ( Pt 2)**, 529-542

56. Leblanc, N., and Hume, J. R. (1990) *Science* **248**, 372-376

57. Sipido, K. R., Maes, M., and Van de Werf, F. (1997) *Circ Res* **81**, 1034-1044

58. Sham, J. S., Cleemann, L., and Morad, M. (1992) *Science* **255**, 850-853

59. Cai, X., and Lytton, J. (2004) *Mol Biol Evol* **21**, 1692-1703

60. Ruknudin, A., and Schulze, D. H. (2002) *Ann N Y Acad Sci* **976**, 103-108

61. Saaf, A., Baars, L., and von Heijne, G. (2001) *J Biol Chem* **276**, 18905-18907

62. Ivey, D. M., Guffanti, A. A., Zemsky, J., Pinner, E., Karpel, R., Padan, E., Schuldiner, S., and Krulwich, T. A. (1993) *J Biol Chem* **268**, 11296-11303

63. Cunningham, K. W., and Fink, G. R. (1996) *Mol Cell Biol* **16**, 2226-2237

64. Hirschi, K. D., Zhen, R. G., Cunningham, K. W., Rea, P. A., and Fink, G. R. (1996) *Proc Natl Acad Sci U S A* **93**, 8782-8786

65. Cheng, N. H., Pittman, J. K., Shigaki, T., and Hirschi, K. D. (2002) *Plant Physiol* **128**, 1245-1254

66. Ottolia, M., John, S., Qiu, Z., and Philipson, K. D. (2001) *J Biol Chem* **276**, 19603-19609.

67. Gabellini, N., Zatti, A., Rispoli, G., Navangione, A., and Carafoli, E. (1996) *Eur J Biochem* **239**, 897-904

68. Li, X. F., and Lytton, J. (1999) *J Biol Chem* **274**, 8153-8160

69. Van Eylen, F., Kamagate, A., and Herchuelz, A. (2001) *Cell Calcium* **30**, 191-198

70. Chung, Y. J., Krueger, C., Metzgar, D., and Saier, M. H., Jr. (2001) *J Bacteriol* **183**, 1012-1021

71. Matsuoka, S., Nicoll, D. A., Reilly, R. F., Hilgemann, D. W., and Philipson, K. D. (1993) *Proc Natl Acad Sci U S A* **90**, 3870-3874.

72. Saier, M. H., Jr., Eng, B. H., Fard, S., Garg, J., Haggerty, D. A., Hutchinson, W. J., Jack, D. L., Lai, E. C., Liu, H. J., Nusinew, D. P., Omar, A. M., Pao, S. S., Paulsen, I. T., Quan, J. A., Sliwinski, M., Tseng, T. T., Wachi, S., and Young, G. B. (1999) *Biochim Biophys Acta* **1422**, 1-56

73. Iwamoto, T., Nakamura, T. Y., Pan, Y., Uehara, A., Imanaga, I., and Shigekawa, M. (1999) *FEBS Lett* **446**, 264-268

74. Philipson, K. D., Longoni, S., and Ward, R. (1988) *Biochim Biophys Acta* **945**, 298-306

75. Durkin, J. T., Ahrens, D. C., Pan, Y. C., and Reeves, J. P. (1991) *Arch Biochem Biophys* **290**, 369-375

76. Hryshko, L. V., Nicoll, D. A., Weiss, J. N., and Philipson, K. D. (1993) *Biochim Biophys Acta* **1151**, 35-42

77. Santacruz-Toloza, L., Ottolia, M., Nicoll, D. A., and Philipson, K. D. (2000) *J Biol Chem* **275**, 182-188

78. Furman, I., Cook, O., Kasir, J., Low, W., and Rahamimoff, H. (1995) *J Biol Chem* **270**, 19120-19127

79. Sahin-Toth, M., Nicoll, D. A., Frank, J. S., Philipson, K. D., and Friedlander, M. (1995) *Biochem Biophys Res Commun* **212**, 968-974

80. Nicoll, D. A., Ottolia, M., Lu, L., Lu, Y., and Philipson, K. D. (1999) *J Biol Chem* **274**, 910-917

81. Doering, A. E., Nicoll, D. A., Lu, Y., Lu, L., Weiss, J. N., and Philipson, K. D. (1998) *J Biol Chem* **273**, 778-783

82. Nicoll, D. A., Hryshko, L. V., Matsuoka, S., Frank, J. S., and Philipson, K. D. (1996) *Ann N Y Acad Sci* **779**, 86-92

83. Qiu, Z., Nicoll, D. A., and Philipson, K. D. (2001) *J Biol Chem* **276**, 194-199.

84. Kasir, J., Ren, X., Furman, I., and Rahamimoff, H. (1999) *J Biol Chem* **274**, 24873-24880

85. Iwata, T., Kraev, A., Guerini, D., and Carafoli, E. (1996) *Ann N Y Acad Sci* **779**, 37-45

86. Ruknudin, A., Valdivia, C., Kofuji, P., Lederer, W. J., and Schulze, D. H. (1997) *Am J Physiol* **273**, C257-265

87. Kraev, A., Chumakov, I., and Carafoli, E. (1996) *Genomics* **37**, 105-112

88. Barnes, K. V., Cheng, G., Dawson, M. M., and Menick, D. R. (1997) *J Biol Chem* **272**, 11510-11517

89. Lee, S. L., Yu, A. S., and Lytton, J. (1994) *J Biol Chem* **269**, 14849-14852

90. Nicholas, S. B., Yang, W., Lee, S. L., Zhu, H., Philipson, K. D., and Lytton, J. (1998) *Am J Physiol* **274**, H217-232

91. Nicholas, S. B., and Philipson, K. D. (1999) *Am J Physiol* **277**, H324-330

92. Muller, J. G., Isomatsu, Y., Koushik, S. V., O'Quinn, M., Xu, L., Kappler, C. S., Hapke, E., Zile, M. R., Conway, S. J., and Menick, D. R. (2002) *Circ Res* **90**, 158-164

93. Shieh, B. H., Xia, Y., Sparkes, R. S., Klisak, I., Lusis, A. J., Nicoll, D. A., and Philipson, K. D. (1992) *Genomics* **12**, 616-617

94. Kikuno, R., Nagase, T., Ishikawa, K., Hirosawa, M., Miyajima, N., Tanaka, A., Kotani, H., Nomura, N., and Ohara, O. (1999) *DNA Res* **6**, 197-205

95. Gabellini, N., Bortoluzzi, S., Danieli, G. A., and Carafoli, E. (2002) *Gene* **298**, 1-7

96. Linck, B., Qiu, Z., He, Z., Tong, Q., Hilgemann, D. W., and Philipson, K. D. (1998) *Am J Physiol* **274**, C415-423

97. Iwamoto, T., and Shigekawa, M. (1998) *Am J Physiol* **275**, C423-430

98. Kofuji, P., Lederer, W. J., and Schulze, D. H. (1994) *J Biol Chem* **269**, 5145-5149

99. Schulze, D. H., Kofuji, P., Valdivia, C., He, S., Luo, S., Ruknudin, A., Wisel, S., Kirby, M. S., duBell, W., and Lederer, W. J. (1996) *Ann N Y Acad Sci* **779**, 46-57

100. Ruknudin, A., He, S., Lederer, W. J., and Schulze, D. H. (2000) *J Physiol* **529 Pt 3**, 599-610

101. Schulze, D. H., Polumuri, S. K., Gille, T., and Ruknudin, A. (2002) *Ann N Y Acad Sci* **976**, 187-196

102. Dyck, C., Omelchenko, A., Elias, C. L., Quednau, B. D., Philipson, K. D., Hnatowich, M., and Hryshko, L. V. (1999) *J Gen Physiol* **114**, 701-711

103. Maack, C., Ganesan, A., Sidor, A., and O'Rourke, B. (2005) *Circ Res* **96**, 91-99

104. Omelchenko, A., Dyck, C., Hnatowich, M., Buchko, J., Nicoll, D. A., Philipson, K. D., and Hryshko, L. V. (1998) *J Gen Physiol* **111**, 691-702

105. Khananshvili, D. (1991) *Ann N Y Acad Sci* **639**, 85-95

106. Hilgemann, D. W., Nicoll, D. A., and Philipson, K. D. (1991) *Nature* **352**, 715-718

107. Matsuoka, S., and Hilgemann, D. W. (1992) *J Gen Physiol* **100**, 963-1001

108. Niggli, E., and Lederer, W. J. (1991) *Nature* **349**, 621-624

109. Goldshlegger, R., Karlish, S. J., Rephaeli, A., and Stein, W. D. (1987) *J Physiol* **387**, 331-355.

110. Khananshvili, D., Weil-Maslansky, E., and Baazov, D. (1996) *Ann N Y Acad Sci* **779**, 217-235.

111. Philipson, K. D., and Nishimoto, A. Y. (1981) *J Biol Chem* **256**, 3698-3702

112. Slaughter, R. S., Sutko, J. L., and Reeves, J. P. (1983) *J Biol Chem* **258**, 3183-3190

113. DiPolo, R., and Beauge, L. (1987) *J Gen Physiol* **90**, 505-525

114. Khananshvili, D. (1991) *J Biol Chem* **266**, 13764-13769

115. Hilgemann, D. W. (1996) *Biophys J* **71**, 759-768

116. Reeves, J. P., and Hale, C. C. (1984) *J Biol Chem* **259**, 7733-7739

117. Bridge, J. H., Smolley, J. R., and Spitzer, K. W. (1990) *Science* **248**, 376-378

118. Blaustein, M. P. (1984) *Soc Gen Physiol Ser* **38**, 129-147

119. Caputo, C., Bezanilla, F., and DiPolo, R. (1989) *Biochim Biophys Acta* **986**, 250-256

120. Crespo, L. M., Grantham, C. J., and Cannell, M. B. (1990) *Nature* **345**, 618-621

121. Rasgado-Flores, H., and Blaustein, M. P. (1987) *Am J Physiol* **252**, C499-504

122. Hinata, M., Yamamura, H., Li, L., Watanabe, Y., Watano, T., Imaizumi, Y., and Kimura, J. (2002) *J Physiol* **545**, 453-461

123. Nicoll, D. A., Hryshko, L. V., Matsuoka, S., Frank, J. S., and Philipson, K. D. (1996) *Journal of Biological Chemistry* **271**, 13385-13391

124. Ottolia, M., Nicoll, D. A., and Philipson, K. D. (2005) *J Biol Chem* **280**, 1061-1069

125. Doyle, D. A., Morais Cabral, J., Pfuetzner, R. A., Kuo, A., Gulbis, J. M., Cohen, S. L., Chait, B. T., and MacKinnon, R. (1998) *Science* **280**, 69-77

126. Wigley, W. C., Corboy, M. J., Cutler, T. D., Thibodeau, P. H., Oldan, J., Lee, M. G., Rizo, J., Hunt, J. F., and Thomas, P. J. (2002) *Nat Struct Biol* **9**, 381-388

127. Philipson, K. D., Bersohn, M. M., and Nishimoto, A. Y. (1982) *Circ Res* **50**, 287-293

128. Hilgemann, D. W., and Ball, R. (1996) *Science* **273**, 956-959

129. He, Z., Feng, S., Tong, Q., Hilgemann, D. W., and Philipson, K. D. (2000) *Am J Physiol Cell Physiol* **278**, C661-666.

130. Philipson, K. D., and Nishimoto, A. Y. (1982) *Am J Physiol* **243**, C191-195

131. Philipson, K. D., and Nishimoto, A. Y. (1984) *J Biol Chem* **259**, 16-19

132. Reeves, J. P., Bailey, C. A., and Hale, C. C. (1986) *J Biol Chem* **261**, 4948-4955

133. Li, Z., Nicoll, D. A., Collins, A., Hilgemann, D. W., Filoteo, A. G., Penniston, J. T., Weiss, J. N., Tomich, J. M., and Philipson, K. D. (1991) *J Biol Chem* **266**, 1014-1020

134. Bers, D. M., Philipson, K. D., and Nishimoto, A. Y. (1980) *Biochim Biophys Acta* **601**, 358-371

135. Matsuda, T., Arakawa, N., Takuma, K., Kishida, Y., Kawasaki, Y., Sakaue, M., Takahashi, K., Takahashi, T., Suzuki, T., Ota, T., Hamano-Takahashi, A., Onishi, M., Tanaka, Y., Kameo, K., and Baba, A. (2001) *J Pharmacol Exp Ther* **298**, 249-256

136. Watano, T., Kimura, J., Morita, T., and Nakanishi, H. (1996) *Br J Pharmacol* **119**, 555-563

137. Vemuri, R., and Philipson, K. D. (1988) *Biochim Biophys Acta* **937**, 258-268

138. Philipson, K. D. (1984) *J Biol Chem* **259**, 13999-14002

139. Vemuri, R., and Philipson, K. D. (1989) *J Biol Chem* **264**, 8680-8685

140. Bers, D. M., Philipson, K. D., and Peskoff, A. (1985) *J Membr Biol* **85**, 251-261

141. DiPolo, R. (1979) *J Gen Physiol* **73**, 91-113

142. Reeves, J. P., and Poronnik, P. (1987) *Am J Physiol* **252**, C17-23

143. Miura, Y., and Kimura, J. (1989) *J Gen Physiol* **93**, 1129-1145

144. Ottolia, M., Philipson, K. D., and John, S. (2004) *Biophys J* **87**, 899-906

145. Levitsky, D. O., Nicoll, D. A., and Philipson, K. D. (1994) *J Biol Chem* **269**, 22847-22852

146. Matsuoka, S., Nicoll, D. A., Hryshko, L. V., Levitsky, D. O., Weiss, J. N., and Philipson, K. D. (1995) *J Gen Physiol* **105**, 403-420

147. Hryshko, L. V., Matsuoka, S., Nicoll, D. A., Weiss, J. N., Schwarz, E. M., Benzer, S., and Philipson, K. D. (1996) *J Gen Physiol* **108**, 67-74

148. Dyck, C., Maxwell, K., Buchko, J., Trac, M., Omelchenko, A., Hnatowich, M., and Hryshko, L. V. (1998) *J Biol Chem* **273**, 12981-12987.

149. Weber, C. R., Ginsburg, K. S., Philipson, K. D., Shannon, T. R., and Bers, D. M. (2001) *J Gen Physiol* **117**, 119-131.

150. Maxwell, K., Scott, J., Omelchenko, A., Lukas, A., Lu, L., Lu, Y., Hnatowich, M., Philipson, K. D., and Hryshko, L. V. (1999) *Am J Physiol* **277**, H2212-2221

151. Hilgemann, D. W., Matsuoka, S., Nagel, G. A., and Collins, A. (1992) *J Gen Physiol* **100**, 905-932

152. Matsuoka, S., and Hilgemann, D. W. (1994) *J Physiol (Lond)* **476**, 443-458

153. Matsuoka, S., Nicoll, D. A., He, Z., and Philipson, K. D. (1997) *J Gen Physiol* **109**, 273-286

154. He, Z., Petesch, N., Voges, K., Roben, W., and Philipson, K. D. (1997) *J Membr Biol* **156**, 149-156

155. Kimura, J., Miyamae, S., and Noma, A. (1987) *J Physiol (Lond)* **384**, 199-222

156. Tibbits, G., CD Moyes and L. Hove-Madsen. (1992) in *Fish Physiology* (Randall, D., AP Farrell, ed) Vol. XIIA, pp. 267-304, Academic Press

157. Bersohn, M. M., Vemuri, R., Schuil, D. W., Weiss, R. S., and Philipson, K. D. (1991) *Biochimica et Biophysica Acta* **1062**, 19-23

158. D'Amico, S., Claverie, P., Collins, T., Georlette, D., Gratia, E., Hoyoux, A., Meuwis, M. A., Feller, G., and Gerday, C. (2002) *Philos Trans R Soc Lond B Biol Sci* **357**, 917-925

159. Fields, P. A. (2001) *Comp Biochem Physiol A Mol Integr Physiol* **129**, 417-431

160. Sheridan, P. P., Panasik, N., Coombs, J. M., and Brenchley, J. E. (2000) *Biochim Biophys Acta* **1543**, 417-433.

161. Russell, N. J. (2000) *Extremophiles* **4**, 83-90.

162. Saunders, N. F., Thomas, T., Curmi, P. M., Mattick, J. S., Kuczek, E., Slade, R., Davis, J., Franzmann, P. D., Boone, D., Rusterholtz, K., Feldman, R., Gates, C., Bench, S., Sowers, K., Kadner, K., Aerts, A., Dehal, P., Detter, C., Glavina, T., Lucas, S., Richardson, P., Larimer, F., Hauser, L., Land, M., and Cavicchioli, R. (2003) *Genome Res* **13**, 1580-1588

163. Kreil, D. P., and Ouzounis, C. A. (2001) *Nucleic Acids Res* **29**, 1608-1615

164. Tekaia, F., Yeramian, E., and Dujon, B. (2002) *Gene* **297**, 51-60

165. Miyazaki, K., Wintrode, P. L., Grayling, R. A., Rubingh, D. N., and Arnold, F. H. (2000) *J Mol Biol* **297**, 1015-1026.

166. Wintrode, P. L., Miyazaki, K., and Arnold, F. H. (2000) *J Biol Chem* **275**, 31635-31640.

167. Svingor, A., Kardos, J., Hajdu, I., Nemeth, A., and Zavodszky, P. (2001) *J Biol Chem* **276**, 28121-28125.

168. Zavodszky, P., Kardos, J., Svingor, and Petsko, G. A. (1998) *Proc Natl Acad Sci U S A* **95**, 7406-7411

169. Fields, P. A., and Somero, G. N. (1998) *Proc Natl Acad Sci U S A* **95**, 11476-11481.

170. Russell, R. J., Gerike, U., Danson, M. J., Hough, D. W., and Taylor, G. L. (1998) *Structure* **6**, 351-361

171. Aghajari, N., Van Petegem, F., Villeret, V., Chessa, J. P., Gerday, C., Haser, R., and Van Beeumen, J. (2003) *Proteins* **50**, 636-647

172. Van Petegem, F., Collins, T., Meuwis, M. A., Gerday, C., Feller, G., and Van Beeumen, J. (2003) *J Biol Chem* **278**, 7531-7539

173. Haney, P. J., Badger, J. H., Buldak, G. L., Reich, C. I., Woese, C. R., and Olsen, G. J. (1999) *Proc Natl Acad Sci U S A* **96**, 3578-3583

174. Chakravarty, S., and Varadarajan, R. (2002) *Biochemistry* **41**, 8152-8161

175. Suhre, K., and Claverie, J. M. (2003) *J Biol Chem* **278**, 17198-17202

176. Haney, P. J., Stees, M., and Konisky, J. (1999) *J Biol Chem* **274**, 28453-28458

177. Chakravarty, S., and Varadarajan, R. (2000) *FEBS Lett* **470**, 65-69

178. Capener, C. E., Kim, H. J., Arinaminpathy, Y., and Sansom, M. S. (2002) *Hum Mol Genet* **11**, 2425-2433

# CHAPTER 2
# TEMPERATURE DEPENDENCE OF CLONED MAMMALIAN AND SALMONID CARDIAC $Na^+/Ca^{2+}$ EXCHANGER ISOFORMS*

Chadwick L. Elias[2,3], Xiao-Hua Xue[1,3], Christian R. Marshall[1], Alexander Omelchenko[2], Larry V. Hryshko[2], and Glen F. Tibbits[1]

[1] Cardiac Membrane Research Laboratory
Simon Fraser University
Burnaby, BC, Canada

[2] Institute of Cardiovascular Sciences
St. Boniface General Hospital Research Centre
The University of Manitoba
Winnipeg, MB, Canada

[3] These authors contributed equally to this study

* This study is published in the *American Journal of Physiology Cell Physiology* under the following reference: Elias C.L., Xue X.H., Marshall C.R., Omelchenko A., Hryshko L.V., and Tibbits G.F. (2001) *Am J Physiol Cell Physiol* **281**: C993-C1000. PMID: 11502576. Reproduced by permission.

## 2.1 Abstract

The cardiac $Na^+$-$Ca^{2+}$ exchanger (NCX), an important regulator of cytosolic $[Ca^{2+}]$ in contraction and relaxation, has been shown in trout heart sarcolemmal vesicles to have high activity at 7°C relative to its mammalian isoform and this unique property is likely due to differences in protein structure. In this study, outward NCX currents ($I_{NCX}$) of the wild type trout (NCX-TR1.0) and canine (NCX 1.1) exchangers expressed in oocytes were measured to explore the potential contributions of regulatory versus transport mechanisms to this observation. cRNA was transcribed in vitro from both wild type cDNA and injected into *Xenopus* oocytes. $I_{NCX}$ of NCX-TR1.0 and NCX1.1 were measured after 3-4 days over a temperature range of 7°C -30°C using the giant excised patch technique. The $I_{NCX}$ for both isoforms exhibited $Na^+$-dependent inactivation and $Ca^{2+}$-dependent positive regulation. The $I_{NCX}$ of NCX1.1 exhibited typical mammalian temperature sensitivities with $Q_{10}$ values of 2.4 and 2.6 for peak and steady-state currents, respectively. However, the $I_{NCX}$ of NCX-TR1.0 was relatively temperature insensitive with $Q_{10}$ values of 1.2 and 1.1 for peak and steady-state currents, respectively. $I_{NCX}$ current decay was fit with single exponential and the resultant rate constant of inactivation ($\lambda$) was determined as a function of temperature. As expected, $\lambda$ decreased monotonically with temperature for both isoforms. Although $\lambda$ was significantly greater in NCX1.1 compared to NCX-TR1.0 at all temperatures, the effect of temperature on $\lambda$ was not different between the two isoforms. These data suggest that the disparities in $I_{NCX}$ temperature dependence between these two exchanger isoforms are unlikely due to differences in their inactivation kinetics. In addition, similar differences in temperature dependence were observed in both isoforms after $\alpha$-chymotrypsin treatment that renders the exchanger in a deregulated state. These data suggest that the differences in $I_{NCX}$ temperature dependence between two isoforms are not due to potential disparities in either the $I_{NCX}$ regulatory mechanisms or structural differences in the cytoplasmic loop but are likely predicated on differences within the transmembrane segments.

## 2.2 Introduction

The plasma membrane integral protein $Na^+$-$Ca^{2+}$ exchanger (NCX) is crucial in cytosolic $Ca^{2+}$ concentration regulation in a variety of cells. The cardiac specific isoform of NCX in mammals (NCX1.1) is critical for mechanical relaxation as it serves as the prime mechanism of $Ca^{2+}$ extrusion from the cardiomyocyte (1, 2, 5). Additionally, it has been postulated that under certain physiological conditions NCX1.1 can operate in reverse mode, in which it contributes to cardiomyocyte $Ca^{2+}$ influx either through depolarization-induced $Ca^{2+}$ influx (18) and/or $Na^+$-current induced $Ca^{2+}$ influx (17). Thus the critical role that NCX1.1 plays in cardiac excitation-contraction (E-C) coupling is well documented.

Cardiac function in active salmonid species such as rainbow trout (*Oncorhynchus mykiss*) is distinguished by its ability to maintain adequate contractility under hypothermic conditions that are cardioplegic to mammals. Achieving this phenomenon poses interesting biological challenges as all of the crucial proteins involved in $Ca^{2+}$ regulation and E-C coupling in the mammalian heart are highly temperature dependent. For example, it has been demonstrated that the $Q_{10}$ (fold change in activity for a 10°C change in temperature) for NCX1.1 is in the range of 2.2 to 4.0 (11, 16). Thus it has been proposed that at least some of the proteins involved in E-C coupling have evolved differently in these species (32) in order to maintain cardiac function under hypothermia. It has been demonstrated in atrial myocytes that the trout NCX plays an important role in excitation-contraction coupling (12). Studies of $Na^+$-$Ca^{2+}$ exchange in trout heart sarcolemmal vesicles have demonstrated properties of this protein that are both unique and common to the mammalian NCX1.1 (33). Similarities include antigenicity, electrogenicity and stimulation by chymotrypsin treatment. Most obvious among the differences is that reducing the temperature from 21 to 7°C dramatically diminishes canine NCX1.1 activity to <10% of the initial level while in trout the activity remains >75% (33). This behavior of NCX was observed in both the native membranes and when the exchangers were reconstituted into asolectin vesicles. These data strongly suggest that the differential temperature dependencies in the mammalian and teleost NCX isoforms are due to differences in their primary structures.

To understand the molecular mechanisms of these differences, we recently cloned trout cardiac NCX and designated it NCX-TR1.0 (36). The NCX-TR1.0 cDNA has an open reading frame that codes for a protein of 968 amino acids with a deduced molecular mass of 108 kDa. Based on the hydropathy analysis and sequence identity, the topology of NCX-TR1.0 is predicted to be similar to that of mammalian NCX1.1, which is now modeled to have 9 transmembrane segments (13, 26). At the amino acid level, sequence comparison including the cleaved leader peptide showed ~75% identity to dog NCX1.1, 66% to rat NCX3, and 61% to rat NCX2. Like all NCXs, the sequence of NCX-TR1.0 shows the most divergence at the N-terminus (34). Sequence identity becomes very high (85%) within the putative transmembrane segments consistent with their functional significance in ion translocation (25). Furthermore, the $\alpha_1$ and $\alpha_2$ repeats within the transmembrane segments, which play a critical role in ion translocation (25) and are modeled to face one another (30), exhibit ~92 and 94% amino acid identity, respectively between these isoforms. Although the amino acid sequence of the intracellular loop of NCX-TR1.0 has only 73% identity overall with NCX1.1, those regions within the loop with known functional importance are well conserved. For example, the endogenous XIP site, consisting of 20 amino acids at the N-terminus of the loop, exhibits a high degree of conservation (17/20 identity with two conservative substitutions) and is critical for $Na^+$-dependent inactivation (19). The regulatory $Ca^{2+}$ binding domains are known to be highly conserved in a wide variety of species (7) including NCX-TR1.0 (~86-90%) (36) and the three consecutive aspartic acid residues characteristic of each of these domains are completely conserved in NCX-TR1.0.

In this study, we characterize in detail the temperature dependencies of the outward currents of trout NCX-TR1.0 and dog NCX1.1 expressed in *Xenopus* oocytes using the giant excised patch technique in order to elucidate the potential contributions of the regulatory domains versus transport mechanisms to temperature sensitivity.

## 2.3 Methods

### 2.3.1 Expression of $Na^+/Ca^{2+}$ Exchanger in *Xenopus* Oocytes

Dog NCX 1.1 and trout NCX-TR1.0 cDNAs were subcloned into modified pBluescript as described previously (36), and then linearized with Hind III. cRNA was synthesized using T3 mMessage mMachine™ In Vitro Transcription Kit (Ambion Inc., Austin, TX). Oocytes were prepared as described previously (20). Oocytes were injected with ~5 ng of cRNA and exchange activity was measured 3-4 days after injection as exchanger current (see below).

### 2.3.2 Assay of $Na^+$-$Ca^{2+}$ Exchange Activity

Outward $Na^+$-$Ca^{2+}$ exchange currents were measured using the giant excised patch technique, as described previously (28) to investigate the potential contributions of regulatory versus transport mechanisms to the differential temperature sensitivities in these two NCX isoforms. Borosilicate glass pipettes were pulled and polished to a final inner diameter of ~20-30 μm and coated with a Parafilm™:mineral oil mixture. The vitellin layer was removed and oocytes were placed in a solution containing (in mM): 100 KOH, 100 MES, 20 HEPES, 5 EGTA, 5 $MgCl_2$; pH 7.0 at room temperature with MES. Gigaohm seals were formed *via* suction and membrane patches (inside-out configuration) were excised by movements of the pipette tip. A computer-controlled, 20-channel solution switcher was used for rapid solution changes. Axon Instruments hardware and software were used for data acquisition and analysis. The pipette solution contained (in mM): 100 NMG-MES, 30 HEPES, 30 TEA-OH, 16 sulfamic acid, 8 $CaCO_3$, 6 KOH, 0.25 ouabain, 0.1 niflumic acid, 0.1 flufenamic acid; pH 7.0 with MES. Outward $Na^+$-$Ca^{2+}$ exchange currents were activated by switching from $Li^+_i$- to $Na^+_i$-based bath solutions containing (in mM): 100 [$Na^+$ or $Li^+$]-aspartate, 20 MOPS, 20 TEA-OH, 20 CsOH, 10 EGTA, 0-7.3 $CaCO_3$, 1.0-1.13 $Mg(OH)_2$; pH 7.0 with MES or LiOH. Magnesium and $Ca^{2+}$ were adjusted to yield free concentrations of 1.0 mM and 0, 1 or 10 μM, respectively, using MAXC software (3). All experiments were conducted first at room temperature (22-23 °C), and then exchange currents were measured at different temperatures (30, 14 and 7 °C) by heating or cooling bath solutions.

### 2.3.3 Data Analysis

All statistical data are shown as means ± SEM. All comparisons between mammalian and trout $Na^+$-$Ca^{2+}$ exchangers were made using unpaired, two-tailed Student's *t*-test. $P < 0.05$ was considered as significantly different.

## 2.4 Results

### 2.4.1 Exchange Currents of NCX-TR1.0 and NCX 1.1

We measured the outward $Na^+$-$Ca^{2+}$ exchange currents in giant patches excised from *Xenopus* oocytes expressing NCX 1.1 and NCX-TR1.0 (Fig.1). Currents were activated by the application of 100 mM $Na^+$ to the cytoplasmic surface of an excised patch of oocyte membrane. As indicated on the overlapping current traces, records were obtained at different concentrations of regulatory $Ca^{2+}$ (0, 1 and 10 μM) at the cytoplasmic surface. Outward $Na^+$-$Ca^{2+}$ exchange currents for both exchanger isoforms displayed similar characteristics. For both dog NCX1.1 and trout NCX-TR1.0 peak and steady-state outward currents were larger in the presence of regulatory $Ca^{2+}$ demonstrating positive regulation of exchange current by $Ca^{2+}{}_i$. Peak current at 10 μM $Ca^{2+}$ was less than at 1 μM $Ca^{2+}{}_i$ for both exchanger isoforms. In addition, both dog NCX1.1 and trout NCX-TR1.0 responded in a similar fashion to $Na^+{}_i$ application. The current increased to a peak value and then slowly decayed in a time dependent manner, indicative of $Na^+{}_i$-dependent inactivation (9).

### 2.4.2 Temperature Effect on Exchange Activity

We examined the temperature dependence of $Na^+$-$Ca^{2+}$ exchange current for the dog NCX1.1 and trout NCX-TR1.0 expressed in *Xenopus* oocytes. Figure 2a shows outward exchange currents activated by the rapid application of 100 mM $Na^+$ to the cytoplasmic surface of an excised patch of oocyte membrane in the presence of 1 μM regulatory $Ca^{2+}$ on the cytoplasmic side. At 30°C, the current properties of NCX1.1 and NCX-TR1.0 are similar. However, with decreasing temperature both peak and steady-state currents of NCX1.1 decreased. The same trend was observed in NCX-TR1.0, but to a much lesser degree. At 7°C, NCX 1.1 maintained about 10% of its peak and steady-

state currents measured at 30°C, while NCX-TR1.0 maintained ~60% of its activity (Fig. 2b and 2c).

Fig. 3 shows an Arrhenius plot of $Na^+$-$Ca^{2+}$ exchange peak and steady-state currents for the wild-type dog NCX1.1 and trout NCX-TR1.0. To allow statistical treatment of data obtained in different patches, each exchange current was normalized to that obtained at 30°C (~303°K). Therefore, the fitting function allowing estimation of the energy of activation, $E_{act}$, is given by the equation:

$$\ln\left(\frac{I}{I_{303}}\right) = -\frac{E_{act}}{R}\left(\frac{303 - T_i}{303 \times T_i}\right)$$

where $I/I_{303}$ is the normalized current, R is the universal gas constant, $T_i$ is the experimental value of temperature (°K). The values of $E_{act}$ for the peak and steady-state currents are 53 ± 1 and 66 ± 9 kJ $mol^{-1}$ for NCX1.1 and 7 ± 2 and 6 ± 0.1 kJ $mol^{-1}$ for NCX-TR1.0, respectively.

The differences in the current inactivation rates for these two exchanger isoforms are shown in Fig. 4. The rate of inactivation was less for trout NCX-TR1.0 than for dog NCX1.1 at both 30°C and 7°C. The inactivation rate constants, λ, of exchange current were obtained by fitting current-time traces to a single exponential. The λ values for NCX-TR1.0 and NCX1.1 were 0.16 ± 0.02 $s^{-1}$ and 0.26 ± 0.03 $s^{-1}$ at 30 °C, 0.10 ± 0.01 $s^{-1}$ and 0.16 ± 0.05 $s^{-1}$ at 14 °C, and 0.10 ± 0.01 $s^{-1}$ and 0.14 ± 0.03 $s^{-1}$ at 7 °C, respectively (Fig.5).

To investigate further whether possible differences in the exchanger regulatory mechanisms are associated with the temperature dependence of exchange activity, we measured current from proteolyzed patches. Fig. 6 shows the exchange outward currents at 30, 14 and 7°C from α-chymotrypsin-treated patches (1 mg $ml^{-1}$ for 1-2 minutes) expressing NCX. Similar to the result observed in dog NCX1.1, proteolysis of the cytoplasmic side of patch for trout NCX-TR1.0 increased the peak current and dramatically reduced the decay. Behaving like wild-type NCX, proteolyzed NCX1.1 yielded temperature-sensitive exchange current, while proteolyzed NCX-TR1.0 yielded relatively temperature-insensitive exchange current. Arrhenius plots of exchange peak

and steady-state currents for proteolyzed NCX1.1 and NCX-TR1.0 are shown in Fig. 7. The values of $E_{act}$ were calculated to be: NCX1.1 54 ± 6 and 72 ± 4 kJ $mol^{-1}$, NCX-TR1.0 14 ± 2 and 17 ± 2 kJ $mol^{-1}$ for the peak and steady-state currents, respectively (Table 1).

The average values of $Q_{10}$ for the wild type and α-chymotrypsin-treated exchangers were calculated for each patch using the equation:

$$Q_{10} = \left( \frac{I_{T_2}}{I_{T_1}} \right)^{10/T_2 - T_1}$$

where $I_{T1}$ and $I_{T2}$ are the currents at the corresponding experimental temperatures $T_1$ or $T_2$. The mean values of $Q_{10}$ for each exchanger averaged from 4-6 patches are presented in Table 2.

## 2.5 Discussion

We have confirmed that cloned trout heart $Na^+$-$Ca^{2+}$ exchanger, NCX-TR1.0, expressed in oocytes, displays similar regulatory properties as mammalian NCX. These properties include $Na^+$-dependent inactivation, characterized by a slow, partial decline in outward exchange current upon application of bath $Na^+$ to initiate exchange, and $Ca^{2+}$-dependent positive regulation characterized by the requirement of the presence of micromolar levels of $Ca^{2+}$ for full activation (9). It is known that these two forms of regulation are dependent on the presence of the XIP site and the $Ca^{2+}$ binding sites of the cytoplasmic loop (22, 23). The similarity in regulation is consistent with the fact that the sequences of both the XIP site and the $Ca^{2+}$ binding sites are highly conserved between trout NCX-TR1.0 and dog NCX1.1 (36). Peak currents for both isoforms declined at 10 μM cytoplasmic $Ca^{2+}$, presumeably reflecting competition between $Na^+$ and $Ca^{2+}$ for the intracellular transport sites (21).

Previous studies have demonstrated unequivocally that NCX activity of mammalian species is highly temperature dependent (11, 15, 16, 29) with $Q_{10}$ values in the range of 2.2-4.0. Using sarcolemmal vesicles, we (33) have demonstrated that the trout heart NCX activity is dramatically less temperature dependent than mammals with a $Q_{10}$ of ~1.2. Comparison of the temperature dependence of exchange activity in

reconstituted proteoliposomes and native membrane indicates that the temperature sensitivity is likely an intrinsic property of the NCX protein rather than dependent on the lipid environment (4, 33). In the present study, the temperature effects on NCX activity were characterized further by measuring outward exchange currents of the cloned trout NCX-TR1.0 and dog NCX1.1 over a temperature range of 7 to 30°C. When the temperature was decreased from 30°C to 7°C, both the peak current and the steady-state current of dog NCX1.1 were greatly reduced (to ~10%) and the derived $Q_{10}$ values of 2.4 for peak current and 2.6 for steady-state current are consistent with previous measurements of mammalian NCX temperature dependence (11, 16, 33). However, when the temperature was reduced from 30 to 7°C, the outward currents of cloned NCX-TR1.0 were largely maintained (~60 %), with the derived $Q_{10}$ values being 1.2 for peak current and 1.1 for steady-state current. These values are strikingly similar with that determined for the calcium uptake by native trout NCX ($Q_{10} \sim 1.2$) in both native and asolectin-reconstituted sarcolemmal vesicles (33).

The energy of activation ($E_{act}$ – expressed as kJ $mol^{-1}$) values for both peak (53 ± 1) and steady state (66 ± 9) $I_{NCX}$ for the expressed canine NCX determined in this study are in a similar range as those observed by others using various mammalian preparations. These results are summarized in Table 3 and a clear distinction can be made between the endothermic mammals in which $E_{act}$ ranges from 48-67 kJ $mol^{-1}$ and the ectothermic lower vertebrates such as frogs (21-25 kJ $mol^{-1}$) and trout (6-7 kJ $mol^{-1}$). This, we believe, is a reflection of the important role that NCX plays in the hearts of these two species under hypothermic conditions.

Characterization of the temperature effect on inactivation kinetics of $Na^+$-$Ca^{2+}$ exchange current was performed by fitting the current decay with single exponential and the inactivation rate constant, $\lambda$, was determined as a function of temperature (Fig.5). $\lambda$ decreased monotonically with temperature for both isoforms, consistent with that observed in myocyte patches by some experimenters (10) but not others (27). The inactivation of NCX-TR1.0 was consistently slower than that of NCX1.1 over the temperature range of 30°C to 7°C. However, the values of $\lambda$ for these two isoforms changed almost in parallel over this temperature range as reflected in fact the inactivation

rate constant $Q_{10}$ values were calculated to be 1.35 for NCX1.1 and 1.34 for NCX-TR1.0, over the range 7°C and 30°C and were not significantly different. However, the derived $Q_{10}$ of the inactivation rate for the cloned canine NCX expressed in oocytes in this study of 1.35 is considerably lower than that of native NCX in excised patches from guinea pig cardiomyocytes ($Q_{10}$ 2.2) observed by Hilgemann et al. (11) and the reasons for this discrepancy are not clear. It is worth noting however that a recent study has shown that there are considerable differences in the rates of $Na^+$-dependent inactivation for $Na^+Ca^{2+}$ exchange, depending upon the model system and technique employed for characterization (8).

To investigate further the relationship between the regulation and temperature dependency of NCX, we treated the cytoplasmic surface of the excised NCX patch with α-chymotrypsin. Although it is not clear whether the 70 kDa fragment generated by chymotrypsin treatment represents either the C terminus (14) or the N terminus (31) of the molecule, it is well-documented that this treatment eliminates all forms of regulation while maintaining the exchange activity (9). Comparable to mammalian NCX, proteolyzed NCX-TR1.0 was deregulated with the exchange current no longer sensitive to changes of cytoplasmic $Ca^{2+}$ concentration (data not shown), and with very little $Na^+$ dependent inactivation (Fig.6). The proteolyzed NCX isoforms from both species exhibited temperature dependencies similar to that of the wild-type exchangers, as the $Q_{10}$ values between wild type and proteolyzed NCX were not significantly different, suggesting that the temperature dependence is not predicated on NCX regulatory mechanisms. Based on the observations that NCX loses its regulatory properties after treatment with α-chymotrypsin (9) and the large cytoplasmic loop is essential for regulation of NCX activity (24), it can be postulated that the substantial sequence differences in the loop are not associated with the disparate temperature dependencies of NCX isoforms. In support of this conclusion, we have preliminary evidence that replacing the cytoplasmic loop of the canine NCX with that of trout NCX-TR1.0 does not reduce the $Q_{10}$ of either the peak or steady state currents of this chimera (35). Therefore the difference in temperature dependence is likely to reside in the transmembrane segments in which NCX1.1 and NCX-TR1.0 exhibit ~85% identity at the amino acid level. The transmembrane segments, especially the α repeats, are known to be involved

in ion binding and translocation. During ion translocation the protein undergoes conformational changes that are determined by the flexibility of the protein structure which in turn are affected by temperature. Further experimentation is required to determine the molecular mechanisms involved in the different temperature sensitivity of these NCX isoforms.

It should be noted that in these experiments no ATP was included in either the bath or pipette solutions because it can activate confounding currents in the oocyte patch. ATP, however, is known to regulate the activity of NCX through the $PIP_2$ pathway (6). Furthermore since most reactions involving phosphorylation and dephosphorylation are known to be temperature dependent, it remains to be seen whether this pathway also contributes to the differential temperature sensitivity between these NCX isoforms.

In summary, we have characterized the temperature differences between the dog and trout myocardial exchangers. These discrepancies are due to intrinsic differences in the NCX isoform structures and are likely related to sequence differences in the transmembrane segments of the protein.

## 2.6 Tables

**Table 1:** Mean $E_{act}$ values (kJ $mol^{-1}$) for the control (-CT) and α-chymotrypsin-treated (+CT) exchangers

| | NCX1.1 | | NCX-TR1.0 | |
|---|---|---|---|---|
| Type of estimate | -CT | +CT | -CT | +CT |
| From peak current | 53 ± 1 | 54 ± 6 | 7 ± 2 | 14 ± 2 |
| From steady-state current | 66 ± 9 | 72 ± 4 | 6 ± 0.1 | 17 ± 2 |

Fitted values of $E_{act}$ for NCX1.1 and NCX-TR1.0, analyzed by Student's *t*-test, were significantly different before and after α-chymotrypsin treatment. Within individual exchanger groups, however, no significant differences were detected between intact and α-chymotrypsin-treated NCX1.1, whereas significant differences were found between intact and α-chymotrypsin-treated NCX-TR1.0.

**Table 2:** Mean $Q_{10}$ values for the control (-CT) and α-chymotrypsin-treated (+CT) exchangers

| | NCX1.1 | | NCX-TR1.0 | |
|---|---|---|---|---|
| Type of estimate | -CT | +CT | -CT | +CT |
| From peak current | 2.4 ± 0.4 | 3.0 ± 0.6 | 1.2 ± 0.1 | 1.2 ± 0.1 |
| From steady-state current | 2.6 ± 0.4 | 3.3 ± 0.5 | 1.1 ± 0.1 | 1.4 ± 0.2 |

Fitted values of $Q_{10}$, analyzed by Student's *t*-test, were significantly different between NCX1.1 and NCX-TR1.0 for both intact and α-chymotrypsin-treated exchangers, but not within a particular exchanger type.

**Table 3:** Energy of activation ($E_{act}$ expressed in kJ $mol^{-1}$) values for NCX activity in various mammalian and lower vertebrate species

| $E_{ACT}$ | NCX Parameter | Species | Preparation | Reference |
|---|---|---|---|---|
| 48 | $I_{NCX}$ –peak | guinea-pig | myocyte patch | (11) |
| 67 | $Ca^{2+}$ uptake velocity | rabbit | native vesicles | (4) |
| 58 | $Ca^{2+}$ uptake velocity | dog | native vesicles | (4) |
| 58 | $Ca^{2+}$ uptake velocity | dog | asolectin vesicles | (4) |
| 62 | $Ca^{2+}$ uptake velocity | dog | native vesicles | (33) |
| 53 | $I_{NCX}$ -peak | dog | oocyte | present study |
| 66 | $I_{NCX}$ –steady state | dog | oocyte | present study |
| | | | | |
| 25 | $Ca^{2+}$ uptake velocity | frog | native vesicles | (4) |
| 21 | $Ca^{2+}$ uptake velocity | frog | asolectin vesicles | (4) |
| | | | | |
| 7 | $Ca^{2+}$ uptake velocity | trout | native vesicles | (33) |
| 7 | $I_{NCX}$ -peak | trout | oocyte | present study |
| 6 | $I_{NCX}$ –steady state | trout | oocyte | present study |

## 2.7 Figures

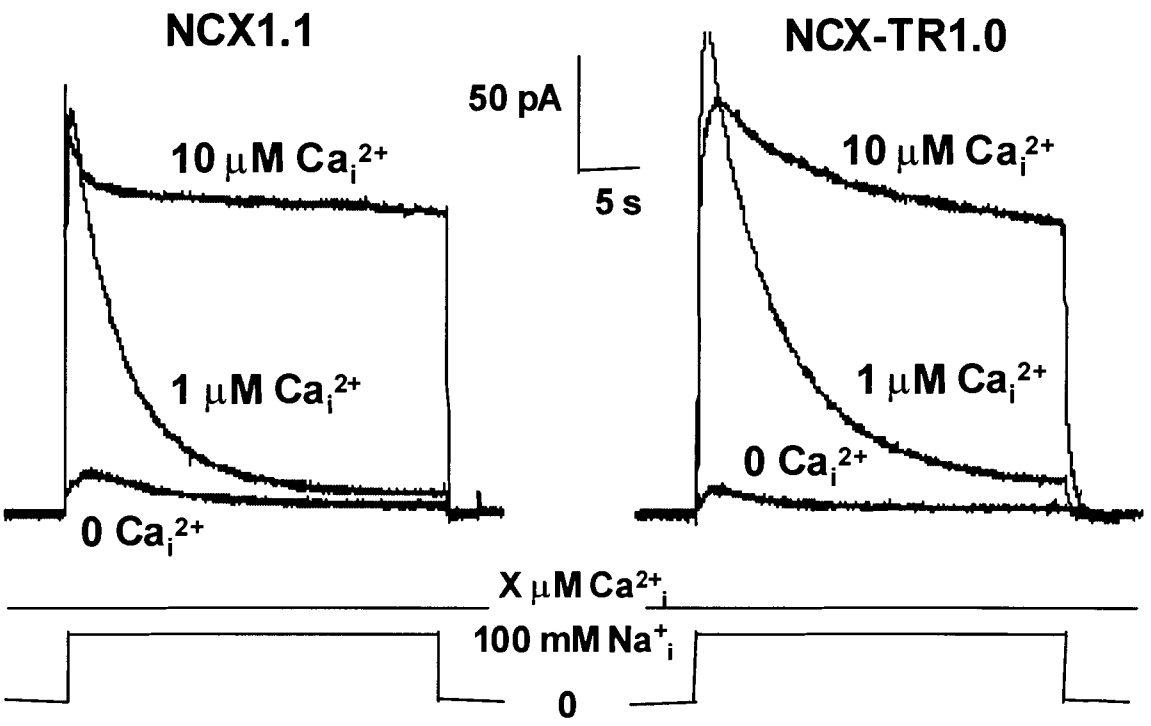


Figure 1

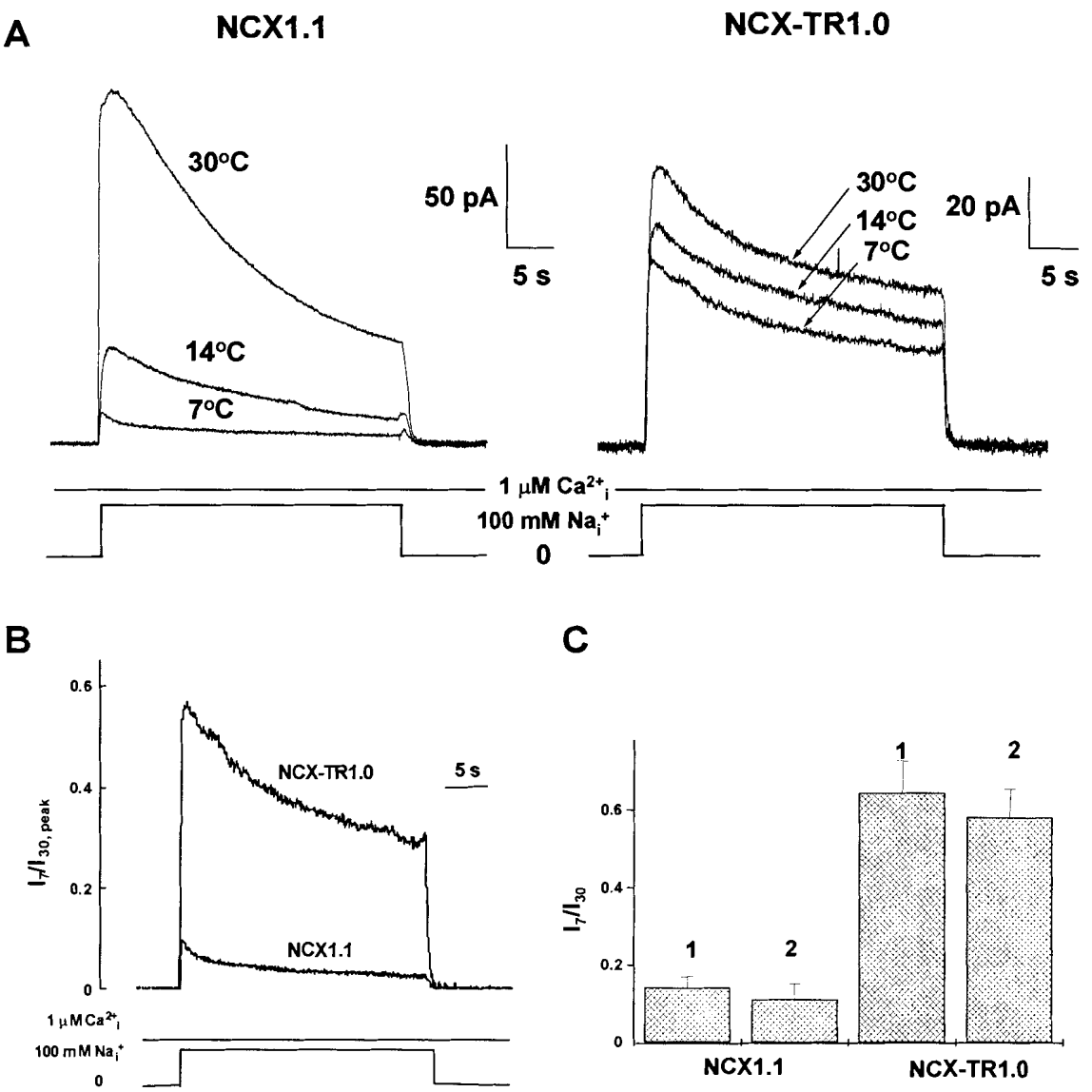
A
NCX1.1
NCX-TR1.0
30°C
50 pA
5 s
14°C
7°C
30°C
14°C
7°C
20 pA
5 s
1 μM Ca2+i
100 mM Na+i
0
B
C
0.6
0.4
0.2
0
I7/I30, peak
NCX-TR1.0
5 s
NCX1.1
1 μM Ca2+i
100 mM Na+i
0
1
2
1
2
I7/I30
0.6
0.4
0.2
0
NCX1.1
NCX-TR1.0

Figure 2

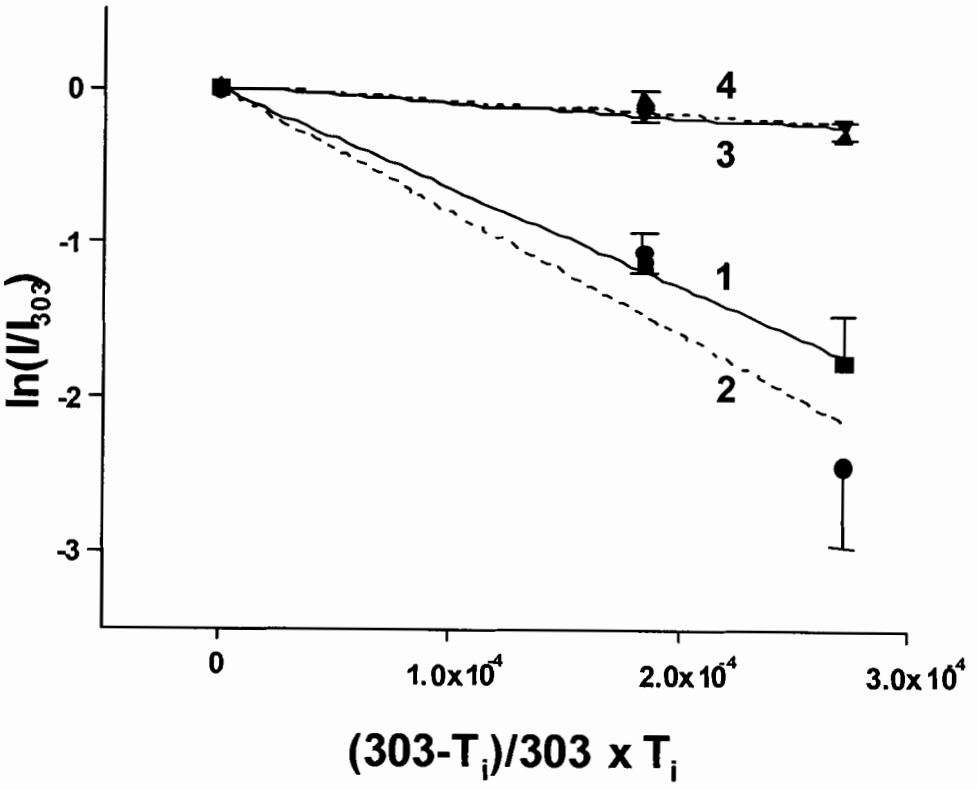


**Figure 3**

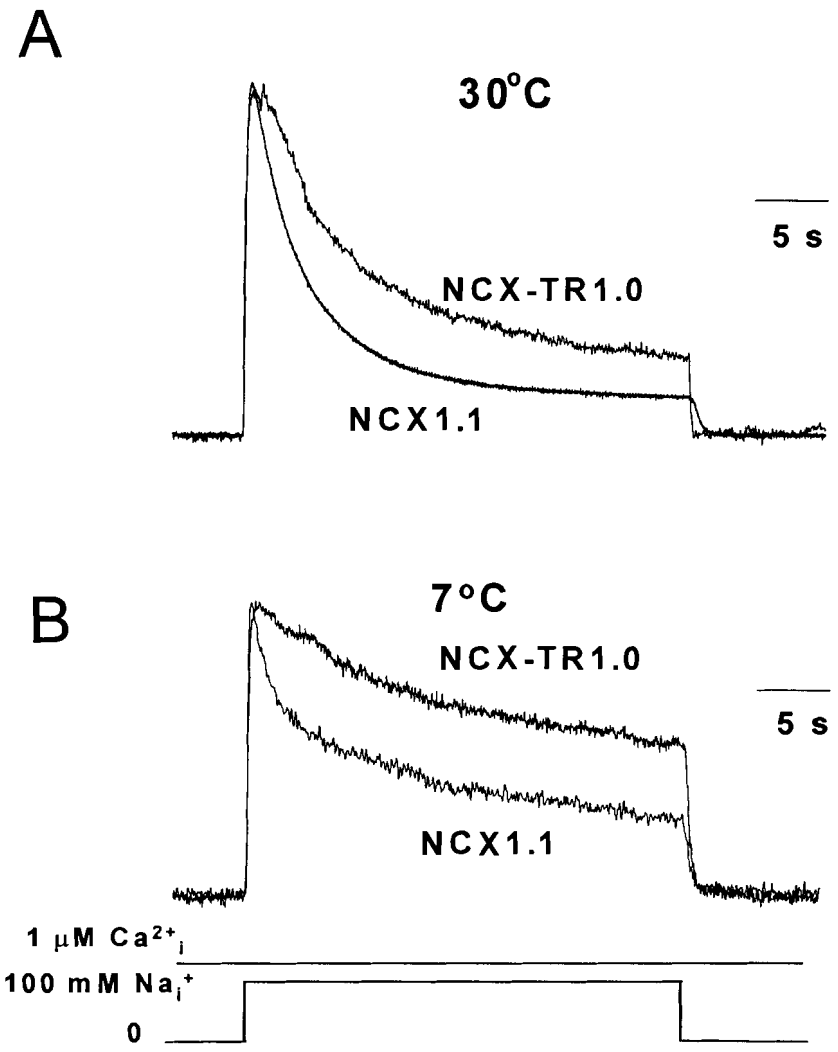
A
30°C
5 s
NCX-TR1.0
NCX1.1
B
7°C
NCX-TR1.0
5 s
NCX1.1
1 μM Ca2+i
100 mM Na+i
0

**Figure 4**

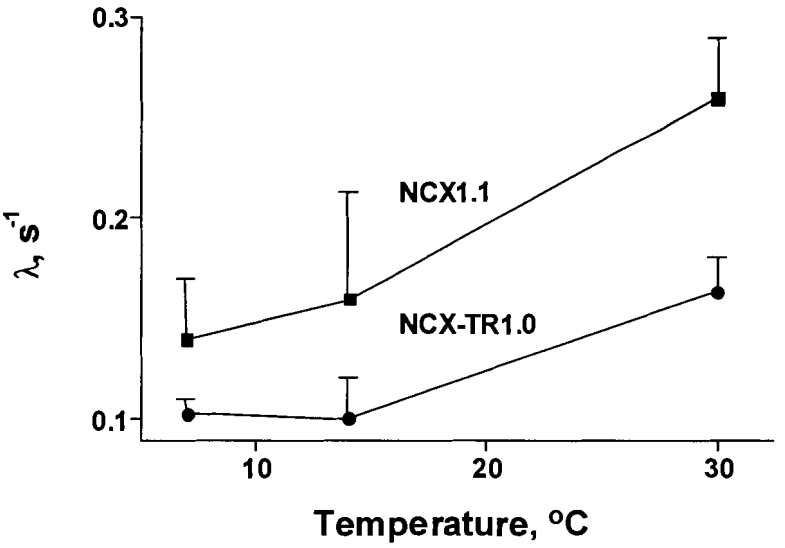


Figure 5

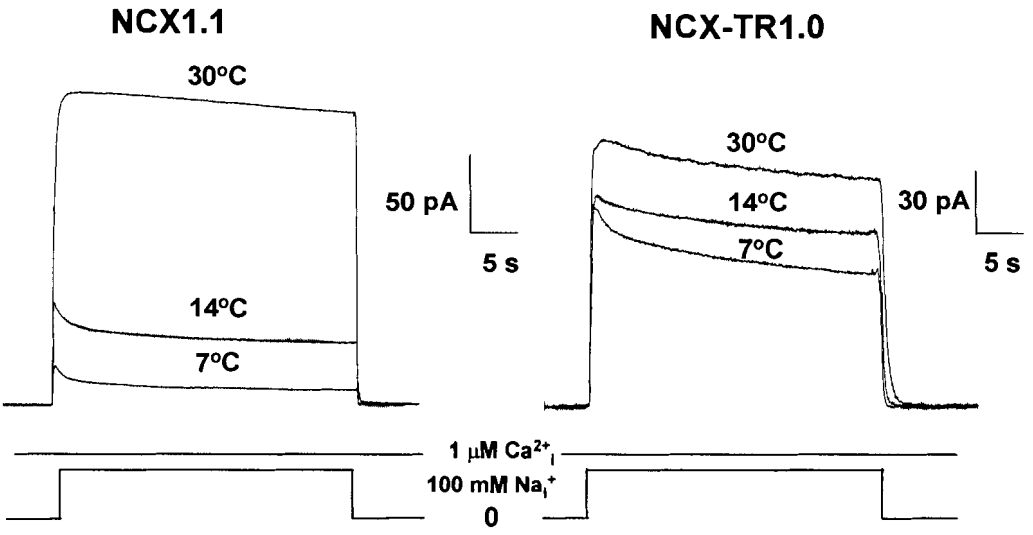


Figure 6

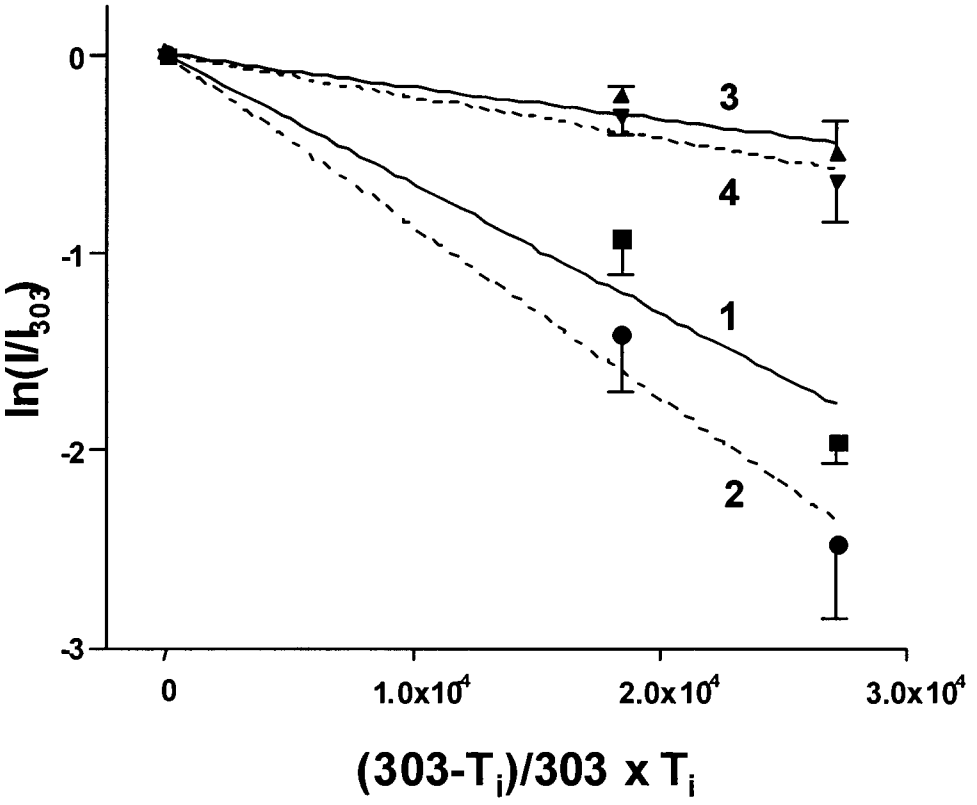


Figure 7

## 2.8 Figure Legends

**Figure 1: $Ca^{2+}$ regulation of $Na^+/Ca^{2+}$ exchange currents**
Typical current traces demonstrating cytoplasmic $Ca^{2+}$ regulation of outward $Na^+$-$Ca^{2+}$ exchange currents obtained from inside-out giant membrane patches. Currents were induced by the rapid application of 100 mM $Na^+$ to the cytoplasmic surface of the patch at the indicated regulatory $Ca^{2+}$ concentrations. $Ca^{2+}$ within the pipette was constant at 8 mM and temperature was 30°C.

**Figure 2: Temperature dependence of $Na^+/Ca^{2+}$ exchange currents**
**(A)** Temperature-dependence of $Na^+$-$Ca^{2+}$ exchange outward current induced by the rapid application of 100 mM $Na^+$ to the cytoplasmic surface of intact patches. 1 μM regulatory $Ca^{2+}$ and 8 mM transport $Ca^{2+}$ were present in the bath and pipette solutions, respectively. **(B)** Representative traces demonstrating influence of temperature on $Na^+$-$Ca^{2+}$ exchange outward current for NCX1.1 and NCX-TR1.0. Currents at 7°C are expressed as a fraction of the respective peak currents at 30°C. **(C)** Influence of temperature on $Na^+$-$Ca^{2+}$ exchange outward current for NCX1.1 and NCX-TR1.0. Values of peak (1) and steady-state (2) currents at 7°C are presented as a fraction of the respective peak and steady-state currents at 30°C. Currents were activated by rapid application of 100 mM $Na^+_i$ in the presence of 1 μM $Ca^{2+}_i$.

**Figure 3: Arrhenius plot of $Na^+/Ca^{2+}$ exchange**
Arrhenius plot of $Na^+$-$Ca^{2+}$ exchange peak (1,3) and steady-state (2,4) currents for the wild-type exchangers: dog (1,2) and trout (3,4) cardiac. For dog NCX1.1, data points represent mean values from 3-4 measurements obtained in 3-4 patches, and those for trout NCX1.0 represent mean values from 3-5 measurements obtained in 3-5 patches. Solid and dashed lines represent linear least-squares fits to the experimental values of the peak and steady-state currents, respectively. To allow statistical treatment of data obtained in different patches, each exchange current was normalized to that obtained at 30°C (~303°K).

**Figure 4: $Na^+$-dependent inactivation of NCX1.1 and NCX-TR1.0**
Representative traces demonstrating difference in the current inactivation rates for dog NCX1.1 and trout NCX-TR1.0 exchangers at 30°C **(A)** and 7°C **(B)**. For each trace, currents were normalized to respective peak current.

**Figure 5: Temperature dependence of the $Na^+$-dependent inactivation**
Temperature-dependence of the inactivation rate constant, λ, of $Na^+$-$Ca^{2+}$ exchange current for NCX1.1 and NCX-TR1.0. For NCX1.1, data points represent mean values from 7 to 30 measurements obtained in 7-16 patches. For NCX-TR1.0, data points represent mean values from 8 to 27 measurements obtained in 4-8 patches. Inactivation rate constants were obtained by fitting current-time traces to a single exponential. The inactivation rate of NCX-TR1.0 was generally slower than that of NCX1.1 over the

temperature range of 7°C to 30°C, although this only achieved statistical significance at 30°C.

**Figure 6: Temperature dependence of deregulated $Na^+/Ca^{2+}$ exchange**
Temperature-dependence of $Na^+$-$Ca^{2+}$ exchange outward current induced by the rapid application of 100 mM $Na^+$ to the cytoplasmic surface of α-chymotrypsin-treated patches. 1 μM regulatory $Ca^{2+}$ and 8 mM transport $Ca^{2+}$ were present in the bath and pipette solutions, respectively.

**Figure 7: Arrhenius plot of $Na^+/Ca^{2+}$ exchange in deregulated patches**
Arrhenius plot of $Na^+$-$Ca^{2+}$ exchange peak (1,3) and steady-state (2,4) currents for α-chymotrypsin-treated exchangers: dog(1,2) and trout (3,4) cardiac. For dog NCX1.1, data points represent mean values from 3-4 measurements obtained in 3-4 patches, and those for trout NCX-TR1.0 represent mean values from 3-5 measurements obtained in 3-5 patches. Solid and dashed lines represent linear least-squares fits to the experimental values of the peak and steady-state currents, respectively. To allow statistical treatment of data obtained in different patches, each exchange current was normalized to that obtained at 30°C (~303°K).

## 2.9 References


1. Bers, D. M. Species differences and the role of sodium-calcium exchange in cardiac muscle relaxation. *Annals of the New York Academy of Sciences* 639: 375-85, 1991.

2. Bers, D. M., J. W. Bassani, and R. A. Bassani. Na-Ca exchange and Ca fluxes during contraction and relaxation in mammalian ventricular muscle. *Annals of the New York Academy of Sciences* 779: 430-42, 1996.

3. Bers, D. M., C. W. Patton, and R. Nuccitelli. A practical guide to the preparation of $Ca^{2+}$ buffers. *Methods in Cell Biology* 40: 3-29, 1994.

4. Bersohn, M. M., R. Vemuri, D. W. Schuil, R. S. Weiss, and K. D. Philipson. Effect of temperature on sodium-calcium exchange in sarcolemma from mammalian and amphibian hearts. *Biochimica et Biophysica Acta* 1062: 19-23, 1991.

5. Bridge, J. H., K. W. Spitzer, and P. R. Ershler. Relaxation of isolated ventricular cardiomyocytes by a voltage-dependent process. *Science* 241: 823-5, 1988.

6. DiPolo, R., and L. Beauge. Effects of vanadate on MgATP stimulation of Na-Ca exchange support kinase-phosphatase modulation in squid axons. *American Journal of Physiology* 266: C1382-91, 1994.

7. Dyck, C., K. Maxwell, J. Buchko, M. Trac, A. Omelchenko, M. Hnatowich, and L. V. Hryshko. Structure-function analysis of CALX1.1, a $Na^{+}$-$Ca^{2+}$ exchanger from Drosophila. Mutagenesis of ionic regulatory sites. *Journal of Biological Chemistry* 273: 12981-7, 1998.

8. Fujioka, Y., K. Hiroe, and S. Matsuoka. Regulation kinetics of $Na^{+}$-$Ca^{2+}$ exchange current in guinea-pig ventricular myocytes. *Journal of Physiology (London)* 529: 611-623, 2000.

9. Hilgemann, D. W. Regulation and deregulation of cardiac $Na^{+}$-$Ca^{2+}$ exchange in giant excised sarcolemmal membrane patches. *Nature* 344: 242-5, 1990.

10. Hilgemann, D. W., A. Collins, and S. Matsuoka. Steady-state and dynamic properties of cardiac sodium-calcium exchange. Secondary modulation by cytoplasmic calcium and ATP. *Journal of General Physiology* 100: 933-61, 1992.

11. Hilgemann, D. W., S. Matsuoka, G. A. Nagel, and A. Collins. Steady-state and dynamic properties of cardiac sodium-calcium exchange. Sodium-dependent inactivation. *Journal of General Physiology* 100: 905-32, 1992.

12. Hove-Madsen, L., A. Llach, and L. Tort. $Na^{+}/Ca^{2+}$-exchange activity regulates contraction and SR $Ca^{2+}$ content in rainbow trout atrial myocytes. *American Journal of Physiology* 279: R1856-64, 2000.

13. Iwamoto, T., T. Y. Nakamura, Y. Pan, A. Uehara, I. Imanaga, and M. Shigekawa. Unique topology of the internal repeats in the cardiac $Na^{+}/Ca^{2+}$ exchanger. *FEBS Letters* 446: 264-8, 1999.

14. Iwata, T., C. Galli, P. Dainese, D. Guerini, and E. Carafoli. The 70 kD component of the heart sarcolemmal $Na^+/Ca^{2+}$-exchanger preparation is the C-terminal portion of the protein. *Cell Calcium* 17: 263-9, 1995.

15. Khananshvili, D., E. Weil-Maslansky, and D. Baazov. Kinetics and mechanism: modulation of ion transport in the cardiac sarcolemma sodium-calcium exchanger by protons, monovalent, ions, and temperature. *Annals of the New York Academy of Sciences* 779: 217-35, 1996.

16. Kimura, J., S. Miyamae, and A. Noma. Identification of sodium-calcium exchange current in single ventricular cells of guinea-pig. *Journal of Physiology (London)* 384: 199-222, 1987.

17. Leblanc, N., and J. R. Hume. Sodium current-induced release of calcium from cardiac sarcoplasmic reticulum. *Science* 248: 372-6, 1990.

18. Levi, A. J., K. W. Spitzer, O. Kohmoto, and J. H. Bridge. Depolarization-induced Ca entry via Na-Ca exchange triggers SR release in guinea pig cardiac myocytes. *American Journal of Physiology* 266: H1422-33, 1994.

19. Li, Z., D. A. Nicoll, A. Collins, D. W. Hilgemann, A. G. Filoteo, J. T. Penniston, J. N. Weiss, J. M. Tomich, and K. D. Philipson. Identification of a peptide inhibitor of the cardiac sarcolemmal $Na^+$- $Ca^{2+}$ exchanger. *Journal of Biological Chemistry* 266: 1014-20, 1991.

20. Longoni, S., M. J. Coady, T. Ikeda, and K. D. Philipson. Expression of cardiac sarcolemmal $Na^+$-$Ca^{2+}$ exchange activity in Xenopus laevis oocytes. *American Journal of Physiology* 255: C870-3, 1988.

21. Matsuoka, S., and D. W. Hilgemann. Steady-state and dynamic properties of cardiac sodium-calcium exchange. Ion and voltage dependencies of the transport cycle. *Journal of General Physiology* 100: 963-1001, 1992.

22. Matsuoka, S., D. A. Nicoll, Z. He, and K. D. Philipson. Regulation of cardiac $Na^+$-$Ca^{2+}$ exchanger by the endogenous XIP region. *Journal of General Physiology* 109: 273-86, 1997.

23. Matsuoka, S., D. A. Nicoll, L. V. Hryshko, D. O. Levitsky, J. N. Weiss, and K. D. Philipson. Regulation of the cardiac $Na^+$-$Ca^{2+}$ exchanger by $Ca^{2+}$. Mutational analysis of the $Ca^{2+}$-binding domain. *Journal of General Physiology* 105: 403-20, 1995.

24. Matsuoka, S., D. A. Nicoll, R. F. Reilly, D. W. Hilgemann, and K. D. Philipson. Initial localization of regulatory regions of the cardiac sarcolemmal $Na^+$-$Ca^{2+}$ exchanger. *Proceedings of the National Academy of Sciences (USA)* 90: 3870-4, 1993.

25. Nicoll, D. A., L. V. Hryshko, S. Matsuoka, J. S. Frank, and K. D. Philipson. Mutation of amino acid residues in the putative transmembrane segments of the cardiac sarcolemmal $Na^+$-$Ca^{2+}$ exchanger. *Journal of Biological Chemistry* 271: 13385-91, 1996.

26. Nicoll, D. A., M. Ottolia, L. Lu, Y. Lu, and K. D. Philipson. A new topological model of the cardiac sarcolemmal $Na^+$-$Ca^{2+}$ exchanger. *Journal of Biological Chemistry* 274: 910-7, 1999.

27. Niggli, E., and J. Lederer. Molecular operations of the sodium-calcium exchanger revealed by conformation currents. *Nature* 349: 612-4, 1991.

28. Omelchenko, A., C. Dyck, M. Hnatowich, J. Buchko, D. A. Nicoll, K. D. Philipson, and L. V. Hryshko. Functional differences in ionic regulation between alternatively spliced isoforms of the $Na^+$-$Ca^{2+}$ exchanger from *Drosophila melanogaster*. *Journal of General Physiology* 111: 691-702, 1998.

29. Powell, T., A. Noma, T. Shioya, and R. Z. Kozlowski. Turnover rate of the cardiac $Na^+$-$Ca^{2+}$ exchanger in guinea-pig ventricular myocytes. *Journal of Physiology (London)* 472: 45-53, 1993.

30. Qiu, Z., D. A. Nicoll, and K. D. Philipson. Helix packing of functionally important regions of the cardiac $Na^+$-$Ca^{2+}$ exchanger. *Journal of Biological Chemistry* 276: 194-199, 2001.

31. Saba, R. I., A. Bollen, and A. Herchuelz. Characterization of the 70 kDa polypeptide of the Na/Ca exchanger. *Biochemical Journal* 338: 139-45, 1999.

32. Tibbits, G. F., C. D. Moyes, and L. Hove-Madsen. Excitation-contraction coupling in the teleost heart. In: *Fish Physiology*, edited by D. J. Randall and A. P. Farrell Academic Press, 1992, p. 267-304.

33. Tibbits, G. F., K. D. Philipson, and H. Kashihara. Characterization of myocardial $Na^+$-$Ca^{2+}$ exchange in rainbow trout. *American Journal of Physiology* 262: C411-7, 1992.

34. Tsuruya, Y., M. M. Bersohn, Z. Li, D. A. Nicoll, and K. D. Philipson. Molecular cloning and functional expression of the guinea pig cardiac $Na^+$-$Ca^{2+}$ exchanger. *Biochimica et Biophysica Acta* 1196: 97-9, 1994.

35. Xue, X. H., C. L. Elias, A. Omelchenko, L. V. Hryshko, and G. F. Tibbits. Temperature dependence of cardiac $Na^+$-$Ca^{2+}$ exchanger: comparison of canine (NCX1) and salmonid (NCX-TR1) isoforms (Abstract). *Biophysical Journal* 78: 54A, 2000.

36. Xue, X. H., L. V. Hryshko, D. A. Nicoll, K. D. Philipson, and G. F. Tibbits. Cloning, expression, and characterization of the trout cardiac $Na^+/Ca^{2+}$ exchanger. *American Journal of Physiology* 277: C693-700, 1999.

# CHAPTER 3
# DETERMINANTS OF CARDIAC $Na^+/Ca^{2+}$ EXCHANGER TEMPERATURE DEPENDENCE: N-TERMINAL TRANSMEMBRANE SEGMENTS*

Christian Marshall[1,4], Chad Elias[2,4], Xiao-Hua Xue[1,4], Hoa Dinh Le[2], Alexander Omelchenko[2], Larry V. Hryshko[2], and Glen F. Tibbits[1,3]

[1] Cardiac Membrane Research Laboratory
Simon Fraser University
Burnaby, BC, Canada

[2] Institute of Cardiovascular Sciences
St. Boniface General Hospital Research Centre
The University of Manitoba
Winnipeg, MB, Canada

[3] Cardiovascular Sciences
BC Research Institute for Children and Women's Health
Vancouver, BC, Canada

[4] These authors contributed equally to this study

* This study is published in the *American Journal of Physiology Cell Physiology* by permission under the following reference: Marshall C., Elias C., Xue X.H., Le H.D., Omelchenko A., Hryshko L.V., and Tibbits G.F. (2002) *Am J Physiol Cell Physiol* **283**: C512-520. PMID: 12107061. Reproduced by permission.

## 3.1 Abstract

The cardiac $Na^+/Ca^{2+}$ exchanger (NCX) in trout exhibits profoundly lower temperature sensitivity in comparison to mammalian NCX. In this study, we attempt to characterize the regions of the NCX molecule responsible for its temperature sensitivity. Chimeric NCX molecules were constructed using wild type trout and canine NCX cDNA, and expressed in *Xenopus* oocytes. NCX-mediated currents were measured at 7, 14 and 30°C using the giant excised patch technique. Using this approach, the differential temperature dependence of NCX was found to reside within the N-terminal region of the molecule. Specifically, we found that approximately 75% of the differential energy of activation is attributable to sequence differences in the region that includes the first four transmembrane segments, and the remainder is attributable to transmembrane segment five and the exchanger inhibitory peptide (XIP) site.

## 3.2 Introduction

The $Na^+$-$Ca^{2+}$ exchanger (NCX) is an integral membrane protein that plays an important role in the regulation of $Ca^{2+}$ concentration in the cytosol. Utilizing the $Na^+$ electrochemical gradient, the NCX transports $Ca^{2+}$ across the membrane with a stoichiometry of three $Na^+$ to one $Ca^{2+}$. Although the NCX is present in many cell types, the cardiac specific isoform (NCX 1.1) has been the most extensively characterized where it serves as the prime mechanism of $Ca^{2+}$ extrusion from the cardiomyocyte (1; 2; 5). Active transporters, such as NCX1.1, involved in ion translocation in the mammalian heart, are highly temperature dependent. For example, it has been demonstrated that the $Q_{10}$ (fold change in activity for a 10°C change in temperature) for NCX1.1 is in the range of 2.2 to 4.0 (12; 16) in mammals. Cardiac function in active salmonid species such as rainbow trout (*Oncorhynchus mykiss*) is distinguished by its ability to maintain adequate contractility under hypothermic conditions that are cardioplegic to mammals. Studies of $Na^+$-$Ca^{2+}$ exchange in trout sarcolemmal vesicles have shown that more than 75% of NCX activity is maintained after reducing the temperature from 21 to 7°C whereas that in canine is diminished to <10% (30). This behavior of NCX was observed in both the native membranes and when exchangers were reconstituted into asolectin vesicles, suggesting that the differential temperature dependencies between isoforms are due to differences in their primary structure. The recent cloning of the trout cardiac NCX (33) provides us with a molecular model for further investigating the temperature dependence of the NCX molecule (7).

The NCX-TR1.0 has predicted topology similar to that of mammalian NCX1.1 based on hydropathy analysis and sequence identity. At the amino acid level the NCX-TR1.0 shows ~75% overall identity to NCX1.1. However, sequence identity between these exchangers is significantly higher in regions of the molecule known to be functionally important, such as the α-repeats (~92%), the XIP site (85%), and regulatory $Ca^{2+}$ binding domains (~86%) (33). Based on these comparisons, the two isoforms appear similar from a molecular perspective, despite exhibiting very different temperature dependencies. In a recent study we characterized in detail the temperature dependencies of NCX1.1 and TR-NCX1.0 wild type exchangers expressed in oocytes by

measuring outward currents using the giant excised patch technique (7). The peak outward current of NCX1.1 exhibited typical mammalian temperature sensitivities with a $Q_{10}$ value of 2.4, while the NCX-TR1.0 peak current was relatively temperature insensitive with a $Q_{10}$ value of 1.2 (7). Furthermore, it was found that the disparities in temperature dependence between these two exchanger isoforms are unlikely due to either differences in inactivation kinetics or NCX regulatory mechanisms (7).

The purpose of this study was to delineate the regions of the NCX molecule responsible for its temperature sensitivity. The strategy used involved the construction of chimeric NCX molecules using cDNA derived from canine and trout NCX wild type cDNA. Outward currents for each chimeric construct were measured in *Xenopus* oocytes over a temperature range of 7 to 30°C using the giant excised patch technique. Using this approach, the majority of the differential temperature dependence of the NCX isoforms was found to reside within the region of the molecule that includes the first four transmembrane segments.

## 3.3 Methods

### 3.3.1 Construction of Chimeras

The strategy used for the construction of the chimeras is shown in Figure 1. Initially, three chimeras were constructed and tested. Wild type dog and trout exchanger cDNA were cut twice at homologous places into three domains: an N-terminal domain that comprises the first five transmembrane segments and the XIP site; the intracellular loop, containing the $Ca^{2+}$ binding domain and alternative splicing site; and a C-terminal domain that includes the final four transmembrane segments. For the trout NCX-TR1.0 (33) a silent mutation was made to introduce a second Bcl I site at nucleotide 2128, relative to the start codon, using the QuikChange™ site-directed mutagenesis kit (Stratagene, La Jolla, CA). The mutations were made in a 548 bp cassette generated by Aat II digestion.

NCX-TR1.0 was digested with Bcl I and the intracellular loop fragment ($T_{loop}$) from amino acid 280 to 710 was isolated, which does not include XIP region but spans most of the intracellular loop (from amino acid 258 to 767). Dog NCX1.1 cDNA was

digested with Bcl I to remove a fragment from amino acid 272 to 711. The construct DTD was generated by inserting the fragment $T_{loop}$ into the digested dog NCX1.1. To generate the chimera DTT, wild-type NCX-TR1.0 cDNA (without the Bcl I site that was introduced) was digested with Bcl I and Bgl II (at nucleotide 49 after the stop codon). The resultant fragment, $T_{loop+TMC}$, was then inserted into NCX1.1 cDNA, which had the region of $D_{loop+TMC}$ removed by digestion with Bcl I and Eag I (at nucleotide 58 after the stop codon). To generate the chimera TDD, the cDNA of wild-type NCX-TR1.0 was digested with Bcl I and Pst I (located at the beginning of the 5' untranslated region) and a fragment, including the N-terminal TM segments and the XIP site ($T_{TMN+XIP}$), was isolated. The cDNA of NCX1.1 was digested with Bcl I and BamH I (located at the beginning of the 5' untranslated region) and the fragment spanning from the beginning of the N-terminus to the XIP site was removed. The remaining NCX1.1 fragment was ligated with the $T_{TMN+XIP}$ to form the construct TDD. A fourth construct called DTTT was produced to isolate the effect of sequence differences within the XIP site and TM5 regions on the differential temperature dependence. For this construct a Stu I site was introduced through silent mutation into the cDNA of NCX-TR1.0 at nucleotide 719 as well as the chimera DTT at nucleotide 695, relative to the start codon, respectively. The cDNA was then digested with Stu I and Bcl I. A fragment from NCX-TR1.0 cDNA spanning the region from amino acid 240 to 279 was inserted into the corresponding region of treated DTT from amino acid 232 to 271 and generating chimera DTTT. All constructs were confirmed by sequencing.

### 3.3.2 Expression of Chimeras in *Xenopus* Oocytes

Expression of chimeric exchangers in *Xenopus* oocytes was carried out as described previously (7; 23). In brief, chimeric cDNA was prepared from XL1-Blue E. coli (Stratagene, La Jolla, CA) using a QIAprep® miniprep kit (Qiagen Inc., Mississauga, ON), then linearized with Hind III. Chimera cRNA was synthesized using T3 mMessage mMachine™ In Vitro Transcription Kit (Ambion Inc., Austin, TX), and run on a 1% agarose gel to assess purity. Oocytes were prepared as described by Longoni *et al.* (18) and injected with 5 ng of cRNA. Exchange activity was measured 3-4 days after injection (see below).

### 3.3.3 Assay of $Na^+/Ca^{2+}$ Exchange Activity

Outward $Na^+$-$Ca^{2+}$ exchange currents were measured using the giant excised patch technique, as described previously (7; 23). Briefly, oocytes were placed in a solution containing (in mM): 100 KOH, 100 MES, 20 HEPES, 5 EGTA, 5 $MgCl_2$; pH 7.0 at room temperature with MES. Gigaohm seals were formed via suction using borosilicate glass pipettes (inner diameter of ≈ 20 - 30 μm) and membrane patches were excised by movements of the pipette tip. The pipette solution contained (in mM): 100 NMG-MES, 30 HEPES, 30 TEA-OH, 16 sulfamic acid, 8 $CaCO_3$, 6 KOH, 0.25 ouabain, 0.1 niflumic acid, 0.1 flufenamic acid; pH 7.0 with MES. Outward $Na^+$-$Ca^{2+}$ exchange currents were activated by switching from $Li^+_i$- to $Na^+_i$-based bath solutions containing (in mM): 100 [$Na^+$ or $Li^+$]-aspartate, 20 MOPS, 20 TEA-OH, 20 CsOH, 10 EGTA, 0-7.3 $CaCO_3$, 1.0-1.13 $Mg(OH)_2$; pH 7.0 with MES or LiOH. Magnesium and $Ca^{2+}$ were adjusted to yield free concentrations of 1.0 mM and either 0 or 1 μM, respectively, using MAXC software (3). All experiments were conducted first at room temperature (22-23°C), and then exchange currents were measured at different temperatures (30°C, 14 °C and 7°C) by heating or refrigerating bath solutions. Axon Instruments hardware and software were used for data acquisition and analysis.

### 3.3.4 Inactivation Kinetics and Temperature Dependence Parameters

To explore further the differences in chimeric and wild type exchangers, we examined the inactivation kinetics and temperature dependence parameters for all constructs. For the inactivation kinetics, we calculated the inactivation rate constant, λ, and the ratio of steady state current to peak current, Fss, for each trace. λ values were obtained by fitting current-time traces to a single exponential (7; 12). The $F_{ss}$ was calculated as the ratio of steady state current over the peak current measured for the same current-time trace, as based on the one-step $I_1$ inactivation model of Hilgemann (12). The energy of activation, $E_{act}$, and temperature coefficient, $Q_{10}$, were calculated for each chimera as indices of temperature dependence. The $E_{act}$ was estimated from the following equation:

$$\ln\left(\frac{I}{I_{303}}\right) = -\frac{E_{act}}{R}\left(\frac{303 - T_i}{303 \times T_i}\right)$$

where $I/I_{303}$ is the normalized current, R is the universal gas constant, and $T_i$ is the experimental temperature (°K). To allow for statistical analysis of data obtained from different patches, exchange current was normalized to that obtained at 30°C, or ~303°K. The $Q_{10}$'s for the chimeric exchangers were estimated for each patch by averaging results calculated for the three pairs of temperatures using the equation:

$$Q_{10} = \left( \frac{I_{T_2}}{I_{T_1}} \right)^{10/T_2 - T_1}$$

where $I_{T1}$ and $I_{T2}$ are the currents at the corresponding experimental temperatures $T_1$ or $T_2$.

### 3.3.5 Data analysis and statistics

Statistical significance of the results was determined by unpaired Student's t test and one-way ANOVA using Microcal Origin and Graphpad software. Unless indicated otherwise, a value of $p < 0.05$ was considered significantly different.

## 3.4 Results

### 3.4.1 Temperature Dependence of Chimeric Proteins

The goal of this study was to determine the domains of the NCX molecule responsible for the unique temperature dependencies observed between mammalian and salmonid NCX. To accomplish this, four different chimeras were constructed from the cDNA of the temperature sensitive canine NCX1.1 and the relatively temperature insensitive trout NCX-TR1.0. We examined the temperature dependence of $Na^+$-$Ca^{2+}$ exchange current for chimeric and wild type exchangers expressed in *Xenopus* oocytes. Representative current traces are shown in Figure 2. Canine NCX1.1 and trout NCX-TR1.0 currents were qualitatively similar at 30°C and both exchangers exhibited decreased peak and steady state currents with decreasing temperature (Figure 2a and b). However, this decrease in current was much more pronounced in the canine NCX1.1, in which the exchanger current at 7°C was less than 10 % of that measured at 30°C. In

contrast, trout NCX-TR1.0 activity remained relatively high at ~60% of its activity at 7°C compared to that at 30°C (7).

To examine the mechanisms of the differential temperature dependence of the NCX molecule, the temperature dependence of four chimeric NCX exchangers was examined. Initially three chimeras, DTD, DTT and TDD, were constructed and their outward currents were measured at 7, 14 and 30°C (Figures 2c-e). All three NCX chimeras displayed a typical outward $Na^+$-$Ca^{2+}$ exchange current with an initial peak current, which then decayed to a steady-state level. However, the temperature dependence of the chimeric exchangers varied and based on the current traces at the different temperatures, each chimera can be qualitatively labeled as having either a predominately trout or dog temperature phenotype. In this regard, it is clear that DTD, which includes the canine N terminal TM segments and trout loop, displays characteristics similar to that of canine NCX1.1 outward exchange current temperature dependence (Figure 2c). At 7°C, DTD maintained only ~10% of the peak and steady-state currents measured at 30°C. DTT, in which the canine portion includes only the five N-terminal transmembrane segments and the XIP site, also displayed a temperature dependence similar to the canine NCX1.1 (Figure 2e). DTT. In contrast, currents from TDD exhibited a temperature phenotype similar to trout NCX-TR1.0 wild type. (Figure 2d). Specifically, at 7°C, TDD maintained ~50% of its peak and steady-state currents measured at 30°C. The TDD construct includes the five N-terminal transmembrane segments and the XIP site, with the rest of the exchanger cDNA being derived from dog. From these results, it appears that the region responsible for the differential temperature dependencies of the NCX molecule is localized within the N-terminal portion of the molecule, a region that includes the XIP site. To determine if the XIP site had any effect on the temperature dependence of the NCX, a fourth chimera was constructed and designated DTTT. In this construct the N terminal end including the first seven amino acids within TM5 are canine and the rest of the exchanger was salmonid wild type. The temperature dependence of DTTT was clearly more similar to that of the dog wild-type exchanger (Figure 2f). At 7°C, DTTT were attenuated to ~20% of the peak and steady state current measured at 30°C. From these results, differences in the sequences within

the TM5 and XIP regions appear to play a rather minor role on the temperature dependence of NCX molecule.

### 3.4.2 Inactivation Kinetics and Temperature Dependence Parameters

To investigate the temperature dependence of the NCX molecule in a more quantitative manner, the effect of temperature on the $Na^+$-dependent inactivation of the chimeric exchangers was examined. The inactivation rate constant, $\lambda$, and $F_{ss}$ values for each current trace were determined. The temperature dependence of $\lambda$ for $Na^+$-$Ca^{2+}$ exchange currents from the chimeric exchangers is shown in Figure 3. In general, the $\lambda$ values decreased monotonically with temperature for all constructs. For the chimeras DTD and DTTT, there is a slight inflection point at 14°C as the mean $\lambda$ value for this temperature is less than the $\lambda$ value at 7°C, however these differences are not statistically significant.

Based on the absolute value of $\lambda$, constructs can be placed into two distinct groups depending on the isoform origin of the N-terminal portion of the exchanger. The $\lambda$ values for the trout wild type (data not shown) and TDD are significantly ($p<0.01$) lower at all temperatures compared to DTD, DTT, and DTTT and canine wild type. From the one-step $I_1$ inactivation model (12), the Fss value characterizes the extent of $I_1$ inactivation since 1-Fss is the fraction of inactivation. For a given exchanger construct, there were no statistically significant differences between $F_{ss}$ values determined at the three different temperatures (Table 1).

The average values of $Q_{10}$ for peak and steady state currents for the chimeras are shown in Table 2. Again, the canine wild type, DTD, DTT, and DTTT can be grouped together having $Q_{10}$ values in the range of 2.0-2.7, whereas the $Q_{10}$ values for TDD and the trout wild type are significantly different and fall within the range of 1.2-1.3.

Previously, it was reported that the $E_{act}$ values for peak and steady-state currents were 53 ± 1 and 66 ± 9 kJ $mol^{-1}$ for canine NCX1.1 and 7 ± 2 and 6 ± 0.1 kJ $mol^{-1}$ for NCX-TR1.0, respectively (7). Arrhenius plots of $Na^+$-$Ca^{2+}$ exchange peak and steady state currents for the chimeric exchangers are shown in Figure 4.

We calculated the $E_{act}$ values for the four chimeras, and these values together with the $E_{act}$ values of wild type dog and trout are summarized in Figure 5. From these $E_{act}$ values, it is clear that DTD and DTT exhibited the canine phenotype, while TDD was trout-like with respect to temperature dependence. The chimera DTTT is clearly closer to the canine than trout phenotype in this regard as the $E_{act}$ calculated from either the peak or steady state currents is about 75% of the canine wild type. Statistical significance of $E_{act}$ values between all exchangers is reported in Table 3.

## 3.5 Discussion

In this study, we attempt to elucidate this temperature dependence discrepancy at the molecular level using chimeric proteins derived from wild-type trout and dog exchangers. The use of chimeric proteins in studies involving NCX (6; 13; 20) and the thermostability of proteins (25; 27) has proven useful in comparing functional differences between isoforms. Qualitative examination of outward exchange currents for the chimeras DTD, DTT, and TDD over a range of temperatures placed the region responsible for NCX temperature dependence within the N-terminal TM segments and XIP site. A fourth chimera, DTTT, revealed that the differences within TM5 and the XIP regions have an effect on the temperature dependence of the NCX molecule, but the contribution is relatively small in comparison to the first four TM segments. This is consistent with earlier findings that deregulation of both wild-type trout and dog exchangers with chymotrypsin treatment had no significant effect on the temperature dependencies of the NCX isoforms (7). However, with the use of chimeras it is possible to more closely examine the relative contribution to the temperature dependence of the NCX by different regions of the molecule. For instance, at 7°C, the chimeras DTD and DTT (in which the N terminal end including TM5 and the XIP site are dog in origin) maintain only ~10% activity of their peak current measured at 30°C. The activity of the chimera DTTT at 7°C is relatively higher, retaining ~20% of peak current measured at 30°C. From this observation it appears that differences in sequence in TM5 and XIP do contribute to the temperature dependence of the NCX molecule, albeit in a relatively minor capacity.

The effect of temperature on the inactivation kinetics of $Na^+/Ca^{2+}$ exchange currents was characterized using the inactivation rate constant, $\lambda$, and the fraction of steady state to peak current, $F_{ss}$. As a general trend, $\lambda$ decreased with temperature for all chimeras measured (Figure 3), consistent with what was found in wild-type trout and dog NCX (7). However, it should be noted that the DTT chimera had abnormally high $\lambda$ values with large standard errors at all temperatures, a phenomenon that cannot currently be explained. The inactivation rates of DTD, DTT, and DTTT were consistently faster than that of TDD over the temperature range of 7-30°C and were not significantly different than canine wild-type. This supports further the conclusion that sequence differences in the N-terminal region of the NCX molecule are responsible for temperature dependence disparities between isoforms and that the XIP site and TM5 have only a small effect on the temperature dependence of the NCX. $F_{ss}$ values were higher for TDD compared to the other chimeras, again indicating that the $Na^+$-dependent inactivation was slower for this construct. However, for each chimera there is no statistically significant difference between $F_{ss}$ values determined over the temperature range of 7-30°C. This indicates that an increase in the inactivation rate with temperature is accompanied by an increase in the rate of recovery from inactivation. The measures of $\lambda$ and $F_{ss}$ to characterize the inactivation kinetics of these chimeras support the idea that the differential temperature dependencies of the NCX isoforms are not related to $Na^+$-dependent inactivation. However, it is apparent that the N-terminal region of the NCX is a determining factor in the phenotype of the NCX inactivation kinetics.

In the present study we calculated $Q_{10}$ values (Table 2) and $E_{act}$ values (Figure 5 and Table 3) for the chimeric exchangers in an attempt to classify their temperature dependence as mammalian or trout-like. Consistent with earlier qualitative observations, the origin of the N-terminal region determines the temperature dependence phenotype exhibited by the chimeric exchangers. Similar to other mammalian species (15; 16), the exchanger activity of DTD and DTT is highly temperature dependent with $Q_{10}$ values in the range of 2.3-2.7. With values in the range of 48-65 kJ/mol, the chimeras DTD and DTT exhibit $E_{act}$ values typical of other mammalian NCX's such as dog (4; 7; 30), rabbit (4) and guinea pig (12). Conversely, the chimera TDD is relatively temperature insensitive exhibiting $Q_{10}$'s (1.2-1.3) and $E_{act}$ values (14-15 kJ/mol) similar to those of the

trout wild type exchanger (7). Using these parameters, the chimera DTTT displays intermediate temperature dependencies. Even though not statistically significant, the $Q_{10}$ values for DTTT are slightly lower than those for canine NCX, and the chimeras DTD and DTT. The $E_{act}$ values for DTTT are 39-40 kJ/mol, making them approximately 75% of the values for canine wild-type (53-66 kJ/mol) (7), but much higher than the $E_{act}$ values for the ectothermic species such as trout (6-7 kJ/mol) (7) and frog (21-25 kJ/mol) (4). These data indicate that the TM5 and XIP region play a relatively minor role in the temperature dependence of the NCX compared to the first four transmembrane segments.

Figure 6 shows a sequence alignment comparing the N-terminal regions of canine NCX1.1 and trout NCX-TR1.0. For convenience, the sequence alignment is split where the restriction cuts were made to make the DTTT chimera. The section of TM5 and the XIP site which is responsible for ~25% of the temperature dependence disparity between the trout and dog NCX contains minor sequence differences. The two non-conservative substitutions in the trout XIP site (F to V and Q to R at XIP positions 5 and 18, respectively) are possible causes for the minor role this region plays in the temperature disparity between isoforms. The structural effects of these substitutions are unknown but they are likely to make the trout XIP site less hydrophobic. The phenylalanine at position 5 (F5) of the XIP site has been found to be important in both the inactivation of the NCX (19) and inhibitory effects of the XIP peptide (10). Matsuoka et al (19) found that making a F5E substitution increased the rate of inactivation six-fold, and decreased $F_{ss}$ two-fold. This substitution, in which an aromatic and hydrophobic amino acid, phenylalanine, is replaced by a negatively charged and hydrophilic amino acid, glutamic acid, appears to induce the conformational changes involved in inactivation more rapidly (19). In the trout XIP site the F5V substitution observed converts the highly hydrophobic amino acid to a non-aromatic and less non-polar amino acid. The data from Matsuoka et al. indicated the importance of the F5 but it is not clear what the impact of the valine substitution is at this point. Related to this is the observation that the potency of the exogenous XIP on NCX inhibition is sensitive to mutations of the phenylalanine at position 5 (10). Exogenously added peptide with the XIP sequence has been shown to inhibit exchanger function, consistent with the hypothesis that the endogenous XIP site has an autoregulatory function (17; 20). Substitution of F5 with a charged group

(glutamate) decreases inhibition by a factor of five while substitution with a conserved residue (tryptophan) has no effect on inhibition (10). Replacing the phenylalanine with an alanine or valine decreases the potency of XIP peptide inhibition by approximately 50% and 30%, respectively (10). Presumably, the XIP binds to the exchanger through hydrophobic interactions and aromatics like F5 are required for maximal inhibition. The valine substitution at this position is the same substitution found in the trout NCX and this may have an effect on the inactivation kinetics of the exchanger. However, further testing with site-directed mutagenesis is needed to confirm this theory. Interestingly, the frog (*Xenopus laevis*) NCX (14) shows complete identity to the canine NCX in the XIP region, even though the bullfrog (*Rana catesbeian)* NCX has a much lower $E_{act}$ than the mammalian NCX isoform. Since the bullfrog NCX $E_{act}$ values are higher than trout NCX $E_{act}$ values (21-25 kJ/mol vs. 6-7 kJ/mol, respectively), perhaps the amino acid substitutions in the XIP region may account for this difference. However, it must be pointed out that sequence differences in the XIP domain play a relatively minor role in the temperature dependence of the NCX molecule.

Although fixed amounts of cRNA of each construct were injected into the oocytes, the absolute value of the peak currents varied substantially. Typically, peak currents for NCX-TR1.0 were lower than that observed for NCX 1.1. The reasons for this difference are not clear but could include disparities in unitary activity, stability of mRNA, and/or stability/longevity/trafficking of the protein in the membrane. These differences in current magnitude are unlikely to alter our conclusions for several reasons. The focus of the present study is on an intrinsic property, specifically the temperature dependence of outward $Na^+/Ca^{2+}$ currents. The magnitude of these currents reflects both the number and unitary currents of exchangers within the patch. While the number of NCX molecules within a patch is likely to vary considerably, possibly reflecting differences cited above and the heterogeneity of pipette and patch geometries, there is no evidence that differences of the number of exchangers within a patch alters its unitary properties. Secondly, the possibility of NCX dimerization has been raised (9; 31) but remains unproven and controversial. In our study, the putative potential of dimerization as an explanation of these results is extremely unlikely as it implies the following: 1)

dimerization occurs; 2) the different constructs have varying propensities for dimerization and 3) dimerization affects the unitary currents.

To date, most studies examining the molecular mechanisms of cold adaptation of proteins have used cytoplasmic enzymes from psychrotrophic bacteria (21; 28; 32) with some studies using enzymes from Antarctic fish (8). As of yet, there is no consensus as to which molecular mechanisms are responsible for low temperature activity (26). General mechanisms by which proteins function at low temperatures include: more polar and less hydrophobic residues; a decrease in or lack of salt bridges; fewer hydrogen bonds, aromatic interactions, and ion pairs; a decrease in the number of arginine and proline residues; and an increase in surface loops with increased polar residues (24; 26). No cold adaptive protein displays all these features, indicating that from an evolutionary perspective, there are multiple routes to cold adaptation (21; 32). However, these mechanisms help increase the conformational flexibility of proteins which is a necessity for function at low temperatures. Even though the NCX is a membrane protein, some of these same principles may apply in its cold adaptation since it must be flexible for ion translocation across the membrane. It has been shown that as few as four amino acid substitutions are sufficient to generate an enzyme whose low temperature activity is significantly greater than its parent enzyme (32). It is therefore not unreasonable to assume that only a few of the amino acid substitutions in the trout NCX-TR1.0 within the first four TM segments are responsible for its relatively high activity at low temperatures. An amino acid sequence comparison of this region between NCXs from mammalian species such as the dog (22), and from ectothermic species such frog (14), trout (33) and squid (11), revealed no general trends regarding the aforementioned adaptive mechanisms proteins use to function at low temperature. The number of prolines (7 for dog and trout, 8 for frog, and 6 for squid) and arginines (5 for dog, and 6 for trout, frog, and squid) in this region are fairly well conserved between species. In addition, substitutions in loop regions between isoforms did not show an overall increase or decrease in polarity (data not shown), nor was there large differences in the number of aromatic residues (21 for dog, 20 for trout, frog and squid). Another feature that may promote structural flexibility are glycine residues, which are thought to be destabilizing in helices and stabilizing in loop regions (26). Within the first four TM segments, the

number of glycine residues is conserved between these four isoforms except in the N-terminal loop (6 for dog, 5 for trout, 3 for frog, and 2 for squid). From sequence analysis there is little to discern the specific mechanisms enabling the trout NCX to function at low temperatures. In fact, it is unlikely that there is one region or a few amino acid substitutions that can totally account for the cold activity of trout NCX-TR1.0. A more likely explanation is that a series of amino acid substitutions in different regions of the molecule all play a role in the activity of the trout NCX at low temperatures.

In summary, we have placed the region responsible for the temperature dependence of the NCX in the N-terminal region of the molecule. The majority of the differential temperature dependence between canine and trout isoforms seems to reside in the first four transmembrane segments, with a minor role played by TM5 and the XIP site. Further mutational analysis is needed to determine the specific amino acids involved in the temperature dependence of the molecule, but we speculate that a series of amino acid substitutions within the first four TM segments are responsible for the activity of the trout NCX at low temperatures.

## 3.6 Tables

**Table 1:** Temperature dependence of $F_{ss}$ values for chimeric NCX

| Exchanger | $F_{SS}$ | | |
|---|---|---|---|
| | 7°C | 14°C | 30°C |
| **Dog WT** | 0.28 ± 0.05 | 0.24 ± 0.04 | 0.17 ± 0.02 |
| **DTD** | 0.24 ± 0.03 | 0.24 ± 0.03 | 0.19 ± 0.04 |
| **DTT** | 0.37 ± 0.05 | 0.23 ± 0.04 | 0.28 ± 0.03 |
| **DTTT** | 0.42 ● 0.06 | 0.38 ± 0.07 | 0.40 ± 0.04 |
| **TDD** | 0.56 ± 0.07 | 0.55 ± 0.08 | 0.48 ± 0.03 |
| **Trout WT** | 0.21 ± 0.04 | 0.23 ± 0.08 | 0.19 ± 0.03 |

**Table 2:** $Q_{10}$ values for chimeric NCX

| Exchanger | $Q_{10}$ | |
|---|---|---|
| | Peak current estimate | Steady-state current estimate |
| **Dog WT** | 2.4 ± 0.4 | 2.6 ± 0.4 |
| **DTD** | 2.3 ± 0.3 | 2.5 ± 0.6 |
| **DTT** | 2.7 ± 0.2 | 2.5 ± 0.1 |
| **DTTT** | 2.0 ± 0.1 | 2.2 ± 0.1 |
| **TDD** | 1.3 ± 0.1* | 1.2 ± 0.0* |
| **Trout WT** | 1.2 ± 0.1* | 1.1 ± 0.1* |

* $p < 0.05$ versus Dog WT, DTD, DTT, and DTTT

**Table 3:** Statistical significance of the differences in $E_{act}$ values

| Exchanger | DTD | | DTT | | DTTT | | TDD | | Trout WT | |
|---|---|---|---|---|---|---|---|---|---|---|
| construct | peak | ss | peak | ss | peak | ss | peak | ss | peak | ss |
| Dog WT | NS | NS | NS | NS | NS | *** | ***** | ***** | ***** | ***** |
| DTD | | | NS | NS | NS | NS | ** | ***** | ***** | ***** |
| DTT | | | | | NS | ***** | **** | ***** | ***** | ***** |
| DTTT | | | | | | | ** | ***** | ***** | ***** |
| TDD | | | | | | | | | NS | ***** |

A comparison of $E_{act}$ values derived from peak and steady state (ss) $I_{NCX}$ for all constructs measured. NS denotes not significant ($p > 0.05$), whereas statistical significance is depicted as follows:

* $p < 0.05$
** $p < 0.01$
*** $p < 0.005$
**** $p < 0.001$
***** $p < 0.0001$

## 3.7 Figures

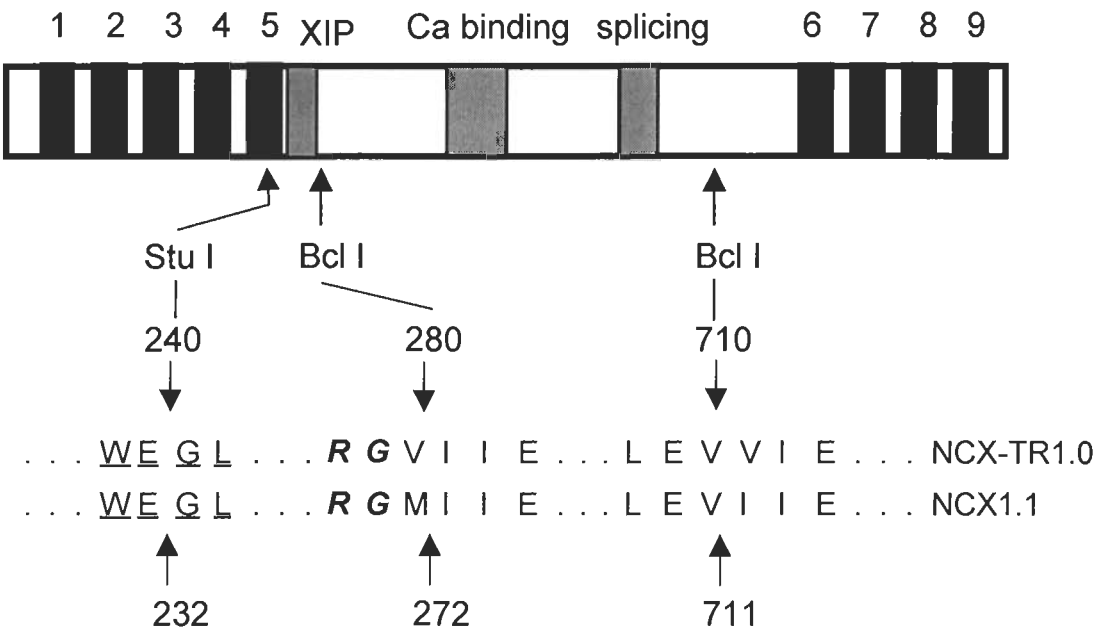


**Figure 1**

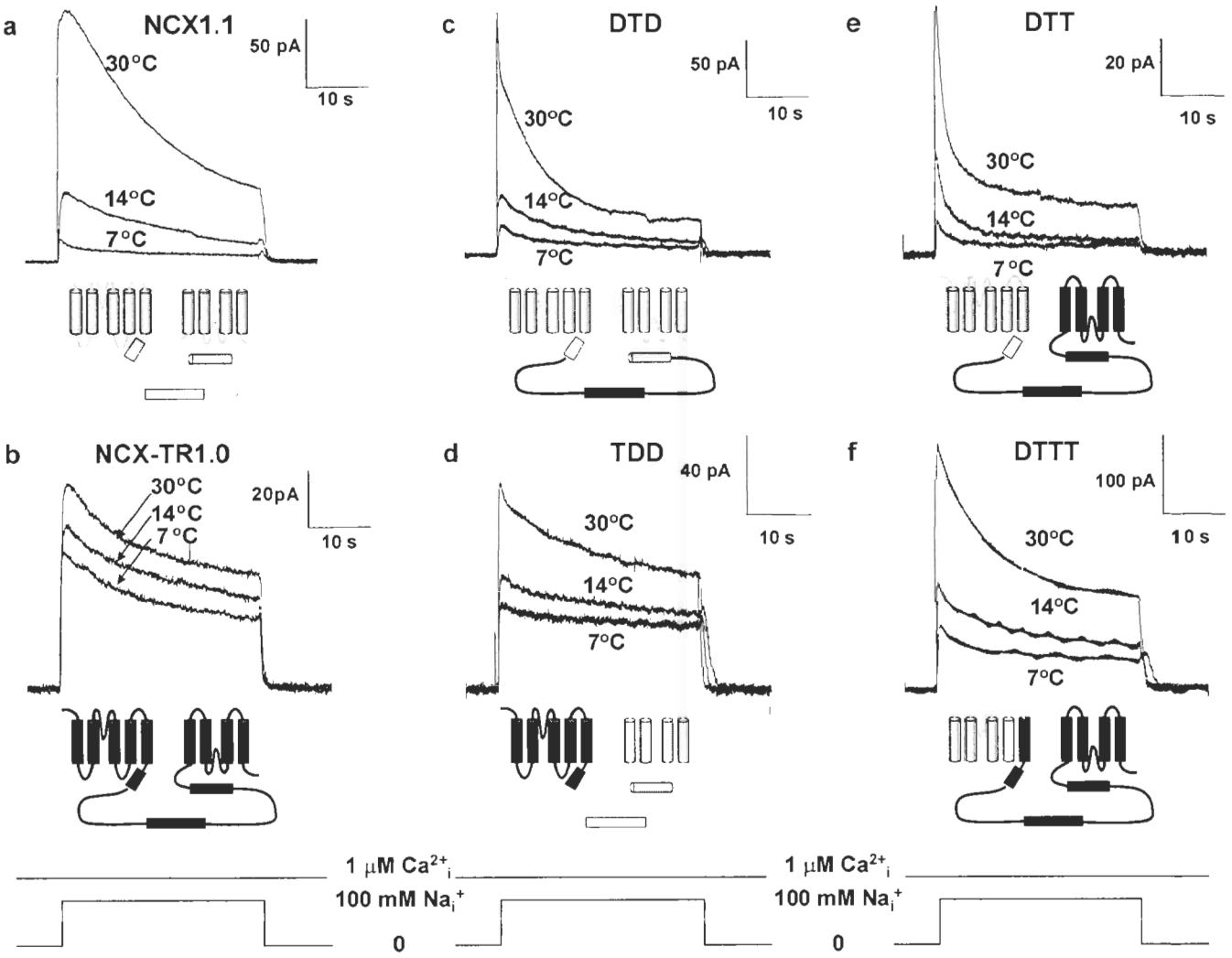
a
NCX1.1
50 pA
10 s
30°C
14°C
7°C
c
DTD
50 pA
10 s
30°C
14°C
7°C
e
DTT
20 pA
10 s
30°C
14°C
7°C
b
NCX-TR1.0
20pA
10 s
30°C
14°C
7°C
d
TDD
40 pA
10 s
30°C
14°C
7°C
f
DTTT
100 pA
10 s
30°C
14°C
7°C
1 μM Ca2+i
100 mM Na+i
0
1 μM Ca2+i
100 mM Na+i
0

Figure 2

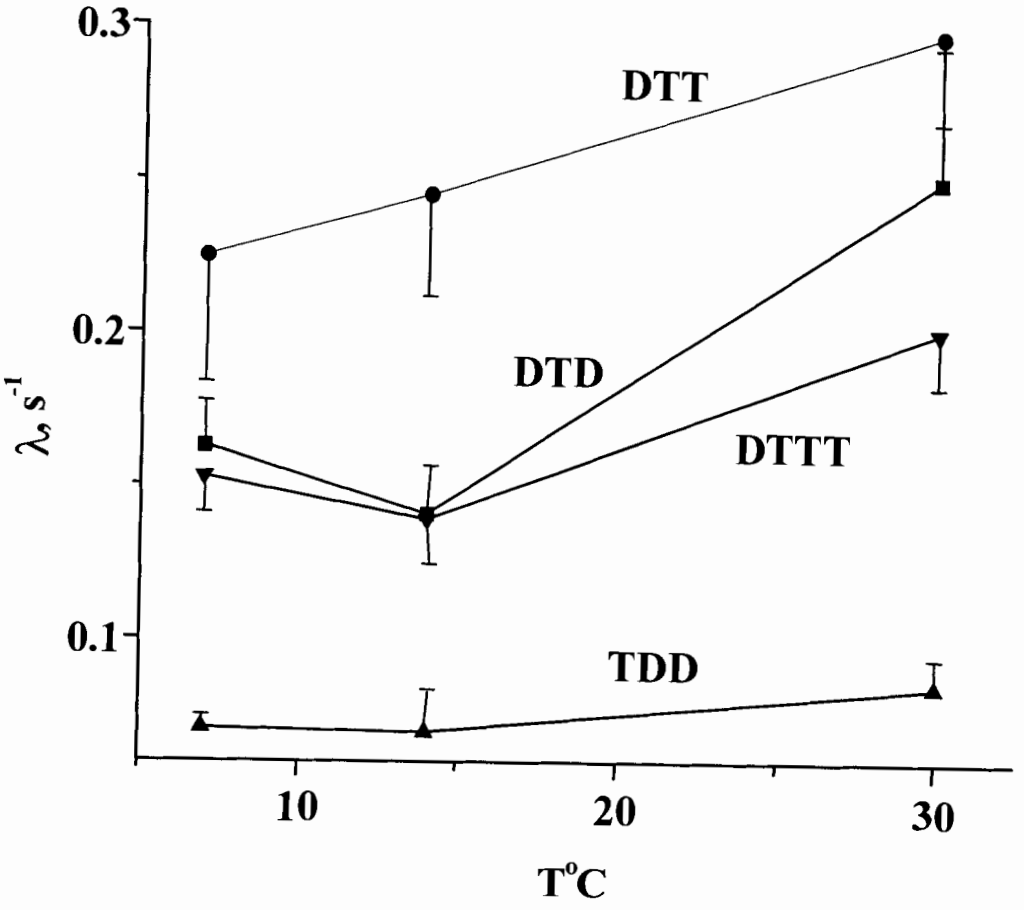


**Figure 3**

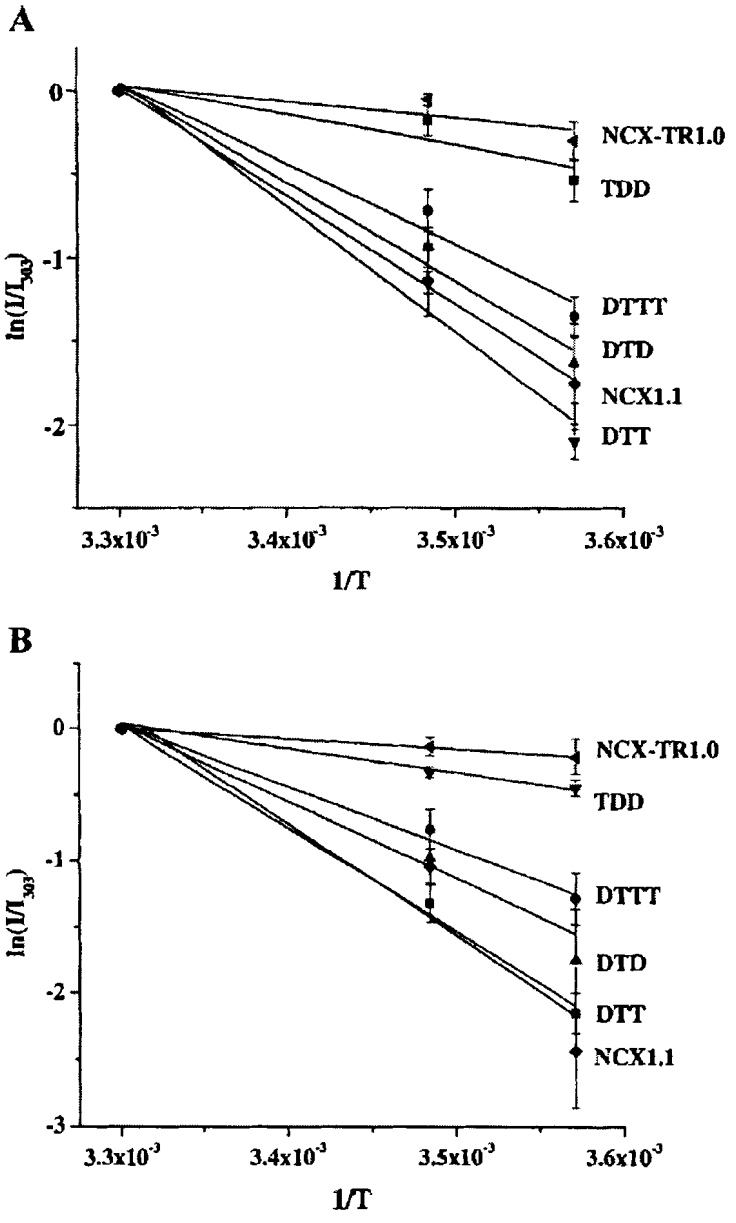
A
0
-1
-2
ln(I/I303)
NCX-TR1.0
TDD
DTTT
DTD
NCX1.1
DTT
3.3x10-3
3.4x10-3
3.5x10-3
3.6x10-3
1/T
B
0
-1
-2
-3
ln(I/I303)
NCX-TR1.0
TDD
DTTT
DTD
DTT
NCX1.1
3.3x10-3
3.4x10-3
3.5x10-3
3.6x10-3
1/T

**Figure 4**

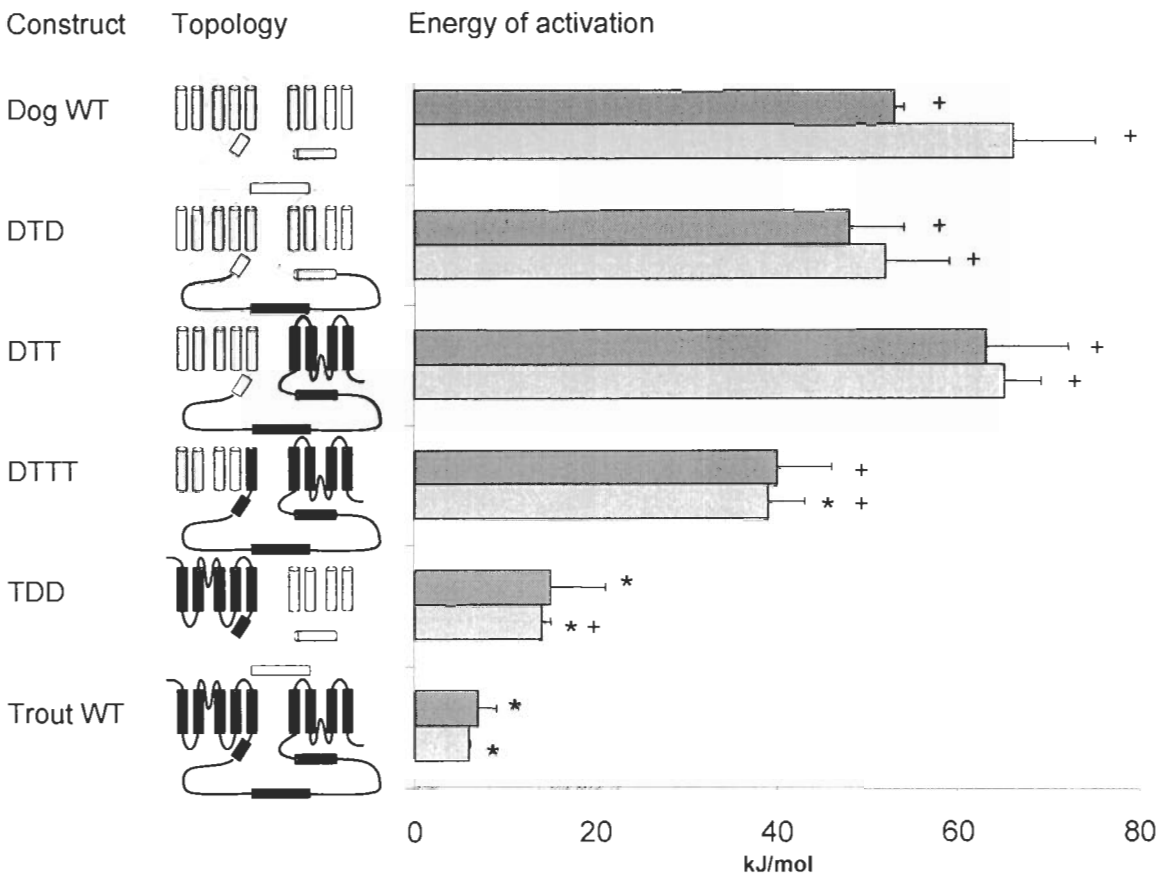
Construct
Topology
Energy of activation
Dog WT
DTD
DTT
DTTT
TDD
Trout WT
0
20
40
60
80
kJ/mol

**Figure 5**

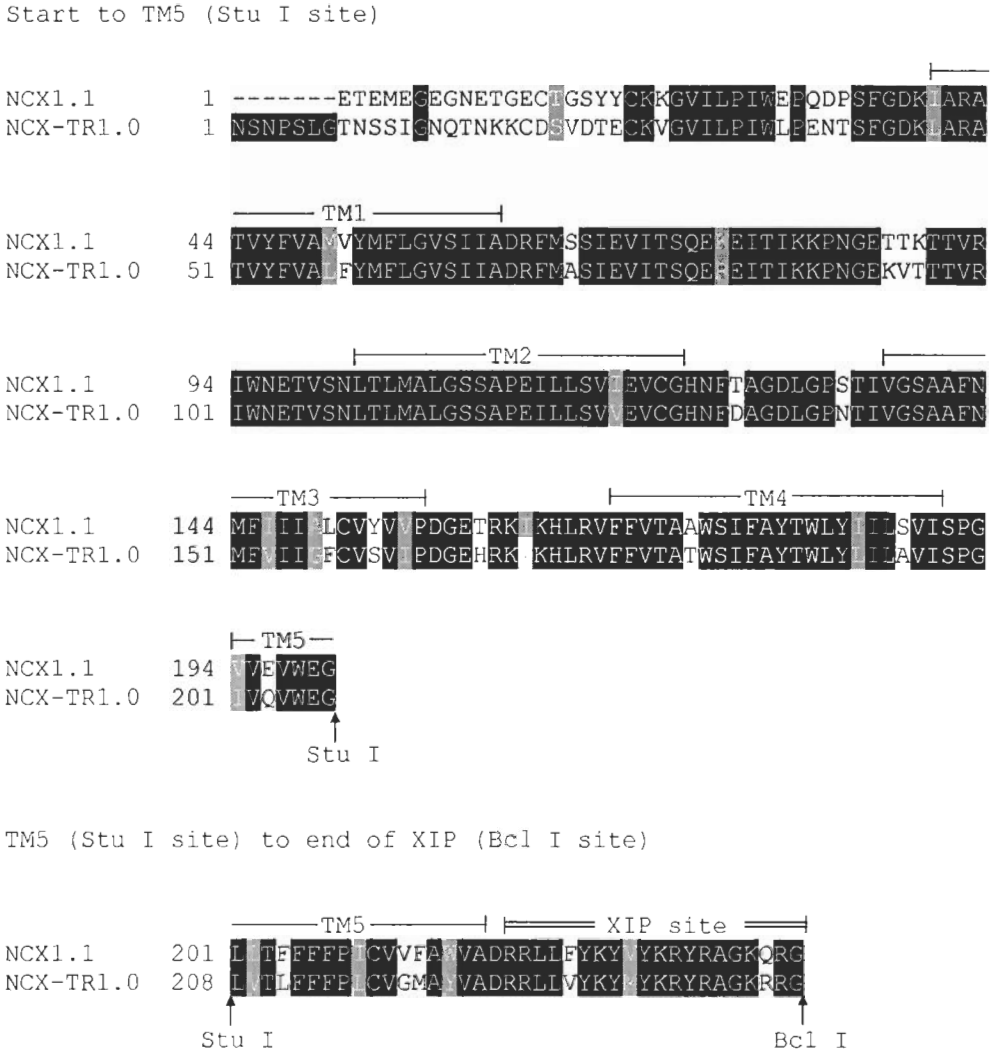
Start to TM5 (Stu I site)
NCX1.1 1 -------ETEMEGEGNETGECIGSYYCKKGVILPIWEPQDPSFGDKIARA
NCX-TR1.0 1 NSNPSLGTNSSICNQTNKKCDSVDTECKVGVILPIWLPENTSFGDKIARA
TM1
NCX1.1 44 TVYFVAMVYMFLGVSIIADRFMSSIEVITSQEKEITIKKPNGETTKTTVR
NCX-TR1.0 51 TVYFVALFYMFLGVSIIADRFMASIEVITSQEREITIKKPNGEKVTTTVR
TM2
NCX1.1 94 IWNETVSNLTLMALGSSAPEILLSVIEVCGHNFTAGDLGPSTIVGSAAFN
NCX-TR1.0 101 IWNETVSNLTLMALGSSAPEILLSVVEVCGHNFDAGDLGPNTIVGSAAFN
TM3
TM4
NCX1.1 144 MFIIIMLCVYVVPDGETRKIKHLRVFFVTAAWSIFAYTWLYIILSVISPG
NCX-TR1.0 151 MFVIIGFCVSVIPDGEHRKIKHLRVFFVTATWSIFAYTWLYIILAVISPG
TM5
NCX1.1 194 VEVWEG
NCX-TR1.0 201 IVQVWEG
Stu I
TM5 (Stu I site) to end of XIP (Bcl I site)
TM5
XIP site
NCX1.1 201 LITFFFFPICVVFAWVADRRLIFYKYIYKRYRAGKQRG
NCX-TR1.0 208 LVTLFFFPLCVGMAYVADRRLIVYKYMYKRYRAGKRRG
Stu I
Bcl I

**Figure 6**

## 3.8 Figure Legends

**Figure 1: Strategy for chimera construction**
Shown is a linear schematic of the NCX topology. Transmembrane segments are depicted as black rectangles and are numbered accordingly. The intracellular loop contains the XIP region, $Ca^{2+}$ binding region, and alternative splicing region as shown. Arrows with relevant restriction enzyme denote approximate areas where the NCX molecule was cut for chimera construction. Sequence alignment is also shown with the numbers indicating the exact amino acid number at which the cut was made.

**Figure 2: Giant patch recordings from *Xenopus* oocytes expressing wild-type and chimeric exchangers**
Representative current traces for wild-type dog (a), trout (b), and chimeric (c-f) $Na^+$-$Ca^{2+}$ exchangers obtained from inside-out giant membrane patches. Currents were induced by the rapid application of 100 mM $Na^+$ to the cytoplasmic surface of the patch. 1 μM regulatory $Ca^{2+}$ and 8 mM transport $Ca^{2+}$ were present in the bath and pipette solutions, respectively. See Figure 5 for chimeric nomenclature.

**Figure 3: Temperature-dependence of the inactivation rate constant, λ, for $I_{NCX}$ from chimeric exchangers**
For DTD, data points represent mean values from 6 patches and 6, 8, and 17 measurements obtained for 7, 14, and 30°C, respectively. For DTT, data points represent mean values from 7 patches and 9, 12, and 28 measurements obtained for 7, 14, and 30°C, respectively. For DTTT, data points represent mean values from 6 patches and 9, 11, and 32 measurements obtained for 7, 14, and 30°C, respectively. For TDD, data points represent mean values from 5 patches and 7, 5, and 17 measurements obtained for 7, 14, and 30°C, respectively. Values of the inactivation rate constants were obtained by fitting current-time traces to a single exponential.

**Figure 4: Arrhenius plots of $I_{NCX}$ for chimeric exchangers**
$I_{NCX}$ peak (panel A) and steady-state (panel B) values for wild type dog (NCX1.1) and trout (NCX-TR1.0) exchangers and various chimeric exchangers, the structures of which are described in Figure 5. Exchange currents were normalized to those obtained at 30°C (~303°K). For the peak currents, data-points are mean values from 3-4 measurements from 3-4 patches, 3-5 measurements from 3-5 patches, 5 measurements from 5 patches, 6 measurements from 6 patches, 6 measurements from 6 patches, and 3-4 measurements from 4 patches for NCX1.1, NCX-TR1.0, DTD, DTT, DTTT, and TDD, respectively. For the steady-state currents, data-points are averaged from 3-4 measurements from 3-4 patches, 3-5 measurements from 3-5 patches, 4 measurements from 4 patches, 5-7 measurements from 7 patches, 6 measurements from 6 patches, and 3-4 measurements from 4 patches for NCX1.1, NCX-TR1.0, DTD, DTT, DTTT, and TDD, respectively. Solid lines represent linear least-squares fit to the experimental values of currents. Fitting of $E_{act}$ values for each exchanger are presented in the table and figure.

**Figure 5: Energy of Activation for wild-type and chimeric exchangers as a function of topology**

For the representation of topology, trout NCX-TR1.0 is shown in black and dog NCX1.1 is shown in gray. $E_{act}$ from peak currents are shown in solid bars and hatched bars represent $E_{act}$ from steady-state currents. + denotes significant difference ($P<0.05$) vs. trout wild type exchanger and * denotes significant difference ($P<0.05$) vs. dog wild type exchanger.

**Figure 6: Amino acid sequence alignment of dog NCX1.1 and trout NCX-TR1.0**

The alignment is split into the first four TM segments and the TM5/XIP site according to the restriction enzyme used to construct the chimera DTTT. Arrows and the corresponding restriction enzyme indicate the site where the exchanger was cut to make the chimera. Identical amino acids are shaded in *black*, conserved amino acids are *shaded*. The sequence alignment was constructed using CLUSTAL W (29).

## 3.9 References


1. **Bers DM.** *Excitation-contraction coupling and cardiac contractile force.* Dordrecht: Kluwer Academic Publishers, 2001.

2. Bers DM, JW Bassani and RA Bassani. Na-Ca exchange and Ca fluxes during contraction and relaxation in mammalian ventricular muscle. *Annals of the New York Academy of Sciences* **779**: 430-442, 1996.

3. Bers DM, CW Patton and R Nuccitelli. A practical guide to the preparation of $Ca^{2+}$ buffers. *Methods in Cell Biology* **40**: 3-29, 1994.

4. Bersohn MM, R Vemuri, DW Schuil, RS Weiss and KD Philipson. Effect of temperature on sodium-calcium exchange in sarcolemma from mammalian and amphibian hearts. *Biochimica et Biophysica Acta* **1062**: 19-23, 1991.

5. Bridge JH, KW Spitzer and PR Ershler. Relaxation of isolated ventricular cardiomyocytes by a voltage-dependent process. *Science* **241**: 823-825, 1988.

6. Dyck C, K Maxwell, J Buchko, M Trac, A Omelchenko, M Hnatowich and LV Hryshko. Structure-function analysis of CALX1.1, a $Na^{+}$-$Ca^{2+}$ exchanger from *Drosophila*. Mutagenesis of ionic regulatory sites. *J Biol Chem* **273**: 12981-12987., 1998.

7. Elias CL, XH Xue, CR Marshall, A Omelchenko, LV Hryshko and GF Tibbits. Temperature dependence of cloned mammalian and salmonid cardiac $Na^{+}/Ca^{2+}$ exchanger isoforms. *Am J Physiol Cell Physiol* **281**: C993-C1000., 2001.

8. Fields PA and GN Somero. Hot spots in cold adaptation: localized increases in conformational flexibility in lactate dehydrogenase A4 orthologs of Antarctic notothenioid fishes. *Proc Natl Acad Sci U S A* **95**: 11476-11481., 1998.

9. Gabellini N, A Zatti, G Rispoli, A Navangione and E Carafoli. Expression of an active $Na^{+}/Ca^{2+}$ exchanger isoform lacking the six C-terminal transmembrane segments. *Eur J Biochem* **239**: 897-904., 1996.

10. He Z, N Petesch, K Voges, W Roben and KD Philipson. Identification of important amino acid residues of the $Na^{+}$-$Ca^{2+}$ exchanger inhibitory peptide, XIP. *J Membr Biol* **156**: 149-156, 1997.

11. He Z, Q Tong, BD Quednau, KD Philipson and DW Hilgemann. Cloning, expression, and characterization of the squid $Na^{+}$-$Ca^{2+}$ exchanger (NCX-SQ1). *J Gen Physiol* **111**: 857-873, 1998.

12. Hilgemann DW, S Matsuoka, GA Nagel and A Collins. Steady-state and dynamic properties of cardiac sodium-calcium exchange. Sodium-dependent inactivation. *J Gen Physiol* **100**: 905-932, 1992.

13. Iwamoto T, A Uehara, TY Nakamura, I Imanaga and M Shigekawa. Chimeric analysis of $Na^{+}/Ca^{2+}$ exchangers NCX1 and NCX3 reveals structural domains important for differential sensitivity to external $Ni^{2+}$ or $Li^{+}$. *J Biol Chem* **274**: 23094-23102., 1999.

14. Iwata T, A Kraev, D Guerini and E Carafoli. A new splicing variant in the frog heart sarcolemmal Na-Ca exchanger creates a putative ATP-binding site. *Ann N Y Acad Sci* **779**: 37-45, 1996.

15. Khananshvili D, E Weil-Maslansky and D Baazov. Kinetics and mechanism: modulation of ion transport in the cardiac sarcolemma sodium-calcium exchanger by protons, monovalent, ions, and temperature. *Ann N Y Acad Sci* **779**: 217-235., 1996.

16. Kimura J, S Miyamae and A Noma. Identification of sodium-calcium exchange current in single ventricular cells of guinea-pig. *J Physiol (Lond)* **384**: 199-222, 1987.

17. Li Z, DA Nicoll, A Collins, DW Hilgemann, AG Filoteo, JT Penniston, JN Weiss, JM Tomich and KD Philipson. Identification of a peptide inhibitor of the cardiac sarcolemmal $Na^+$- $Ca^{2+}$ exchanger. *J Biol Chem* **266**: 1014-1020, 1991.

18. Longoni S, MJ Coady, T Ikeda and KD Philipson. Expression of cardiac sarcolemmal $Na^+$-$Ca^{2+}$ exchange activity in *Xenopus laevis* oocytes. *American Journal of Physiology* **255**: C870-873, 1988.

19. Matsuoka S, DA Nicoll, Z He and KD Philipson. Regulation of cardiac $Na^+$-$Ca^{2+}$ exchanger by the endogenous XIP region. *J Gen Physiol* **109**: 273-286, 1997.

20. Matsuoka S, DA Nicoll, RF Reilly, DW Hilgemann and KD Philipson. Initial localization of regulatory regions of the cardiac sarcolemmal $Na^+$-$Ca^{2+}$ exchanger. *Proc Natl Acad Sci U S A* **90**: 3870-3874., 1993.

21. Miyazaki K, PL Wintrode, RA Grayling, DN Rubingh and FH Arnold. Directed evolution study of temperature adaptation in a psychrophilic enzyme. *J Mol Biol* **297**: 1015-1026., 2000.

22. Nicoll DA, S Longoni and KD Philipson. Molecular cloning and functional expression of the cardiac sarcolemmal $Na^+$-$Ca^{2+}$ exchanger. *Science* **250**: 562-565, 1990.

23. Omelchenko A, C Dyck, M Hnatowich, J Buchko, DA Nicoll, KD Philipson and LV Hryshko. Functional differences in ionic regulation between alternatively spliced isoforms of the $Na^+$-$Ca^{2+}$ exchanger from *Drosophila melanogaster*. *J Gen Physiol* **111**: 691-702, 1998.

24. Russell NJ. Toward a molecular understanding of cold activity of enzymes from psychrophiles. *Extremophiles* **4**: 83-90., 2000.

25. Satoh T, Y Takahashi, N Oshida, A Shimizu, H Shinoda, M Watanabe and T Samejima. A chimeric inorganic pyrophosphatase derived from *Escherichia coli* and *Thermus thermophilus* has an increased thermostability. *Biochemistry* **38**: 1531-1536., 1999.

26. Sheridan PP, N Panasik, JM Coombs and JE Brenchley. Approaches for deciphering the structural basis of low temperature enzyme activity. *Biochim Biophys Acta* **1543**: 417-433., 2000.

27. Sode K, K Watanabe, S Ito, K Matsumura and T Kikuchi. Thermostable chimeric PQQ glucose dehydrogenase. *FEBS Lett* **364**: 325-327., 1995.

28. Svingor A, J Kardos, I Hajdu, A Nemeth and P Zavodszky. A better enzyme to cope with cold. Comparative flexibility studies on psychrotrophic, mesophilic, and thermophilic IPMDHs. *J Biol Chem* **276**: 28121-28125., 2001.

29. Thompson JD, DG Higgins and TJ Gibson. CLUSTAL W: improving the sensitivity of progressive multiple sequence alignment through sequence weighting, position-specific gap penalties and weight matrix choice. *Nucleic Acids Res* **22**: 4673-4680., 1994.

30. Tibbits GF, KD Philipson and H Kashihara. Characterization of myocardial $Na^+$-$Ca^{2+}$ exchange in rainbow trout. *Am J Physiol* **262**: C411-417, 1992.

31. Van Eylen F, A Kamagate and A Herchuelz. A new Na/Ca exchanger splicing pattern identified in situ leads to a functionally active 70kDa $NH_2$-terminal protein. *Cell Calcium* **30**: 191-198., 2001.

32. Wintrode PL, K Miyazaki and FH Arnold. Cold adaptation of a mesophilic subtilisin-like protease by laboratory evolution. *J Biol Chem* **275**: 31635-31640., 2000.

33. Xue XH, LV Hryshko, DA Nicoll, KD Philipson and GF Tibbits. Cloning, expression, and characterization of the trout cardiac $Na^+/Ca^{2+}$ exchanger. *Am J Physiol* **277**: C693-700, 1999.

# CHAPTER 4
# CONTRIBUTION OF N-TERMINAL TRANSMEMBRANE DOMAIN TO $Na^+/Ca^{2+}$ EXCHANGER TEMPERATURE DEPENDENCE: A CHIMERIC AND COMPARATIVE ANALYSIS*

Christian Marshall[1,3], Hoa Dinh Le[2], Alexander Omelchenko[2], Larry V. Hryshko[2], and Glen F. Tibbits[1,3]

[1] Department of Molecular Biology and Biochemistry
Simon Fraser University
Burnaby, BC, Canada

[2] Institute of Cardiovascular Sciences
St. Boniface General Hospital Research Centre
The University of Manitoba
Winnipeg, MB, Canada

[3] Cardiovascular Sciences
BC Research Institute for Children and Women's Health
Vancouver, BC, Canada

* These data have yet to be published

## 4.1 Introduction

As demonstrated in previous chapters, the cardiac $Na^+/Ca^{2+}$ exchanger (NCX) in trout is much less sensitive to decreasing temperatures compared to mammalian NCX1.1. Prior to the molecular cloning of trout cardiac NCX-TR1.0, isolated native protein from trout and mammalian sarcolemmal vesicles suggested this differential temperature sensitivity was an intrinsic property of the NCX protein itself and not influenced by membrane lipid composition (1). This was further confirmed by Elias *et al* (2) using cloned trout NCX-TR1.0 and mammalian NCX1.1 expressed in *Xenopus* oocytes. Trout NCX-TR1.0 peak and steady state currents from giant excised patches measured over a range of 7-30 °C exhibited $E_{act}$ values of 7 and 6 kJ/mol, respectively. Conversely, mammalian NCX1.1 displayed higher sensitivity to temperature with $E_{act}$ values of 53 and 66 kJ/mol for peak and steady state currents, respectively, measured over the same temperature range. In a subsequent study by Marshall *et al* (3), a chimeric strategy was used in an attempt to elucidate the molecular regions responsible for NCX temperature. Chimeras derived from trout and mammalian NCX cDNA were expressed in *Xenopus* oocytes and exchanger currents were measured using the giant excised patch technique. Using this approach, we unequivocally demonstrated that the region responsible for NCX temperature dependence encompasses the N-terminal TMS region of the protein up to the end of the XIP site. Furthermore, we found that approximately 75% of the differential energy of activation is attributable to sequence differences in the region that includes the first four TMS and the remainder to TMS5 and the exchanger inhibitory peptide (XIP) site.

The following set of data is an extension of this initial chimera study and includes the temperature dependence phenotypes of wild type squid and fly exchangers. In the first set of experiments, we continued with a chimera strategy to determine if a region within the N-terminal TMS segment is responsible for NCX temperature dependence phenotypes. Insertion of two additional homologous restriction sites in trout NCX-TR1.0 and canine NCX1.1 proximal and distal to intracellular loop b allowed construction of four additional chimeras with various combinations of genotypes. Specifically, this allowed rough isolation of the N-terminus and TM1, loop b, and TMS2-4 including the

alpha-1 region. NCX-mediated currents from the new chimeric constructs yielded equivocal results, and failed to define further a region within the N-terminal TMS responsible for NCX temperature dependence. In the second set of experiments we measured the temperature dependence of fruit fly CALX and squid NCX-SQ1. As expected, NCX-SQ1 functions well in low temperatures and has similar temperature dependence to trout NCX-TR1.0 whereas CALX has intermediate temperature dependence. A multiple sequence alignment of these NCX isoforms points to amino acid positions that may confer NCX temperature dependence, specifically a position in loop C of the α-1 repeat that is a threonine in NCX1.1 but a negatively charged residue (i.e. aspartic or glutamic acid) in the cold adaptive species. However, mutation of this residue in a NCX1.1 background did not significantly change the temperature dependence. Most likely, a combination of residues in the N-terminal region is responsible for NCX temperature dependence.

## 4.2 Methods

### 4.2.1 Chimera Construction and Mutations

The strategy used for the construction of all N-terminal chimeras, including the four new ones from this study, is shown in Figure 1. Our approach was to increase the trout genotype in a stepwise manner from the carboxy end towards the amino terminal using the previously constructed chimera DTTT (3) and trout NCX-TR1.0. All mutations for chimera construction were generated in 200-500 bp cassettes using the QuikChange™ site-directed mutagenesis kit (Stratagene, La Jolla, CA) and confirmed by sequencing. For the DTTT chimera, a pair of restriction sites, AvrII and TthIII1, were introduced through silent mutation at nucleotide positions (from start codon) 258 and 390, respectively. The trout NCX-TR1.0 cDNA contains an endogenous TthIII1 site at nucleotide position 414; however the AvrII site had to be introduced through silent mutation at position 282. The chimeras were constructed by rearranging homologous regions of trout NCX-TR1.0 and the DTTT chimera using the newly introduced sites (AvrII and TthIII1) and the StuI site previously introduced (see Figure 1). For dog NCX1.1, the AvrII, TthIII1, and StuI sites are located at amino acid positions (mature

protein) 54, 98, and 199, respectively. AvrII, TthIII1, and StuI positions for trout NCX-TR1.0 are at amino acid positions 62, 106, and 207, respectively.

### 4.2.2 Expression of NCX Constructs in *Xenopus* Oocytes

NCX cRNA was synthesized and expressed in *Xenopus* oocytes as described previously (3). All chimeric constructs and wild-type dog NCX1.1, trout NCX-TR1.0, and fruit fly CALX constructs were subcloned in a modified pBluescript SK+ containing the 3' untranslated region of a $Na^+$/glucose transported with a poly(A)$^+$ tail (4). cDNA from these clones was linearized with HindIII, and cRNA was synthesized *in vitro* using the T3 mMessage mMachine Kit (Ambion, Austin, TX). The squid NCX-SQ1 construct, having poor expression in the modified pBluescript SK+, was subcloned in pBSTA vector containing the 5' and 3' untranslated regions of *Xenopus* β-globin (5). The squid NCX-SQ1 was linearized with SacII and cRNA was synthesized *in vitro* using the T7 kit mMessage mMachine Kit (Ambion, Austin, TX). The cRNA amount was assessed spectroscopically, while cRNA purity was determined with a 1% agarose RNA gel. Oocytes were prepared as described previously (6), and injected with 46 nl of cRNA diluted to 0.5 ng/nl. Exchange activity was assessed 3-7 days after injection using the giant excised patch technique (see below).

### 4.2.3 Electrophysiology, Analysis, and Statistics

Assay of NCX activity and measurement of temperature dependence was performed as described previously (3). Outward $Na^+/Ca^{2+}$ exchange currents were activated by switching from $Li^+$- to $Na^+$-based bath solution and recorded at 30, 14, and 7 $^oC$. To account for current rundown within a single patch, multiple current traces at all three temperatures were measured. Axon Instruments (Union City, CA) hardware and software were used for data acquisition and analysis. The energy of activation, $E_{act}$, and temperature coefficient, $Q_{10}$, were calculated as indices of temperature dependence as described by Marshall *et al* (3). The inactivation rate constant, $\lambda$, and ratio of steady-state to peak current, $F_{ss}$, were calculated as kinetic properties as described previously (3). All values are displayed as means ± standard error of means (SEM). Statistical significance of the results was determined by mean comparison using Tukey's test and

one-way ANOVA performed with Microcal Origin and Graphpad software. Unless indicated otherwise, a value of $p<0.05$ was considered significantly different.

## 4.3 Results and Discussion

### 4.3.1 Temperature Dependence of N-terminal Chimeras

Using chimeras we have previously determined that the N-terminal TMS domain is solely responsible for determining NCX temperature dependence (3). In the mature protein, this region is ~240 residues, constituting approximately one quarter of the overall length of NCX. Isolation of TMS5 and the XIP site showed that, although having an effect, this region was not the main contributor to NCX temperature dependence. Continuing with this chimeric strategy, two more restriction sites where introduced in the N-terminal region allowing the construction of four new chimeras that roughly isolated the effect of loop b and the TMS2-4 on NCX temperature sensitivity. Representative traces of NCX mediated outward currents measured at 7, 14 and 30 °C for wild-type and chimeric exchangers are shown in Figure 2. Even from the raw traces it is evident that all chimeras display varying degrees of intermediate temperature dependence. The chimera TDTTT (containing dog TMS2-4) has a temperature dependence phenotype similar to canine NCX, whereas the chimera TDTTTT (containing dog loop b) has predominately trout-like temperature sensitivity. Chimeras DTTTT and DTTTTT, differing only by the genetic origin of loop b, have temperature dependence phenotypes that are intermediate to trout and dog. These observations are reflected in the temperature dependence parameters, $Q_{10}$ and $E_{act}$, displayed in Figures 3 and 4, respectively. For comparison, wild-type dog and trout NCX along with the chimeras DTT, DTTT and TDD from previous studies are shown. Unfortunately, due to the low signal to noise ratio resulting from small absolute currents, the limited number of temperatures measured, and the small number of chimeras used, it is very difficult to attach a quantitative value to the contribution of each region. Previously a comparison of DTT and DTTT $Q_{10}$ and $E_{act}$ values indicated that TMS5 and the XIP site contributed ~25% to NCX temperature dependence (3). However, in this study analysis of the new chimeras often gave conflicting results. For example, comparison of DTTT and DTTTT indicates TMS2-4

has a small effect on temperature dependence whereas the chimera TDTTT shows that this region's contribution is large. Similarly, a comparison of TDTTT and DTTT indicates the N-terminus and TMS1 has no effect on NCX temperature dependence but the chimera DTTTTT would indicate otherwise. What is apparent from Figures 3 and 4 is a general trend showing temperature phenotype being proportional to genotype origin (i.e. trout or dog NCX). This observation argues against the idea that a single region within the N-terminal TMS domain dictates NCX temperature dependence. Rather, it is likely that NCX temperature dependence phenotype is defined by several sequence differences in positions located throughout the primary sequence of the N-terminal region. It is possible that these residues are close in tertiary space; however, this is not known since very little information on the 3D structure of NCX is available. $Q_{10}$ and $E_{act}$ values for all chimeras are shown in Table 1, along with the inactivation parameter values, $\lambda$ and $F_{ss}$. For the inactivation parameters, no significant trends exist except that $\lambda$ decreases with temperature for all constructs. We have previously shown that NCX temperature dependence is independent of regulatory properties such as $Na^+$-dependent inactivation and $Ca^{2+}$ dependent inactivation (2).

### 4.3.2 Species Comparison of NCX Temperature Dependence

In a previous study, we completed a detailed analysis comparing the temperature dependence of wild-type canine NCX1.1 and trout NCX-TR1.0 (2). It was shown that the temperature dependence of NCX is an intrinsic property of the protein itself and is not dependent on differences in NCX regulatory properties between isoforms. Results from our chimera studies indicate that the whole N-terminal TMS domain is important for NCX temperature dependence and is not attributable to a single region within this domain. A comparison of amino acid sequence shows ~40 differences between trout NCX-TR1.0 and canine NCX1.1 in the N-terminal TMS domain, which is ~240 residues in length. To establish a link between genotype and temperature sensitivity, we expanded our phenotypic data by measuring the temperature dependence of NCX isoforms from the ectotherms, fruit fly and squid. We hypothesized that NCX isoforms from cold adapted ectothermic species may have residues conserved in positions that are important for

function at low temperatures. Further, warm-adapted species would have different residues in the same position.

Figure 5 shows a comparison of NCX-mediated outward currents measured at 7, 14, and 30 °C for wild-type canine NCX1.1, fruit fly CALX, squid NCX-SQ1, and trout NCX-TR1.0. Representative current traces are shown together with averages of the temperature dependence parameters $Q_{10}$ and $E_{act}$. As expected, the squid NCX-SQ1 has similar temperature dependence to trout NCX-SQ1 since the species typically inhabits ocean waters off the coast of Southern California (~ 13 °C) (7). The $Q_{10}$ values for NCX-SQ1 are almost identical to the trout NCX-TR1.0 (~1.2), whereas the $E_{act}$ values are slightly higher, but not significantly greater. The fruit fly is capable of surviving over a larger range of environmental temperatures than (>30 °C range) (8) trout or squid species and as such one would expect its proteins to adequately function over a large range of temperatures. This is reflected in fruit fly CALX mediated currents, which have a temperature dependence that is intermediate to trout NCX-TR1.0 and canine NCX1.1. $Q_{10}$ values for steady state CALX outward currents are 2.0 and 1.7, respectively, and the $E_{act}$ values are 50 and 35 kJ/mol, respectively. Interestingly, the temperature dependence of CALX peak currents is closer to canine NCX1.1 values whereas the steady state temperature dependence is more intermediate between NCX1.1 and NCX-TR1.0. This disparity may be a result of the relatively fast inactivation rates of CALX compared to the other isoforms, especially at 30 °C. Figure 6 shows a multiple sequence alignment of the N-terminal TMS domains for all four NCX isoforms. Immediately noticeable is the high overall identity amongst isoforms despite their diverse phylogenetic origins, especially in the TMS and α-1 repeat region. In comparing genotypes with respect to temperature dependence phenotype, it had proven difficult to find sequence patterns. This is due to the high variability in positions where sequence differences do exist and the relatively small sample size of sequences. However, using this strategy did point to one interesting sequence position, located in the extracellular loop spanning TMS2 and 3. This extracellular loop is part of the α-1 repeat region, and is thought to form a re-entrant loop in a manner similar to the pore forming loops of ion channels (9). Position 127 of the mature NCX1.1 (159 with the signal peptide) is denoted by an asterisk in Figure 6. At this position the highly temperature sensitive NCX1.1 has a threonine, while the

ectothermic species all have a negatively charged glutamic (NCX-SQ1 and CALX) or aspartic acid (NCX-TR1.0). Since this position is in a region important for ion translocation, we reasoned it could have an effect on NCX temperature dependence and therefore replaced the threonine in NCX1.1 with an aspartic acid. The temperature dependence of the NCX1.1 T127D mutant compared to wild-type NCX1.1 is displayed in Figure 7. As clearly shown, there is no significant difference in the temperature dependence of NCX mediated outward currents between the wild-type and mutant exchanger. On its own, the T127D mutation does not affect NCX temperature sensitivity; however, it is possible that in combination with other substitutions this position is important for conferring differential temperature dependence phenotypes.

## 4.4 Conclusions and Perspective

In conclusion, the molecular interactions determining NCX temperature dependence are complex and multifaceted in nature. Our chimera studies show the entire N-terminal TMS domain is required to confer a temperature dependence phenotype, and further is not associated with any particular region within this domain. A comparison of NCX temperature dependence phenotype and genotype from four different species did not point to obvious mutations that may affect NCX temperature sensitivity. Taken together, these data indicate that a series of mutations throughout the N-terminal TMS domain are responsible for NCX temperature dependence.

These studies represent the first attempt at linking NCX genotype to temperature dependence phenotype through comparison of multiple isoforms. Although in its rudimentary stages, sequence analyses in this manner has proved a viable strategy to derive specific hypotheses as to which residues are important for NCX temperature dependence. However, only a small number of sequences were used and more importantly, the evolutionary relationship between these isoforms is largely unknown. For instance, it is not currently known if the NCX homologs used in the above studies represent paralogous or orthologous sequences. It is clear that the number of NCX sequences needs expanding and that the molecular phylogeny of the exchanger needs to be clarified.

## 4.5 Tables

**Table 1:** Temperature Dependence and Inactivation Parameters for NCX Chimeras

| CONSTRUCT | | TEMPERATURE DEPENDENCE | | | | INACTIVATION PARAMETERS | | | | | |
|---|---|---|---|---|---|---|---|---|---|---|---|
| Name | Topology | $Q_{10}$ | | $E_{act}$ (kJ/mol) | | lambda | | | $F_{ss}$ | | |
| | | $I_{peak}$ | $I_{ss}$ | $I_{peak}$ | $I_{ss}$ | 7 °C | 14 °C | 30 °C | 7 °C | 14 °C | 30 °C |
| NCX1.1 | 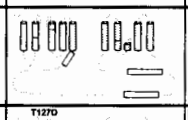 | 2.4±0.4 (n=4) | 2.6±0.4 (n=4) | 53±1.0 (n=4) | 66±9.0 (n=4) | 0.135 ±0.030 (n=7) | 0.159 ±0.053 (n=7) | 0.258 ±0.031 (n=16) | 0.28±0.05 (n=7) | 0.24±0.04 (n=7) | 0.17±0.02 (n=16) |
| $NCX1.1_{T127D}$ | 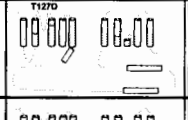 | 2.7±0.2 (n=7) | 2.8±0.2 (n=7) | 62±4.5 (n=5) | 63±6.1 (n=5) | 0.134 ±0.006 (n=6) | 0.204 ±0.017 (n=7) | 0.262 ±0.025 (n=7) | 0.31±0.04 (n=7) | 0.37±0.06 (n=7) | 0.39±0.08 (n=7) |
| DTD | 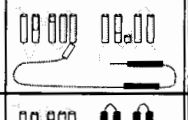 | 2.3±0.3 (n=5) | 2.5±0.6 (n=4) | 48±6.0 (n=5) | 52±7.0 (n=4) | 0.163 ±0.015 (n=6) | 0.149 ±0.021 (n=6) | 0.25 ±0.075 (n=6) | 0.24±0.03 (n=6) | 0.24±0.03 (n=6) | 0.19±0.04 (n=6) |
| DTT | 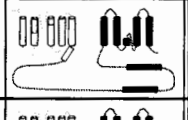 | 2.7±0.2 (n=6) | 2.5±0.1 (n=5) | 63±9.0 (n=6) | 65±4.0 (n=5) | 0.222 ±0.054 (n=5) | 0.269 ±0.052 (n=5) | 0.296 ±0.052 (n=7) | 0.37±0.05 (n=5) | 0.23±0.04 (n=5) | 0.28±0.03 (n=7) |
| DTTT | 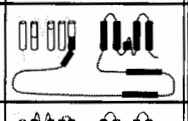 | 2.0±0.1 (n=6) | 2.2±0.1 (n=6) | 40±6.0 (n=6) | 39±4.0 (n=6) | 0.154 ±0.017 (n=6) | 0.137 ±0.024 (n=6) | 0.203 ±0.032 (n=6) | 0.42±0.06 (n=6) | 0.38±0.07 (n=6) | 0.40±0.04 (n=6) |
| DTTTT | 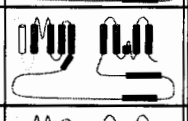 | 1.7±0.1 (n=9) | 1.9±0.1 (n=9) | 30±4.3 (n=9) | 34±10 (n=9) | 0.117 ±0.011 (n=6) | 0.106 ±0.014 (n=6) | 0.112 ±0.021 (n=6) | 0.42±0.06 (n=12) | 0.53±0.05 (n=12) | 0.52±0.05 (n=12) |
| DTTTTT | 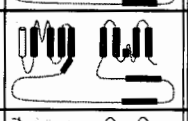 | 1.5±0.1 (n=9) | 1.6±0.1 (n=9) | 27±4.5 (n=9) | 33±5.6 (n=9) | 0.148 ±0.021 (n=9) | 0.136 ±0.010 (n=9) | 0.172 ±0.019 (n=9) | 0.50±0.04 (n=9) | 0.56±0.03 (n=9) | 0.60±0.03 (n=9) |
| TDTTT | 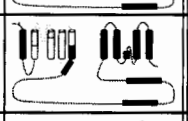 | 2.2±0.1 (n=11) | 2.3±0.1 (n=11) | 40±4.0 (n=6) | 42±7.3 (n=6) | 0.116 ±0.018 (n=12) | 0.154 ±0.031 (n=12) | 0.256 ±0.073 (n=12) | 0.38±0.07 (n=12) | 0.41±0.07 (n=12) | 0.37±0.06 (n=12) |
| TDTTTT |  | 1.4±0.1 (n=6) | 1.5±0.1 (n=5) | 19±3.7 (n=5) | 22±6.8 (n=5) | 0.151 ±0.017 (n=8) | 0.171 ±0.024 (n=8) | 0.236 ±0.029 (n=8) | 0.26±0.08 (n=7) | 0.29±0.08 (n=7) | 0.29±0.07 (n=7) |
| TDD |  | 1.3±0.1 (n=4) | 1.2±0.0 (n=4) | 15±6.0 (n=4) | 14±1.0 (n=4) | 0.069 ±0.005 (n=5) | 0.077 ±0.020 (n=3) | 0.084 ±0.016 (n=5) | 0.56±0.07 (n=5) | 0.55±0.08 (n=3) | 0.48±0.03 (n=5) |
| NCX-TR1.0 |  | 1.2±0.1 (n=5) | 1.1±0.1 (n=5) | 7.0±2.0 (n=5) | 6.0±0.1 (n=5) | 0.103 ±0.007 (n=5) | 0.101 ±0.020 (n=4) | 0.166 ±0.016 (n=9) | 0.21±0.04 (n=5) | 0.23±0.08 (n=4) | 0.19±0.03 (n=9) |

## 4.6 Figures

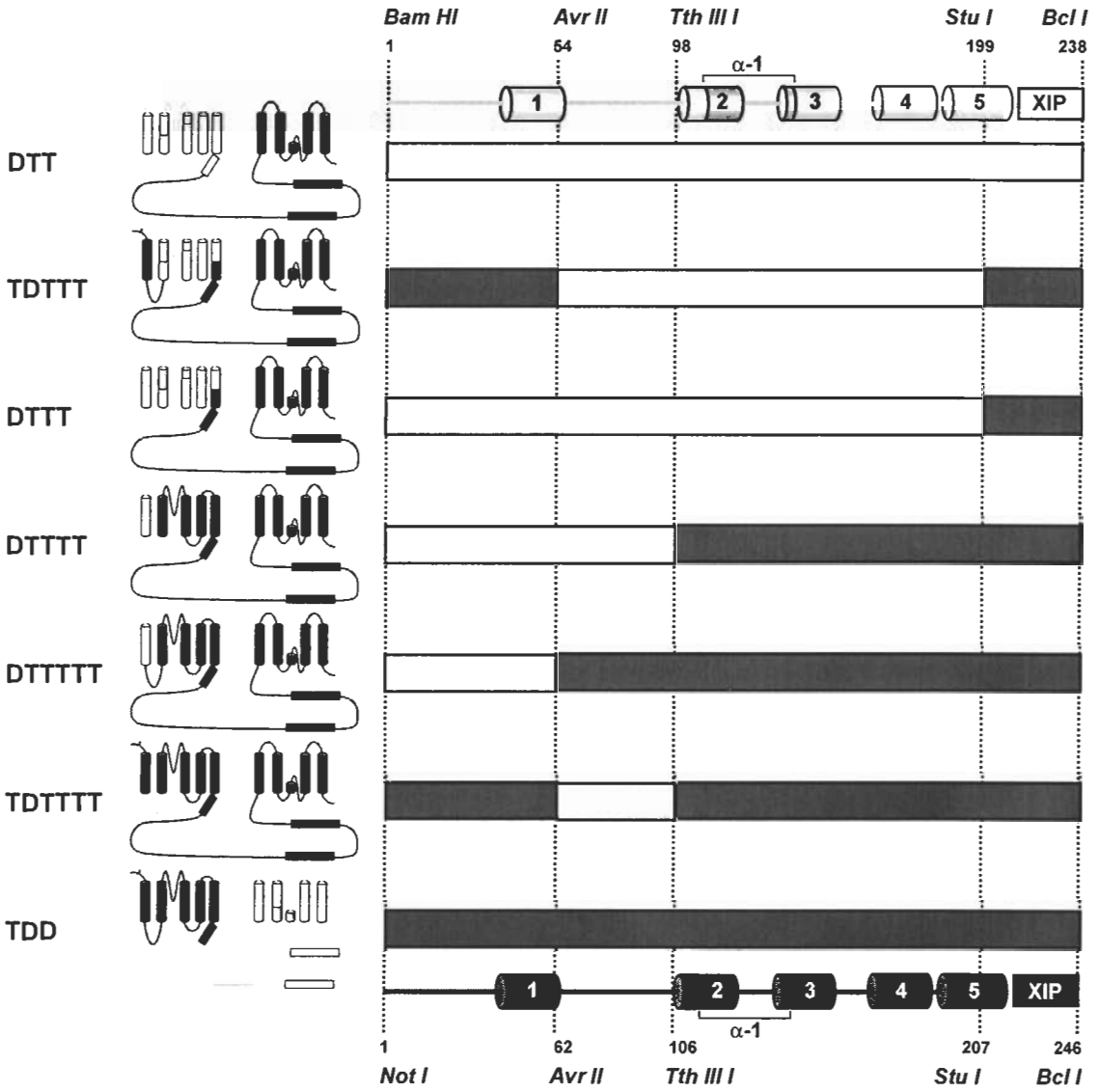


**Figure 1**

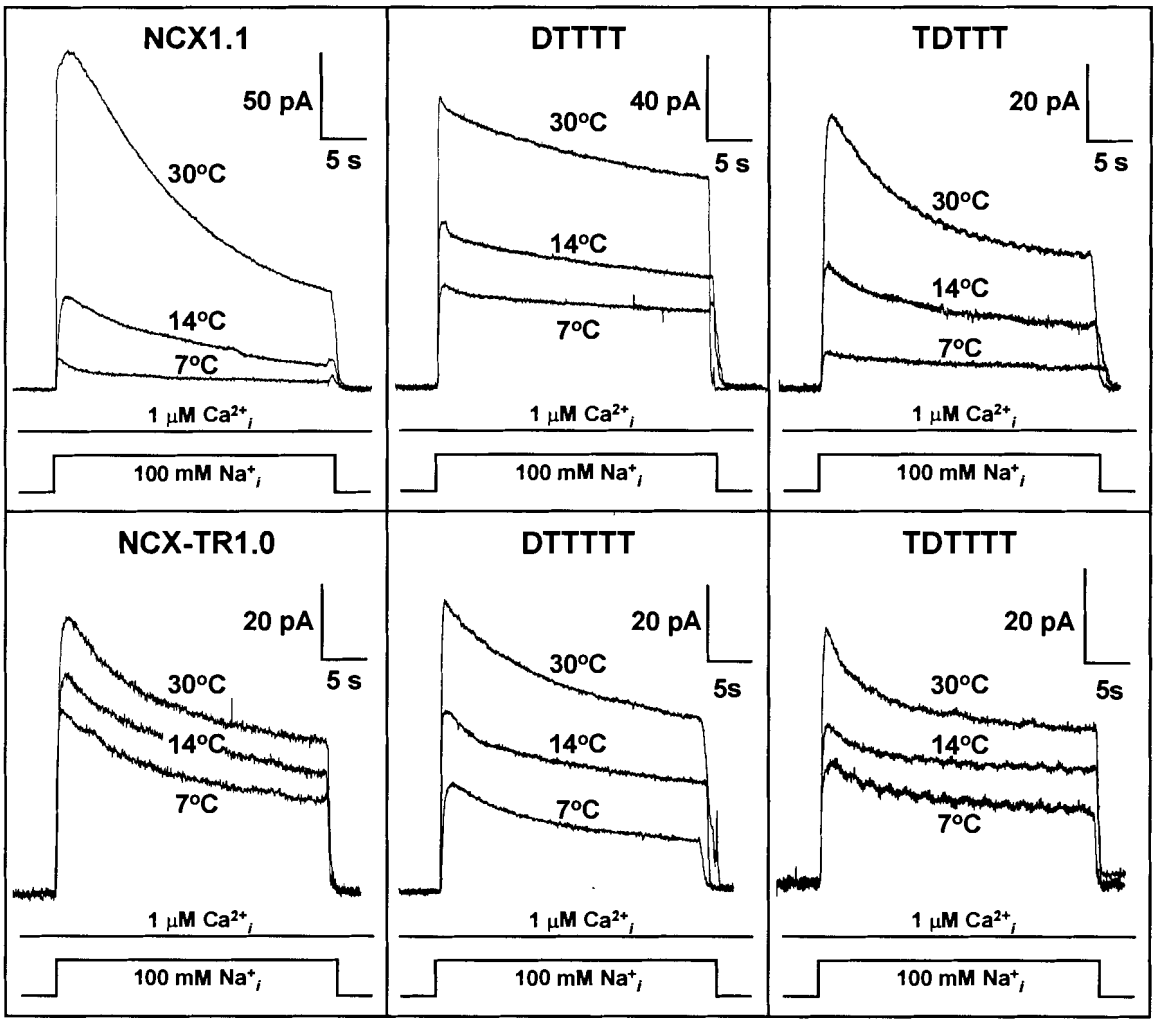
NCX1.1
50 pA
5 s
30°C
14°C
7°C
1 μM Ca2+i
100 mM Na+i
DTTTT
40 pA
5 s
30°C
14°C
7°C
1 μM Ca2+i
100 mM Na+i
TDTTT
20 pA
5 s
30°C
14°C
7°C
1 μM Ca2+i
100 mM Na+i
NCX-TR1.0
20 pA
5 s
30°C
14°C
7°C
1 μM Ca2+i
100 mM Na+i
DTTTTT
20 pA
5s
30°C
14°C
7°C
1 μM Ca2+i
100 mM Na+i
TDTTTT
20 pA
5s
30°C
14°C
7°C
1 μM Ca2+i
100 mM Na+i

**Figure 2**

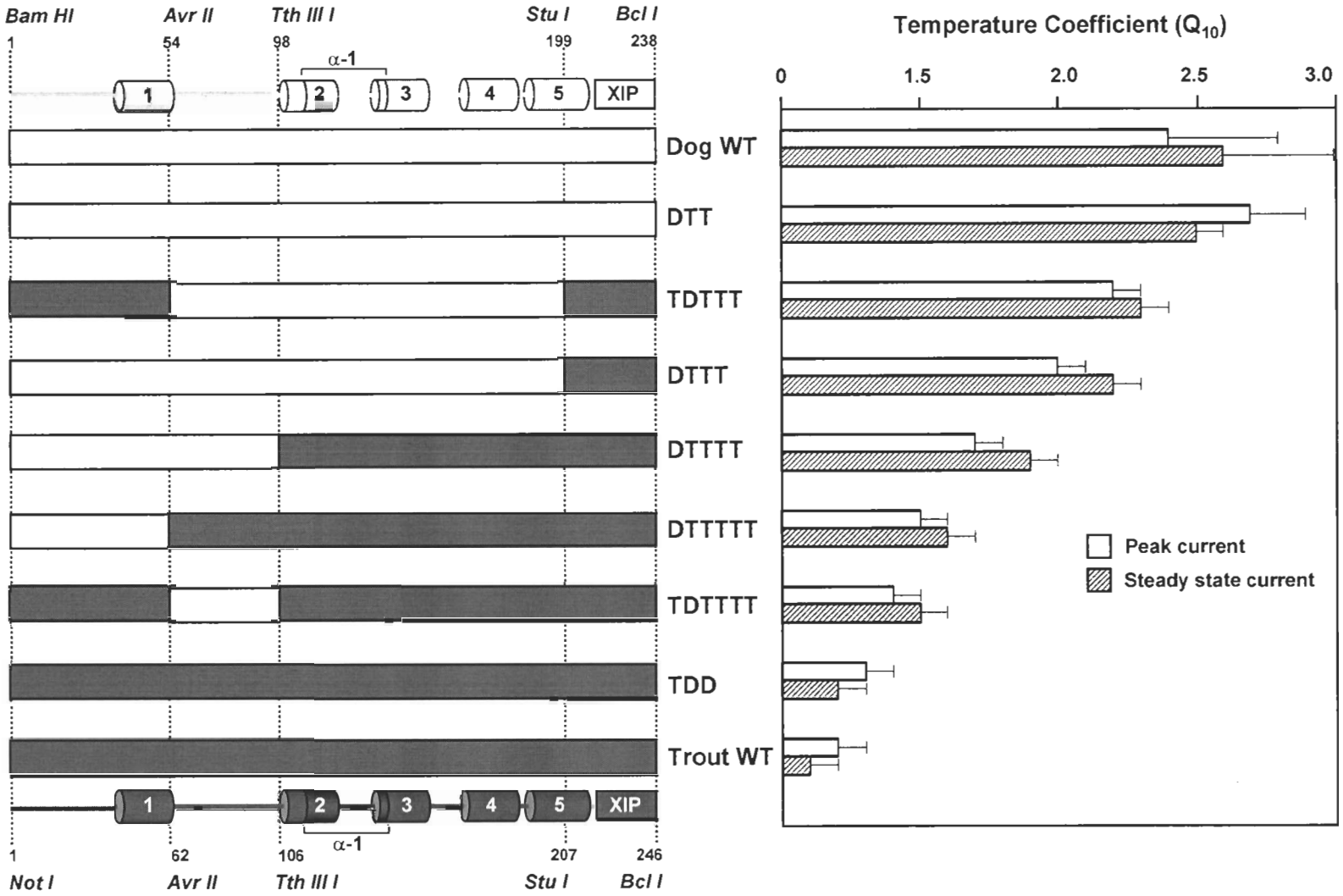
Bam HI
Avr II
Tth III I
Stu I
Bcl I
1
54
98
199
238
α-1
1
2
3
4
5
XIP
Dog WT
DTT
TDTTT
DTTT
DTTTT
DTTTTT
TDTTTT
TDD
Trout WT
1
62
106
207
246
α-1
Not I
Avr II
Tth III I
Stu I
Bcl I
Temperature Coefficient (Q10)
0
1.5
2.0
2.5
3.0
Peak current
Steady state current

Figure 3

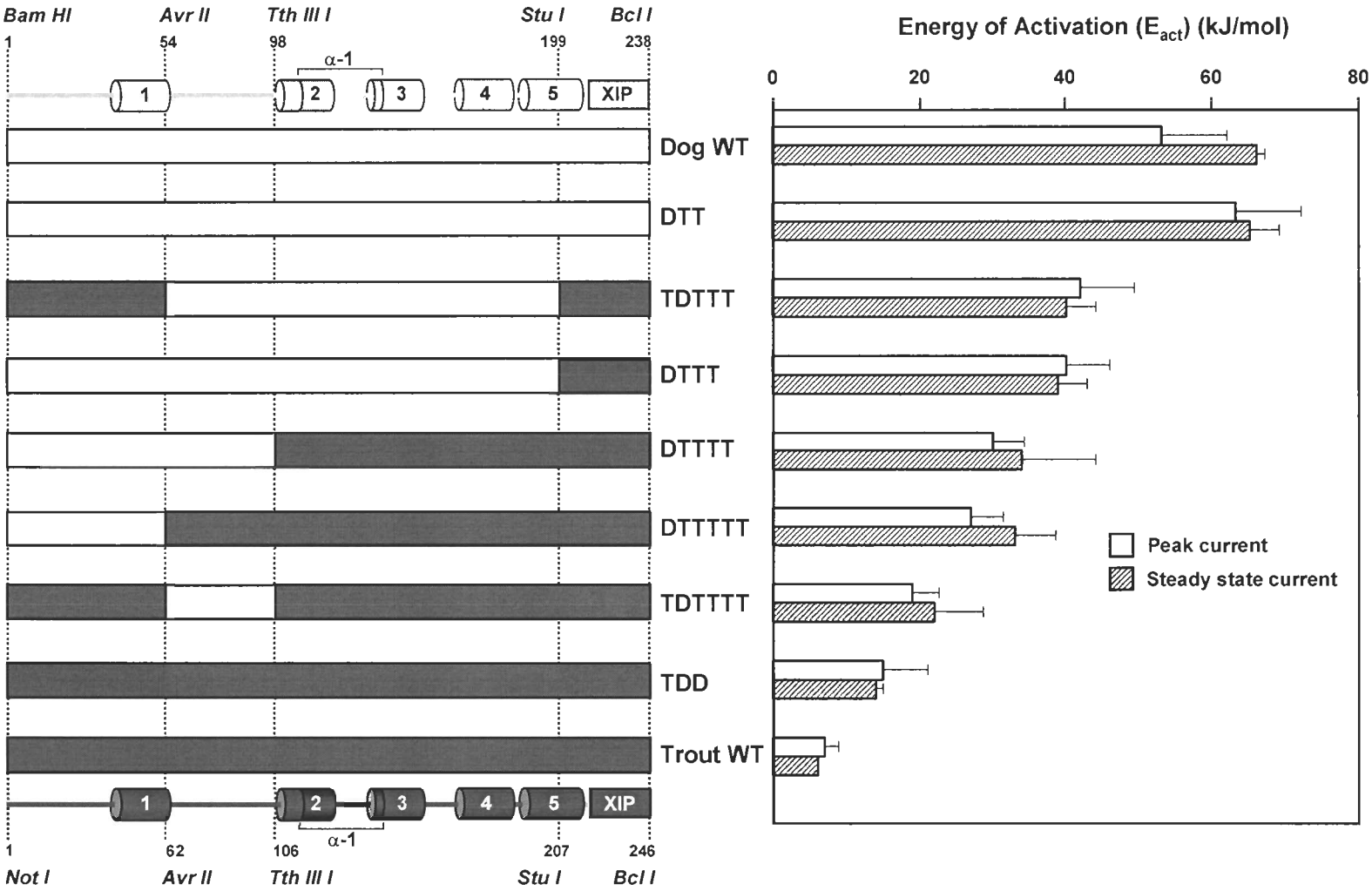
Bam HI
Avr II
Tth III I
Stu I
Bcl I
1
54
98
199
238
α-1
1
2
3
4
5
XIP
Dog WT
DTT
TDTTT
DTTT
DTTTT
DTTTTT
TDTTTT
TDD
Trout WT
1
62
106
207
246
α-1
Not I
Avr II
Tth III I
Stu I
Bcl I
Energy of Activation (E$_{act}$) (kJ/mol)
0
20
40
60
80
Peak current
Steady state current

Figure 4

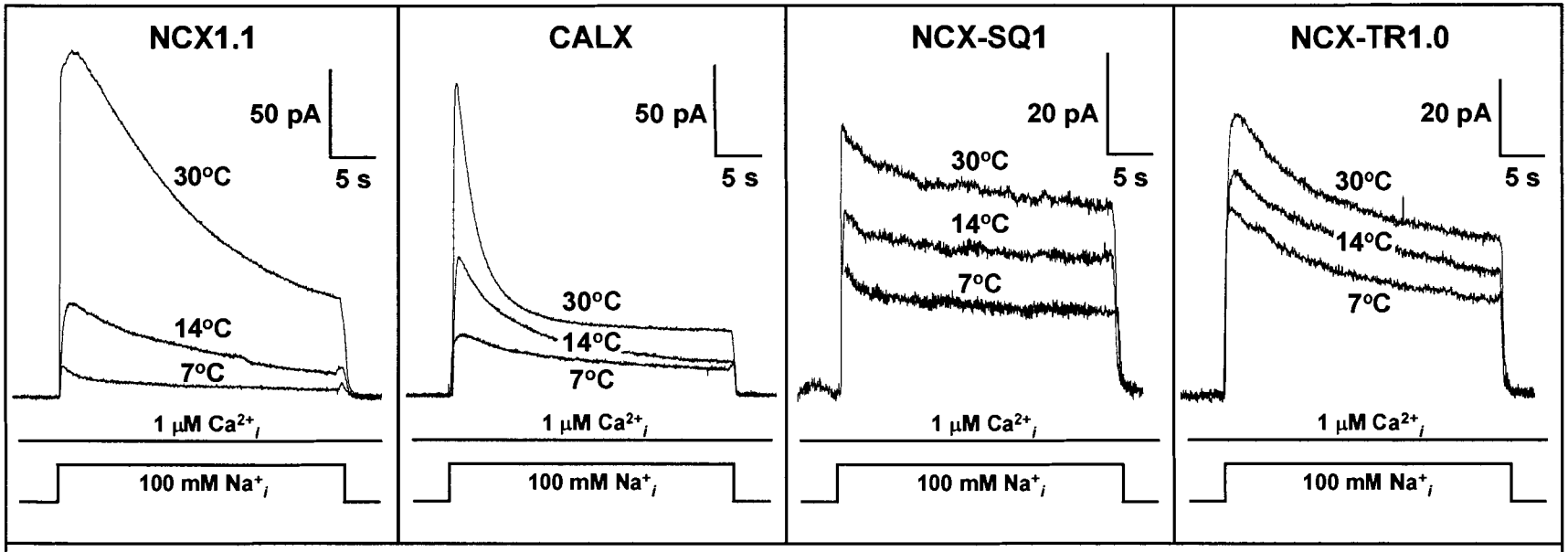


| TEMPERATURE COEFFICIENT ($Q_{10}$) | | | | | | | |
|---|---|---|---|---|---|---|---|
| $I_{peak}$ | $I_{SS}$ | $I_{peak}$ | $I_{SS}$ | $I_{peak}$ | $I_{SS}$ | $I_{peak}$ | $I_{SS}$ |
| 2.4 ± 0.4 | 2.6 ± 0.4 | 2.0 ± 0.1 | 1.7 ± 0.1 | 1.2 ± 0.1 | 1.2± 0.1 | 1.2 ± 0.1 | 1.1 ± 0.1 |
| ENERGY OF ACTIVATION ($E_{act}$) | | | | | | | |
| $I_{peak}$ | $I_{SS}$ | $I_{peak}$ | $I_{SS}$ | $I_{peak}$ | $I_{SS}$ | $I_{peak}$ | $I_{SS}$ |
| 53 ± 1.0 | 66 ± 1.0 | 50 ± 4.0 | 35 ± 3.0 | 14 ± 3.4 | 13 ± 1.5 | 7.0 ± 2.0 | 6.0 ± 0.1 |

Figure 5

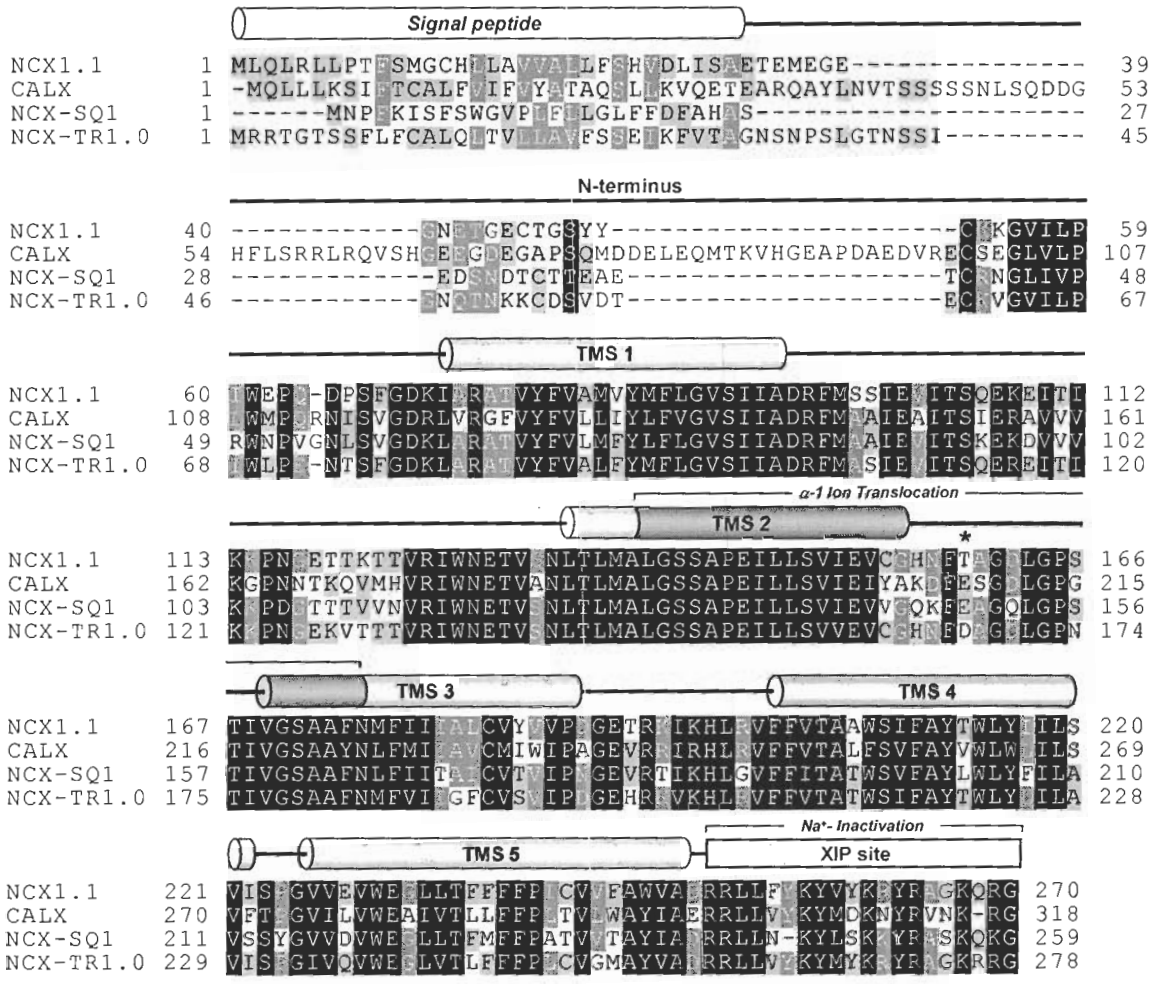
Signal peptide
N-terminus
TMS 1
α-1 Ion Translocation
TMS 2
TMS 3
TMS 4
Na+- Inactivation
TMS 5
XIP site
NCX1.1
CALX
NCX-SQ1
NCX-TR1.0

**Figure 6**

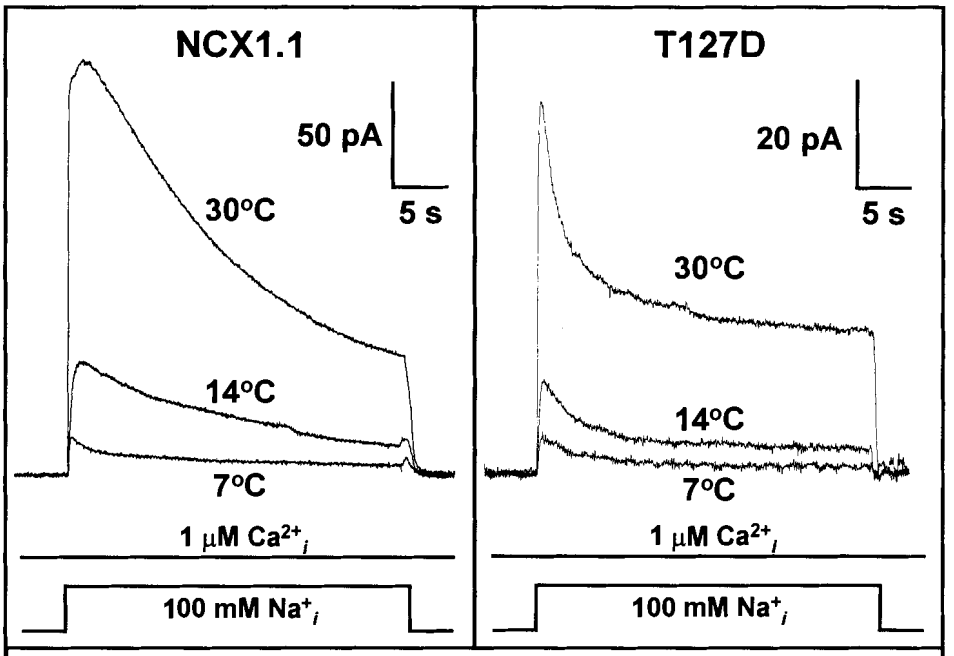


| TEMPERATURE COEFFICIENT ($Q_{10}$) | | | |
|---|---|---|---|
| $I_{peak}$ | $I_{SS}$ | $I_{peak}$ | $I_{SS}$ |
| 2.4 ± 0.4 | 2.6 ± 0.4 | 2.7 ± 0.2 | 2.8 ± 0.2 |
| **ENERGY OF ACTIVATION ($E_{act}$)** | | | |
| $I_{peak}$ | $I_{SS}$ | $I_{peak}$ | $I_{SS}$ |
| 53 ± 1.0 | 66 ± 1.0 | 62 ± 4.5 | 63 ± 6.1 |

**Figure 7**

## 4.7 Figure Legends

**Figure 1: Strategy for Construction of N-terminal Chimeras**
NCX is currently modelled to have nine transmembrane spanning segments (TMS) with five in the N-terminal domain separated from four in the C-terminal domain by a large intracellular loop. Chimeras were constructed by substituting regions of trout NCX-TR1.0 (T) with homologous regions of dog NCX1.1 (D), and named based on the genotype of the specific region. Overall NCX topology is shown to the right of the chimera name, with trout and canine regions depicted in dark grey and light grey, respectively. All chimeras except for TDD have a trout genotype after the XIP site. To the right of the overall topology is a detailed schematic of the N-terminal TMS domain, which extends to the end of the XIP site. Restriction enzyme cut sites are shown by broken lines and trout and canine substituted regions are depicted in dark grey and light grey, respectively. Numbers indicate the amino acid residue number of the mature protein where each restriction enzyme cuts. NCX secondary structure is shown at the top (NCX1.1) and bottom (NCX-TR1.0), with numbered cylinders representing TMS, a rectangular box denoting the XIP site, and α-1 repeat shown between TMS2 and 3.

**Figure 2: Giant Excised Patch Recordings for Wild-type and Chimeric Exchangers**
Representative outward currents from canine NCX1.1, trout NCX-TR1.0, and chimeric exchangers were obtained from inside-out giant membrane patches. Currents were induced by the rapid application of 100 mM $Na^+$ to the cytoplasmic surface of the patch. Pipettes contained 8 mM $Ca^{2+}$ and currents were generated by the rapid application of 100 mM intracellular $Na^+$ ($Na^+_i$) to the cytoplasmic surface of the patch in the continuous presence of 1 μM regulatory intracellular $Ca^{2+}$ ($Ca^{2+}_i$) at the temperatures indicated.

**Figure 3: Temperature Coefficients for Wild-type and Chimeric Exchangers**
The left panel shows chimera topology as described in Figure 1. In the right panel, temperature coefficient ($Q_{10}$) values for peak (*open bars*) and steady-state (*hatched bars*) currents are shown as a function of NCX topology. Error bars represent standard error of means.

**Figure 4: Energy of Activation for Wild-type and Chimeric Exchangers**
The left panel shows chimera topology as described in Figure 1. In the right panel, energy of activation ($E_{act}$) values for peak (*open bars*) and steady-state (*hatched bars*) are shown as a function of NCX topology. Error bars represent standard error of means.

**Figure 5: Giant Excised Patch Recordings and Temperature Parameters for Wild-type Canine NCX1.1, Fruit fly CALX, Squid NCX-SQ1, and Trout NCX-TR1.0.**
The top panel shows representative outward currents from inside-out giant membrane patches from *Xenopus* oocytes expressing canine NCX1.1, fruit fly CALX, squid NCX-SQ1, and trout NCX-TR1.0. Currents were induced by the rapid application of 100 mM $Na^+$ to the cytoplasmic surface of the patch. Pipettes contained 8 mM $Ca^{2+}$ and currents were generated by the rapid application of 100 mM intracellular $Na^+$ ($Na^+_i$) to the cytoplasmic surface of the patch in the continuous presence of 1 μM regulatory

intracellular $Ca^{2+}$ ($Ca^{2+}_i$) at the temperatures indicated. The lower panels show temperature coefficients ($Q_{10}$) and energy of activation ($E_{act}$ – kJ/mol) values (± SEM) for all species.

**Figure 6: Multiple Sequence Alignment of the NCX N-terminal TMS domain**
Sequences were acquired from the National Center for Biotechnology Information (NCBI) non redundant protein database under the following accession numbers: rainbow trout NCX-TR1.0 (GI 6273849), canine NCX1.1 (GI 127793), fruit fly CALX (GI 2266953), and squid NCX-SQ1 (GI 1947092). Sequences were aligned with ClustalX (Version 1.83) (REF Alsutch, 1990) using the default parameters then imported into Genedoc (Version 2.6.002) (REF Nicolas) for manual editing. Exchanger topology is represented schematically above the sequence alignment. The N-terminal domain is modelled to have 5 TMS (*light gray cylinders*) and a signal peptide (*open cylinder*) that is cleaved during biosynthesis. The α1-repeat region (*shaded dark gray*) is important for ion translocation and the XIP site (*light gray box*) is implicated in $Na^+$-dependent inactivation. The asterisk (*) denotes a threonine at position 127 of mature canine NCX1.1, which was mutated to an aspartic acid (see Figure 7). This mutation was found to have no effect on NCX temperature dependence.

**Figure 7: Giant Excised Patch Recordings and Temperature Parameters for Wild-type Canine NCX1.1 and Mutant Canine NCX1.1 T127D.**
The top panel shows representative outward currents from inside-out giant membrane patches from *Xenopus* oocytes expressing canine NCX1.1 and the NCX1.1 T127D mutant. Currents were induced by the rapid application of 100 mM $Na^+$ to the cytoplasmic surface of the patch. Pipettes contained 8 mM $Ca^{2+}$ and currents were generated by the rapid application of 100 mM intracellular $Na^+$ ($Na^+_i$) to the cytoplasmic surface of the patch in the continuous presence of 1 μM regulatory intracellular $Ca^{2+}$ ($Ca^{2+}_i$) at the temperatures indicated. The lower panels show temperature coefficients ($Q_{10}$) and energy of activation ($E_{act}$ –kJ/mol) values (± SEM). No significant differences exist between the temperature dependence of the wild-type and mutant NCX1.1.

## 4.8 References


1. Tibbits, G. F., Philipson, K. D., and Kashihara, H. (1992) *Am J Physiol* **262**, C411-417
2. Elias, C. L., Xue, X. H., Marshall, C. R., Omelchenko, A., Hryshko, L. V., and Tibbits, G. F. (2001) *Am J Physiol Cell Physiol* **281**, C993-C1000.
3. Marshall, C., Elias, C., Xue, X. H., Le, H. D., Omelchenko, A., Hryshko, L. V., and Tibbits, G. F. (2002) *Am J Physiol Cell Physiol* **283**, C512-520
4. Matsuoka, S., Nicoll, D. A., Reilly, R. F., Hilgemann, D. W., and Philipson, K. D. (1993) *Proc Natl Acad Sci U S A* **90**, 3870-3874.
5. He, Z., Tong, Q., Quednau, B. D., Philipson, K. D., and Hilgemann, D. W. (1998) *J Gen Physiol* **111**, 857-873
6. Longoni, S., Coady, M. J., Ikeda, T., and Philipson, K. D. (1988) *American Journal of Physiology* **255**, C870-873
7. Rosenthal, J. J., and Bezanilla, F. (2002) *J Exp Biol* **205**, 1819-1830
8. Kimura, M. T. (2004) *Oecologia* **140**, 442-449
9. Doyle, D. A., Morais Cabral, J., Pfuetzner, R. A., Kuo, A., Gulbis, J. M., Cohen, S. L., Chait, B. T., and MacKinnon, R. (1998) *Science* **280**, 69-77

# CHAPTER 5
# PHYLOGENY OF $Na^+$-$Ca^{2+}$ EXCHANGER (NCX) GENES FROM GENOMIC DATA IDENTIFIES NEW GENE DUPLICATIONS AND A NEW FAMILY MEMBER IN FISH SPECIES*

Christian R. Marshall[1,2,3], Joanne A. Fox[4], Stefanie L. Butland[4], B.F. Francis Ouellette[4],Fiona S.L. Brinkman[1], and Glen F. Tibbits[1,2,3]

[1] Department of Molecular Biology & Biochemistry
Simon Fraser University
Burnaby, BC, Canada

[2] Cardiovascular Sciences
BC Research Institute for Children's & Women's Health
Vancouver, BC, Canada

[3] Cardiac Membrane Research Laboratory
Simon Fraser University
Burnaby, BC, Canada

[4] UBC Bioinformatics Centre
University of British Columbia
Vancouver, BC, Canada

* This study is published in *Physiological Genomics* by permission under the following reference: Marshall C.R., Fox J.A., Butland S.L., Ouellette B.F., Brinkman F.S., Tibbits G.F. (2005) *Physiol Genomics* **21**:161-73. PMID: 15741504. Reproduced with permission.

## 5.1 Abstract

The $Na^+$-$Ca^{2+}$ exchanger (NCX) is a member of the cation:$Ca^{2+}$ antiporter (CaCA) family and plays a key role in maintaining cellular $Ca^{2+}$ homeostasis in a variety of cell types. NCX is present in a diverse group of organisms and exhibits high overall identity across species. To date, three separate genes – NCX1, NCX2, NCX3 – have been identified in mammals. However, phylogenetic analysis of the exchanger has been hindered by the lack of non-mammalian NCX sequences. In this study, we expand and diversify the list of NCX sequences by identifying NCX homologs from whole genome sequences accessible through the Ensembl Genome Browser. We identified and annotated thirteen new NCX sequences, including four from zebrafish, four from Japanese pufferfish, two from chicken, and one each from honeybee, mosquito and chimpanzee. Examination of NCX gene structure, together with construction of phylogenetic trees, provided novel insights into the molecular evolution of NCX and allowed us to more accurately annotate NCX gene names. For the first time, we report the existence of NCX2 and NCX3 in organisms other than mammals yielding the hypothesis that two serial NCX gene duplications occurred around the time vertebrates and invertebrates diverged. In addition, we have found a putative new NCX protein, named NCX4 that is related to NCX1 but has been observed only in fish species' genomes. These findings present a stronger foundation for our understanding of the molecular evolution of the NCX gene family and provide a framework for further NCX phylogenetic and molecular studies.

## 5.2 Introduction

Transport across biological membranes is fundamental to cellular processes, and thus it is not surprising that ~400 families of transport proteins have evolved to manage this diverse and complex task (1,2). $Ca^{2+}$ is a ubiquitous and highly versatile intracellular messenger used in practically all cell types spanning plant (3), animal (4), protist (5), and bacterial (6) kingdoms. Cytosolic $Ca^{2+}$ concentrations are tightly regulated and differentially interpreted to allow modulation of a variety of cellular functions (7). This $Ca^{2+}$ concentration plasticity is absolutely required for fine tuning of intracellular signaling, and hence $Ca^{2+}$ is in constant flux across the membrane. Nature has evolved multiple systems to regulate intracellular $Ca^{2+}$, including $Na^{+}$-$Ca^{2+}$ exchange. The $Na^{+}$-$Ca^{2+}$ exchanger (NCX) is a polytopic membrane transporter which catalyzes the counter-transport of three $Na^{+}$ for one $Ca^{2+}$ (8,9). Forming an essential part of the $Ca^{2+}$ efflux system, the NCX competes with other $Ca^{2+}$ transport systems to restore resting cytosolic levels, thereby maintaining $Ca^{2+}$ homeostasis. The molecular cloning of the mammalian NCX greatly accelerated our understanding of $Ca^{2+}$ exchange (10). This provided the impetus for the biochemical and functional characterization of the NCX at the molecular level, and further led to the discovery and cloning of NCX homologs in various species (11-13). The current era of informatics is marked by the availability of an increasing number of genome sequences from prokaryotes and from metazoan organisms (14). Mining of genomic databases affords tremendous potential in discovering new NCX homologs, which in turn would offer insights into NCX phylogeny and the evolution of the protein from a molecular and genetic perspective (15).

NCX is a member of the cation:$Ca^{2+}$ antiporter (CaCA) family, which corresponds to family 2.A.19 of the Transport Classification Database (TCDB) (see http://tcdb.ucsd.edu/index.php) (1). Recently, Cai and Lytton (16) performed an extensive sequence comparison and phylogenetic analysis of 147 sequences in the CaCA family. They defined the NCX group as one of five major subgroups of the CaCA family, and furthermore, found the group to be almost exclusively composed of sequences with animal origins (16). The NCX genes are classified as members of the CaCA family based on two defining characteristics: conserved α-repeats in the

transmembrane segments (TMS) (12), and hydrophobicity plots that predict ~10 TMS (8). The presence of intramolecular homology and relative conservation of TMS throughout the CaCA family suggests its members arose from an ancient intragenic gene duplication event, in which a primordial gene encoding a protein with 5-6 TMS duplicated internally to give one protein with twice the TMS (2). To date, no primordial 'half' exchanger has been found and it appears that – at least for NCX – both the N- and C-terminal hydrophobic domains are needed for proper membrane trafficking and function (17).

The architecture of the NCX protein is shown in Figure 1. Based on the topological models of Iwamoto *et al.* (18) and Nicoll *et al.* (19), the mature NCX is modeled to have 9 putative TMS organized in N- and C-terminal hydrophobic domains of 5 and 4 TMS, respectively. A signal sequence of ~30 residues is cleaved during initial processing (20,21), which makes the mature NCX protein ~900 residues in length depending upon the isoform. Within the hydrophobic domains are the opposing α-1 and α-2 repeats, which are critical for ion translocation (22). The intracellular loop comprises more than half the protein and contains sites important for $Ca^{2+}$ regulation, $Na^{+}$-dependent inactivation, and alternative splicing. So far, little information on NCX tertiary structure is available, although an extracellular disulfide bond has been shown to exist between cysteines in the N- and C-terminal hydrophobic domains (23). In addition, Qui *et al* (24) found the helix packing of TMS 2, 3, 7 and 8 is such that the two α-repeats may be adjacent to each other in the tertiary configuration.

NCX is present in most plasma membranes where its relative abundance is correlative with the importance of $Na^{+}$ -$Ca^{2+}$ exchange in that cell type. Expression of NCX is especially high in heart, brain and kidney tissue, where NCX clearly plays an important role in $Ca^{2+}$ homeostasis (25,26). The NCX family contains three separate gene products exhibiting differential expression, NCX1 (10), NCX2 (27), and NCX3 (28). NCX1 is highly expressed in the heart but is virtually ubiquitous, whereas NCX2 and NCX3 are found exclusively in brain and skeletal muscle (26). The NCX1 gene is organized into 12 exons, although most of the protein is coded by exon 2 (29). In mammalian isoforms, the exon boundaries of all three NCX genes are identical, except

that the long coding exon 2 found in NCX1 and NCX3 is split into three exons in NCX2 (29-31). The protein products of all three NCX genes display an overall identity of ~70%; however, no major functional differences occur between genes (32). It appears that two sequential gene replication events gave rise to the three NCX genes, but the date of these replications is unknown. In addition to having three separate gene products, tissue specific expression of the NCX is further diversified by alternative splicing. Alternative splice variants of NCX arise from a region in the intracellular loop where six small exons, designated A-F, are encoded. Exons A and B are mutually exclusive and are used in combination with cassette exons C through F to express splice variants in a tissue specific manner (33). The functional significance of NCX alternative splicing remains unclear, and needs to be investigated further.

The early evolutionary emergence of NCX predicts that all metazoans should express some exchanger isoform. To date, most cloned NCX genes are from mammalian origins; however, NCX1 orthologs have been cloned and characterized from lower vertebrates such as trout (*Oncorhynchus mykiss*) (13) and frog (*Xenopus laevis*) (34) and the invertebrates fruit fly (*Drosophila melanogaster*) (12,35), squid (*Loligo opalescens*) (11) and nematode (*Caenorhabditis elegans*) (29). Previously, no NCX2 or NCX3 orthologs have been found in non-mammalian species leading to the hypothesis that non-mammalian exchangers diverged before mammalian exchangers split into NCX1, NCX2 and NCX3 (16). Phylogenetic analysis of the NCX family has been hindered by the lack of non-mammalian NCX sequences available in public databases. The increase in availability of whole genomes from both vertebrates and non-vertebrates provides the opportunity to increase the number of NCX sequences available for phylogenetic analysis.

In this study, we have expanded the phylogenetic examination of NCX by increasing the number and diversity of full length sequences available for analysis. Combined with NCX sequences currently present in the protein databases, these new NCX sequences were subjected to a comprehensive sequence comparison and phylogenetic analysis. The inclusion of thirteen new NCX sequences from six different organisms provides novel insights into the molecular evolution and function of NCX.

## 5.3 Methods

### 5.3.1 Sequence Data

A complete list of all the NCX sequences used in this study is shown in Table 1 (see Supplementary Figure 1 for FASTA amino acid sequences). All sequences used in this study were obtained from either the National Center for Biotechnology Information (NCBI) (Bethesda, MD) non-redundant (nr) protein database or the Ensembl Genome Browser (Wellcome Trust Genome Campus, Hinxton, Cambridge UK) (36,37). BLASTP (38) was used to screen the nr protein database at NCBI, using canine NCX1.1 (GenBank GI number 127793) or trout NCX-TR1.0 (GenBank GI number 6273849) amino acid sequences as queries. Default parameters for BLASTP were used, except the descriptions option was set to 1000 to increase the number of reported hits and to ensure all NCX sequences were found. We ensured that other members of the CaCA family (e.g. NCKX) were identified in our search, providing further confidence that no NCX sequences were missed. The frog NCX1 full length gene was constructed by splicing together the N- and C-terminal portions of the exchanger, GenBank GI numbers 1019101 and 109099, respectively.

The Ensembl Genome Browser was used to search for new NCX sequences within six complete genomes (five non-mammalian) including zebrafish (*Danio rerio*) (Version 23.3c.1), Japanese pufferfish (*Fugu rubripes*) (Version 23.2c.1), honeybee (*Apis mellifera*) (Version 1 pre), chimpanzee (*Pan troglodytes*) (Version 23.1.1), chicken (*Gallus gallus*) (Version 23.1a.1) and mosquito (*Anopheles gambiae*) (Version 23.2b.1). The genomes at Ensembl are from sequencing projects from various institutions. Zebrafish sequence data were produced by the Zebrafish Genome Sequencing Group at the Sanger Institute (Hinxton, UK) and can be obtained from http://www.ensembl.org/Danio_rerio/exportview. Fugu Ensembl is a joint project between the IMCB (Singapore) and the EMBL - EBI to produce and maintain an automatic annotation of the Fugu Genome, using data sequenced by the Fugu Consortium. The honeybee genome sequence was determined by whole genome shotgun at the Human Genome Sequencing Center at Baylor College of Medicine (Houston, USA). The chimpanzee genome was sequenced by the Chimpanzee Sequencing

Consortium headed by the Genome Sequencing Center (St. Louis, USA) and The Broad Institute at MIT (Boston, USA). The chicken genome sequence was determined by the Genome Sequencing Center at Washington University (St Louis, USA). Finally, assembly of the mosquito genome was prepared by The International Anopheles Genome project.

TBLASTN was used to search the above genomes with varying NCX protein sequences as queries depending upon the genome being searched. All vertebrate genomes were searched with mammalian NCX1-3, whereas the fruitfly CALX (GenBank GI number 2266953) was used to TBLASTN the insect genomes. Due to the high degree of sequence similarity amongst all NCX isoforms, all NCX queries produced similar TBLASTN results. Segments of genomic DNA that encompassed both the N- and C-terminus were obtained (~10-100 Kb) and coding exons manually identified using a combination of the original TBLASTN results, the Ensembl Contig view, and previously cloned NCX sequences. Full length proposed NCX protein and cDNA sequences were then constructed by splicing together the coding exons and then these sequences were added to our list of NCX sequences identified from the NCBI nr database.

### 5.3.2 Sequence Alignments

All acquired NCX sequences were initially aligned using the default parameters of ClustalX (Version 1.83) (39). The resulting alignment was then imported into Genedoc (Version 2.6.002) (40) for manual examination and editing. Partial, duplicated and alternatively spliced isoforms were discarded to ensure that only one NCX gene of each type from each species was used, and further that this gene was a full length and non-redundant sequence. The variable alternative splice site region of NCX (illustrated schematically in Figure 1) was not included in subsequent phylogenetic analyses due the high potential for homoplasy in that region.

### 5.3.3 Phylogenetic Analysis

Phylogenetic analyses were performed using ClustalX (primarily for initial tree constructions and manipulations) and the PHYLIP package for verification of the initially derived trees (Version 3.6b, Joe Felsenstein, Department of Genome Sciences, University

of Washington, Seattle, WA) (41). Included in the alignments were two outgroup sequences, AtMHX from mouse-ear cress (*Arabidopsis thaliana*) (GenBank GI number 6492237) and a $Na^{+}$-$Ca^{2+}$ exchanger from the bacterium *Pirellula sp* (GenBank GI number 32475149). These sequences appear at the base of the NCX subgroup in the unrooted tree of Cai and Lytton's (16) recent phylogenetic analysis of the CaCA family.

Neighbor-Joining (NJ) trees (42) were generated using ClustalX, followed by tree evaluation with bootstrap resampling (1000 times). Further phylogenetic analysis (including confirmation of the ClustalX-based NJ tree topologies) was performed using the PHYLIP package, where trees were also constructed using maximum parsimony (MP) and maximum likelihood (ML) methods. Bootstrapping was performed with 100 replicates in such cases. The program TREEVIEW (Version 1.6.6) (43) was used to examine and display all trees.

## 5.4 Results and Discussion

NCX is characterized by two transmembrane spanning domains separated by a large intracellular hydrophilic loop (8). Signifying its importance in regulating intracellular $Ca^{+2}$ concentrations, NCX is present and highly conserved across phyla within the animal kingdom. Studies of the molecular phylogeny of NCX have used limited sequences or have been part of larger studies on the CaCA family in general. In 1996, Kraev *et al* (29) found an NCX homolog in *C. elegans* and compared its genomic structure to human NCX1, and a year later, Schwarz and Benzer (12) first noted the intramolecular homology of NCX in their multiple alignment of 20 exchangers related to fruitfly CALX. Philipson and Nicoll (8) performed BLAST searches of the GenBank protein database and designated the NCX family as one of four subfamilies of the exchanger superfamily. However, this analysis contained only 8 NCX sequences and 29 in total. This study was expanded in the first comprehensive phylogenetic analysis of the CaCA family, which was recently undertaken by Cai and Lytton (16). They categorized 147 members of the CaCA family into five subfamilies, with the NCX subfamily containing 22 proteins. Of these NCX proteins, only seven were non-mammalian, including two from non-mammalian vertebrates. Cloning and functional characterization of the NCX has always had a strong mammalian bias despite the protein's early

emergence in evolution. From our initial searches, ~75% of all publicly available NCX protein sequences were from mammalian origins. The dearth of sequence data from non-mammalian species has greatly impaired evolutionary analyses of the NCX family. This study builds on previous research through inclusion of additional NCX sequences derived from sequenced genomes, and represents the first phylogenetic analysis specifically focused on NCX.

### 5.4.1 NCX is Present in a Diverse Group of Organisms

All NCX sequences identified and used in this study are listed in Table 1 (see Supplementary Figure 1 for FASTA amino acid sequences). A BLASTP search of the NCBI nr database produced almost identical results when dog NCX1.1 or trout NCX-TR1.0 were used as a query. 80 NCX amino acid sequences were initially obtained from the search and pared down to 25 full-length non-redundant NCX sequences. An additional 13 previously unidentified NCX sequences were obtained from analysis of six genome sequences available through the Ensembl genome browser. These included four NCX sequences from zebrafish, four from Japanese pufferfish, two from chicken, and one each from honeybee, mosquito and chimpanzee. For some of the above species, additional NCX genes were found on other chromosomes but were incomplete or lacked sufficient identity to be included. In total, 38 full length non-redundant NCX sequences from 23 species were used in our analyses, including 16 mammalian NCX sequences and 22 non-mammalian sequences. Of the 22 non-mammalian NCX sequences, eight were from invertebrates and 14 from lower vertebrates. These NCX proteins range in size from 861 to 973 amino acids due to gene isoform and splice variant differences.

It should be noted that not all of the NCX sequences obtained from the Ensembl genome browser were annotated correctly, illustrating the difficulties currently faced in whole genome annotation (44-46) and gene prediction (47,48). Genes at Ensembl are computationally annotated based on gene prediction and comparison to protein, cDNA and EST databases. These methods result in some annotation errors that can be resolved by manual re-annotation. In general, NCX coding exons displaying high identity across many species were annotated correctly, whereas erroneous annotation of intron-exon boundaries tended to occur in less conserved regions or in the alternative splice region in

which individual coding exons are small. In most cases the start codon and portions of the signal peptide were also missing since this region is poorly conserved amongst NCX isoforms. The NCX sequences were manually re-annotated using a combination of strategies, including TBLASTN searches and manual translation of coding areas to find intron/exon boundaries. Due to incomplete genome sequencing, some final NCX sequences contained gaps (e.g. zebrafish NCX2 is only 747 amino acids). The addition of 13 (12 non-mammalian) previously unidentified NCX sequences is crucial to expanding the phylogenetic analyses of the exchanger.

### 5.4.2 NCX Identity in the Ion Translocation and Regulatory Regions is High

The conservation of the NCX throughout evolution is evidenced by the overall high identity of the full sequence alignment (see Supplementary Figure 2 for full multiple sequence alignment). The relatively high identity in the TMS of NCX is a feature consistent throughout the CaCA family, in which the intracellular loop is poorly conserved between independent clades (16). The data are consistent with the findings that only the N- and C-terminal hydrophobic domains are required for ion transport (17,49) and further supports the idea that the hydrophilic loop has evolved to gain specific regulatory properties.

The α-1 and α-2 repeats, together with the immediate surrounding TMS, are central to ion translocation function of the NCX. An alignment of these regions using a representative list of 26 NCX sequences is shown in Figure 2. An immediate and striking observation is the high identity across all NCX species and isoforms (35/55 identical residues for α-1 region and 32/53 identical residues for α-2 region), particularity for those residues modeled to be within the membrane. Previous studies have shown that residues in these regions are extremely sensitive to mutation, especially the acidic (glutamate and aspartate), polar (threonine, serine, asparagine), and flexible (glycine, proline, alanine) groups of amino acids (8,50,51).

There are several conserved acidic residues in the α-repeats and surrounding TMS. E148 in TMS2 and D849 in TMS7 in human NCX1.1, are completely conserved throughout the CaCA family (16) and are absolutely required for NCX ion translocation

function (50). TMS2 has an additional conserved glutamate E155, which would place the charged residue on the same side of the helix as E148. Mutational studies have shown that mutation of Glu-155 reduces NCX activity by 50% (50). TMS3 lacks the presence of charged amino acids, but the proximal end of the reentrant loop between TMS7 and 8 has two conserved aspartate residues: D860 and D864. D860 is very sensitive to mutation, whereas D864 is not (8). These conserved acidic residues throughout the region are likely involved in neutralizing the positive charges of $Na^+$ and $Ca^{2+}$, thereby allowing transport of the cations through the membrane (16).

In addition to negatively charged residues, the α-repeats and surrounding TMS have a number of conserved polar (serine, threonine, asparagine) amino acids (Figure 2). In TMS2, 3, and 7, the polar residues are spaced at regular intervals of 3-4 residues, making these helices amphipathic. The conservation of polar residues in this region is consistent with expected functional modifications based on previous mutational analyses (50). The hydrophilic faces of the amphipathic TMS2, 3, and 7 are believed to form a portion of the ion translocation pathway (24) and may help coordinate cation binding or provide the hydrophilic environment necessary for ion translocation (16).

The α-repeat regions are also rich in conserved glycine and proline residues, even within the regions modeled to be TMS helices. The α-1 region has three proline and two glycine residues that are conserved across all species and isoforms. These residues do not appear to be absolutely required for ion translocation, but not all have been tested (Figure 2). In contrast, the α-2 region has one conserved proline and five conserved glycine residues, with mutation of the glycines at positions 844, 881, and 883 modifying transport properties. The latter two glycine residues flank a G(I/L)G sequence that is similar to the GYG motif in the P-loop of $K^+$ channels (52) and the GIG motif in the pore region of the sarcoplasmic $Ca^{2+}$ release channels (RyR) (53,54). However, other than being a tight turn within the re-entrant loop, this motif in NCX has not been shown to have any functional significance. The presence of proline and glycine residues in the middle of TMS2 and 7 may provide the helix flexibility needed for the conformational changes that occur upon ion binding and translocation (16).

In addition to being substrates, $Na^+$ and $Ca^{2+}$ also have a role in the regulation of the NCX in the forms of $Na^+$-dependent inactivation and $Ca^{2+}$-dependent activation, respectively. The regions responsible for this regulation are located in the large intracellular loop and an alignment of these regions is shown in Figure 3. $Na^+$-dependent inactivation causes inactivation of NCX current to a steady state level (55) and is attributed, at least in part, to the XIP (e*X*changer *I*nhibitory *P*eptide) site. Immediately apparent in Figure 3A is the lack of sequence similarity of the nematode XIP sites compared to all other species, despite high identity in the TMS5. It is not known whether nematode NCX isoforms display $Na^+$-dependent inactivation, but based on lack of sequence similarity in the XIP site, it is unlikely. Even amongst the rest of the species, sequence identity is low except for the start of the XIP site beginning with the consensus RRLL(X)nG. $Na^+$-dependent inactivation has been demonstrated in different NCX isoforms (32) and in NCX from different species including squid (11), fruitfly (56) and trout (57). Consistent with low XIP identity across all species, mutations in this region do not affect ion translocation of the NCX but rather have modulating effects on inactivation (58,59). The relatively low evolutionary conservation in the XIP site may be due to indirect binding of $Na^+$ to the XIP site.

Conversely, the $Ca^{2+}$-dependent activation does require the binding of $Ca^{2+}$, and this is reflected in two highly conserved binding sites located in the intracellular loop (Figure 3B). Regulatory $Ca^{2+}$ is not translocated but is required for exchange activity, binding with high affinity at two aspartate and glutamate rich sites in the regulatory loop (60). The zebrafish NCX2 sequence shown in Figure 3B is missing the first binding site due to incomplete genomic sequencing and the tilapia NCX1.1 has a frame shift in this region due to sequencing error (unpublished observations, CR Marshall). Mutations in this region (especially the first trio of aspartates) do not affect ion translocation, but do affect $Ca^{2+}$ binding and regulation properties (61). Interestingly, regulatory $Ca^{2+}$ binding in the fruitfly CALX decreases exchanger activity, which is opposite to the observed effect in other NCX isoforms. It is not known whether this is the case in the related exchangers from the honeybee and mosquito, but must be due to an allosteric effect in the protein since the $Ca^{2+}$ binding sites themselves have high identity.

In overall sequence identity, there is a core of consensus residues that are needed for full NCX function and regulation. Surprisingly, not all residues that are conserved across all species are essential to NCX function; however, any residue that is known to be very sensitive to mutation is conserved across all species. NCX sequence similarity follows that of the CaCA family in general, with high relative sequence identity in the TMS and lower sequence identity in the cytoplasmic regulatory loop (16). This in turn is consistent with the expected sequence-function relationship: the TMS of NCX are absolutely required for ion translocation and have therefore remained relatively intact throughout evolution, whereas regions in the hydrophilic loop have evolved separately amongst NCX isoforms to confer species specific regulatory properties.

### 5.4.3 NCX Gene Families have Similar Genomic Structure and Intron-Exon Boundaries

In searching for new NCX sequences in sequenced genomes, we found multiple NCX isoforms in three of the six organisms – chicken, zebrafish, and Japanese pufferfish. The genomic organization of the coding exons for the 13 NCX sequences found at Ensembl is shown in Figure 4, and can be a useful tool in examining NCX evolution. Human NCX1, NCX2 and NCX3 genes have been previously mapped to chromosomes 2p22.1 (29), 19q13.2 (62), and 14q24.2 (30), respectively. We found the three human NCX genes at Ensembl and used them as reference sequences in our analysis (Figure 4). A couple of features regarding the human NCX genes are of note. First, the NCX sequences contain only the coding exons, and do not contain portions of 5' and 3' untranslated regions. Previously, it has been shown that the start codon of NCX1 and NCX3 is in exon 2, a large 1.8 kb exon that extends to the alternative splice site (29,30). In Figure 4, the untranslated exon 1 is not shown and exon numbering begins with the first coding exon. Human NCX2 displays the same exon boundaries as NCX1 and NCX3, except the long initial coding exon is split into three exons. Secondly, the coding regions of human NCX1 and NCX3 genes have been reported to stretch over ~200 kb (29) and ~126 kb (30) of genomic DNA, respectively. According to the human NCX genes at Ensembl, these distances are ~316 kb for NCX1 and ~126 kb for NCX3. The reason for this length discrepancy in the NCX 1 gene is unknown, but is solely

attributable to differences in intron length and is not due to miscalculation of the gene boundaries. There are a couple of possible reasons for this discrepancy. First, it is possible that there are errors in the assembly of the human genome sequence at Ensembl; however examination of the human genomic sequence encompassing the NCX1 gene is of high quality and it is unlikely that errors in genome assembly exist. Supporting the genomic assembly of human NCX1 at Ensembl is the fact that the closely related chimpanzee genome yields an NCX1 gene that spans a similar distance to the human NCX1 gene. Secondly, Kraev *et al* (29) did not sequence the introns completely and therefore it is possible that their length was underestimated.

In addition to having a different initial coding exon structure, the human NCX2 gene is very compact, stretching over only ~36 kb of genomic DNA. In general, the NCX isoforms from other species followed these trends with NCX2 having more compact genomic DNA compared to NCX1 and NCX3. NCX2 also has a greater number of exons before the alternative splice region, a trend which is also common in the invertebrates' NCX. In contrast, NCX1 and NCX3 typically have a single large initial coding exon separated from the alternative splice site by a very long intron. This suggests that the NCX1 and NCX3 genes of vertebrates have undergone some form of intron loss, effectively fusing together all their coding exons up to the alternative splice site. Based on similarities in exon structures and genomic organization, NCX1 and NCX3 appear to be more closely related to each other than either gene is to NCX2.

### 5.4.4 Non-Mammalian Vertebrates Have Multiple NCX Genes

In addition to insights into the evolution of the NCX gene, similarities in gene structure can be used to annotate new NCX genes. Using the human NCX genes as a reference, the 13 NCX isoforms from Ensembl were annotated based on an examination of the sequence alignment (see Supplementary Figure 2) and genomic organization of exons (Figure 4). The chimpanzee NCX1 sequence shares 99% amino acid identity with human NCX1, and has an almost identical exon structure. Frame shifts due to sequencing errors in the chimpanzee genome gave different NCX exon boundaries compared with human NCX in the first exon, but correction would yield identical NCX exons for human and chimpanzee. Both NCX2 and NCX3 are present in the chimpanzee

genome, but contained too many gaps to warrant inclusion in our sequence lists. The mosquito and honeybee NCX sequences did not display high amino acid or intron-exon boundary similarity to NCX1, 2 or 3, and are therefore unclassified. This is consistent with the literature, in which no invertebrate NCX isoform has been classified as one of NCX1, 2, or 3. The chicken genome had NCX1, NCX2 and NCX3 genes, but as was the case for chimpanzee isoforms, NCX2 was not added to the list due to presence of partial sequence only. Both zebrafish and Japanese pufferfish genomes contained NCX1, NCX2 and NCX3. For all NCX genes, the Japanese pufferfish isoforms had the shortest introns, consistent with this species having a genome that is ~7.5 times as compact as the human genome (63,64). The NCX isoforms from chicken, zebrafish, and Japanese pufferfish represent the first NCX2 and NCX3 sequences from non-mammalian species.

To further confirm the annotation of the NCX sequences from Ensembl, the alternative splice site was aligned and examined (Figure 5). The exons expressed in this region, both in terms of number and sequence, can offer insight into the identity of the NCX gene. In vertebrate NCX genes exons A and B are mutually exclusive, and produce tissue specific variants when expressed in combination with exons CDEF. The NCX1 gene has exons ABCDEF, whereas NCX2 has only AC and NCX3 only ABC (26). The NCX sequences of invertebrates do not have alternative splicing to the same extent as isoforms from vertebrate species, but do have a variant of exon A/B. For all sequences except fugu NCX3, either exon A or B was found and showed significant sequence identity for it to be categorized as NCX1, NCX2, or NCX3 specific. Interestingly, both exons A and B were found for chicken and Japanese pufferfish NCX1, which to our knowledge is the first time both exons have been shown in non-mammalian species. Exon A likely exists in the zebrafish NCX1 gene, but was not found due to genomic sequence gaps. Some of the smaller cassette exons (CDE) present in NCX1 could not be found in non-mammalian species because they were either too small (5-7 amino acids) or lacked sufficient similarity to be picked up by BLAST analysis. These exons (CDEF) are predicted to exist in both zebrafish and Japanese pufferfish NCX1 isoforms, since all are present in trout NCX1.0 and tilapia NCX1.1 with fairly high similarity to the mammalian exons. However, it is possible that the cassette exons have been lost in some species or have diverged to a point that they cannot be identified using sequence similarity methods.

This may be the case for NCX3, where exon C, which is present in mammalian NCX genes could not be found in chicken, zebrafish or Japanese pufferfish. Conversley, exon C in the NCX2 subfamily was found in both zebrafish and Japanese pufferfish and appears to be highly conserved in all species. In general, the alternative splice region within NCX subfamilies displays high similarity in both exon structure and exon sequence. The fact that this region has maintained a high degree of conservation throughout evolution implicates its role in creating functionally different NCX splice variants through the differential expression of exons – a strategy that is employed in species ranging from lower vertebrates to mammals.

### 5.4.5 NCX Gene Duplication Events Occurred Before Emergence of Mammals

Phylogenetic analysis of all 38 NCX sequences offered further insight into the evolution of NCX (Figure 6 and Supplementary Figure 3). Phylogenetic analysis using different tree building methods have often shown a lack of uniformity in their results (65), therefore we have used three different methods in the phylogenetic reconstruction of NCX. Figure 6 shows the rooted NJ tree for all 38 NCX sequences, together with the 2 outgroup sequences. There is clear delineation between the invertebrate NCX sequences, which further branch into groups containing the nematodes, insects, and squid. The vertebrate NCX sequences are distinctly grouped into clades, including the three familiar NCX1, NCX2, NCX3 proteins. Within the NCX1, NCX2, and NCX3 groups, mammalian and non-mammalian sequences are separated and grouped in a manner that seems to be consistent with the evolution of the organisms. In their analysis, Cai and Lytton (16) determined that invertebrate and non-mammalian vertebrate exchangers diverged before mammalian exchangers split into NCX1, NCX2, and NCX3. Increasing the number of NCX sequences for phylogenetic analysis has allowed us to fashion a rudimentary account of the molecular evolution of the NCX. The divergence of NCX into three genes occurred after the divergence of invertebrate exchangers but before the divergence of vertebrate exchangers, indicating these duplication events took place at least 450 million years ago. After the separation of the invertebrate NCX clade, the ancestor to the vertebrate NCX gene family underwent two separate gene duplication events. From our analysis it appears the vertebrate NCX2 gene evolved from the first

duplication event, while the other gene underwent a subsequent duplication giving rise to NCX1 and NCX3. The actual timing of these serial duplications cannot be estimated due to the lack of NCX sequences from organisms spanning the evolutionary gap between invertebrate and lower vertebrate fish species (~100-150 million year period). Sequencing of genomes from species spanning this time frame (e.g. hagfish, lampreys) should help pinpoint the actual timing of NCX gene duplications. This theory of NCX evolution is supported by the MP method in supplementary Figure 3A, as it produced virtually the same tree topology as the NJ approach. The ML tree (Supplementary Figure 3B) is similar to the above trees with a few exceptions that offer an alternative theory to the evolution of NCX. The tree topology shows the split in the invertebrate and vertebrate NCX isoforms, and groups the vertebrate isoforms in the same NCX groups as the NJ and MP trees. However, the ML tree shows that the NCX1 group was the first to diverge and then NCX2 and NCX3 arose from gene duplication. Although this theory is plausible, it is not supported by the similarity of exon structures shared between NCX1 and NCX3, compared to NCX2. Expanding the number and diversity of NCX sequences for phylogenetic analysis should resolve these discrepancies and create a clearer picture of the evolution of NCX.

### 5.4.6 Fish Species Have a Fourth NCX Gene Related to NCX1

Both zebrafish and Japanese pufferfish have a fourth NCX isoform that has high identity to an exchanger from the green spotted pufferfish (GenBank GI number 47219419). Collectively, these putative genes are distinct from NCX1-3, and therefore we have tentatively named them NCX4. So far, NCX4 is present in only in fish genomes as orthologs could not be found in any non-fish species. Based on sequence similarity, fish NCX4 is most closely related to NCX1; however, it is not known if this gene is expressed in fish or functions as an exchanger. In terms of exon structure, the fugu NCX4 is more similar to NCX2, whereas the zebrafish NCX4 has an exon structure more similar to both NCX1 and NCX3 (Figure 4). At the NCX4 alternative splice site, only exon A/B was found and it is not known whether any of the cassette exons exist. This new NCX isoform appears to be a result of a separate gene duplication of NCX. NJ and MP trees both suggest that it evolved from a gene duplication of the ancestor of NCX1

and NCX4, and that the duplication may have occurred after the divergence of fish from other vertebrates (Figure 6 and Supplementary Figure 3A). The date of this duplication is unknown but appears to have occurred early in the evolution of NCX due to the degree of divergence between NCX4 and NCX1 and the fact that NCX4 is not present in mammalian or avian species. The ML tree is not consistent, suggesting instead that NCX4 evolved from an older gene duplication that may be ancestral to the divergence of NCX1, NCX2 and NCX3 (Supplementary Figure 3A). However, it should be noted that bootstrap values for this component of the tree are not very reliable. In addition, the fish NCX4 shares its highest identity with NCX1, meaning these proteins would have diverged at a much slower rate than NCX2 and NCX3 if the ML tree was a representation of true NCX evolution.

In summary, this study has built on previous work to present the first comprehensive sequence and phylogenetic analysis of the NCX family, which now includes 13 new NCX sequences derived from whole genome sequencing projects. Integration of sequence alignment, gene structure, and phylogenetic data has generated a solid framework for future analyses and has provided novel insights into the molecular evolution of the NCX. For the first time, NCX2 and NCX3 have been shown to exist in non-mammalian species, and we propose that a NCX4 gene exists in fish species'.

## 5.5 Tables

**Table 1:** Organism name, Common name, Gene name, and GI numbers of NCX sequences used for analyses in this study

| Organism Name | Common Name | Gene Name | Sequence Identifier (GI) | Database | Code Name^ |
|---|---|---|---|---|---|
| *Mus musculus* | house mouse | NCX1.1 | 2829482 | GenBank | ncx1.1_mouse |
| *Macaca mulatta* | rhesus monkey | NCX1.3 | 4140706 | GenBank | ncx1.3_monkey |
| *Tetraodon nigroviridis* | green spotted pufferfish | NCX4 | 47219419 | GenBank | ncx4_green_puffer |
| *Oryctolagus cuniculus* | rabbit | NCX1.2 | 1279782 | GenBank | ncx1.2_rabbit |
| *Oreochromis mossambicus* | tilapia | NCX1.1 | 30908988 | GenBank | ncx1.1_tilapia |
| *Mus musculus* | house mouse | NCX2.1 | 22507355 | GenBank | ncx2.1_mouse |
| *Homo sapiens* | human | NCX1.1 | 10863913 | GenBank | ncx1.1_human |
| *Rattus norvegicus* | norway rat | NCX1.1 | 1346652 | GenBank | ncx1.1_rat |
| *Rattus norvegicus* | norway rat | NCX3.3 | 17530969 | GenBank | ncx3.3_rat |
| *Felis catus* | cat | NCX1.1 | 134650 | GenBank | ncx1.1_cat |
| *Canis familiaris* | dog | NCX1.1 | 127793 | GenBank | ncx1.1_dog |
| *Oncorhynchus mykiss* | rainbow trout | NCX-TR1.0 | 6273849 | GenBank | ncx1.0_trout |
| *Cavia porcellus* | guinea pig | NCX1.1 | 1346649 | GenBank | ncx1.1_guinea_pig |
| *Mus musculus* | mouse | NCX3.1 | 17978254 | GenBank | ncx3.1_mouse |
| *Bos taurus* | cow | NCX1.1 | 28603740 | GenBank | ncx1.1_cow |
| *Loligo opalescens* | squid | NCX_SQ1 | 1947092 | GenBank | ncx_squid |
| *Homo sapiens* | human | NCX3.3 | 22087483 | GenBank | ncx3.3_human |
| *Homo sapiens* | human | NCX2.1 | 10720116 | GenBank | ncx2.1_human |
| *Rattus norvegicus* | norway rat | NCX2.1 | 17530967 | GenBank | ncx2.1_rat |
| *Drosophila melanogaster* | fruit fly | CALX | 2266953 | GenBank | ncx_fly |
| *Xenopus laevis* | clawed frog | NCXN | 1019101 | GenBank | ncx1_frog |
| *Xenopus laevis* | clawed frog | NCXC | 1019099 | GenBank | |
| *Caenorhabditis elegans* | nematode | NCX-1 (Y113G7A.4) | 17566438 | GenBank | Y113G7A.4_c.elegans |
| *Caenorhabditis briggsae* | nematode | NCX-1 | 39595924 | GenBank | CBG12917_c.briggsae |
| *Caenorhabditis elegans* | nematode | NCX-2 (C10G8.5) | 20901918 | GenBank | C10G8.5_c.elegans |
| *Caenorhabditis briggsae* | nematode | NCX-2 | 39593024 | GenBank | CBG06769_c.briggsae |
| *Gallus Gallus* | chicken | NCX1 | N/A | EnsEMBL | ncx1_chicken* |
| *Gallus Gallus* | chicken | NCX3 | N/A | EnsEMBL | ncx3_chicken* |
| *Fugu Rubripes* | pufferfish | NCX1 | N/A | EnsEMBL | ncx1_fugu* |
| *Fugu Rubripes* | pufferfish | NCX2 | N/A | EnsEMBL | ncx2_fugu* |
| *Fugu Rubripes* | pufferfish | NCX3 | N/A | EnsEMBL | ncx3_fugu* |
| *Fugu Rubripes* | pufferfish | NCX | N/A | EnsEMBL | ncx4_fugu* |
| *Apis Mellifera* | honeybee | NCX | N/A | EnsEMBL | ncx_honeybee* |
| *Anopheles gambiae* | mosquito | NCX | N/A | EnsEMBL | ncx_mosquito* |
| *Pan troglodytes* | chimpanzee | NCX1.1 | N/A | EnsEMBL | ncx_chimpanzee* |
| *Danio rerio* | zebrafish | NCX1 | N/A | EnsEMBL | ncx1_danio* |
| *Danio rerio* | zebrafish | NCX2 | N/A | EnsEMBL | ncx2_danio* |
| *Danio rerio* | zebrafish | NCX3 | N/A | EnsEMBL | ncx3_danio* |
| *Danio rerio* | zebrafish | NCX4 | N/A | EnsEMBL | ncx4_danio* |

* denotes sequences derived from whole genomes at Ensembl Genome browser
^ denotes code name used in alignments and phylogenetic trees

## 5.6 Figures

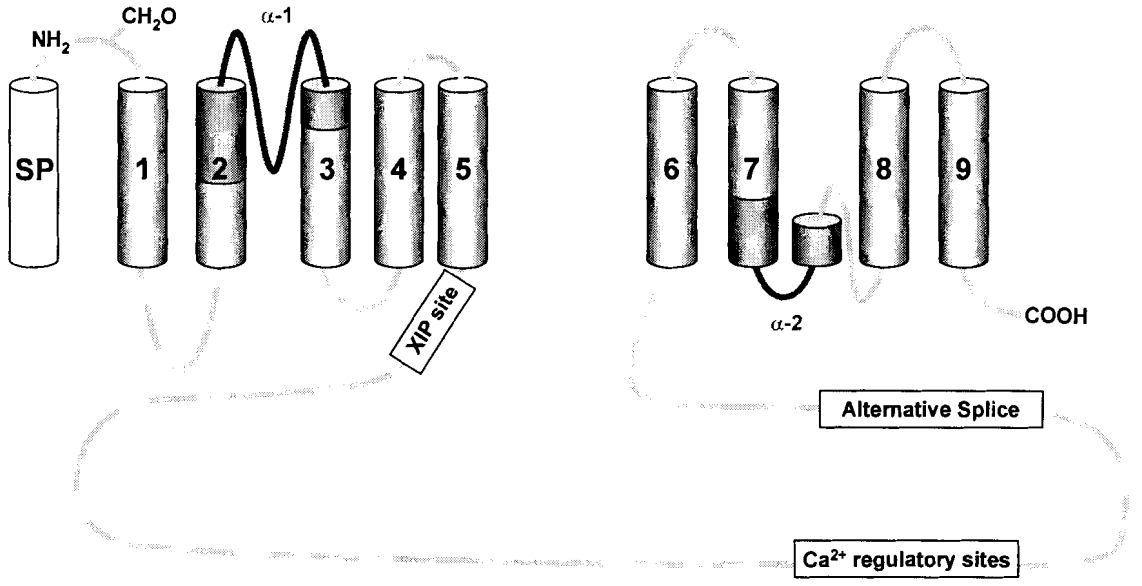


**Figure 1**

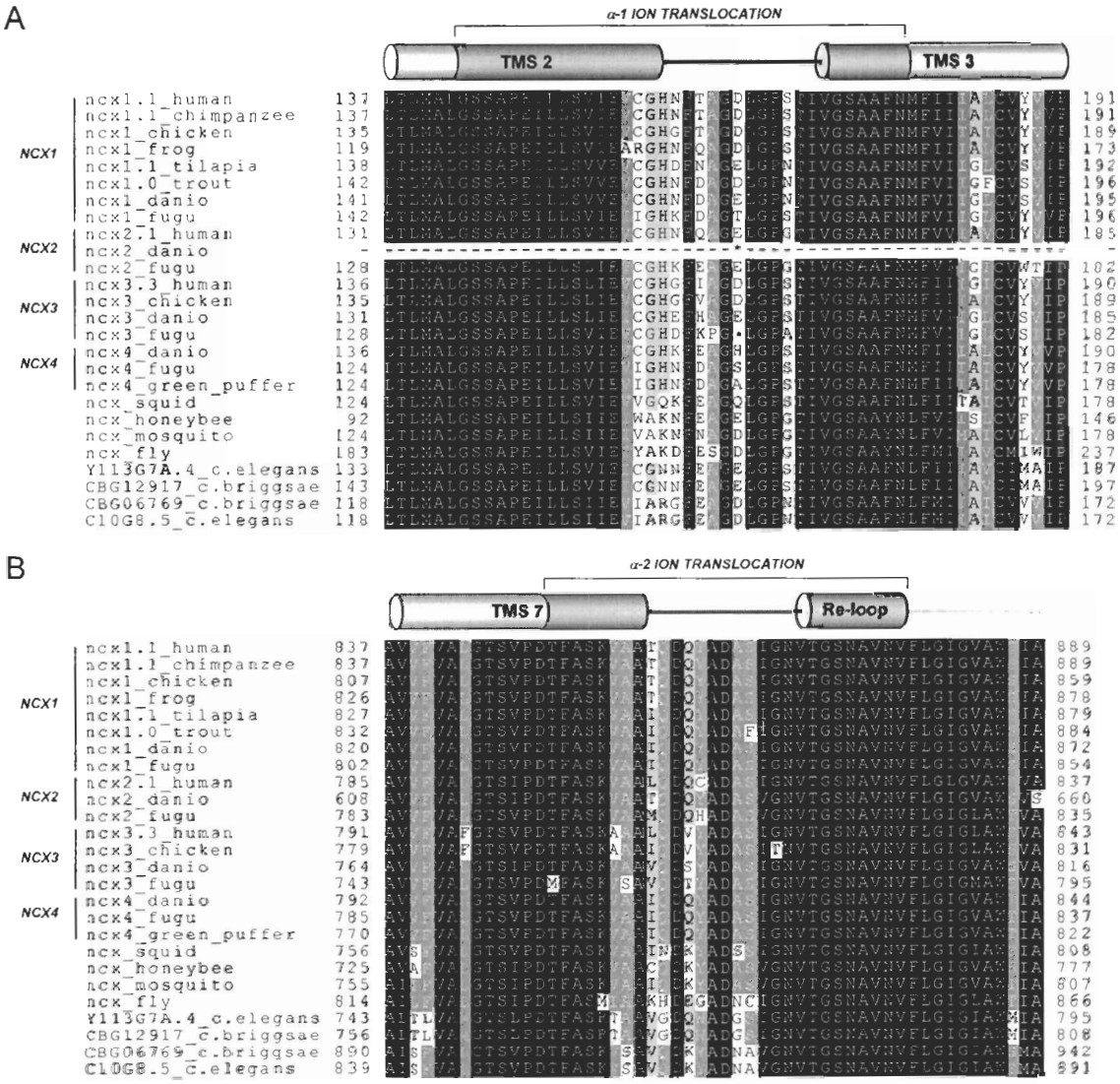
A
α-1 ION TRANSLOCATION
TMS 2
TMS 3
NCX1
NCX2
NCX3
NCX4
ncx1.1_human
ncx1.1_chimpanzee
ncx1_chicken
ncx1_frog
ncx1.1_tilapia
ncx1.0_trout
ncx1_danio
ncx1_fugu
ncx2.1_human
ncx2_danio
ncx2_fugu
ncx3.3_human
ncx3_chicken
ncx3_danio
ncx3_fugu
ncx4_danio
ncx4_fugu
ncx4_green_puffer
ncx_squid
ncx_honeybee
ncx_mosquito
ncx_fly
Y113G7A.4_c.elegans
CBG12917_c.briggsae
CBG06769_c.briggsae
C10G8.5_c.elegans
B
α-2 ION TRANSLOCATION
TMS 7
Re-loop
NCX1
NCX2
NCX3
NCX4
ncx1.1_human
ncx1.1_chimpanzee
ncx1_chicken
ncx1_frog
ncx1.1_tilapia
ncx1.0_trout
ncx1_danio
ncx1_fugu
ncx2.1_human
ncx2_danio
ncx2_fugu
ncx3.3_human
ncx3_chicken
ncx3_danio
ncx3_fugu
ncx4_danio
ncx4_fugu
ncx4_green_puffer
ncx_squid
ncx_honeybee
ncx_mosquito
ncx_fly
Y113G7A.4_c.elegans
CBG12917_c.briggsae
CBG06769_c.briggsae
C10G8.5_c.elegans

**Figure 2**

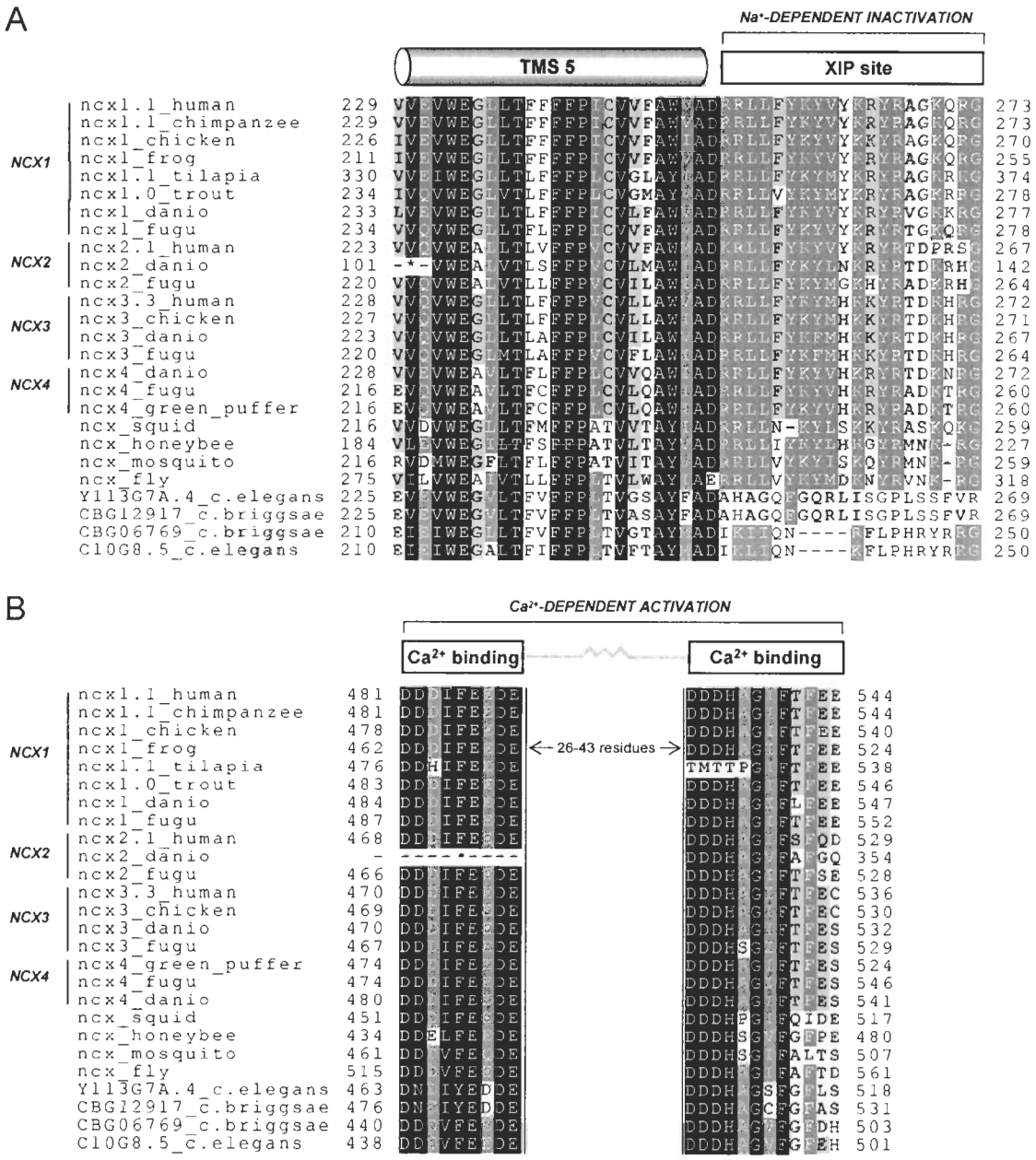
A
Na+-DEPENDENT INACTIVATION
TMS 5
XIP site
NCX1
NCX2
NCX3
NCX4
ncx1.1_human 229 273
ncx1.1_chimpanzee 229 273
ncx1_chicken 226 270
ncx1_frog 211 255
ncx1.1_tilapia 330 374
ncx1.0_trout 234 278
ncx1_danio 233 277
ncx1_fugu 234 278
ncx2.1_human 223 267
ncx2_danio 101 142
ncx2_fugu 220 264
ncx3.3_human 228 272
ncx3_chicken 227 271
ncx3_danio 223 267
ncx3_fugu 220 264
ncx4_danio 228 272
ncx4_fugu 216 260
ncx4_green_puffer 216 260
ncx_squid 216 259
ncx_honeybee 184 227
ncx_mosquito 216 259
ncx_fly 275 318
Y113G7A.4_c.elegans 225 269
CBG12917_c.briggsae 225 269
CBG06769_c.briggsae 210 250
C10G8.5_c.elegans 210 250
B
Ca2+-DEPENDENT ACTIVATION
Ca2+ binding
Ca2+ binding
26-43 residues
ncx1.1_human 481 544
ncx1.1_chimpanzee 481 544
ncx1_chicken 478 540
ncx1_frog 462 524
ncx1.1_tilapia 476 538
ncx1.0_trout 483 546
ncx1_danio 484 547
ncx1_fugu 487 552
ncx2.1_human 468 529
ncx2_danio 354
ncx2_fugu 466 528
ncx3.3_human 470 536
ncx3_chicken 469 530
ncx3_danio 470 532
ncx3_fugu 467 529
ncx4_green_puffer 474 524
ncx4_fugu 474 546
ncx4_danio 480 541
ncx_squid 451 517
ncx_honeybee 434 480
ncx_mosquito 461 507
ncx_fly 515 561
Y113G7A.4_c.elegans 463 518
CBG12917_c.briggsae 476 531
CBG06769_c.briggsae 440 503
C10G8.5_c.elegans 438 501

**Figure 3**

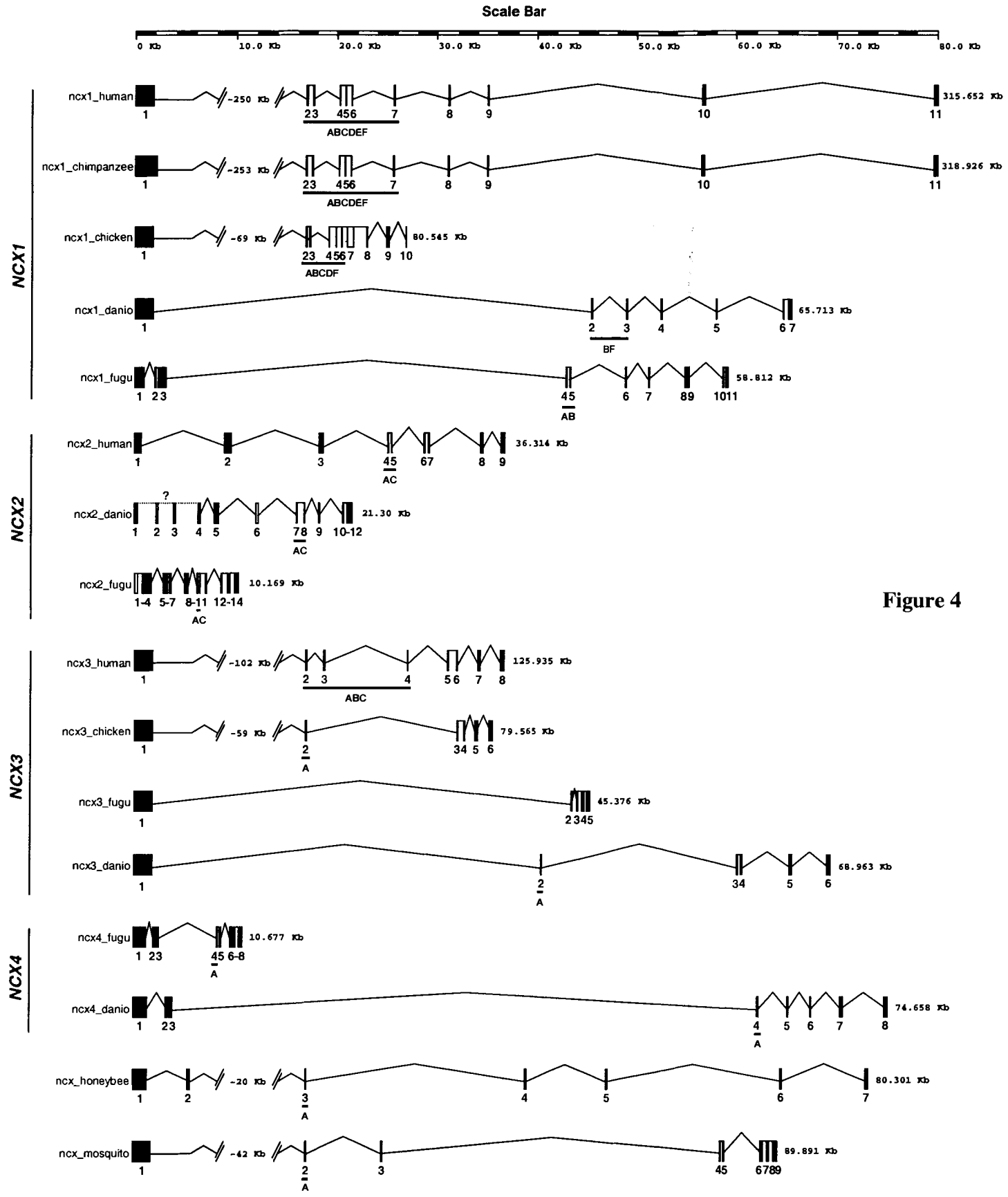
Scale Bar
0 Kb
10.0 Kb
20.0 Kb
30.0 Kb
40.0 Kb
50.0 Kb
60.0 Kb
70.0 Kb
80.0 Kb
NCX1
ncx1_human
~250 Kb
315.652 Kb
ABCDEF
ncx1_chimpanzee
~253 Kb
318.926 Kb
ABCDEF
ncx1_chicken
~69 Kb
80.545 Kb
ABCDF
ncx1_danio
65.713 Kb
BF
ncx1_fugu
58.812 Kb
AB
NCX2
ncx2_human
36.314 Kb
AC
ncx2_danio
21.30 Kb
AC
ncx2_fugu
10.169 Kb
AC
NCX3
ncx3_human
~102 Kb
125.935 Kb
ABC
ncx3_chicken
~59 Kb
79.565 Kb
A
ncx3_fugu
45.376 Kb
ncx3_danio
68.963 Kb
A
NCX4
ncx4_fugu
10.677 Kb
A
ncx4_danio
74.658 Kb
A
ncx_honeybee
~20 Kb
80.301 Kb
A
ncx_mosquito
~42 Kb
89.891 Kb
A

**Figure 4**

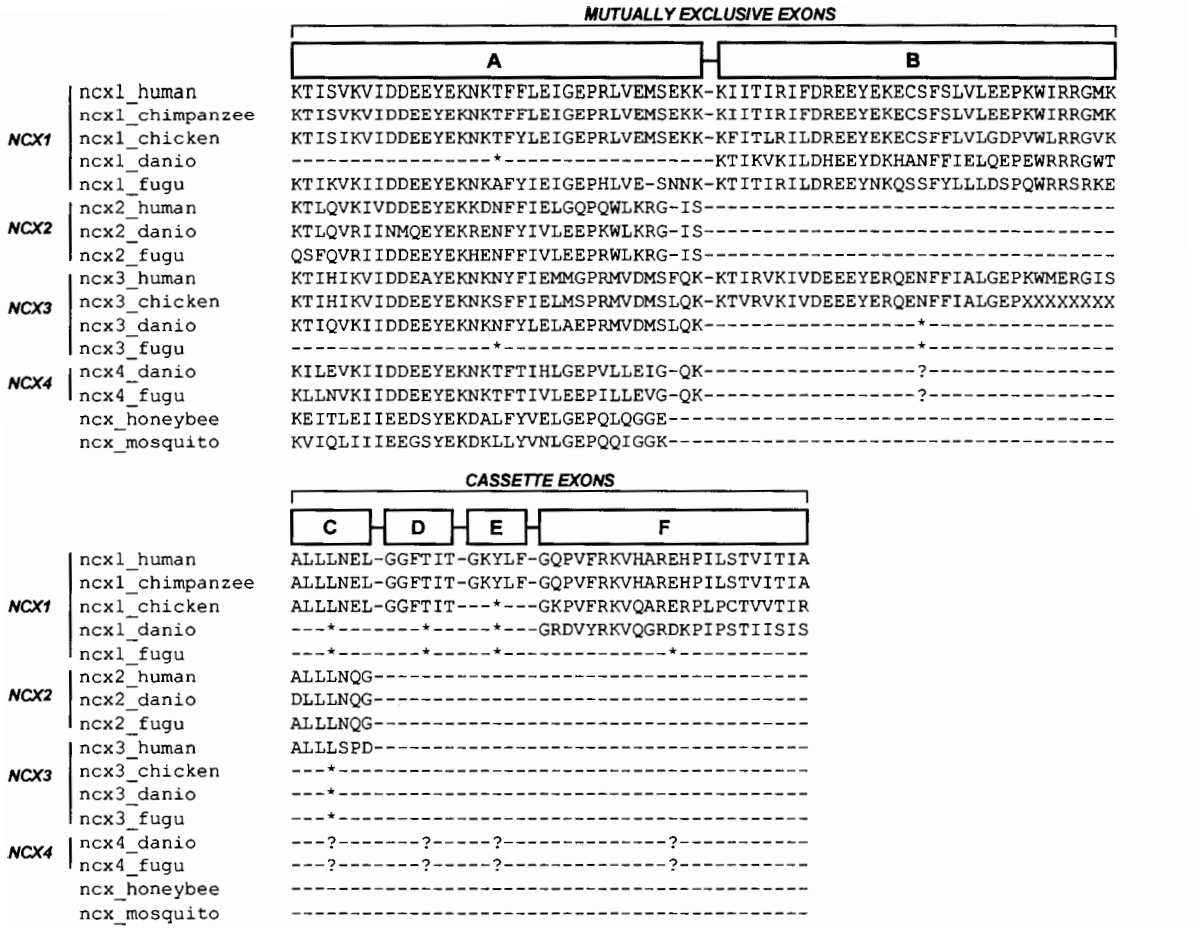
MUTUALLY EXCLUSIVE EXONS
A
B
ncx1_human KTISVKVIDDEEYEKNKTFFLEIGEPRLVEMSEKK-KIITIRIFDREEYEKECSFSLVLEEPKWIRRGMK
ncx1_chimpanzee KTISVKVIDDEEYEKNKTFFLEIGEPRLVEMSEKK-KIITIRIFDREEYEKECSFSLVLEEPKWIRRGMK
NCX1 ncx1_chicken KTISIKVIDDEEYEKNKTFYLEIGEPRLVEMSEKK-KFITLRILDREEYEKECSFFLVLGDPVWLRRGVK
ncx1_danio ----------*----------KTIKVKILDHEEYDKHANFFIELQEPEWRRRGWT
ncx1_fugu KTIKVKIIDDEEYEKNKAFYIEIGEPHLVE-SNNK-KTITIRILDREEYNKQSSFYLLLDSPQWRRSRKE
ncx2_human KTLQVKIVDDEEYEKKDNFFIELGQPQWLKRG-IS----------
NCX2 ncx2_danio KTLQVRIINMQEYEKRENFYIVLEEPKWLKRG-IS----------
ncx2_fugu QSFQVRIIDDEEYEKHENFFIVLEEPRWLKRG-IS----------
ncx3_human KTIHIKVIDDEAYEKNKNYFIEMMGPRMVDMSFQK-KTIRVKIVDEEEYERQENFFIALGEPKWMERGIS
NCX3 ncx3_chicken KTIHIKVIDDEEYEKNKSFFIELMSPRMVDMSLQK-KTVRVKIVDEEEYERQENFFIALGEPXXXXXXXX
ncx3_danio KTIQVKIIDDEEYEKNKNFYLELAEPRMVDMSLQK----------*----------
ncx3_fugu ----------*----------*----------
NCX4 ncx4_danio KILEVKIIDDEEYEKNKTFTIHLGEPVLLEIG-QK----------?----------
ncx4_fugu KLLNVKIIDDEEYEKNKTFTIVLEEPILLEVG-QK----------?----------
ncx_honeybee KEITLEIIEEDSYEKDALFYVELGEPQLQGGE----------
ncx_mosquito KVIQLIIIEEGSYEKDKLLYVNLGEPQQIGGK----------
CASSETTE EXONS
C
D
E
F
ncx1_human ALLLNEL-GGFTIT-GKYLF-GQPVFRKVHAREHPILSTVITIA
ncx1_chimpanzee ALLLNEL-GGFTIT-GKYLF-GQPVFRKVHAREHPILSTVITIA
NCX1 ncx1_chicken ALLLNEL-GGFTIT---*---GKPVFRKVQARERPLPCTVVTIR
ncx1_danio ---*-------*-----*---GRDVYRKVQGRDKPIPSTIISIS
ncx1_fugu ---*-------*-----*----------*----------
ncx2_human ALLLNQG----------
NCX2 ncx2_danio DLLLNQG----------
ncx2_fugu ALLLNQG----------
ncx3_human ALLLSPD----------
NCX3 ncx3_chicken ---*----------
ncx3_danio ---*----------
ncx3_fugu ---*----------
NCX4 ncx4_danio ---?-------?-----?----------?----------
ncx4_fugu ---?-------?-----?----------?----------
ncx_honeybee ----------
ncx_mosquito ----------

**Figure 5**

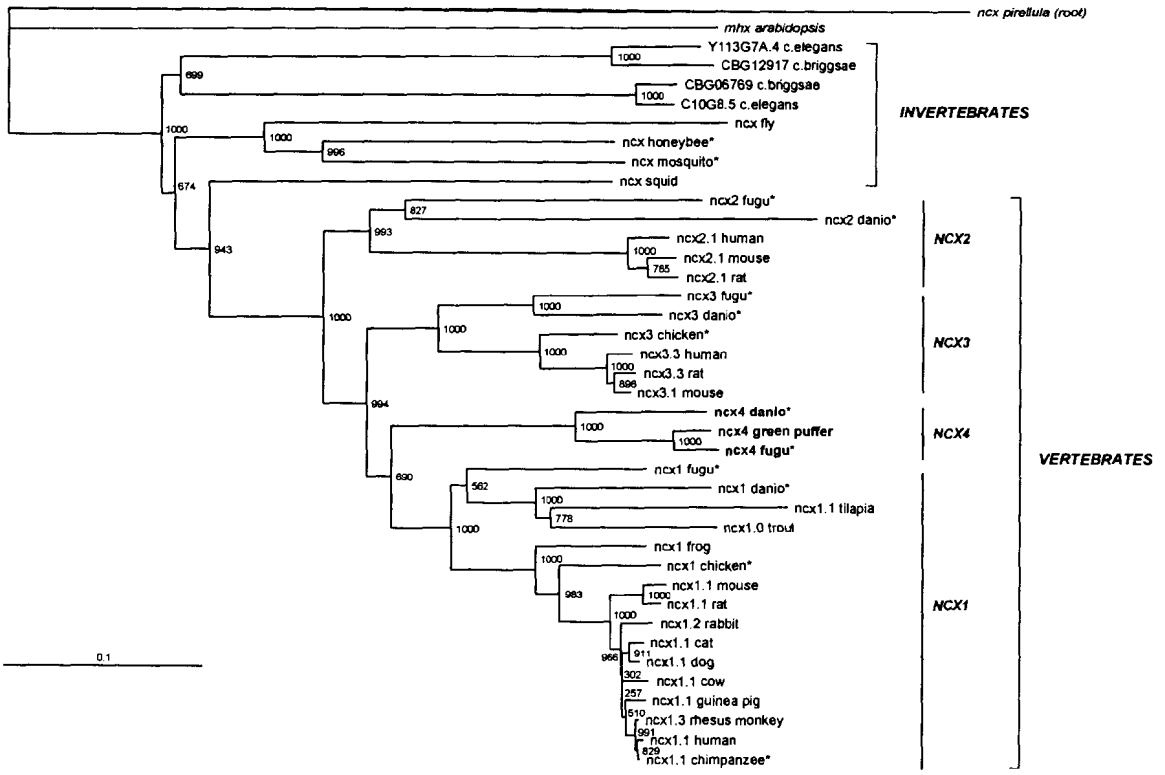
ncx pirellula (root)
mhx arabidopsis
Y113G7A.4 c.elegans
CBG12917 c.briggsae
CBG06769 c.briggsae
C10G8.5 c.elegans
ncx fly
ncx honeybee*
ncx mosquito*
ncx squid
INVERTEBRATES
ncx2 fugu*
ncx2 danio*
ncx2.1 human
ncx2.1 mouse
ncx2.1 rat
NCX2
ncx3 fugu*
ncx3 danio*
ncx3 chicken*
ncx3.3 human
ncx3.3 rat
ncx3.1 mouse
NCX3
ncx4 danio*
ncx4 green puffer
ncx4 fugu*
NCX4
ncx1 fugu*
ncx1 danio*
ncx1.1 tilapia
ncx1.0 trout
ncx1 frog
ncx1 chicken*
ncx1.1 mouse
ncx1.1 rat
ncx1.2 rabbit
ncx1.1 cat
ncx1.1 dog
ncx1.1 cow
ncx1.1 guinea pig
ncx1.3 rhesus monkey
ncx1.1 human
ncx1.1 chimpanzee*
NCX1
VERTEBRATES
0.1

**Figure 6**

## 5.7 Figure Legends

**Figure 1: Topology of the $Na^+$-$Ca^{2+}$ exchanger**
The $Na^+$-$Ca^{2+}$ exchanger (NCX) is modeled to have 9 putative transmembrane segments (TMS), based on experimental evidence of Nicoll *et al.* (19) and Iwamoto *et al.* (18). The TMS are shown as *shaded cylinders*, with 5 in the N-terminal ($NH_2$) domain and 4 in the C-terminal domain (COOH). The NCX has a ~32 residue signal peptide (SP) that is cleaved during processing and is indicated by an *open cylinder*. On opposite sides of the membrane between TMS 2-3 and TMS 7-8 are the respective α-1 and α-2 repeats, shown in dark grey. These regions display intramolecular similarity and are important in ion translocation. The N- and C-terminal TMS clusters are separated by a large hydrophilic intracellular loop (~550 residues) that is important in exchanger regulation. The XIP site is implicated in $Na^+$-dependent inactivation, and $Ca^{2+}$ binding sites in $Ca^{2+}$-dependent activation. In addition, the C-terminal end of the hydrophilic loop contains an alternative splice region.

**Figure 2: Multiple sequence alignment of α-repeat regions and surrounding TMS**
Multiple sequence alignments of the α-1 (A) and α-2 (B) internal repeats and surrounding TMS are shown. This region is important for ion translocation. The predicted secondary structure profile as described in Fig. 1 is shown above the alignment, with the α-repeats shown in dark grey. The mammalian NCX sequences in these regions display 100% identity, and are therefore represented by human isoforms of NCX1, NCX2, and NCX3. GI numbers for all NCX sequences are shown in Table I. NCX sequences are grouped based on NCX isoform, with the residues flanking the alignment numbered from the start codon. The asterisk (*) in the zebrafish NCX2 sequence signifies a gap in sequence due to incomplete sequencing of the zebrafish genome.

**Figure 3: Multiple sequence alignment of regulatory regions from selected NCX sequences**
Alignments of the TMS5 and XIP site (A) and $Ca^{2+}$-regulatory region (B) are shown. The XIP site has been implicated in $Na^+$-dependent inactivation and the $Ca^{2+}$-binding sites in $Ca^{2+}$-dependent activation. The predicted secondary structure profile as described in Fig. 1 is shown above the alignment. The mammalian NCX sequences in these regions display nearly 100% identity, and are therefore represented by human isoforms of NCX1, NCX2, and NCX3. GI numbers for all NCX sequences are shown in Table I. NCX sequences are grouped based on NCX isoform, with the residues flanking the alignment numbered from the start codon. The asterisk (*) in the zebrafish NCX2 sequence signifies a gap in sequence due to incomplete sequencing of the zebrafish genome.

**Figure 4: Gene structure of NCX sequences derived from whole genomes**
The gene structures of the 13 new NCX sequences and representative human NCX1, NCX2, and NCX3 were constructed from intron-exon data at Ensembl. The genes are grouped based on NCX isoform, with the invertebrate NCX isoforms being unclassified. Exons are denoted by *black* boxes, beginning with the start codon and terminating with the stop codon. Exons only represent the coding sequence of the NCX gene and are

numbered accordingly from the start codon. Previously, it has been shown that exon 1 of the NCX genes is not translated and therefore we have not included it in this schematic. The start codon is in exon 2, which is designated exon 1 in this figure. Introns are indicated by *lines* connecting the exons. The exon and intron widths are drawn approximately to scale based on their nucleotide size over 80 Kb of genomic DNA. Genes that extend beyond 80 Kb have the longest intron given simply by their length so as to fit the scalebar. Total genomic distance each gene stretches is given to the right of the last exon in Kb. Exons belonging to the alternative splice region are underlined and lettered accordingly. It should be noted that not all of the alternative splice exons predicted to exist in these species were found. The mutually exclusive exons A and B are both shown in the schematic in cases where they could both be found in the genomic data. Due to sequencing errors in the chimpanzee genome, the first exon of NCX1 was split into three exons, each separated by a single nucleotide. Since the actual chimpanzee NCX1 gene would not contain these insertions, we have numbered the exons the same as human NCX1. Exon 6 in both the chicken NCX1 and the danio NCX2 contain gaps, and are indicated by open boxes. Exons 2 and 3 from zebrafish NCX2 were not present due to incomplete sequencing of the zebrafish genome and are indicated by open boxes and a question mark (?).

**Figure 5: Multiple sequence alignment of alternative splice region from NCX sequences derived from whole genomes**

The alternative splice regions of NCX genes derived in this study were aligned with human NCX splice variants for reference. The sequences are grouped by isoform, with boxes above the alignment denoting mutually exclusive (A or B, gray boxes) and cassette (CDEF, white boxes) exons. In instances where exons A and B were found in a species' genome, both are shown. The asterisks (*) denote exons that should be present in the species but were not found, while the question mark (?) indicates that it is not known if homologous cassettes exist in NCX4. The X's in exon B of chicken NCX3 denote amino acids that cannot be identified due to incomplete genome sequencing.

**Figure 6: Phylogenetic analysis of the NCX family**

The Neighbour-Joining (NJ) tree was constructed with resampling (bootstrap, 1000 datasets) using ClustalX. Vertebrate and invertebrate sequences are enclosed with brackets, while vertebrate NCX genes are labeled with vertical lines. The tree is rooted with a $Na^{+}$-$Ca^{2+}$ exchanger from *Pirellula sp*, and rooting with AtMHX from *A. thaliana* did not change the tree topology. NCX4 (bold) refers to our putative NCX group that is unique to the fish species, and asterisks (*) denote NCX isoforms that where derived from whole genomes.

## 5.8 References


1. Busch, W., and Saier, M. H., Jr. (2003) *Methods Mol Biol* 227, 21-36
2. Saier, M. H., Jr. (2003) *Mol Microbiol* 48, 1145-1156
3. White, P. J., and Broadley, M. R. (2003) *Ann Bot (Lond)* 92, 487-511
4. Berridge, M. J., Lipp, P., and Bootman, M. D. (2000) *Nat Rev Mol Cell Biol* 1, 11-21
5. Moreno, S. N., and Docampo, R. (2003) *Curr Opin Microbiol* 6, 359-364
6. Norris, V., Grant, S., Freestone, P., Canvin, J., Sheikh, F. N., Toth, I., Trinei, M., Modha, K., and Norman, R. I. (1996) *J Bacteriol* 178, 3677-3682
7. Macrez, N., and Mironneau, J. (2004) *Curr Mol Med* 4, 263-275
8. Philipson, K. D., and Nicoll, D. A. (2000) *Annu Rev Physiol* 62, 111-133
9. Blaustein, M. P., and Lederer, W. J. (1999) *Physiol Rev* 79, 763-854
10. Nicoll, D. A., Longoni, S., and Philipson, K. D. (1990) *Science* 250, 562-565
11. He, Z., Tong, Q., Quednau, B. D., Philipson, K. D., and Hilgemann, D. W. (1998) *J Gen Physiol* 111, 857-873
12. Schwarz, E. M., and Benzer, S. (1997) *Proc Natl Acad Sci U S A* 94, 10249-10254
13. Xue, X. H., Hryshko, L. V., Nicoll, D. A., Philipson, K. D., and Tibbits, G. F. (1999) *Am J Physiol* 277, C693-700
14. Ureta-Vidal, A., Ettwiller, L., and Birney, E. (2003) *Nat Rev Genet* 4, 251-262
15. Baxevanis, A. D. (2003) *Mol Med* 9, 185-192
16. Cai, X., and Lytton, J. (2004) *Mol Biol Evol* 21, 1692-1703
17. Ottolia, M., John, S., Qiu, Z., and Philipson, K. D. (2001) *J Biol Chem* 276, 19603-19609.
18. Iwamoto, T., Nakamura, T. Y., Pan, Y., Uehara, A., Imanaga, I., and Shigekawa, M. (1999) *FEBS Lett* 446, 264-268
19. Nicoll, D. A., Ottolia, M., Lu, L., Lu, Y., and Philipson, K. D. (1999) *J Biol Chem* 274, 910-917
20. Durkin, J. T., Ahrens, D. C., Pan, Y. C., and Reeves, J. P. (1991) *Arch Biochem Biophys* 290, 369-375
21. Hryshko, L. V., Nicoll, D. A., Weiss, J. N., and Philipson, K. D. (1993) *Biochim Biophys Acta* 1151, 35-42
22. Nicoll, D. A., Hryshko, L. V., Matsuoka, S., Frank, J. S., and Philipson, K. D. (1996) *Journal of Biological Chemistry* 271, 13385-13391

23. Santacruz-Toloza, L., Ottolia, M., Nicoll, D. A., and Philipson, K. D. (2000) *J Biol Chem* 275, 182-188

24. Qiu, Z., Nicoll, D. A., and Philipson, K. D. (2001) *J Biol Chem* 276, 194-199.

25. Kofuji, P., Hadley, R. W., Kieval, R. S., Lederer, W. J., and Schulze, D. H. (1992) *Am J Physiol* 263, C1241-1249

26. Quednau, B. D., Nicoll, D. A., and Philipson, K. D. (1997) *Am J Physiol* 272, C1250-1261

27. Li, Z., Matsuoka, S., Hryshko, L. V., Nicoll, D. A., Bersohn, M. M., Burke, E. P., Lifton, R. P., and Philipson, K. D. (1994) *J Biol Chem* 269, 17434-17439

28. Nicoll, D. A., Quednau, B. D., Qui, Z., Xia, Y. R., Lusis, A. J., and Philipson, K. D. (1996) *J Biol Chem* 271, 24914-24921

29. Kraev, A., Chumakov, I., and Carafoli, E. (1996) *Genomics* 37, 105-112

30. Gabellini, N., Bortoluzzi, S., Danieli, G. A., and Carafoli, E. (2002) *Gene* 298, 1-7

31. Li, X. F., Kraev, A. S., and Lytton, J. (2002) *J Biol Chem* 277, 48410-48417

32. Linck, B., Qiu, Z., He, Z., Tong, Q., Hilgemann, D. W., and Philipson, K. D. (1998) *Am J Physiol* 274, C415-423

33. Kofuji, P., Lederer, W. J., and Schulze, D. H. (1994) *J Biol Chem* 269, 5145-5149

34. Iwata, T., Kraev, A., Guerini, D., and Carafoli, E. (1996) *Ann N Y Acad Sci* 779, 37-45

35. Ruknudin, A., Valdivia, C., Kofuji, P., Lederer, W. J., and Schulze, D. H. (1997) *Am J Physiol* 273, C257-265

36. Birney, E., Andrews, T. D., Bevan, P., Caccamo, M., Chen, Y., Clarke, L., Coates, G., Cuff, J., Curwen, V., Cutts, T., Down, T., Eyras, E., Fernandez-Suarez, X. M., Gane, P., Gibbins, B., Gilbert, J., Hammond, M., Hotz, H. R., Iyer, V., Jekosch, K., Kahari, A., Kasprzyk, A., Keefe, D., Keenan, S., Lehvaslaiho, H., McVicker, G., Melsopp, C., Meidl, P., Mongin, E., Pettett, R., Potter, S., Proctor, G., Rae, M., Searle, S., Slater, G., Smedley, D., Smith, J., Spooner, W., Stabenau, A., Stalker, J., Storey, R., Ureta-Vidal, A., Woodwark, K. C., Cameron, G., Durbin, R., Cox, A., Hubbard, T., and Clamp, M. (2004) *Genome Res* 14, 925-928

37. Hubbard, T., Barker, D., Birney, E., Cameron, G., Chen, Y., Clark, L., Cox, T., Cuff, J., Curwen, V., Down, T., Durbin, R., Eyras, E., Gilbert, J., Hammond, M., Huminiecki, L., Kasprzyk, A., Lehvaslaiho, H., Lijnzaad, P., Melsopp, C., Mongin, E., Pettett, R., Pocock, M., Potter, S., Rust, A., Schmidt, E., Searle, S., Slater, G., Smith, J., Spooner, W., Stabenau, A., Stalker, J., Stupka, E., Ureta-Vidal, A., Vastrik, I., and Clamp, M. (2002) *Nucleic Acids Res* 30, 38-41

38. Altschul, S. F., Gish, W., Miller, W., Myers, E. W., and Lipman, D. J. (1990) *J Mol Biol* 215, 403-410

39. Thompson, J. D., Gibson, T. J., Plewniak, F., Jeanmougin, F., and Higgins, D. G. (1997) *Nucleic Acids Res* 25, 4876-4882

40. Nicholas, K. B., Nicholas, H. B. J., and Deerfield, D. W. I. (1997) *EMBNET NEWS* 4, 1-4

41. Felsenstein, J. (1996) *Methods Enzymol* 266, 418-427

42. Saitou, N., and Nei, M. (1987) *Mol Biol Evol* 4, 406-425

43. Page, R. D. (1996) *Comput Appl Biosci* 12, 357-358

44. Brenner, S. E. (1999) *Trends Genet* 15, 132-133

45. Devos, D., and Valencia, A. (2001) *Trends Genet* 17, 429-431

46. Iliopoulos, I., Tsoka, S., Andrade, M. A., Enright, A. J., Carroll, M., Poullet, P., Promponas, V., Liakopoulos, T., Palaios, G., Pasquier, C., Hamodrakas, S., Tamames, J., Yagnik, A. T., Tramontano, A., Devos, D., Blaschke, C., Valencia, A., Brett, D., Martin, D., Leroy, C., Rigoutsos, I., Sander, C., and Ouzounis, C. A. (2003) *Bioinformatics* 19, 717-726

47. Guigo, R., Agarwal, P., Abril, J. F., Burset, M., and Fickett, J. W. (2000) *Genome Res* 10, 1631-1642

48. Mathe, C., Sagot, M. F., Schiex, T., and Rouze, P. (2002) *Nucleic Acids Res* 30, 4103-4117

49. Matsuoka, S., Nicoll, D. A., Reilly, R. F., Hilgemann, D. W., and Philipson, K. D. (1993) *Proc Natl Acad Sci U S A* 90, 3870-3874.

50. Nicoll, D. A., Hryshko, L. V., Matsuoka, S., Frank, J. S., and Philipson, K. D. (1996) *Ann N Y Acad Sci* 779, 86-92

51. Doering, A. E., Nicoll, D. A., Lu, Y., Lu, L., Weiss, J. N., and Philipson, K. D. (1998) *J Biol Chem* 273, 778-783

52. Doyle, D. A., Morais Cabral, J., Pfuetzner, R. A., Kuo, A., Gulbis, J. M., Cohen, S. L., Chait, B. T., and MacKinnon, R. (1998) *Science* 280, 69-77

53. Gao, L., Balshaw, D., Xu, L., Tripathy, A., Xin, C., and Meissner, G. (2000) *Biophys J* 79, 828-840

54. Balshaw, D., Gao, L., and Meissner, G. (1999) *Proc Natl Acad Sci U S A* 96, 3345-3347

55. Hilgemann, D. W. (1990) *Nature* 344, 242-245

56. Hryshko, L. V., Matsuoka, S., Nicoll, D. A., Weiss, J. N., Schwarz, E. M., Benzer, S., and Philipson, K. D. (1996) *J Gen Physiol* 108, 67-74

57. Elias, C. L., Xue, X. H., Marshall, C. R., Omelchenko, A., Hryshko, L. V., and Tibbits, G. F. (2001) *Am J Physiol Cell Physiol* 281, C993-C1000.

58. Matsuoka, S., Nicoll, D. A., He, Z., and Philipson, K. D. (1997) *J Gen Physiol* 109, 273-286

59. He, Z., Petesch, N., Voges, K., Roben, W., and Philipson, K. D. (1997) *J Membr Biol* 156, 149-156

60. Levitsky, D. O., Nicoll, D. A., and Philipson, K. D. (1994) *J Biol Chem* 269, 22847-22852

61. Matsuoka, S., Nicoll, D. A., Hryshko, L. V., Levitsky, D. O., Weiss, J. N., and Philipson, K. D. (1995) *J Gen Physiol* 105, 403-420

62. Kikuno, R., Nagase, T., Ishikawa, K., Hirosawa, M., Miyajima, N., Tanaka, A., Kotani, H., Nomura, N., and Ohara, O. (1999) *DNA Res* 6, 197-205

63. Brenner, S., Elgar, G., Sandford, R., Macrae, A., Venkatesh, B., and Aparicio, S. (1993) *Nature* 366, 265-268

64. Aparicio, S., Chapman, J., Stupka, E., Putnam, N., Chia, J. M., Dehal, P., Christoffels, A., Rash, S., Hoon, S., Smit, A., Gelpke, M. D., Roach, J., Oh, T., Ho, I. Y., Wong, M., Detter, C., Verhoef, F., Predki, P., Tay, A., Lucas, S., Richardson, P., Smith, S. F., Clark, M. S., Edwards, Y. J., Doggett, N., Zharkikh, A., Tavtigian, S. V., Pruss, D., Barnstead, M., Evans, C., Baden, H., Powell, J., Glusman, G., Rowen, L., Hood, L., Tan, Y. H., Elgar, G., Hawkins, T., Venkatesh, B., Rokhsar, D., and Brenner, S. (2002) *Science* 297, 1301-1310

65. Sjolander, K. (2004) *Bioinformatics* 20, 170-179

# CHAPTER 6
# cDNA CLONING AND EXPRESSION OF CARDIAC $Na^+/Ca^{2+}$ EXCHANGER (NCX) FROM MOZAMBIQUE TILAPIA (*Oreochromis Mossambicus*) REVEALS TELEOST MEMBRANE TRANSPORTER WITH MAMMALIAN TEMPERATURE DEPENDENCE*‡

Christian R. Marshall[1,2], Tien-Chien Pan[3], Hoa Dinh Le[4], Alexander Omelchenko[4], Pung Pung Hwang[3], Larry V. Hryshko[4] and Glen F. Tibbits[1,2]

[1] Department of Molecular Biology & Biochemistry and the
Cardiac Membrane Research Laboratory
Simon Fraser University
Burnaby, BC, Canada

[2] Cardiovascular Sciences
BC Research Institute for Children's & Women's Health
Vancouver, BC, Canada

[3] Institute of Cellular and Organismic Biology
Academia Sinica Nankang,
Taipei, Taiwan

[4] Institute of Cardiovascular Sciences
St. Boniface General Hospital Research Centre
The University of Manitoba
Winnipeg, MB, Canada

* This study is published in the *Journal of Biological Chemistry* by permission under the following reference: Marshall C.R., Pan T.C., Le H.D., Omelchenko A., Hwang P.P., Hryshko L.V., and Tibbits G.F. (2005) *J Biol Chem* Jun 3. PMID: 15937330. Reproduced with permission.

‡ The nucleotide sequence reported in this manuscript has been submitted to GenBank™ with the accession number AY283779

## 6.1 Abstract

The complete cDNA sequence of the tilapia cardiac $Na^+/Ca^{2+}$ exchanger (*NCX-TL1.0*) was determined. The 3.1 kb transcript encodes a protein 957 amino acids in length, with a predicted signal peptide cleaved at residue 31. Hydropathy analysis and sequence comparison predicted a mature protein with nine transmembrane spanning segments, which is consistent with the structural topologies of other known mammalian and teleost NCX isoforms. Overall sequence comparison shows high identity to both trout NCX-TR1.0 (~81%) and mammalian NCX1.1 (~73%), and phylogenetic analyses confirms NCX-TL1.0 as a member of the *NCX1* gene family expressing exons A, C, D, and F in the alternative splice region. When expressed in *Xenopus* oocytes, NCX-TL1.0 displayed both positive regulation by $Ca^{2+}$ and $Na^+$-dependent inactivation in a manner similar to trout NCX-TR1.0. However, the tilapia NCX-TL1.0 exhibits a relatively high sensitivity to temperature compared to the trout NCX-TR1.0. Whereas trout NCX-TR1.0 currents display energy of activation ($E_a$) values of ~7 kJ/mol, the tilapia NCX-TL1.0 currents show mammalian-like temperature dependence with peak and steady state current $E_{act}$ values of 53 ± 9 kJ/mol and 67 ± 21 kJ/mol, respectively. Using comparative sequence analysis, we highlight 10 residue positions in the N-terminal domain of NCX that, in combination, may confer exchanger temperature dependence through subtle changes in protein flexibility. Tilapia NCX-TL1.0 represents the first non-mammalian NCX to exhibit a mammalian temperature dependence phenotype, and will prove a useful model in defining the interplay between molecular flexibility versus stability in NCX function.

## 6.2 Introduction

The $Na^+/Ca^{2+}$ exchanger (NCX) is a polytopic membrane protein belonging to the cation:$Ca^{2+}$ antiporter (CaCA) superfamily of $Ca^{2+}$ transporters. Catalyzing the electrogenic exchange of three $Na^+$ for one $Ca^{2+}$, the NCX plays a key role in regulating cytosolic $Ca^{2+}$ concentrations in many different cell types. The NCX is present in a wide array of species with high overall sequence identity and conservation of ion transport and regulatory components (1,2). However, knowledge of molecular function of the NCX is based primarily on examination of mammalian isoforms and is therefore restrictive from a phylogenetic perspective. Examination of non-mammalian isoforms has previously provided valuable insights into NCX function (3-5). The *NCX* gene family consists of three cloned members present in vertebrates, *NCX1* (6), *NCX2* (7), and *NCX3* (8). Phylogenetic analyses suggests that these exchanger isoforms arose from separate gene duplication events occurring before the emergence of vertebrates, as evidenced by the presence of all three *NCX* genes in fish species (2). In addition, a putative fourth member of the *NCX* family present only in fish species was derived from genomic data, but has unknown function and expression patterns at this time (2).

The relative expression of NCX amongst tissues varies greatly, and generally is correlative with the need for a high degree of transmembrane $Ca^{2+}$ flux regulated in a precise manner. Whereas NCX2 and NCX3 are found exclusively in brain and skeletal muscle, expression of NCX1 is virtually ubiquitous with the highest levels present in excitable tissues (9). In addition, differential expressions of exons from the alternative splice region yield an array of NCX splice variants that are expressed in a tissue specific manner (9,10). The highest exchange activity is in the heart, where the role of the cardiac NCX1.1 in excitation-contraction (EC) coupling has been studied extensively (11-13). NCX1.1 serves as the prime mechanism of $Ca^{2+}$ extrusion from the cardiomyocyte and is, therefore, an important contributor to relaxation (14,15). It has been suggested that reverse mode exchange can contribute to cardiac contraction via $Ca^{2+}$ influx (16-18), a role that is increased in both the failing heart and neonate heart (19-21). In addition, NCX1 has been implicated in several cardiac pathophysiologies including arrhythmogenesis (22-24) and cellular damage associated with ischemia/reperfusion

injury (25,26). Elucidating the molecular mechanisms behind NCX function is crucial to understanding and manipulating its role in the heart.

Previously, we have used temperature as a probe to gain insight into the molecular function of the NCX (3,27). Proteins involved with $Ca^{2+}$ active transport and regulation in the mammalian heart, such as NCX1.1, are highly temperature dependent (3,28). Homologous proteins in cold adaptive species have evolved differently in order to maintain adequate cardiac function in conditions that are cardioplegic to mammals. Using both native (29) and cloned (3) protein, it has been shown that temperature dependence of NCX1 from cold- and warm-adapted species vary substantially. Comparison of peak outward exchange currents from cloned trout NCX-TR1.0 and canine NCX1.1 gave $Q_{10}$ values (fold change in activity per 10 °C change in temperature) of 1.1 and 2.4, respectively (3). Furthermore, these disparities in temperature dependence are not due to differences in inactivation kinetics or NCX regulatory properties. At the amino acid level, these isoforms exhibit high overall identity (~73%), which is significantly higher in the alpha repeat region (~92%), XIP site (~85%), and $Ca^{2+}$ regulatory binding domains (95%). Construction of trout and canine NCX chimeras revealed that the region responsible for the differential temperature dependence between isoforms was within the $NH_2$-terminal transmembrane domain (27). This region comprises approximately a third of the protein, including the first five transmembrane segments up to the end of the XIP site. Further attempts to define specific areas or substitutions responsible for the temperature dependence of the exchanger have proven difficult and given equivocal results (unpublished observations).

Despite the high overall identity between trout NCX-TR1.0 and canine NCX1.1, the species are separated by ~450 million years of evolution (30). To make a more accurate comparison between NCX proteins adapted to high and low temperatures, examination of more closely related NCX isoforms may reduce the number of substitution permutations required to confer the temperature dependence phenotype. Teleosts successfully populate habitats over a large temperature range, and as such their proteins have evolved to function accordingly. Tilapias (*Oreochromis sp)* are euryhaline teleosts that inhabit environments ranging from freshwater to seawater of high salinity and can withstand temperatures as high as 42 °C (31,32). Due to their tolerance of

relatively extreme environments, tilapias have gained important roles as model organisms in the laboratory (31,33,34) and as a prominent fish in aquaculture (32,35). In this study, we have chosen the Mozambique Tilapia (*Oreochromis mossambicus*) as a model system because the cardiac NCX from this species has likely adapted to function at temperatures similar to those in the mammalian heart but lethal to the trout. We report here the cDNA cloning and characterization of the tilapia NCX-TL1.0 and for the first time demonstrate a non-mammalian NCX with mammalian like temperature dependence of $Na^+/Ca^{2+}$ exchange.

## 6.3 Methods

### 6.3.1 Animals

Cultured tilapia (*Oreochromis mossambicus*), weighing 40 ~ 50 g, were maintained at the Institute of Zoology (Academia Sinica, Taipei, Taiwan) in freshwater (local tap water) at 27 °C under a 14hr:10hr light:dark photoperiod.

### 6.3.2 RNA Extraction

Tilapia were killed with a sharp blow to the head. An appropriate amount of heart tissue (~0.5 g) was collected and homogenized in 4 mL of solution containing 4 M guanidine thiocyanate, 1.25 M sodium citrate, 35% N-Lauroylsar-cosine-Na-salt and 0.1 M 2-ME (2-Mercaptoethanol). Tissue homogenates were mixed with 0.4 mL 2 M sodium acetate, 0.8 mL choloroform-isopropanol (49:1) and 4 mL phenol and shaken thoroughly. After centrifugation at 4 °C and 13,000 rpm for 30 min, the supernatants were mixed with an equal volume of isopropanol. Pellets were precipitated by another centrifugation at 4 °C and 13,000 rpm for 30 min, washed with 70% alcohol and stored at -20 °C before use. The amount and quality of the total RNA was determined by measuring absorbance at 260 nm and 280 nm with a spectrophotometer (Hitachi U-2000, Tokyo, Japan) and by running RNA denatured gels.

### 6.3.3 cDNA Cloning and Sequencing

For cloning and sequencing, mRNA was purified from the total RNA of three tilapia hearts using an Oligotex mRNA kit (Qiagen, Hilden, Germany). The cDNA used for all subsequent PCR cloning was prepared by 5'- and 3'- rapid amplification of cDNA ends (RACE) using a SMART™ RACE cDNA Amplification Kit (Clontech, CA, USA). A partial cDNA fragment was amplified by PCR using forward (5'-AARCARAARCAYCCNGA-3') and reverse (5'-ACRAAYTGYTCNCKCCA-3') degenerate primers based on conserved domains within the intracellular loop of canine *NCX1.1* (GenBank™ accession number M57523). The forward primer corresponds to a region just downstream of the XIP site (nucleotides 1018-1035); whereas the reverse primer, matches a region just before TMS6 (nucleotides 2248-2265). For PCR amplification, 2 μL cDNA was used as template in a 50 μL final reaction volume containing 0.25 mM dNTP, 2.5 units *Ex Taq*™ DNA polymerase (TaKaRa, Shiga, Japan), and 0.2 μM of each primer. For PCR the reaction conditions were: initial denaturation at 95 °C for 3 min, followed by 30 cycles of denaturation at 95 °C for 30 s, annealing at 50 °C for 30s, extension at 72 °C for 1 min, and final extension at 72 °C for 10 min. PCR products were purified and subcloned into the pGEM-T Easy vector (Promega, WI, USA). Nucleotide sequencing was determined with an ABI 377 Automated DNA Sequencer (ABI, Warrington, UK). From these partial sequences, specific 5'- and 3'- RACE primers were designed and used for subsequent PCR steps. PCR products were subcloned into the pGEM-T Easy vector and sequenced. The full length tilapia *NCX-TL1.0* clone was covered by three overlapping fragments, each ~1 kb in length. These three fragments were ligated together to produce the full length clone.

### 6.3.4 Expression of Tilapia NCX-TL1.0 in *Xenopus* Oocytes

The full length tilapia *NCX-TL1.0* was subcloned from the original sequencing pGEM-T Easy vector into the expression vector pBSTA. To do this, *Bgl*II sites were introduced at the start and stop codons of the tilapia *NCX-TL1.0* in the pGEM-T Easy vector using the QuickChange™ Site-Directed Mutagenesis Kit (Stratagene, La Jolla, CA). The pBSTA vector contains the 5' and 3' untranslated regions (UTRs) of *Xenopus* β-globin, which in the final construct replaces the endogenous tilapia UTRs and flank the

coding region. The pBSTA vector containing the full length tilapia *NCX-TL1.0* was linearized with *Sac*II and cRNA was synthesized *in vitro* using the T7 mMessage mMachine Kit (Ambion, Austin, TX). The cRNA amount was assessed spectroscopically, while cRNA purity was determined with a 1% agarose RNA gel. Oocytes were prepared as described previously (36), and injected with 46 nl of cRNA diluted to 0.5 ng/nl. Tilapia NCX-TL1.0 exchange activity was assessed 3-7 days after injection using the giant excised patch technique (see below).

### 6.3.5 Electrophysiology

Using the giant excised patch technique, outward $Na^+/Ca^{2+}$ exchange currents were measured as described previously (3,27). Briefly, oocytes with the vitellin layer removed were placed in a solution containing (in mM): 100 KOH, 100 MES, 20 HEPES, 5 EGTA, 5 $MgCl_2$; pH 7.0 at room temperature (~22-23 °C) with MES. Borosilicate glass pipettes were polished (inner diameter of ~20 - 30 μm) and coated with a Parafilm-mineral oil mixture. Suction was used to form gigaohm seals and membrane patches were excised by moving the pipette tip. The pipette (extracellular) solution contained (in mM): 100 NMG-MES, 30 HEPES, 30 TEA-OH, 16 sulfamic acid, 8 $CaCO_3$, 6 KOH, 0.25 ouabain, 0.1 niflumic acid, 0.1 flufenamic acid; pH 7.0 with MES. The bath (cytosolic) solutions contained (in mM): 100 [$Na^+$ or $Li^+$]-aspartate, 20 MOPS, 20 TEA-OH, 20 CsOH, 10 EGTA, 0-7.3 $CaCO_3$, 1.0-1.13 $Mg(OH)_2$; pH 7.0 with MES or LiOH. MAXC software (37) was used to adjust $Mg^{2+}$ and $Ca^{2+}$ to yield free concentrations of 1 mM and either 0, 1, or 10 μM, respectively. Outward $Na^+/Ca^{2+}$ exchange currents were activated by switching from $Li^+$- to $Na^+$-based bath solution and recorded at 30, 14, and 7 °C. To account for current rundown within a single patch, multiple current traces at all three temperatures were measured. Axon Instruments (Union City, CA) hardware and software were used for data acquisition and analysis.

### 6.3.6 Current Trace Analyses and Statistics

Inactivation kinetics and temperature dependence parameters for the tilapia NCX-TL1.0 currents were calculated as described previously (3). The inactivation rate constant, λ, was obtained by fitting current-time traces to a single exponential. The

energy of activation, $E_{act}$, and temperature coefficient, $Q_{10}$, were calculated as indices of temperature dependence as described by Marshall et al (27). All values are displayed as means ± standard error of means (SEM). Statistical significance of the results was determined by mean comparison using Tukey's test and one-way ANOVA performed with Microcal Origin and Graphpad software. Unless indicated otherwise, a value of $p<0.05$ was considered significantly different.

### 6.3.7 Sequence Alignments and Phylogenetic Analysis

Sequence and phylogenetic analyses were performed as previously described (2). Sequence data were acquired from either the National Center for Biotechnology Information (NCBI) non redundant protein database, or derived from whole genome sequences. The following sequences were obtained from NCBI (GenBank™ GI number): human NCX1.1 (GI 10863913), human NCX2.1 (GI 10720116), human NCX3.3 (GI 22087483), rainbow trout NCX-TR1.0 (GI 6273849), and green spotted pufferfish NCX (GI 47219419). NCX1, NCX2, NCX3, and NCX4 from *Fugu rubripes* (Japanese pufferfish) and *Danio rerio* (zebrafish) were derived from whole genome sequences (2). Acquired NCX sequences were aligned with ClustalX (Version 1.83) (38) using the default parameters. The alignment was then imported into Genedoc (Version 2.6.002) (39) for manual editing and creation of figures. Neighbor-Joining (NJ) trees were generated using ClustalX, followed by tree evaluation with bootstrap resampling (1000 times). The program TREEVIEW (Version 1.6.6) (40) was used to examine and display the resulting phylogram and was rooted with the invertebrate CALX (GI 2266953) from fruit fly. The variable alternative splice site region of NCX was not included in subsequent phylogenetic analyses due the high potential for homoplasy in that region.

## 6.4 Results

### 6.4.1 Tilapia NCX-TL1.0 cDNA and Deduced Protein Topology

A 3106-bp cDNA clone was isolated from the heart of Mozambique tilapia (GenBank™ Accession number AY283779) using a combination of RT-PCR and 5'- and

3'-RACE. An open reading frame of 2871-bp is initiated by a methionine at nucleotide 59 associated with a partial Kozak initiation site, ACC*ATG*A (start codon italicized). This open reading frame encodes a protein of 957 amino acids, designated NCX-TL1.0, with a deduced molecular weight of 107 kDa. The 174-bp 3'-untranslated region (excluding the stop codon) does not contain a polyadenylation signal.

The deduced amino acid sequence for tilapia *NCX-TL1.0* is shown in Figure 1. The only other teleost NCX to be cloned and characterized, trout *NCX-TR1.0* (Genbank™ Accession AF175313), is aligned for comparison of the sequences. The topology of tilapia NCX-TL1.0 is similar to that of trout NCX-TR1.0 (41) and canine NCX1.1 (6) based on hydropathy analysis (42) and prediction of secondary structure using PSI-PRED (43) (data not shown). For tilapia NCX-TL1.0, an N-terminal signal peptide with a cleavage site between residues 31 and 32 was predicted both through homology to experimentally determined NCX signal peptides (44,45) and by the prediction program SignalP 3.0 (46). In the N-terminal region of the mature tilapia NCX-TL1.0 (between signal cleavage site and first TMS) there are two potential N-linked glycosylation sites at positions 10 and 15 (aspargines). If glycosylation of tilapia NCX-TL1.0 and mammalian NCX1 is similar, then N10 of NCX-TL1.0 would be glycosylated, however this requires experimental conformation. In addition, the cysteines at positions 19 and 25 are homologous with positions 14 and 20 of the mammalian NCX1, which are thought to be involved in a disulfide bond with cysteine 792 (47). This latter cysteine is located in the extracellular loop between TMS 6 and 7 and corresponds to C780 in the tilapia NCX-TL1.0.

Overall sequence comparison of full length tilapia NCX-TL1.0 and trout NCX-TR1.0 shows ~81% identity at the amino acid level. As expected, identity is especially high in the α-repeats (~95%), XIP site (90%) and $Ca^{2+}$ binding sites (100%). Phylogenetic analysis confirms NCX-TL1.0 as a member of the *NCX1* gene family, expressing exons A, C, D, and F in the alternative splice site. The phylogram in Figure 2 shows the evolutionary relationship of all known NCX isoforms from fish.

### 6.4.2 Functional Expression of Tilapia NCX-TL1.0 and Exchange Currents

To confirm that the tilapia NCX-TL1.0 was functional, we expressed the exchanger in *Xenopus* oocytes and measured outward $Na^+/Ca^{2+}$ exchange currents in giant excised patches (Figure 3). With the pipette (extracellular surface) containing 8 mM $Ca^{2+}$, currents were activated by switching from a 100 mM $Li^+$ to 100 mM $Na^+$ solution applied to the intracellular surface of the excised patch. Tilapia NCX-TL1.0 outward exchange currents show characteristics similar to those of both trout and mammalian NCX1 isoforms. As shown in Figure 3A, the tilapia NCX-TL1.0 demonstrates positive regulation by intracellular $Ca^{2+}$. At 1 μM intracellular $Ca^{2+}$, the outward current increases to a peak value then decays slowly in a time dependent manner indicative of $Na^+$-dependent inactivation (48). Increased regulatory intracellular $Ca^{2+}$ (10 μM) eliminates $Na^+$-dependent inactivation, thereby increasing steady state current (Figure 3B). The current-voltage (I-V) relationship for tilapia NCX-TL1.0 recorded in the presence of 100 mM $Na^+_i$ and 1 μM $Ca^{2+}_i$ is shown in Figure 3C. To obtain the I-V plot, a series of 10 mV voltage steps from a holding potential of 0 mV were applied from -100 to +100 mV for 10 ms intervals. This voltage clamp protocol was applied both in the presence and absence of $Na^+$ to allow for leak subtraction. The I-V plot obtained for tilapia NCX-TL1.0 was similar to that of trout NCX-TR1.0.

### 6.4.3 Temperature Effect on Tilapia NCX-TL1.0 Exchange Activity

We examined the effects of temperature on $Na^+/Ca^{2+}$ exchange from tilapia NCX-TL1.0 expressed in *Xenopus* oocytes in comparison to that of previously published trout NCX-TR1.0 temperature sensitivity (3). Figure 4A shows outward exchange currents of tilapia NCX-TL1.0 and trout NCX-TR1.0 measured in giant patches at 7, 14 and 30 °C. The current properties of tilapia NCX-TL1.0 and trout NCX-TR1.0 are similar; however, they display very different responses to decreasing temperature. At 7 °C, the trout NCX-TR1.0 maintains ~60% of its activity measured at 30 °C whereas the tilapia NCX-TL1.0 sustains only ~10% of its activity.

Arrhenius plots of $Na^+/Ca^{2+}$ exchange peak and steady currents of tilapia NCX-TL1.0 and NCX-TR1.0 are shown in Figure 4B. Within the same patch, currents at 7 and

14 °C were normalized to that of 30 °C. The $E_{act}$ was obtained from the slope of a linear regression fit of the logarithms of normalized currents (Figure 4C). Previously, we have used the $E_{act}$ as an indication of NCX temperature dependence (3,27). For tilapia NCX-TL1.0, the $E_{act}$ values were 53 ± 9 kJ/mol and 67 ± 21 kJ/mol, for peak and steady state currents, respectively. Compared to trout NCX-TR1.0 (peak and steady-state $E_{act}$ are 7.0 ± 2.0 kJ/mol and 6.0 ± 0.1 kJ/mol, respectively), tilapia NCX-TL1.0 exchange activity is highly temperature dependent. This phenomenon is corroborated by comparison of tilapia NCX-TL1.0 and trout NCX-TR1.0 $Q_{10}$'s (Figure 4D). The $Q_{10}$ values for the peak and steady state currents are 2.2 ± 0.1 and 2.8 ± 0.3, respectively for tilapia NCX-TL1.0 compared to 1.2 ± 0.1 and 1.1 ± 0.1 for trout NCX-TR1.0, respectively.

The inactivation rate constant (λ) was obtained by fitting tilapia NCX-TL1.0 current-time traces at 7, 14, and 30 °C to a single exponential (Figure 4E). For comparison, the λ values published by Elias et al (3) for the trout NCX-TR1.0 are also shown. The respective λ values for tilapia NCX-TL1.0 and trout NCX-TR1.0 are 0.14 ± 0.03 and 0.16 ± 0.02 at 30 °C, 0.12 ± 0.04 and 0.10 ± 0.01 at 14 °C, and 0.19 ± 0.03 and 0.10 ± 0.01 at 7 °C. The reason for the increase in λ value for the tilapia NCX-TL1.0 at 7 °C is not known, but may be a result of poor fitting due to small absolute currents.

### 6.4.4 Examination of Sequence Differences in the N-terminal Domain

Figure 5 shows a multiple sequence alignment of the N-terminus, previously shown to be the area solely responsible for NCX temperature dependence (27). The alignment contains all known fish species NCX isoforms and uses human NCX isoforms as mammalian representatives. A sequence comparison based on common temperature phenotypes highlights 10 residue positions (P70, V87, N163, L186, T196, A210, V230, L238, L249, F259) numbered from the tilapia start codon that may confer NCX temperature sensitivity. All residues except for N163 (T in mammal) and 249L (F in mammal) are common between mammalian NCX1.1 and tilapia NCX-TL1.0 but different than trout NCX-TR1.0.

## 6.5 Discussion

With the underlying motivation of finding a teleost NCX capable of functioning at mammalian core temperatures, we have cloned, expressed, and characterized an NCX from tilapia heart. Hydropathy and secondary structure analyses of tilapia NCX-TL1.0 yield similar results to that of other NCX1 isoforms. Currently, NCX is modeled to have nine TMS, five in the N-terminal domain and four in the C-terminal domain (49,50). These TMS domains are important for ion translocation (51) and are separated by a large intracellular loop that confers NCX regulatory properties and alternative splicing. In addition, known NCX1 post-translational modifications including signal peptide cleavage, N-linked glycosylation, and intramolecular disulfide bond formation are predicted to be conserved in tilapia NCX-TL1.0. Thus, the overall topology of tilapia NCX-TL1.0 is unlikely to be different from that proposed for NCX1.

Sequence and evolutionary analyses support the assignment of NCX-TL1.0 as a member of the NCX1 subfamily. Fish species' genomes have recently been shown to possess up to four separate *NCX* genes, whereas other vertebrate species have only three *NCX* genes (2). However, the degree and distribution of *NCX* gene expression in fish species is largely unknown with the exception of the trout NCX1 ortholog (NCX-TR1.0), which is known to be expressed in cardiac tissue (41). Phylogenetic analysis places the tilapia NCX-TL1.0 as a member of the teleost NCX1 family, with its most closely related isoform being trout NCX-TR1.0. Sequence comparison at the amino acid level shows an overall identity of ~81% with trout NCX-TR1.0 and ~73% with mammalian NCX1. Conversely, comparison of tilapia NCX-TL1.0 protein sequence with other NCX paralogs (NCX2, NCX3, and NCX4) yields lower identities in the range of 60-65%. Consistent with the NCX subfamily as a whole, the tilapia NCX-TL1.0 sequence displays the highest divergence in the N-terminal region but is highly conserved in the TMS and regulatory regions (1,2).

Tissue specific NCX splice variants are created through differential expression of six small exons (A-F) located in the C-terminal region of the large intracellular loop (9,10,52). Exons A and B are mutually exclusive and are used in conjunction with the cassette exons C, D, E, and F to produce alternatively spliced NCX isoforms (10). In

mammals, the cardiac specific NCX isoform is designated NCX1.1 and uses the exons A, C, D, E, and F. Interestingly, the tilapia NCX-TL1.0 cloned in this study expresses exons A, C, D, and F, the same combination present in trout NCX-TR1.0 cloned from heart tissue (41). Both cardiac specific NCX isoforms from fish species appear to lack exon E, which is only five amino acids in length. The functional significance of the alternative splice region remains unclear as it is not essential for ion transport (53). Potential roles of the region including modulation of NCX current through PKA sensitivity (54,55), $Ca^{2+}$ dependent activation (55,56) and $Na^{+}$ inactivation (56,57) have been suggested. However, the specific physiological relevance of exon E is not known, and its absence in the unique splice variant combination of A, C, D, and F is thus far restricted to expression in fish hearts (thus named NCX1.0). Based on phylogenetic analyses and examination of exon expression patterns in the alternative splice region, it is clear that we have expressed a cardiac specific NCX1 from tilapia.

The high sequence identity of tilapia NCX-TL1.0 with trout NCX-TR1.0 in known regulatory regions is reflected in its $Na^{+}/Ca^{2+}$ exchange current. The tilapia NCX-TL1.0 is positively regulated by $Ca^{2+}$ making it similar to trout NCX-TR1.0 (41), mammalian NCX1 (58), and squid NCX-SQ1 (4) but opposite to fruit fly CALX, which is characterized by decreased current in response to increased cytoplasmic $Ca^{2+}$ (5). At 30 °C, the $\lambda$ values for trout NCX-TR1.0 and tilapia NCX-TL1.0 (~0.15) are indicative of slower inactivation rates than those previously reported for mammalian cloned ($\lambda \sim 0.25$) (3) and native ($\lambda \sim 0.23$) (60) NCX1.1 outward currents. $Na^{+}$-dependent inactivation in NCX1 is attributed in part to the highly conserved XIP site, which is comprised of 20 residues and is located in the first portion of the intracellular loop just past TMS5 (59). Common to tilapia NCX-TL1.0 and trout NCX-TR1.0 are a methionine and arginine at positions 9 and 18, respectively (numbering from start of XIP site). Mammalian NCX1.1 has a valine and glutamine at these respective positions. To our knowledge, these residue positions have not undergone mutational analysis and may be directly or indirectly involved in altering NCX inactivation rates. The physiological significance of fish NCX isoforms having slower $Na^{+}$-dependent inactivation is not known. We have thus confirmed that tilapia NCX-TL1.0 is functional when expressed in oocytes, and that it is regulated in a manner similar to that of trout NCX-TR1.0.

Mammalian cardiac NCX1 activity measured in cardiac myocytes (60,61), sarcolemmal vesicles (29), and *Xenopus* oocytes (3) has been shown to be highly temperature dependent with $E_{act}$ values in the range of 48-66 kJ/mol. In contrast, trout NCX-TR1.0 currents exhibit $E_{act}$ values of ~7 kJ/mol when expressed in *Xenopus* oocytes (3). The relative insensitivity of trout NCX-TR1.0 to temperature compared to mammalian NCX1.1 has been shown to be an intrinsic property of the protein rather than dependent on lipid environment (29). In the present study, we measured the temperature dependence of cardiac NCX-TL1.0 cloned from the warm-adapted fish species, Mozambique tilapia. This teleost is tolerant of environmental temperatures greater than mammalian body temperature (up to 42 °C) and has an optimal growth temperature (~30 °C) that is lethal to the trout. Conversely, the lower temperature limit of tilapia (~14 °C) coincides with the optimal temperature for trout survival. The relatively high $E_{act}$ values (~60 kJ/mol) we recorded for tilapia NCX-TL1.0 in giant excised patches are consistent with the tilapia's environmental temperature range, and are typical values of a warm adaptive species. To our knowledge this is the first NCX from non-mammalian species shown to display mammalian-like temperature dependence. The only other non-mammalian NCX temperature dependence reported is from frog NCX, which has intermediate temperature sensitivity with $E_{act}$ values of ~25 kJ/mol (62).

Elucidating the specific molecular determinants of NCX temperature dependence has proven a difficult undertaking. Previous chimeric studies using mammalian NCX1.1 and trout NCX-TR1.0 have shown that the region responsible for the differential temperature dependence between these isoforms is attributable to the N-terminal hydrophobic domain (27). This includes the XIP region and makes up only a quarter of the mature protein, consisting of approximately ~240 residues. There are 50 substitutions between trout NCX-TR1.0 and tilapia NCX-TL1.0 in this region, with over half of these substitutions residing in the highly variable N-terminus before the putative TMS1. The rest of the hydrophobic region (TMS1 to end of XIP site) is highly conserved with only 22 substitutions. It is generally accepted that proteins adapted to cold temperatures, like the trout NCX-TR1.0, gain catalytic efficiency through increased flexibility in structural moieties involved in catalysis (63,64) (also see reviews (65-67)). The opposite also holds true in that adaptation to high temperatures is postulated to involve increased rigidity for

thermal stability. Unfortunately, this relationship between flexibility and stability does not allow prediction of single amino acid effects on protein temperature dependence. There is no absolute consensus as to which residues modify protein flexibility suggesting that evolution has utilized numerous strategies to confer function over a range of temperatures. In addition, it is not known if membrane proteins – which may make up ~30% of an organisms proteome – employ the same adaptations to temperature as soluble proteins. The vast majority of functional data examining protein temperature adaptation is derived from soluble proteins (64,68-70) and, in the case of comparative proteomic studies (71-73), fail to differentially treat soluble and membrane proteins in their analysis. These caveats advocate the study of membrane protein temperature dependence on a case-by-case basis, preferably using orthologs that are highly conserved. The tilapia NCX-TL1.0 is potentially a very good model to study NCX temperature dependence since it is evolutionarily close to the trout NCX-TR1.0, but displays a mammalian temperature dependence phenotype.

A simple sequence analysis comparing amino acids that are common to tilapia NCX-TL1.0 and mammalian NCX1.1 but different in trout NCX-TR1.0, yields ten residue positions in the N-terminal domain that may alter exchanger flexibility (Figure 5). These highlighted substitutions are spread throughout the N-terminus and not localized to a single area in the primary sequence; however, since little of the NCX tertiary structure is known, it is possible some of these residues are in close proximity in the tertiary structure. All residues except N163 and L249 (numbering is from tilapia NCX-TL1.0 start codon) are identical between tilapia and mammalian NCX, but different in trout NCX-TR1.0. Tilapia residue N163 (D in trout and T in mammal) is predicted to be in re-entrant loop of the α-1 repeat, spanning TMS2 and TMS3. The TMS portion of the α-1 repeat is known to be important for ion translocation and is highly conserved, whereas the reentrant loop shows more variability amongst NCX isoforms (2) and has a less defined role in ion exchange. Recent mutational analysis at this position showed no effect on ion translocation or intracellular $Na^+$ affinity, arguing against the role of N163 in the ion translocation mechanism (74). Tilapia residue L249 (M in trout, F in mammal) is located in TMS5 and is implicated in sensitivity to the NCX inhibitor SEA0400 (75). The remaining tilapia NCX-TL1.0 residues (P70, V87, L186, T196, A210, V230, L238,

F259) are identical to NCX1.1. F259 has been shown to modify $Na^+$-dependent inactivation (59), but the remaining residues have not undergone mutational analysis and have unknown roles in NCX function. The most interesting of these positions is tilapia residue P70, located in the N-terminus just upstream of TMS1. In all vertebrate species a proline is located at this position, except in the trout NCX-TR1.0 which has a threonine. This substitution introduces a potential N-linked glycosylation site (consensus NXS/TX, where X is any residue except P) in the trout NCX-TR1.0 that is not found in any other vertebrate NCX isoform. Glycosylation in mammalian NCX1 occurs ~23 residues upstream from this position and has been experimentally determined to not modify exchange based on the parameters measured to date (45). However the effect of glycosylation on NCX temperature dependence is not known. The addition of a glycosylation site in trout NCX-TR1.0 close to TMS1 raises the intriguing possibility of glycosylation being involved in temperature dependence of NCX.

In general, the high variability amongst NCX orthologs and paralogs at these positions is consistent with the fact that none of the residues has been shown to be important for NCX ion translocation. It is likely that NCX contains two types of amino acid residues, one group that is conserved throughout evolution and is critical for the core function of ion translocation and regulation, and a second group that is not essential for NCX function but rather confers the subtle "tweaking" of the protein to function optimally under its respective environmental conditions. NCX temperature dependence is therefore dictated by a series of substitutions in positions that may or may not be common among homologs, indicating each isoform has evolved independent mechanisms to adapt to temperature. Further, these substitutions most likely modify the flexibility of NCX core regions in an allosteric manner that allows function at different temperatures.

In summary, we have cloned and characterized NCX-TL1.0 from tilapia heart and show it displays mammalian like temperature dependence. The tilapia NCX-TL1.0 is a potentially good model to study the temperature dependence of NCX and should lead to a better understanding of NCX function in general.

## 6.6 Figures

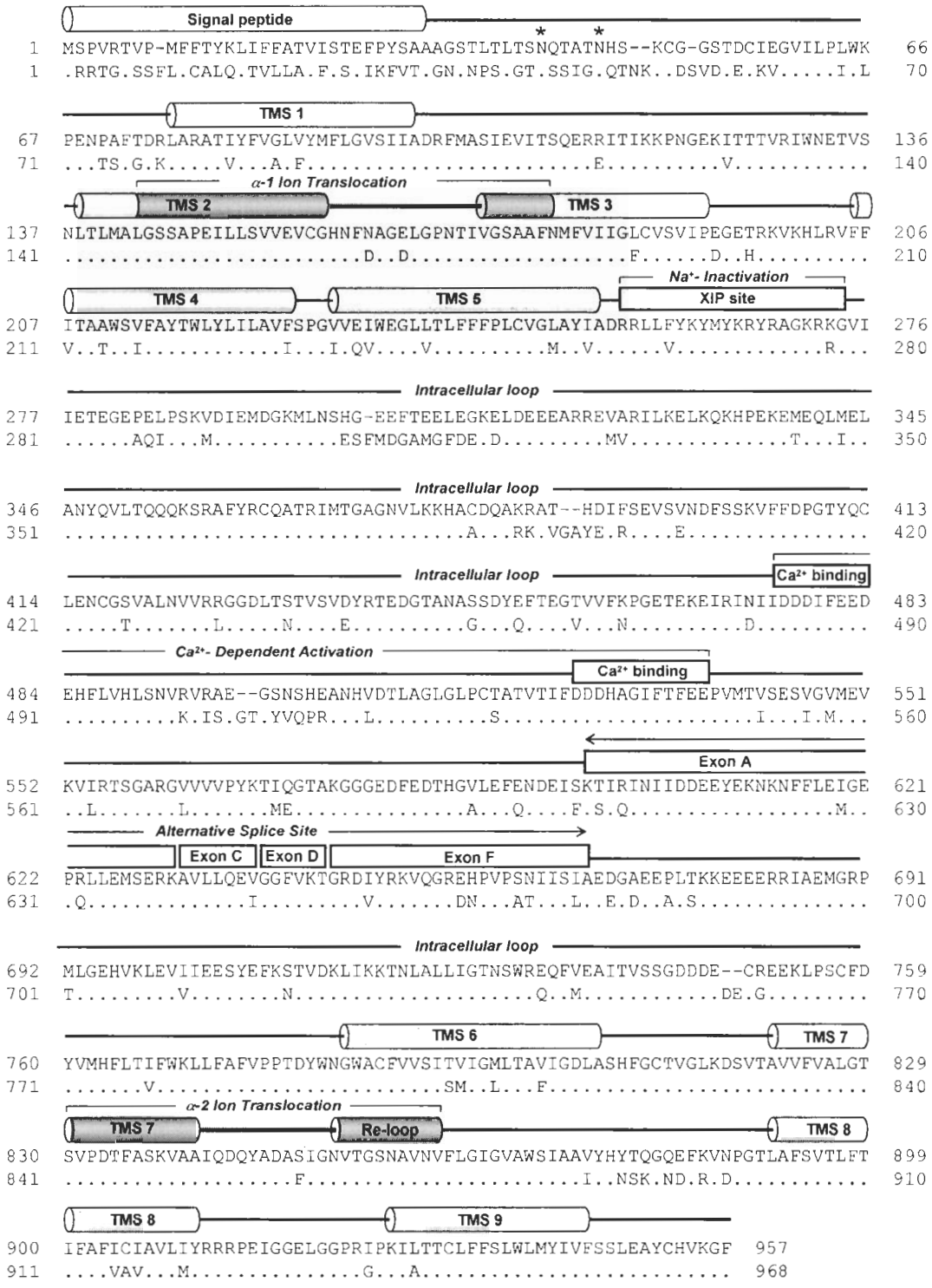


**Figure 1**

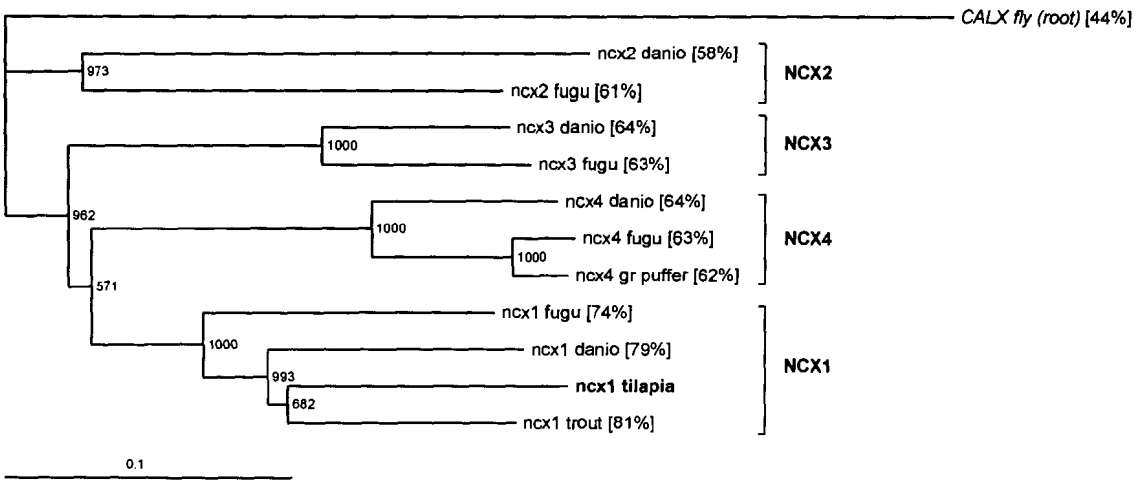
CALX fly (root) [44%]
ncx2 danio [58%]
973
ncx2 fugu [61%]
NCX2
ncx3 danio [64%]
1000
ncx3 fugu [63%]
NCX3
ncx4 danio [64%]
962
1000
ncx4 fugu [63%]
1000
ncx4 gr puffer [62%]
NCX4
571
ncx1 fugu [74%]
1000
ncx1 danio [79%]
993
ncx1 tilapia
682
ncx1 trout [81%]
NCX1
0.1

**Figure 2**

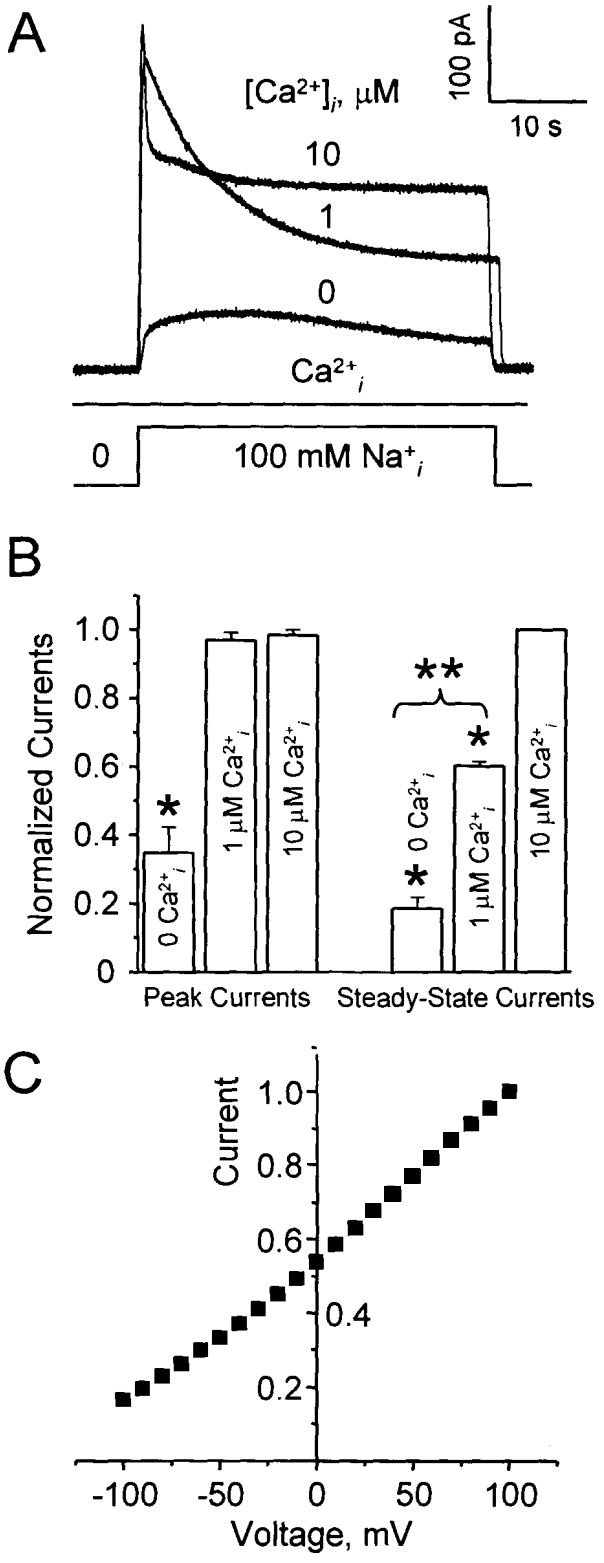
A
[Ca2+]i, μM
100 pA
10 s
10
1
0
Ca2+i
0
100 mM Na+i
B
Normalized Currents
1.0
0.8
0.6
0.4
0.2
0
0 Ca2+i
1 μM Ca2+i
10 μM Ca2+i
0 Ca2+i
1 μM Ca2+i
10 μM Ca2+i
Peak Currents
Steady-State Currents
C
Current
1.0
0.8
0.6
0.4
0.2
-100
-50
0
50
100
Voltage, mV

**Figure 3**

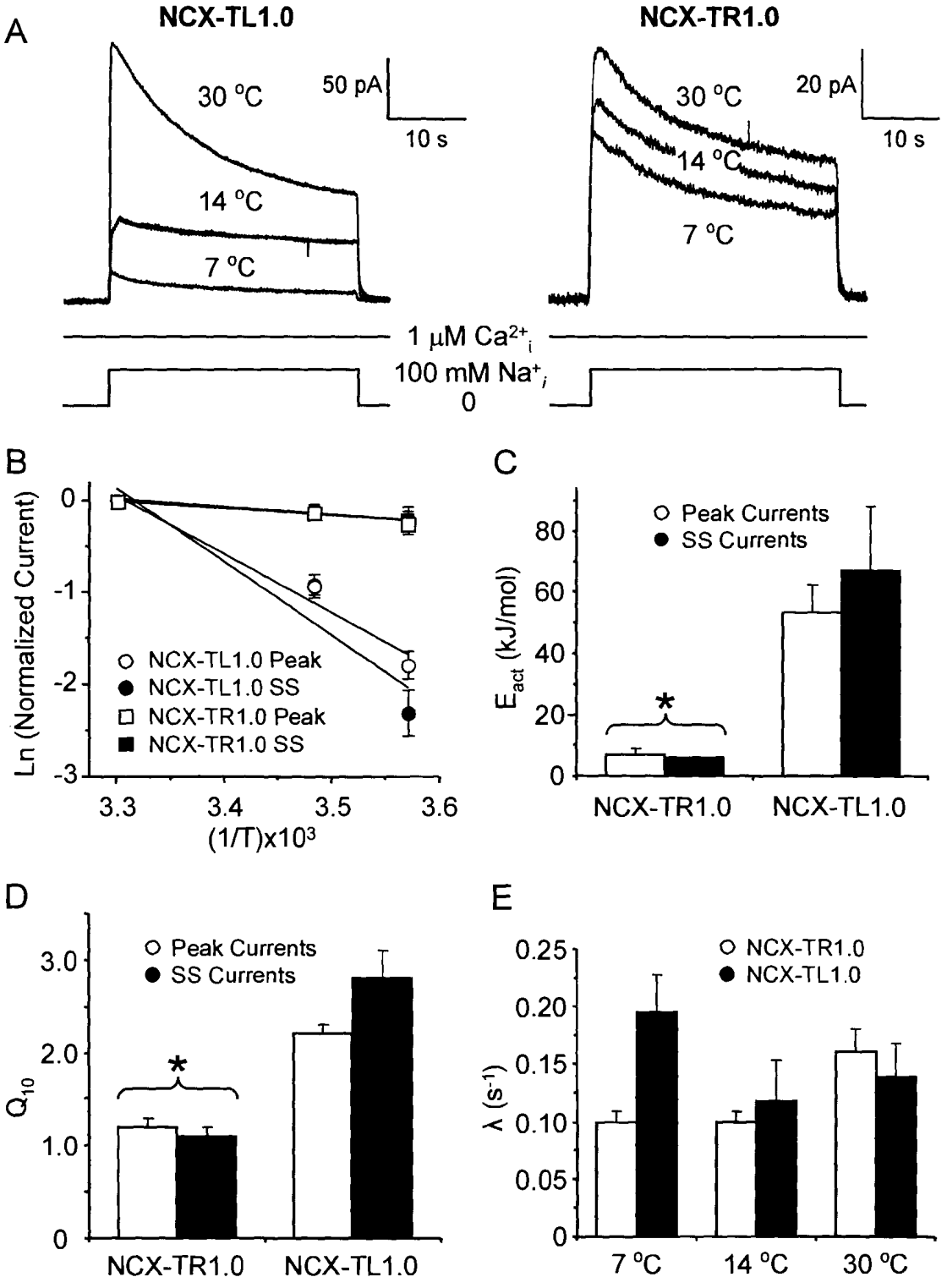
A
NCX-TL1.0
NCX-TR1.0
30 °C
50 pA
10 s
14 °C
7 °C
20 pA
1 μM Ca2+i
100 mM Na+i
0
B
Ln (Normalized Current)
0
-1
-2
-3
3.3
3.4
3.5
3.6
(1/T)x10³
NCX-TL1.0 Peak
NCX-TL1.0 SS
NCX-TR1.0 Peak
NCX-TR1.0 SS
C
Eact (kJ/mol)
80
60
40
20
0
Peak Currents
SS Currents
*
NCX-TR1.0
NCX-TL1.0
D
Q10
3.0
2.0
1.0
0
Peak Currents
SS Currents
*
NCX-TR1.0
NCX-TL1.0
E
λ (s-1)
0.25
0.20
0.15
0.10
0.05
0
NCX-TR1.0
NCX-TL1.0
7 °C
14 °C
30 °C

**Figure 4**

A

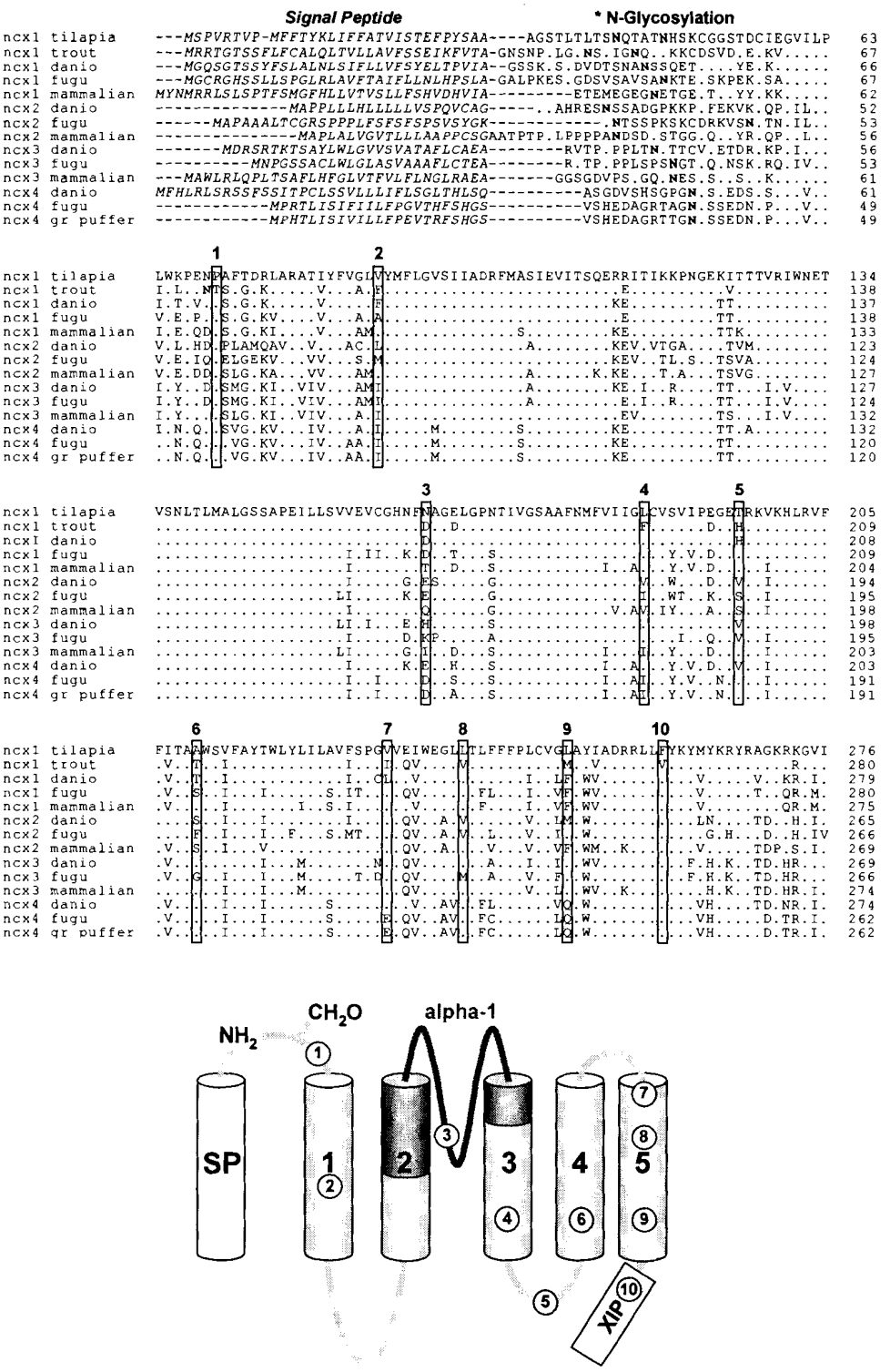
Signal Peptide
* N-Glycosylation
ncx1 tilapia
ncx1 trout
ncx1 danio
ncx1 fugu
ncx1 mammalian
ncx2 danio
ncx2 fugu
ncx2 mammalian
ncx3 danio
ncx3 fugu
ncx3 mammalian
ncx4 danio
ncx4 fugu
ncx4 gr puffer
1
2
3
4
5
6
7
8
9
10

B


NH2
CH2O
alpha-1
SP
1
2
3
4
5
XIP

**Figure 5**

## 6.7 Figure Legends

**Figure 1: Amino acid sequence and topology of tilapia NCX-TL1.0**
The full length deduced amino acid sequence of tilapia NCX-TL1.0 (*upper sequence*) is compared to trout NCX-TR1.0 (*lower sequence*) with dots representing identity between species. Exchanger topology is represented schematically above the sequence alignment. The NCX is modeled to have nine TMS (gray cylinders) and a signal peptide (*open cylinder*) that is cleaved during biosynthesis. The α-repeat regions (*shaded dark gray*) are show intra-molecular sequence similarity and are important for ion translocation. Also shown (*labeled boxes*) are important regions of the large intracellular loop: the exchanger inhibitory peptide (XIP) site, $Ca^{2+}$ regulatory binding sites, and alternative splice site. Asterisks (*) denote potential N-linked glycosylation sites in the N-terminal region of tilapia NCX-TL1.0.

**Figure 2: Phylogeny of NCX from fish species**
Neighbor-Joining (NJ) phylogram of fish species *NCX* gene family constructed with bootstrap re-sampling (1000 datasets). Rainbow trout NCX-TR1.0 (ncx1 trout) and green spotted pufferfish NCX (ncx4 gr puffer) were obtained from the non-redundant protein database at NCBI. NCX1, NCX2, NCX3, and NCX4 from *Fugu rubripes* (ncx1-4 fugu) and *Danio rerio* (ncx1-4 danio) were previously derived from whole genome sequences (2). The tree is rooted with CALX exchanger from the fruit fly, and the tilapia NCX-TL1.0 is shown in bold. Percentages in square brackets display percent identity to tilapia NCX-TL1.0.

**Figure 3: Outward exchange currents of tilapia NCX-TL1.0**
Panel A shows overlapping outward $Na^+/Ca^{2+}$ exchange currents mediated by tilapia NCX-TL1.0. Pipettes contained 8 mM $Ca^{2+}$ and currents were generated by the application of 100 mM intracellular $Na^+$ ($Na^+_i$) in the continuous presence of regulatory intracellular $Ca^{2+}$ ($Ca^{2+}_i$)at the concentration indicated. Temperature was held constant at 30 °C. In panel B pooled data from 4 patches are shown illustrating the intracellular $Ca^{2+}$-dependence of peak and steady-state outward currents. Currents were normalized to the largest peak or steady-state current attained within the same patch. In the absence of regulatory $Ca^{2+}_i$, peak and steady-state currents were minimal and not well-defined. Therefore, the maximal current in the trace was taken as the peak value and the current measured at the end of the 32 second trace was taken as the steady-state value. Single asterisks (*) illustrate statistically significant differences ($p<0.05$) between mean values with respect to that in the presence of 10 μM $Ca^{2+}_i$. The double asterisk (**) indicates a significant difference between mean values found at 0 and 1 μM regulatory $Ca^{2+}_i$. Panel C shows a leak subtracted current-voltage relationship obtained in the presence of 100 mM $Na^+_i$ and 1 μM $Ca^{2+}_i$. This relationship was obtained using 10 ms voltage steps from -100 to 100 mV in 10 mV increments from a holding potential of 0 mV.

**Figure 4: Temperature dependence of tilapia NCX-TL1.0**
Panel A shows representative overlapping traces of tilapia NCX-TL1.0 and the previously published trout NCX-TR1.0 (3). Pipettes contained 8 mM $Ca^{2+}$ and currents

were generated by the rapid application of 100 mM intracellular $Na^+$ ($Na^+_i$) to the cytoplasmic surface of the patch in the continuous presence of 1 μM regulatory intracellular $Ca^{2+}$ ($Ca^{2+}_i$) at the temperatures indicated. In panel B, Arrhenius plots for peak and steady-state currents are presented for tilapia NCX-TL1.0 (*circles*) and trout NCX-TR1.0 (*squares*). For tilapia NCX-TL1.0 data were pooled from 7 patches, while trout NCX-TR1.0 points are as previously measured. Within the same patch, currents at 7 and 14 °C were normalized to that at 30 °C, which was the highest temperature studied. Energies of activation ($E_{act}$), obtained from the slope of a linear regression fit of the logarithms of normalized peak (*open bars*) and steady-state (*shaded bars*) currents are shown in panel C. The single asterisk (*) illustrate statistically significant differences ($p<0.05$) for mean peak and steady current $E_A$ values between trout NCX-TR1.0 and tilapia NCX-TL1.0. For the 7-30 °C interval, the values of temperature coefficients, $Q_{10}$, for peak (*open bars*) and steady state (*shaded bars*) currents are shown in panel D. The single asterisk (*) illustrate statistically significant differences ($p<0.001$) for mean peak and steady current $Q_{10}$ values between trout NCX-TR1.0 and tilapia NCX-TL1.0. Panel E illustrates the temperature dependence of the current decay rate, $\lambda$ ($s^{-1}$) for trout NCX-TR1.0 (*open bars*) and tilapia NCX-TL1.0 (*shaded bars*). ANOVA and mean comparison using Tukey's test did not reveal significant differences at the temperatures indicated.

**Figure 5: Multiple sequence alignment of NCX N-terminal domain**

Panel A shows a multiple sequence alignment of the NCX N-terminal domain from representative species. Sequences were aligned in ClustalX (Version 1.83) using the default parameters and imported into Genedoc (Version 2.6.002) for manual editing. Human NCX1.1 (ncx1 mammalian), human NCX2.1 (ncx2 mammalian), human NCX3.3 (ncx3 mammalian), rainbow trout NCX-TR1.0 (ncx1 trout) and green spotted pufferfish NCX (ncx4 gr puffer) were obtained from the non-redundant protein database at NCBI. NCX1, NCX2, NCX3, and NCX4 from *Fugu rubripes* (ncx1-4 fugu) and *Danio rerio* (ncx1-4 danio) were previously derived from whole genome sequences (2). Due to almost complete identity in this region amongst mammals, human NCX sequences were used as representatives. Residues thought to comprise the signal peptide are shown in italics, while asparagine residues part of a potential glycosylation site (NXS/TX, where X is not a proline) are shown in bold. Residue positions that potentially confer NCX temperature dependence are highlighted and numbered. Panel B shows the approximate location of the highlighted residues in a topological model of the NCX N-terminal domain.

## 6.8 References


1. Cai, X., and Lytton, J. (2004) *Mol Biol Evol* **21**, 1692-1703
2. Marshall, C. R., Fox, J. A., Butland, S. L., Ouellette, B. F., Brinkman, F. S., and Tibbits, G. F. (2005) *Physiol Genomics* Mar 1; [Epub ahead of print] PMID: 15741504
3. Elias, C. L., Xue, X. H., Marshall, C. R., Omelchenko, A., Hryshko, L. V., and Tibbits, G. F. (2001) *Am J Physiol Cell Physiol* **281**, C993-C1000.
4. He, Z., Tong, Q., Quednau, B. D., Philipson, K. D., and Hilgemann, D. W. (1998) *J Gen Physiol* **111**, 857-873
5. Hryshko, L. V., Matsuoka, S., Nicoll, D. A., Weiss, J. N., Schwarz, E. M., Benzer, S., and Philipson, K. D. (1996) *J Gen Physiol* **108**, 67-74
6. Nicoll, D. A., Longoni, S., and Philipson, K. D. (1990) *Science* **250**, 562-565
7. Li, Z., Matsuoka, S., Hryshko, L. V., Nicoll, D. A., Bersohn, M. M., Burke, E. P., Lifton, R. P., and Philipson, K. D. (1994) *J Biol Chem* **269**, 17434-17439
8. Nicoll, D. A., Quednau, B. D., Qui, Z., Xia, Y. R., Lusis, A. J., and Philipson, K. D. (1996) *J Biol Chem* **271**, 24914-24921
9. Quednau, B. D., Nicoll, D. A., and Philipson, K. D. (1997) *Am J Physiol* **272**, C1250-1261
10. Kofuji, P., Hadley, R. W., Kieval, R. S., Lederer, W. J., and Schulze, D. H. (1992) *Am J Physiol* **263**, C1241-1249
11. Blaustein, M. P., and Lederer, W. J. (1999) *Physiol Rev* **79**, 763-854
12. Hilgemann, D. W. (2004) *Am J Physiol Cell Physiol* **287**, C1167-1172
13. Philipson, K. D., and Nicoll, D. A. (2000) *Annu Rev Physiol* **62**, 111-133
14. Bers, D. M., Bassani, J. W., and Bassani, R. A. (1996) *Annals of the New York Academy of Sciences* **779**, 430-442
15. Bridge, J. H., Spitzer, K. W., and Ershler, P. R. (1988) *Science* **241**, 823-825
16. Bers, D. M. (2002) *Nature* **415**, 198-205
17. Leblanc, N., and Hume, J. R. (1990) *Science* **248**, 372-376
18. Wasserstrom, J. A., and Vites, A. M. (1996) *J Physiol* **493 ( Pt 2)**, 529-542
19. Weber, C. R., Piacentino, V., 3rd, Houser, S. R., and Bers, D. M. (2003) *Circulation* **108**, 2224-2229
20. Weisser-Thomas, J., Piacentino, V., 3rd, Gaughan, J. P., Margulies, K., and Houser, S. R. (2003) *Cardiovasc Res* **57**, 974-985
21. Piacentino, V., 3rd, Weber, C. R., Gaughan, J. P., Margulies, K. B., Bers, D. M., and Houser, S. R. (2002) *Ann N Y Acad Sci* **976**, 466-471

22. Pogwizd, S. M., Schlotthauer, K., Li, L., Yuan, W., and Bers, D. M. (2001) *Circ Res* **88**, 1159-1167

23. Pogwizd, S. M., and Bers, D. M. (2004) *Trends Cardiovasc Med* **14**, 61-66

24. Sipido, K. R., Volders, P. G., Schoenmakers, M., De Groot, S. H., Verdonck, F., and Vos, M. A. (2002) *Ann N Y Acad Sci* **976**, 438-445

25. Kusuoka, H., Camilion de Hurtado, M. C., and Marban, E. (1993) *J Am Coll Cardiol* **21**, 240-248

26. Imahashi, K., Kusuoka, H., Hashimoto, K., Yoshioka, J., Yamaguchi, H., and Nishimura, T. (1999) *Circ Res* **84**, 1401-1406

27. Marshall, C., Elias, C., Xue, X. H., Le, H. D., Omelchenko, A., Hryshko, L. V., and Tibbits, G. F. (2002) *Am J Physiol Cell Physiol* **283**, C512-520

28. Hilgemann, D. W., Collins, A., and Matsuoka, S. (1992) *J Gen Physiol* **100**, 933-961

29. Tibbits, G. F., Philipson, K. D., and Kashihara, H. (1992) *Am J Physiol* **262**, C411-417

30. Hedges, S. B. (2002) *Nat Rev Genet* **3**, 838-849

31. Wilson, P. J., Wood, C. M., Walsh, P. J., Bergman, A. N., Bergman, H. L., Laurent, P., and White, B. N. (2004) *Physiol Biochem Zool* **77**, 537-555

32. Costa-Pierce, B. A., and Riedel, R. (2000) in *Tilapia Aquaculture in the Americas* (Costa-Pierce, B. A., and Rakocy, J., eds) Vol. Volume 2, pp. 1-20, 2 vols., World Aquaculture Society Books, Baton Rouge

33. Loretz, C. A., Pollina, C., Hyodo, S., Takei, Y., Chang, W., and Shoback, D. (2004) *J Biol Chem* **279**, 53288-53297

34. Sardella, B. A., Cooper, J., Gonzalez, R. J., and Brauner, C. J. (2004) *Comp Biochem Physiol A Mol Integr Physiol* **137**, 621-629

35. Maclean, N., Rahman, M. A., Sohm, F., Hwang, G., Iyengar, A., Ayad, H., Smith, A., and Farahmand, H. (2002) *Gene* **295**, 265-277

36. Longoni, S., Coady, M. J., Ikeda, T., and Philipson, K. D. (1988) *American Journal of Physiology* **255**, C870-873

37. Bers, D. M., Patton, C. W., and Nuccitelli, R. (1994) *Methods in Cell Biology* **40**, 3-29

38. Altschul, S. F., Gish, W., Miller, W., Myers, E. W., and Lipman, D. J. (1990) *J Mol Biol* **215**, 403-410

39. Nicholas, K. B., Nicholas, H. B. J., and Deerfield, D. W. I. (1997) *EMBNET NEWS* **4**, 1-4

40. Page, R. D. (1996) *Comput Appl Biosci* **12**, 357-358

41. Xue, X. H., Hryshko, L. V., Nicoll, D. A., Philipson, K. D., and Tibbits, G. F. (1999) *Am J Physiol* **277**, C693-700

42. Kyte, J., and Doolittle, R. F. (1982) *J Mol Biol* **157**, 105-132

43. Jones, D. T. (1999) *J Mol Biol* **292**, 195-202

44. Durkin, J. T., Ahrens, D. C., Pan, Y. C., and Reeves, J. P. (1991) *Arch Biochem Biophys* **290**, 369-375

45. Hryshko, L. V., Nicoll, D. A., Weiss, J. N., and Philipson, K. D. (1993) *Biochim Biophys Acta* **1151**, 35-42

46. Bendtsen, J. D., Nielsen, H., von Heijne, G., and Brunak, S. (2004) *J Mol Biol* **340**, 783-795

47. Santacruz-Toloza, L., Ottolia, M., Nicoll, D. A., and Philipson, K. D. (2000) *J Biol Chem* **275**, 182-188

48. Hilgemann, D. W. (1990) *Nature* **344**, 242-245

49. Iwamoto, T., Nakamura, T. Y., Pan, Y., Uehara, A., Imanaga, I., and Shigekawa, M. (1999) *FEBS Lett* **446**, 264-268

50. Nicoll, D. A., Ottolia, M., Lu, L., Lu, Y., and Philipson, K. D. (1999) *J Biol Chem* **274**, 910-917

51. Nicoll, D. A., Hryshko, L. V., Matsuoka, S., Frank, J. S., and Philipson, K. D. (1996) *Journal of Biological Chemistry* **271**, 13385-13391

52. Lee, S. L., Yu, A. S., and Lytton, J. (1994) *J Biol Chem* **269**, 14849-14852

53. Matsuoka, S., Nicoll, D. A., Reilly, R. F., Hilgemann, D. W., and Philipson, K. D. (1993) *Proc Natl Acad Sci U S A* **90**, 3870-3874.

54. Schulze, D. H., Polumuri, S. K., Gille, T., and Ruknudin, A. (2002) *Ann N Y Acad Sci* **976**, 187-196

55. Ruknudin, A., He, S., Lederer, W. J., and Schulze, D. H. (2000) *J Physiol* **529 Pt 3**, 599-610

56. Dyck, C., Omelchenko, A., Elias, C. L., Quednau, B. D., Philipson, K. D., Hnatowich, M., and Hryshko, L. V. (1999) *J Gen Physiol* **114**, 701-711

57. Maack, C., Ganesan, A., Sidor, A., and O'Rourke, B. (2005) *Circ Res* **96**, 91-99

58. Matsuoka, S., Nicoll, D. A., Hryshko, L. V., Levitsky, D. O., Weiss, J. N., and Philipson, K. D. (1995) *J Gen Physiol* **105**, 403-420

59. Matsuoka, S., Nicoll, D. A., He, Z., and Philipson, K. D. (1997) *J Gen Physiol* **109**, 273-286

60. Hilgemann, D. W., Matsuoka, S., Nagel, G. A., and Collins, A. (1992) *J Gen Physiol* **100**, 905-932

61. Kimura, J., Miyamae, S., and Noma, A. (1987) *J Physiol (Lond)* **384**, 199-222

62. Bersohn, M. M., Vemuri, R., Schuil, D. W., Weiss, R. S., and Philipson, K. D. (1991) *Biochimica et Biophysica Acta* **1062**, 19-23

63. Zavodszky, P., Kardos, J., Svingor, and Petsko, G. A. (1998) *Proc Natl Acad Sci U S A* **95**, 7406-7411

64. Olufsen, M., Smalas, A. O., Moe, E., and Brandsdal, B. O. (2005) *J Biol Chem*

65. D'Amico, S., Claverie, P., Collins, T., Georlette, D., Gratia, E., Hoyoux, A., Meuwis, M. A., Feller, G., and Gerday, C. (2002) *Philos Trans R Soc Lond B Biol Sci* **357**, 917-925

66. Fields, P. A. (2001) *Comp Biochem Physiol A Mol Integr Physiol* **129**, 417-431

67. Russell, N. J. (2000) *Extremophiles* **4**, 83-90.

68. Miyazaki, K., Wintrode, P. L., Grayling, R. A., Rubingh, D. N., and Arnold, F. H. (2000) *J Mol Biol* **297**, 1015-1026.

69. Svingor, A., Kardos, J., Hajdu, I., Nemeth, A., and Zavodszky, P. (2001) *J Biol Chem* **276**, 28121-28125.

70. Fields, P. A., and Somero, G. N. (1998) *Proc Natl Acad Sci U S A* **95**, 11476-11481.

71. Saunders, N. F., Thomas, T., Curmi, P. M., Mattick, J. S., Kuczek, E., Slade, R., Davis, J., Franzmann, P. D., Boone, D., Rusterholtz, K., Feldman, R., Gates, C., Bench, S., Sowers, K., Kadner, K., Aerts, A., Dehal, P., Detter, C., Glavina, T., Lucas, S., Richardson, P., Larimer, F., Hauser, L., Land, M., and Cavicchioli, R. (2003) *Genome Res* **13**, 1580-1588

72. Suhre, K., and Claverie, J. M. (2003) *J Biol Chem* **278**, 17198-17202

73. Chakravarty, S., and Varadarajan, R. (2000) *FEBS Lett* **470**, 65-69

74. Ottolia, M., Nicoll, D. A., and Philipson, K. D. (2005) *J Biol Chem* **280**, 1061-1069

75. Iwamoto, T., Kita, S., Uehara, A., Imanaga, I., Matsuda, T., Baba, A., and Katsuragi, T. (2004) *J Biol Chem* **279**, 7544-7553

# CHAPTER 7
# GENERAL DISCUSSION

## 7.1 Summary

Before the undertaking of this thesis, little was known regarding the function of lower vertebrate NCX isoforms and their molecular adaptations to low temperature. Cardiac function in ectothermic species such as teleosts has adapted to operate at temperatures debilitating to the mammalian heart. Orthologous proteins that share function between species have evolved to work optimally over an array of temperatures, often with only minor changes in primary sequence. Thus nature's design affords us comparative models to study the adaptability of protein function to environmental perturbations, as is the case in this study with NCX and temperature dependence.

It has been previously shown that NCX isolated from trout heart was relatively insensitive to temperature compared to mammalian NCX (1); however, the molecular determinants of this observation were unknown. With the cloning of NCX-TR1.0 from trout heart in 1999 by Xue *et al* (2), an avenue for the molecular examination of NCX temperature dependence was opened. The conclusions drawn from this dissertation are widespread and have significantly advanced our understanding of NCX. Using temperature as a probe in combination with comparative sequence analyses provided insight into relationship between NCX genotype and phenotype. Also, despite not being an original goal of this thesis, a comprehensive phylogenetic analysis of NCX was borne out of the need to classify all sequences originally examined for insights into temperature dependence. In a broader context these results have implications for the structure function relationship of proteins in general, especially as it pertains to the intricate balance between protein stability and flexibility. This chapter will discuss the major findings of this thesis, first discussing some of the main caveats of the study then summarizing NCX phylogeny and then NCX temperature dependence.

## 7.2 Main Critiques of the Study

There are several caveats that must be taken into account when drawing conclusions from these studies, some of which will be discussed here. For our molecular studies the main critiques arises from the difficulties associated with the NCX temperature dependent assay. Although extremely sensitive, the giant excised patch technique is very difficult to do especially when isoform specific NCX expression is very low. Due to its low relative expression, we were not able to perform experiments on NCX-TR1.0 that would have given further insight into its function (e.g. half reaction cycles). Charge movement experiments run on NCX-TR1.0 and NCX1.1 would have definitively defined potential differences in ion translocation between the isoforms.

We also could not control or account for different levels of protein expression between NCX isoforms. In all cases the trout NCX-TR1.0, or those chimeras containing substantial trout NCX-TR1.0 genotype typically expressed poorly and gave lower currents than that of other species. The effect of protein expression on modulation of NCX regulation or ion translocation is not known. Over expression of NCX may have a stabilizing effect on the protein thereby altering its translocation properties. The issue of dimerization has also been raised, which could potentially be driven by protein concentration. Dimerization of NCX, although never proven to occur, may fundamentally alter NCX translocation perhaps resulting in differences in the measured current. However, the overwhelming consensus to date is that dimerization of NCX does not occur (personal communication with Dr. Ken Philipson) but the notion that NCX expression level is a modulator of ion translocation cannot be refuted at this time.

Since it is difficult to keep patches stable over a long period of time, we were also severely limited in the number of different temperatures that we could test. Patches undergo a natural current rundown in a time dependent manner. Since we had to make absolutely sure the patches reached a stable temperature, single temperature dependent experiments would run for as long as 30 minutes and be subject to current rundown. We corrected for rundown by measuring exchange current at 30 $^{o}$C after measurements at 7 and 14 $^{o}$C and defining a linear rundown value for each patch. Unfortunately, it is not known if current rundown is completely linear over the whole experiment or if rundown

itself has a temperature dependent component. Both of these contentions are sources of errors.

An alternative would be measuring the temperature dependence of NCX activity using $^{45}Ca^{+2}$ uptake experiments; however, this method only gives an indication of bulk exchanger activity and does not provide insight into the subtleties of NCX currents. Having only three temperatures, we had to approximate temperature dependence in a linear manner, when in reality the temperature dependence profile of NCX would likely have a non-linear relationship. This is most evident in the observation that for our Arrhenius plots, the temperature dependence between 7 and 14 °C was always greater than the temperature dependence between 14 and 30 °C. It would be beneficial to have data at more temperatures to establish if there is a 'break point' that gave the Arrhenius plot a convex shape instead of a linear one. Possible sources for the non-linearity of the Arrhenius plot include changes in lipid fluidity, protein denaturation, change in ion translocation mechanism, or a change in the rate limiting step of the reaction. The latter two points are likely not relevant in our system but protein denaturation may effect the slope of the Arrhenius plot. This is especially true for NCX-TR1.0 since temperatures of 30 °C are lethal to the trout. It is possible that NCX-TR1.0 is becoming denatured at 30 °C, thus impairing its function and underestimating its temperature dependence. Measurement at more temperatures in smaller increments above and below 21 °C would help clarify this question. Regardless, in fitting the Arrhenius plot to linear equation we are assuming that the discussed parameters do not change appreciably over the range of temperatures we used. Currently, it is difficult to surmise if NCX-TR1.0 has gained function at cold temperatures or has lost the ability to function at warm temperatures or visa versa with NCX1.1.

A final point of discussion lies in the interpretation of the $E_{act}$ values derived from the Arrhenius plot and how they are related to temperature dependence. As discussed in the Introduction, we are defining NCX $E_{act}$ values to indicate the minimal amount of energy required for ion translocation to occur. The activation energy of catalyzed reaction is related to the overall free energy, $\Delta G = \Delta H - T\Delta S$, by the equation $\Delta H = E_{act} - RT$. $E_{act}$ is separate, but energetically related to the binding energy of the substrates ($Ca^{2+}$

and $Na^+$ ions) and the overall catalytic efficiency of the translocation. The stability of the ion-protein complex can have a large effect on the $E_{act}$; furthermore the rate of ion translocation per exchanger is also related to the energy barrier of the reaction, which in turn is dependent on the flexibility of the exchanger. In the case of our study, we do not know the optimal temperature of each NCX isoform since, due to technical limitations, we only measured three temperatures across a relatively narrow temperature range. For all exchangers measured, we observed an increase in absolute current with temperature indicating that the optimal temperature of all isoforms is greater than 30 °C. To get an estimation of catalytic efficiency one would have to measure the unitary currents of each isoform at their respective optimal temperature. Unfortunately, the slow turnover rate of the exchanger compared to an ion channel makes this impossible. One would hypothetically expect that for any given temperature, the catalytic efficiency would be higher for a cold versus a warm adapted exchanger and this would be reflected in lower $E_{act}$ values. Presumably, exchangers from ectotherms overcome the disadvantage of working at low temperatures (i.e. catalytic efficiency decreases with temperature) by lowering the $E_{act}$ for ion translocation. Lower $E_{act}$ values for an NCX isoform reflects an increase in protein flexibility so that ion binding and translocation can occur faster. Conversely, NCX isoforms from warm adapted species need the conformational stability to function at higher temperatures. This additional structural stability of the ion translocation apparatus will result in increased $E_{act}$ values for NCX from warm adapted species. Thus NCX, like all proteins, has adapted to function adequately at different environmental temperatures through alterations in protein flexibility-stability and these structural modifications are reflected in an NCX isoform's $E_{act}$ value.

## 7.3 Phylogeny of NCX

Prior to this dissertation very little information on NCX phylogeny was available, and that which was known suffered from a general lack of sequences and a strong mammalian bias of the sequences that did exist (3). The dearth in NCX sequence information was most evident in the lack of those from lower vertebrates and invertebrates. This is despite a high conservation of structure and function throughout the NCX family, and the insight already gained from characterization of non-mammalian

NCX isoforms (4-6). Evolutionary analysis at the molecular level can be valuable for finding residues that are important for protein function.

The elucidation of NCX phylogeny was not an intended goal at the outset of this project but became a fundamental aspect when the current literature was found lacking. The result was the first comprehensive phylogenetic and molecular evolutionary analysis of the NCX gene family. Initially we set out to gather as many NCX sequences as possible from a diverse group of organisms. We hypothesized that a large scale amino acid comparison of cold and warm adaptive NCX sequences would point to residues that are important for temperature adaptation. Cloned NCX isoforms present in protein databases are mostly of mammalian origin; fortunately the sequencing of full genomes has matured to the point that full length genes can extracted. Data mining of genomes resulted in the identification and annotation of thirteen new NCX sequences from six different species. Most importantly twelve of these sequences were derived from non-mammalian species, providing a greater evolutionary scope of NCX sequences. Interestingly, we found multiple NCX sequences in species other than mammals which prompted the need for their classification. Examination of NCX gene structure, together with construction of phylogenetic trees, provided novel insights into the molecular evolution of NCX. For the first time, we reported the existence of NCX2 and NCX3 in lower vertebrates yielding the hypothesis that two serial NCX gene duplications occurred around the time vertebrates and invertebrates diverged.

We also found a putative new NCX gene named NCX4 that is related to NCX1, but has been observed only in fish species' genomes. It is not known where or if NCX4 is expressed, nor is it known what type of function it may have. Since fish species need to maintain ionic homeostasis throughout a wide range of environments it is not surprising that additional proteins have adapted to deal with ionic regulation. We have not been able to find NCX4 in species other than fish, leading to the possibilities that a separate gene duplication event occurred only in fish or that the gene has been lost in terrestrial species due to a lack of selective pressure.

Finally, multiple sequence alignments confirmed NCX to be a protein highly conserved throughout evolution. The alignments have provided a basis for further

sequence comparison that though statistical analysis will highlight residues responsible for NCX temperature dependence. Overall, these findings present a stronger foundation for our understanding of the molecular evolution of the NCX gene family and provide a framework for further NCX phylogenetic and molecular studies.

## 7.4 The Temperature Dependence of NCX

Previous studies have shown mammalian NCX, like active transporters in general, is highly temperature dependent (7,8). NCX temperature dependence of trout (1) and frog (9) isoforms is considerably less, but these data are derived from native preparations and offer little mechanistic information. In the first study presented in this thesis, a comprehensive comparative analysis of NCX function was carried out using cloned canine NCX1.1 and trout NCX-TR1.0 isoforms. We were able to duplicate the previous results found from native proteins and show NCX-TR1.0 displayed significantly less temperature sensitivity than its mammalian ortholog when expressed in *Xenopus* oocytes. For example, typical $Q_{10}$ values for NCX-TR1.0 (both peak and steady-state current)s were ~1.1, compared to ~2.5 for canine NCX1.1. One possibility was that this temperature dependence differential was due to differences in regulatory or transport mechanisms between isoforms.

### 7.4.1 NCX Regulatory Properties and Temperature Dependence

Characterization of currents showed similar regulatory properties for NCX-TR1.0 and NCX1.1 as both displayed $Na^+$-dependent inactivation and $Ca^{2+}$-dependent positive regulation. This is perhaps not surprising due to the high overall sequence identity between isoforms in the XIP site and $Ca^{2+}$ binding region. One minor difference in $Na^+$-dependent inactivation between NCX-TR1.0 and NCX1.1 is the rate of current decay. Although displaying identical temperature dependencies, the $Na^+$-dependent inactivation of NCX-TR1.0 is consistently slower than that of NCX1.1 at all temperatures measured. The reason for the slower inactivation of NCX-TR1.0 is not known as 17/20 residues in the XIP site are completely conserved between isoforms. It is well established that $Na^+$-dependent inactivation is associated with the XIP site (10); however the slower inactivation rates of NCX-TR1.0 could be attributed to differences in other parts of the

exchanger that are thought to interact with the XIP site and modulate $Na^+$-dependent regulation (11,12). Regardless of these differences, measurement of NCX-TR1.0 and NCX1.1 currents in deregulated patches indicates NCX temperature sensitivity is not predicated on NCX regulatory mechanisms. Although the exact mechanism is uncertain, it is well documented that proteinase treatment of patches with α-chymotrypsin eliminates all forms of NCX regulation while maintaining exchange activity (13). The proteolyzed NCX-TR1.0 and NCX1.1 exhibited temperature dependencies similar to that of wild-type exchangers with $Q_{10}$ values not being significantly different. Based on the observation that NCX is deregulated after α-chymotrypsin treatment (13) and that the large intracellular loop is essential for NCX regulation (14) it was concluded that sequence differences in the loop are not associated with the disparate temperature dependencies of NCX isoforms. From these results it was hypothesized that sequence differences in the TMS are responsible for NCX temperature dependence, either with a modification of the translocation mechanism or in protein flexibility.

### 7.4.2 NCX Transport and Temperature Dependence

The TMS, especially the α-repeats, are known to be involved in ion exchange (15) and thus it is likely that sequence differences can indeed alter translocation to function at different temperatures. To test this hypothesis we employed the use of chimeras made from NCX-TR1.0 and NCX1.1. The use of chimeric proteins in studies involving NCX (4,14,16,17) and the thermostability of proteins (18,19) has proven a useful strategy in determining the molecular basis of functional differences between isoforms. As presented in Chapters 3 and 4, we attempted to find the molecular determinants for NCX temperature dependence.

The amino acid identity between NCX-TR1.0 and NCX1.1 is higher (~85%) within the TMS domains compared to the intracellular loop (~74%). Our strategy was to isolate the contributions of the TMS domains by cutting the exchanger in roughly three sections: the N-terminal TMS domain, the large hydrophilic loop, and the C-terminal TMS domain. Examination of outward currents for the first set of chimeras – DTT, DTD, and TDD – unequivocally showed that NCX temperature dependence was solely attributable to a region including the N-terminal TMS and XIP site. The N-terminal TMS

domain of the mature NCX is ~240 in length, constituting approximately one quarter of the overall length of the exchanger. In accordance with our previous finding in wild-type NCX-TR1.0 and NCX1.1, the inactivation kinetics of the chimeric proteins did not contribute to NCX temperature dependence. We continued with a chimera strategy to determine if one or more regions within the N-terminal TMS domains are responsible for NCX temperature dependence phenotypes. Specifically, this allowed rough isolation of the N-terminus and TMS1, loop b, and TMS2-4 including the alpha-1 region, and TMS5 and the XIP site. Unfortunately, measurement of chimera temperature dependence produced equivocal results. What was apparent from the data was a general trend showing temperature dependence phenotype being proportional to genotype origin (i.e. trout or dog NCX). This observation argues against the idea that a single region within the N-terminal TMS domain dictates NCX temperature dependence. Rather, it is likely that NCX temperature dependence phenotype is defined by several sequence differences in positions located throughout the primary sequence of the N-terminal region. From a direct comparison of NCX-TR1.0 and NCX1.1 sequences, there are few amino acid substitutions that immediately stand out nor do the sequences differences follow a pattern that one may predict for strategies to produce a cold-adaptive protein (e.g. an increase in polar residues) (20).

Instead of making random single residue mutations, we decided to obtain temperature dependence data on other NCX isoforms in an attempt to relate genotype with phenotype. We hypothesized that NCX isoforms from cold-adapted ectothermic species may have residues conserved in positions that are important for function at low temperatures. In contrast, warm adapted species would have different residues in these same positions. We measured the temperature dependencies of outward exchange currents from the previously cloned fruit fly CALX and squid NCX-SQ1. Consistent with the environments in which they live, the squid NCX-SQ1 ($Q_{10}$ ~1.2) displayed a temperature dependence similar to NCX-TR1.0 while the fly CALX ($Q_{10}$ ~1.8) was intermediate to NCX-TR1.0 and NCX1.1. A sequence alignment of these four species led to the testing of a single point mutation T127D in a NCX1.1 background. Modelled to be in the re-entrant loop of the $\alpha$-1 repeat, the mutation did not affect NCX function or temperature dependence.

One problem with this type of analyses is the evolutionary diversity of the species used. The canine and trout isoforms belong to the NCX1 gene family but CALX and NCX-SQ1 belong to invertebrate species that are far removed from vertebrates from a phylogenetic perspective. It is possible that different gene families of NCX have evolved differently to deal with temperature, since it has been shown that nature has employed a multitude of ways for proteins to deal with cold-adaptation (21,22). These caveats prompted two separate, but simultaneous, courses of action: 1) data-mining of sequence databases and genomes to increase the number of NCX sequences available for analysis 2) the search for a better comparative NCX model. Both strategies, albeit in entirely different manners, were to assist in the targeting of residues that could alter NCX temperature dependence. The former point culminated in the first full phylogenetic analysis of NCX and the novel insights therein as already described above. The latter resulted in the cloning and characterization of an NCX1 isoform from tilapia, a warm adapted teleost.

Teleost fish exhibit an extraordinary biodiversity, making up half of all vertebrate species. As such, orthologous proteins have evolved to function in many different environmental conditions, including a wide array of temperatures. In the tilapia, we had a good comparative match to the trout due to a relatively close evolutionary relatedness coupled with its ability to live at mammalian temperatures (i.e. 37 °C). The tilapia NCX, which we termed NCX-TL1.0, shares ~80% identity to trout NCX-TR1.0 and has highly similar functional and regulatory properties. However, NCX-TL1.0 displayed $Q_{10}$ values of ~2.5, marking the first time a non-mammalian NCX isoform displayed mammalian-like temperature dependence. Comparison of sequences in the N-terminal TMS domain highlighted ten residues common to tilapia NCX-TL1.0 and dog NCX1.1, but different to trout NCX-TR1.0. We reasoned that these residues would be under high selective pressure to be conserved in the dog and tilapia despite being evolutionary removed by ~450 million years. Supporting our chimera data, the ten residues are not localized to a single region but are scattered throughout the N-terminal TMS domain. Since little of NCX tertiary structure is available, it is not known if these residues are in proximity in the native protein but it remains an intriguing possibility.

## 7.5 Overall Conclusion

When this project started, there was a possibility that the differential temperature dependence between NCX-TR1.0 and NCX1.1 was due to different regulatory or ion transport mechanisms. Our studies with deregulated patches and with chimeras clearly show that NCX regulatory properties do not play a role in NCX temperature dependence. However, the issue of NCX isoforms from cold adaptive species having a different transport mechanism, as has been demonstrated in squid NCX, is feasible.

It has been shown previously that the electrogenic transport reactions in NCX-SQ1 are different than that for NCX1.1. Upon measurement of half reaction cycles the charge movement was found to accompany $Ca^{2+}$ in NCX-SQ1, which is the opposite of that observed in the mammalian NCX1.1 (5). Thus, $Ca^{2+}$ transport may be the rate limiting step in NCX-SQ1 ion exchange, whereas it is generally accepted to be $Na^{+}$ transport in NCX1.1 (23). It should be noted that the consecutive exchange mechanism in NCX-SQ1 has not been rigorously verified. A recent revised model of the consecutive mechanism in NCX1 suggests two separate cation binding sites, one that can bind 2 $Na^{+}$ or 1 $Ca^{2+}$ and another that only binds 1 $Na^{+}$ (24). In this model, the exchanger is capable of multiple transport modes where NCX1 can transport not only 1 $Ca^{2+}$ for 3 $Na^{+}$, but also 1 $Ca^{2+}$ with 1 $Na^{+}$ ion at a low rate. The role of different transport modes or mechanisms amongst species in NCX temperature dependence is not known.

Although NCX-TR1.0 and NCX-SQ1 have similar temperature dependences, charge movement experiments have not been attempted in NCX-TR1.0 since the method is extremely difficult to perform reliably especially in isoforms producing low currents. It is possible that NCX isoforms from ectotherms have adapted to function at cold temperatures by using $Ca^{2+}$ instead of $Na^{+}$ as the charge carrier. However, this seems highly unlikely for NCX-TR1.0 given it is much more closely related to NCX1.1 then NCX-SQ1 from a phylogenetic perspective. Both NCX1.1 and NCX-TR1.0 were cloned from heart tissue, and as orthologous proteins would have the same function. NCX-SQ1 was cloned from squid optic lobe and is not a member of the NCX1 subfamily and therefore could have evolved a different translocation mechanism. Underlying the different translocation mechanisms one would expect to see sequences differences in

areas important for ion exchange, namely the α-1 repeat region. A sequence comparison of this region shows five differences between NCX1.1 and NCX-SQ1, whereas only two sequence differences exist between NCX1.1 and NCX-TR1.0. One of these differences, T127 of NCX1.1 (D in NCX-TR1.0 and E in NCX-SQ1), is modelled to be in the re-entrant loop of α-1 and was shown in Chapter 4 to not play a role in NCX temperature dependence on its own. A recent mutational analysis of α-1 showed that residues in the re-entrant loop do not substantially affect ion transport; however mechanistic effects on ion translocation were not addressed (25). Our chimeric data also argues against NCX-TR1.0 having a different translocation mechanism that confers function at low temperatures. Trout-dog NCX1 chimeras showed that all regions of the N-terminal TMS domain contribute to NCX temperature dependence. If NCX temperature dependence were an issue of ion translocation mechanism, one may expect a specific region within the N-terminal TMS domain to have been localized. Finally, the residues highlighted from the tilapia paper corroborate this point since they are scattered throughout the N-terminal TMS domain.

In summary, there are several points regarding NCX temperature dependence that can be made. First, the temperature dependence of NCX is not due to regulatory properties, and is probably not due to differences in ion transport mechanisms that exist between species. The N-terminal TMS domain up to and including the XIP site is solely responsible for NCX temperature dependence; however it is not one residue or even region within this domain that allows NCX to function at different temperatures. It is likely that NCX contains two types of amino acid residues, one group that is conserved throughout evolution and is critical for the core function of ion translocation and regulation, and a second group that is not essential for NCX function but rather confers the subtle "tweaking" of the protein to function optimally under its respective environmental conditions. NCX temperature dependence is therefore dictated by a series of substitutions in positions that may or may not be common among homologs, indicating each isoform has evolved independent mechanisms to adapt to temperature. Further, these substitutions most likely modify the flexibility of NCX core regions in an allosteric manner that allows function at different temperatures. It is hoped that mutational analysis

directed by comparison of genotypes will uncover the identity of these substitutions and that this information can be used to infer structural information.

## 7.6 Future Directions

Much knowledge has been gained from this thesis regarding both NCX phylogeny and temperature dependence; however there is still a lot that needs to be done. In fact this thesis has merely provided a framework for further studies whose results should be more definitive.

In terms of NCX temperature dependence, we are using sequence data in two different comparative approaches to single out amino acids important for temperature dependence. The first approach is currently underway with examination of the ten residues were highlighted from the tilapia study. Our strategy is to decrease the temperature dependence of NCX1.1 by mutating all ten residues to the amino acids present in NCX-TR1.0. If successful, each residue will be examined as its contribution to NCX temperature dependence. The second comparative strategy involves a more theoretical approach using the multiple sequence alignment data gathered for the phylogenetic analysis. Though comparison of NCX sequences derived from cold and warm adaptive species, it should be possible to separate residues responsible for core exchanger function (i.e. those conserved) and other residues that may modify protein flexibility. Inference of residues that are important for protein function from a multiple sequence alignment is hardly a new idea, but the search in this case is complicated by the fact that residues altering NCX flexibility are probably not conserved amongst isoforms. A further complication in this manner is the fact that each NCX gene family has been evolving independently since the divergence of vertebrates and invertebrates. If the temperature dependence of NCX is in fact governed by slight alterations in protein flexibility or stability, it is entirely possible that each individual NCX gene family, or even isoform, has adapted to temperature independently. It may be a case where only cold and warm adapted NCX isoforms within a gene family can be compared. Current research is in the midst of trying to find a way to statistically predict which residues are candidates for mutation based on some type of conservation scoring system.

Future work on the phylogeny of NCX is also warranted. Additional NCX sequences from the mining of genomes should help clarify NCX molecular evolution. For example, we have recently found only one NCX gene in the early chordate *Ciona intestinalis*, indicating that the duplication events giving rise to the four NCX gene families occurred later in evolution. The release of genomes from species that preceded teleosts, such as hagfish and lampreys, should give a more accurate evolutionary timeframe of NCX duplication events. Since it is well known that fish genomes have undergone a separate round of genome duplication, the search for more NCX genes in fish species is a possibility and is one that is being explored currently. Another issue that needs resolution is the presence of NCX4 in fish genomes and if it is product of a separate fish gene duplication event or if it occurred before the divergence of fish from other vertebrates. We have recently shed some light on this controversy by finding the NCX4 gene in the amphibian *Xenopus tropicalis*, indicating that NCX4 was present before the divergence of fish species. We have yet to find any traces of NCX4 in any terrestrial species, raising the intriguing possibility that NCX4 is unique to aquatic species perhaps functioning as for ion homeostasis. Presumably, NCX4 was once present in mammalian and avian genomes but has been lost due to loss of selective pressure. Though gene synteny, it may be possible to locate the remnants of NCX4 in these genomes and represents another avenue of exploration. Finally, there is much to be gained through comparison of the gene structures of both paralogous and orthologous NCX genes. Knowing the genomic sequence of NCX isoforms affords the unique possibility of examining the evolution of NCX introns and exons and how alternative splicing came to be.

## 7.7 References


1. Tibbits, G. F., Philipson, K. D., and Kashihara, H. (1992) *Am J Physiol* **262**, C411-417
2. Xue, X. H., Hryshko, L. V., Nicoll, D. A., Philipson, K. D., and Tibbits, G. F. (1999) *Am J Physiol* **277**, C693-700
3. Cai, X., and Lytton, J. (2004) *Mol Biol Evol* **21**, 1692-1703
4. Dyck, C., Maxwell, K., Buchko, J., Trac, M., Omelchenko, A., Hnatowich, M., and Hryshko, L. V. (1998) *J Biol Chem* **273**, 12981-12987.
5. He, Z., Tong, Q., Quednau, B. D., Philipson, K. D., and Hilgemann, D. W. (1998) *J Gen Physiol* **111**, 857-873
6. Hryshko, L. V., Matsuoka, S., Nicoll, D. A., Weiss, J. N., Schwarz, E. M., Benzer, S., and Philipson, K. D. (1996) *J Gen Physiol* **108**, 67-74
7. Hilgemann, D. W., Matsuoka, S., Nagel, G. A., and Collins, A. (1992) *J Gen Physiol* **100**, 905-932
8. Kimura, J., Miyamae, S., and Noma, A. (1987) *J Physiol (Lond)* **384**, 199-222
9. Bersohn, M. M., Vemuri, R., Schuil, D. W., Weiss, R. S., and Philipson, K. D. (1991) *Biochimica et Biophysica Acta* **1062**, 19-23
10. Matsuoka, S., Nicoll, D. A., He, Z., and Philipson, K. D. (1997) *J Gen Physiol* **109**, 273-286
11. Maxwell, K., Scott, J., Omelchenko, A., Lukas, A., Lu, L., Lu, Y., Hnatowich, M., Philipson, K. D., and Hryshko, L. V. (1999) *Am J Physiol* **277**, H2212-2221
12. Weber, C. R., Ginsburg, K. S., Philipson, K. D., Shannon, T. R., and Bers, D. M. (2001) *J Gen Physiol* **117**, 119-131.
13. Hilgemann, D. W. (1990) *Nature* **344**, 242-245
14. Matsuoka, S., Nicoll, D. A., Reilly, R. F., Hilgemann, D. W., and Philipson, K. D. (1993) *Proc Natl Acad Sci U S A* **90**, 3870-3874.
15. Nicoll, D. A., Hryshko, L. V., Matsuoka, S., Frank, J. S., and Philipson, K. D. (1996) *Journal of Biological Chemistry* **271**, 13385-13391
16. Iwamoto, T., Uehara, A., Nakamura, T. Y., Imanaga, I., and Shigekawa, M. (1999) *J Biol Chem* **274**, 23094-23102.
17. Iwamoto, T., Kita, S., Uehara, A., Imanaga, I., Matsuda, T., Baba, A., and Katsuragi, T. (2004) *J Biol Chem* **279**, 7544-7553
18. Satoh, T., Takahashi, Y., Oshida, N., Shimizu, A., Shinoda, H., Watanabe, M., and Samejima, T. (1999) *Biochemistry* **38**, 1531-1536.
19. Sode, K., Watanabe, K., Ito, S., Matsumura, K., and Kikuchi, T. (1995) *FEBS Lett* **364**, 325-327.

20. Russell, N. J. (2000) *Extremophiles* **4**, 83-90.

21. Miyazaki, K., Wintrode, P. L., Grayling, R. A., Rubingh, D. N., and Arnold, F. H. (2000) *J Mol Biol* **297**, 1015-1026.

22. Wintrode, P. L., Miyazaki, K., and Arnold, F. H. (2000) *J Biol Chem* **275**, 31635-31640.

23. Hilgemann, D. W., Nicoll, D. A., and Philipson, K. D. (1991) *Nature* **352**, 715-718

24. Kang, T. M., and Hilgemann, D. W. (2004) *Nature* **427**, 544-548

25. Ottolia, M., Nicoll, D. A., and Philipson, K. D. (2005) *J Biol Chem* **280**, 1061-1069